UNCERTAINTY IN PREDICTIONS OF THERMAL COMFORT IN BUILDINGS

Proefschrift

ter verkrijging van de graad van doctor
aan de Technische Universiteit Delft,
op gezag van de Rector Magnificus prof.ir. K.F. Wakker,
voorzitter van het College voor Promoties,
in het openbaar te verdedigen op maandag 25 juni 2001 om 16.00 uur

door

Michael Stendert DE WIT

natuurkundig ingenieur
geboren te Valkenswaard

Dit proefschrift is goedgekeurd door de promotoren:

Prof.ir. A.C.W.M. Vrouwenvelder
Prof.ir. G.L.M. Augenbroe

Samenstelling promotiecommissie:

Rector Magnificus, voorzitter	
Prof.ir. A.C.W.M. Vrouwenvelder	Technische Universiteit Delft, promotor
Prof.ir. G.L.M. Augenbroe	Georgia Institute of Technology, Atlanta, USA, promotor
Prof.ir. J.J.M. Cauberg	Technische Universiteit Delft
Prof.dr. R.M. Cooke	Technische Universiteit Delft
Prof. K.J. Lomas	De Montfort University, Leicester, UK
Prof.drs.ir. J.K. Vrijling	Technische Universiteit Delft
Prof. H.W. Tieleman	Virginia Polytechnic Institute and State University, Blacksburg, USA

ISBN 90-9014884-1

Omslagontwerp: Martijn Baljon

Printed in The Netherlands.

Abstract

Building performances play an important role in choices between alternative building designs. When expressed in suitable indicators, they provide the decision-maker with a quantitative measure of the extent to which a building alternative satisfies the design requirements and objectives. Predictions of building performances in the design stage imply uncertainty. Quantitative appraisal of this uncertainty can contribute to more rational design decisions.

In current design practice though, the uncertainties in the majority of the performance predictions are not explicitly quantified. This certainly holds for performances related to the heat regulation of a building, such as thermal comfort performance or annual energy consumption. In the literature on the simulation of these performance aspects, uncertainties have received some attention, but several questions have been left open. Firstly, it has been acknowledged that many of the uncertainties cannot be estimated by straightforward statistical analysis of available data. This raises the question by which method these uncertainties could be assessed and whether such a method would be applicable in design practice. Secondly, although intuitive arguments have been put forward to emphasize the relevance of quantitative uncertainty information for design decisions, no attempts have been made to show how a decision maker could use this information to improve his decision.

The research underlying this thesis aims to provide an answer to these two questions. The questions are addressed in the context of a specific case, which concerns the performance of a four story, naturally ventilated office building with respect to the thermal comfort of its occupants. To quantify this performance aspect, two indicators are selected, which are commonly used in Dutch design practice. Prediction of these indicators involves computer simulations on the basis of a thermal building model.

First, a crude assessment is made of the uncertainty that should be attributed to predictions of the comfort indicators in the case at hand. In this analysis, the uncertainties in all of the building model parameters are estimated by the author on the basis of the literature. A sensitivity analysis is carried out to identify the parameters, which contribute most to the prediction uncertainty.

Subsequently, two sets of parameters of which the uncertainties cannot be derived by straightforward statistics, are selected for further analysis from the top 5 important parameters. For both parameter sets, structured expert judgment is used to assess the uncertainties involved. The parameters in the first set concern physically observable quantities and the experts are asked to state their uncertainties over these parameters directly. Their assessments are combined by weighted averaging. The experts' weights are derived from a statistical comparison of their assessments with measured data. The uncertainties in the second set of parameters are calculated in a similar way, but an extra step is involved. As these parameters are abstract and highly model-specific, the experts' assessments are elicited over a set of related variables, which are physically observable. The uncertainties in the parameters of interest are obtained by probabilistic inversion of the model relating the parameters to the elicitation variables. In both analyses, the performance of the applied method and its practical applicability are evaluated.

Finally, the uncertainty in the prediction of the two performance indicators is assessed. A demonstration is given how this uncertainty can constructively be used in design decisions through a Bayesian decision analysis.

Contents

1 Introduction 1

2 Performance assessment 7

2.1 Introduction ... 7
2.2 Case description ... 8
2.3 Thermal building simulation ... 11
2.3.1 Introduction ... 11
2.3.2 Building space ... 14
2.3.3 External sunblind ... 17
2.3.4 Ventilation modeling ... 18
2.3.5 From component models to building model ... 21
2.3.6 Quantification of model parameters ... 22
2.3.7 Implementation and verification ... 25
2.4 Performance criteria for thermal comfort ... 25
2.4.1 Introduction ... 25
2.4.2 Thermal comfort models ... 27
2.4.3 Performance indicators ... 33
2.5 Discussion ... 33
2.6 Summary ... 34

3 Crude uncertainty analysis 35

3.1 Introduction ... 35
3.2 Uncertainty in model parameters ... 38
3.2.1 Introduction ... 38
3.2.2 Physical properties of materials and components ... 39
3.2.3 Space dimensions ... 39
3.2.4 Wind reduction factor ... 40
3.2.5 Wind pressure coefficients ... 41
3.2.6 Discharge coefficients ... 43
3.2.7 Internal convective heat transfer coefficients ... 43
3.2.8 External convective heat transfer coefficients ... 45
3.2.9 Albedo ... 46
3.2.10 Convective heat transfer at sunblind and window ... 46
3.2.11 Distribution of absorption of the incident solar radiation ... 48
3.2.12 Air temperature stratification ... 48
3.2.13 Radiant temperature of surrounding buildings ... 50
3.2.14 Outdoor ambient temperature ... 50
3.2.15 Discussion and summary ... 50
3.3 Propagation of uncertainty ... 51
3.4 Sensitivity analysis ... 52
3.4.1 Introduction ... 52
3.4.2 Technique ... 53
3.4.3 Results ... 55
3.5 Discussion and conclusions ... 57

4 Uncertainty in wind pressure coefficients 59

4.1 Introduction ... 59
4.2 Case definition ... 60
4.2.1 Introduction ... 60
4.2.2 Building and its surroundings ... 60
4.2.3 Simulated boundary layer ... 61
4.2.4 Wind pressure difference coefficients ... 62
4.3 Calculation models for wind pressure coefficients ... 63
4.3.1 Introduction ... 63
4.3.2 Summary of model features ... 63
4.3.3 Comparison of model outputs ... 66
4.4 Expert judgment study ... 68
4.4.1 Introduction ... 68
4.4.2 Questionnaire ... 70
4.4.3 Selection of the experts ... 72
4.4.4 Expert training ... 73
4.4.5 Dry-run ... 73
4.4.6 Elicitation ... 74
4.4.7 Wind tunnel experiments ... 74
4.5 Results 77
4.5.1 Wind tunnel results ... 77
4.5.2 Experts' assessments ... 78
4.6 Analysis of the expert data ... 80
4.6.1 Introduction ... 80
4.6.2 From quantile values to a marginal distribution ... 81
4.6.3 Performance ... 81
4.6.4 Combination of the experts' marginal distributions ... 84
4.6.5 Combination of the experts' dependencies ... 86
4.6.6 Robustness analysis ... 87
4.7 Discussion ... 88
4.7.1 Introduction ... 88
4.7.2 Disaggregation ... 88
4.7.3 Expert judgment compared to wind tunnel ... 91
4.8 Conclusions and recommendations ... 93

5 Uncertainty in the indoor air temperature distribution 95

5.1 Introduction ... 95
5.2 Description of the space ... 97
5.3 Modeling of the air temperature distribution ... 98
5.3.1 Introduction ... 98
5.3.2 Current modeling approach ... 98
5.3.3 Alternative modeling approaches ... 100
5.4 Uncertainty ... 102
5.5 Modeling under uncertainty ... 102
5.6 Heuristic model ... 103
5.6.1 Introduction ... 103
5.6.2 Modeling of the difference between exhaust air temperature and mean air temperature ... 104
5.6.3 Modeling of the difference between temperature experienced by an occupant and mean air temperature ... 108
5.6.4 Modeling of the mean air temperature ... 108
5.6.5 Discussion ... 109

5.7 Expert judgment study 110
5.7.1 Introduction 110
5.7.2 Main features of the expert judgment study 110
5.7.3 Questionnaire 111
5.7.4 Selection of the experts 116
5.7.5 Dry-run 117
5.7.6 Elicitation 117
5.7.7 Results 118
5.7.8 Analysis and combination of the experts' assessments 120
5.8 Probabilistic inversion 121
5.8.1 Introduction 121
5.8.2 Solution scheme 122
5.8.3 Implementation in the study 125
5.8.4 Results 126
5.9 Discussion and conclusions 132

6 Propagation and implications of uncertainty 137

6.1 Introduction 137
6.2 Propagation of the uncertainty 138
6.2.1 Introduction 138
6.2.2 Wind pressure difference coefficients 138
6.2.3 Indoor air temperature distribution 141
6.2.4 All parameters 143
6.3 Implications for design decisions 144
6.3.1 Introduction 144
6.3.2 Advice on the basis of 'best' estimates 145
6.3.3 Bayesian decision analysis 145
6.3.4 Example 149
6.4 Discussion 154
6.5 Summary 156

7 Closure 157

7.1 Summary and conclusions 157
7.2 Recommendations 160

References 163

Appendix A 175

Appendix B 181

Appendix C 185

Appendix D 201

Symbols and abbreviations 211

Samenvatting 213

Dankwoord 217

Curriculum vitae 219

1 Introduction

A crucial element in building design and construction is decision-making. From the initial exploration of objectives and requirements to the final brush of paint, a tremendous number of choices have to be made. These choices touch on a variety of disciplines and involve a spectrum of specialists and consultants to advise the decision maker(s) involved. Dependent on the context, a consultant's advice may serve in e.g. further clarifying the decision-maker's objectives and requirements, proposing new or adapted design alternatives, surveying the possible consequences of certain design decisions and/or quantifying these consequences.

In this thesis we focus on a particular type of consultant and on a particular aspect of advice. The consultant, or rather the domain the consultant represents, is building physics. The advice aspect is the quantification of the consequences of one or more design choices, which are considered by the responsible decision-maker.

The domain of expertise of the building physics consultant traditionally covers phenomena related to heat, moisture, ventilation/wind, lighting and acoustics in the built environment. This expertise gives him a part in a diversity of problem areas, such as indoor climate in buildings, acoustics of concert halls, wind discomfort in built-up areas, or lighting conditions in office spaces.

In quantifying the consequences of design actions, the first step is to identify in which terms this should be done. A decision-maker, for instance the client or the future user of the building, will generally have rather abstract (functional) requirements or objectives in view. An evaluation of the consequences of a design action should enable him to score to which degree the action contributes to these objectives. Hence, before a quantitative evaluation of consequences can be made, one or more quantities must be defined, on which the decision-maker can measure the level of achievement on his objectives.
These quantities, which form the link between the qualitative requirements on the one hand and the technical implications of a design decision on the other hand, are in the building industry commonly referred to as performances or performance indicators.
An example of a performance indicator is one that measures the ventilation systems' capacity to maintain a building space near optimum indoor air quality. It translates the requirement to maintain healthy conditions in a given building zone into a quantitative indicator, which can be calculated from air flow rates and resulting spatial contaminant distributions obtained in standardized experiments.

Assessment of building physics related performance indicators in a design context has two main characteristics. First, it commonly requires insight in the response of the building to 'external' conditions such as the outdoor temperature, the wind velocity, and the occupants. As the building is still under design, commonly of a unique nature, and in

many respects a complex system, it is not surprising that computer simulation is often deployed.
Second, there is always lack of information. This is inherent in the design context. Indeed, only as the design process advances, more and more information becomes available about the building as it will be delivered. But even a final design plan does not completely determine the building, due to imprecision in the construction process and natural variability in the properties of building components and materials. Moreover, in addition to the lack of knowledge about the building itself, several external factors, which affect the building performance, are not precisely known during the design process. Finally, the complexity of the building makes it necessary to introduce simplifications in the computer simulation models. Together with the lack of information about the building and the external factors it will be exposed to, these simplifications lead to uncertainty in the assessment of the building performance. This uncertainty is the central issue in this thesis.

It is, however, a far from central issue in current building physics consultancy. Explicit appraisal of uncertainty is the exception rather than the rule and most decisions are based on single valued estimates for performance indicators.

From a conceptual point of view, this lack of concern for uncertainty is surprising. If we consider advice as an exchange of information, which aims to contribute to a decision-makers understanding and overview of the decision problem, it seems natural that uncertainties in building performances are assessed and communicated.
Moreover, quantitative information about the uncertainties can be used in the development of the building model. Specific attention can be given to those parts of the model, which give a disproportionate contribution to the performance uncertainty. If a model part causes too much uncertainty, measures can be considered such as more refined modeling or collection of additional information by e.g. an experiment. On the other hand, model components that prove to be overly sophisticated may be simplified to reduce the time and effort involved in generating model input and running the computer simulations.

From a practical perspective, though, the lack of focus on uncertainty is quite natural. In current practice, building performance is commonly assessed with commercially available building simulation tools. Such tools facilitates the modeling and simulation of complex building systems within the limitations on time and money that apply in practical design situations. However, the tools provide virtually no handles to explore and quantify uncertainty in performance assessments.
First, no information is supplied about the magnitudes of the various uncertainties that come into play. Libraries with data on e.g. material properties and model parameters, which are included in almost all simulation tools, specify default or 'best' values, but lack information on the spread in these values. Second, with the exception of one or two, none of these tools offer methods to carry out a systematic sensitivity analysis or to propagate uncertainty. Finally, the possibilities to selectively refine or simplify model aspects are limited in most simulation environments.

The above reflection on the deterministic approach in current practice specifically holds for thermal building simulation. Thermal building simulation is used to quantify performance aspects, which are related to the heat regulation of a building, such as the maximum temperature in a building space over a given period, the thermal comfort in the building, the annual energy consumption, the required peak power of a heating plant, etc. In the rest of this thesis we will focus entirely on these building performance aspects and the simulation tools that can be used to assess the associated performance indicators.

In the research field from which these building simulation tools have emerged, several studies have been dedicated to uncertainty in the output of building simulations and the building performance derived from these outputs. Report of the research that is most relevant to the study in this thesis can be found in Lomas and Bowman (1988), Clarke et al. (1990), Pinney et al. (1991), Lomas and Eppel (1992), Lomas (1993), Martin (1993), Fürbringer (1994), Jensen (1994), Wijsman (1994), Rahni et al. (1997), De Wit (1997c), MacDonald et al. (1999). As these studies will be cited at various points throughout this thesis, a full discussion is omitted here. Instead we will give a concise overview of the state-of-the-art:

- Overall, the data and knowledge on the various uncertainties that may contribute to the uncertainty in building performance is limited. Uncertainties related to natural variability, which can sensibly be quantified on the basis of statistical analysis such as spread in e.g. material properties and building dimensions, are relatively well-covered. Modeling uncertainties, though, and other uncertainties which cannot be comprehensively derived from observed relative frequencies, received restricted attention. If they were assessed, it was on an ad-hoc basis.
- Several of the studies focus on a comparison of techniques for model sensitivity analysis and propagation of uncertainty. When we combine the results of these studies with the more general literature in this field, an overview of methods results, which provides sufficient possibilities for direct application. However, as mentioned before, these techniques have hardly pervaded commercially available tools for building simulation.
- All analyses restrict their focus to a given model structure, often suggested by a particular simulation tool. The issue of how explicit information about uncertainty can be used to selectively simplify or refine (part of) the model is not addressed.
- Virtually no attention is given to the question how quantitative uncertainty can be dealt with in decision analysis, in such a way that it contributes to further insight into the decision problem at hand, rather than to a growing vagueness. Some of the studies attempt to deal with uncertainty within the paradigm of current practice: 'best' estimates of performance as a basis for decisions. However, the value of the information in this approach is judged by the consultant, who, from his perspective, has only a partial view of the total decision problem. The person who can value the information properly is the decision maker. Clearly, this requires not only the proper attitude of the decision-maker, but also the knowledge and skill to deal with uncertainty in decision making.

- The majority of the uncertainty analyses focus on energy consumption and plant power in winter situations. Although it is difficult to compare the uncertainties resulting from the various studies due to differences in approach (e.g. a comparison of the outputs from different simulation tools versus a systematic uncertainty analysis), assumptions (which uncertainties are taken into account and which are not) and context (e.g. building design versus model validation), it seems that predictions of these performances have associated uncertainties in the order of 10 – 50%. Instantaneous, time-averaged, and peak temperatures have also been considered, especially in studies with a model validation context. Only Wijsman (1994) explicitly addresses thermal comfort performance in a design context. In an experiment, where different analysts were given the same case and the same simulation tool, differences in building performance of up to 100% were observed. When the analysts' 'errors' were removed, this range was decreased well below 40%.

This overview has triggered the questions, which are the focus of the research underlying this thesis:

- The uncertainty in thermal comfort performance in summer is potentially much larger than in performance indicators like annual energy use for heating in winter. However, no systematic uncertainty analyses have been reported in literature. Is the uncertainty in this aspect of building performance indeed significant in a design context?
- Many of the relevant uncertainties cannot be derived from straightforward statistical analysis of available data. By which method could these uncertainties be assessed? Is such a technique applicable in consultancy practice?
- How can quantitative information on the uncertainties be used to selectively refine or simplify the building model?
- What is the relevance of the explicit and quantitative appraisal of uncertainty for building physics advice in a decision context?

These questions have been addressed in a case study, which focuses on a specific performance aspect, i.e. thermal comfort in summer. The building in the case study is a naturally ventilated low-rise office building.

An office building has been selected as thermal comfort is an important issue in this type of building. The choice for thermal comfort was, apart from the relative lack of attention this performance aspect has received in uncertainty analyses in the literature, motivated by two considerations.

First, a demand regarding indoor climate performance is usually included in the design requirements for (office) buildings. This concern for the indoor climate is not surprising as the majority of complaints about working conditions in Dutch office buildings are temperature-related (Voskamp, 1995).

Second, practically all buildings in The Netherlands are equipped with heating plant, whereas cooling plant is much less common. In the absence of a cooling system, uncomfortably high temperatures in summer have to be avoided by measures such as solar shading, reduced glazing areas, additional thermal mass, and (natural) ventilation. Obviously, most of these measures may have side effects on other performance

characteristics. Conversely, many design alterations, although not (primarily) targeted at the indoor climate, may well affect performance with respect to this climate. Hence, to be able to properly consider the effect of design choices, an evaluation of performance is required at every step of the design evolution.

The outline of the thesis is as follows. First, Chapter 2 describes the office building, the approach towards thermal modeling and simulation of the building performance, and the definition of and background to, the thermal comfort indicators that have been considered. Chapter 3 discusses a crude uncertainty analysis. The uncertainties from different sources are identified, quantified and propagated through the model. Sensitivity analysis points out which model parameters (parameter sets) contribute most to the uncertainty in the building performance indicators. Two of these important parameter sets are selected for further analysis. These analyses, one on wind pressure coefficients and another on the temperature distribution in the indoor air, are reported in Chapters 4 and 5 respectively. The focus of these chapters is on a proper assessment of the uncertainties, both methodologically and regarding content. Moreover, Chapter 5 illustrates the issue of model development in tandem with the appraisal of uncertainty. Chapter 6 starts with the propagation of the uncertainties, including those that have been (re-)assessed in Chapters 4 and 5. Subsequently, on the basis of the results a method by which quantitative information on uncertainty can be used in design decisions is illustrated. Chapter 7 completes the thesis with conclusions and recommendations.

2 Performance assessment

2.1 Introduction

The focus of this thesis is on building physics advice, elicited in the design phase of a building to support design decisions. As explained in Chapter 1, a specific aspect of advice is considered, i.e. the quantification of the consequences of (design) actions. These consequences are quantified in terms of performance indicators. A performance indicator rates the degree to which the result of a design action satisfies the decision maker's objectives or demands. A more elaborate discussion on the role of performance indicators in the decision process is deferred to Chapter 6.

Chapter 1 also indicates that a specific case is addressed in this study. The case considers a naturally ventilated office building, which is evaluated with respect to its performance on indoor climate. This performance is assessed by simulation.

The current chapter describes the selected case, discusses the definition of relevant performance indicator(s) and explains the simulation process. These issues are addressed separately in the following sections. However, before going into the details, we give a brief outline of simulation based performance assessment.

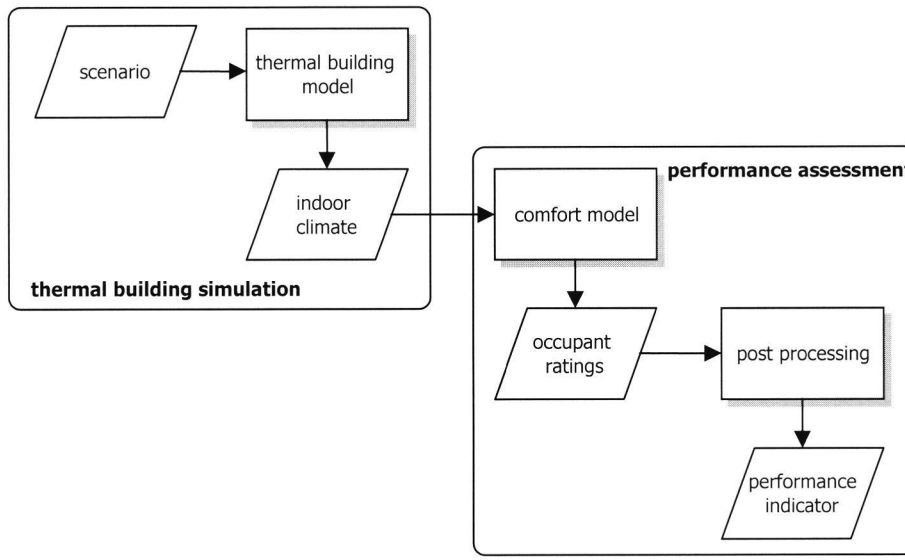

Figure 2.1 Schema for building performance evaluation with respect to thermal comfort.

Loosely stated, the indictors that are used in The Netherlands to rate buildings with respect to indoor climate are based on the fraction of time that occupants are (dis)satisfied with the climatic conditions in the building. To quantify this fraction of time in a design context, when measurements are infeasible for obvious reasons, (computer) simulation is a frequently used technique. Graphically, the process of performance simulation can be rendered as shown in Figure 2.1.

First, the indoor climate is simulated dynamically with a thermal building model. This model is developed on the basis of the design specifications of the building. The inputs to the model, collectively referred to as the scenario, specify the 'external' conditions as a function of time. These conditions include among other things a time series of the outdoor climatic conditions, heat gains from people, lighting and equipment in the building and the control of sunblinds and windows. This component of the performance simulation process is referred to as thermal building simulation.

Subsequently, the building performance is assessed. This process is divisible into two parts. First, the occupants' comfort ratings in response to the calculated climatic conditions are estimated with a comfort model. Then, in the post-processing these ratings are combined into the performance indicator.

The simulation approach, as outlined in the previous three paragraphs, has been followed in the study underlying this thesis. In the implementation, however, two important choices have been made. First, in accordance with mainstream building simulation, the scope of the building models has been restricted to temperatures only. Other aspects of the indoor climate such as humidity and air velocity have not been part of the simulations. Details about the development of the building model, the compilation of the scenario, and the simulation are discussed in Section 2.3.
Second, only global models for thermal comfort have been considered. These models describe occupant ratings in terms of the global (or average) ambient climatic conditions. Local effects of e.g. cold floors, asymmetric radiant fields or draught at head level are not accounted for by the models. The performance assessment process is discussed more elaborately in Section 2.4.
Before addressing the issues of modeling and simulation, though, we first describe the subject of these efforts, i.e. the case of interest.

2.2 Case description

As mentioned earlier, this study focuses on a specific building. More adequately put, it focuses on a specific *model* of this building. Section 2.3 aims to describe the principles of this model. That section will often refer to specific characteristics of the building, which require or allow a certain modeling approach. It is the goal of the current section to provide the necessary information on these characteristics.

The case concerns the advanced design stage of a (hypothetical) four-story office building in a sub-urban/urban environment in The Netherlands. Figure 2.2 shows a front view of the office building with its main dimensions.

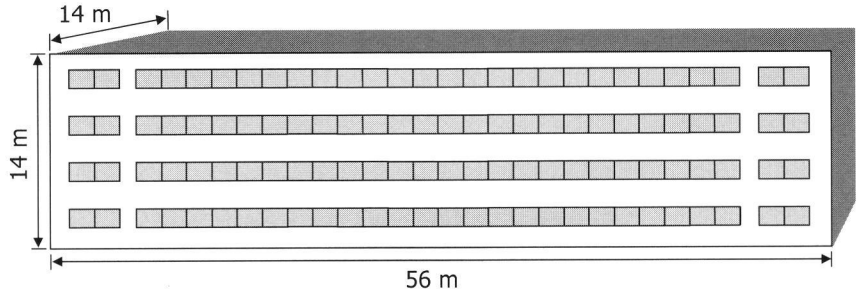

Figure 2.2 Schematic view of the office building with its main dimensions.

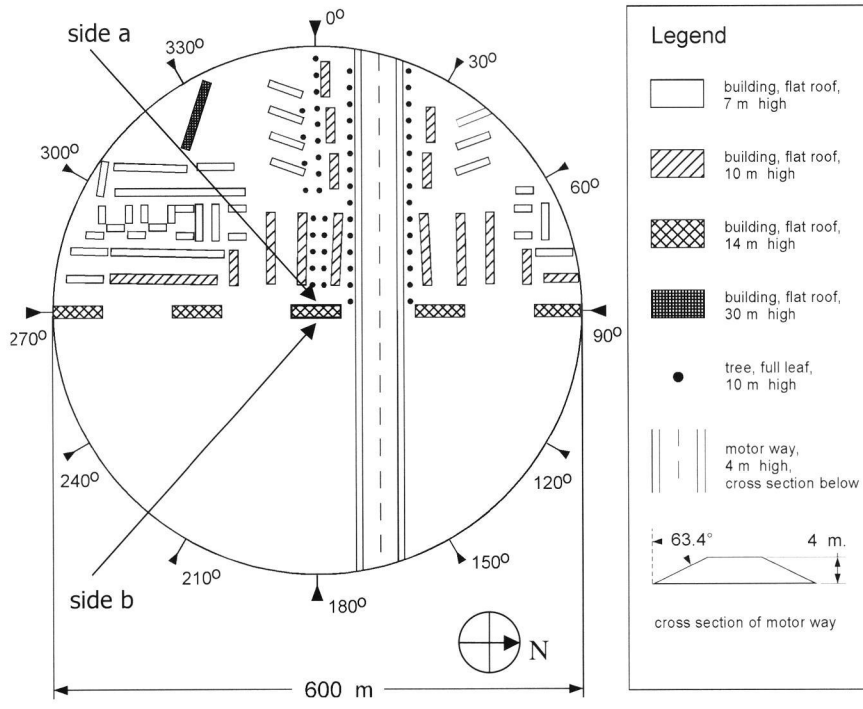

Figure 2.3 Schematic layout of the building in its environment.

In Figure 2.3 the layout of the building environment is outlined within a radius of 300 m. The upper half of the area shows a typical urban setting, which was modeled after a part of the Dutch town Delft. The lower half is left void, with exception of the embankment of the roadway. This mimics a large open space in an otherwise urban environment.

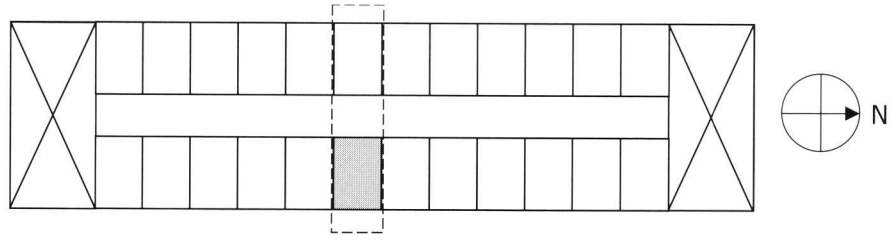

Figure 2.4 Plan of the top floor. A corridor separates the two rows of office spaces at the long façades. The crosses at both ends of the building indicate the stairwells, which are separated from the corridors by airtight fire doors. The orientation of the building is indicated. The office space under study is grayed. The dashed rectangle encloses the part of the building that will be modeled in detail (see Section 2.3.2).

The building relies on natural ventilation. Without cooling plant in the building it will be especially difficult to maintain acceptable climatic conditions in the spaces on the top floor, especially those oriented to the east (see e.g. Wapenaar, 1992). Hence, as a first step in the assessment of the performance of the building with respect to indoor climate, the thermal conditions in one of these office spaces will be studied in detail. Figure 2.5 shows an impression of the selected space with its main dimensions.

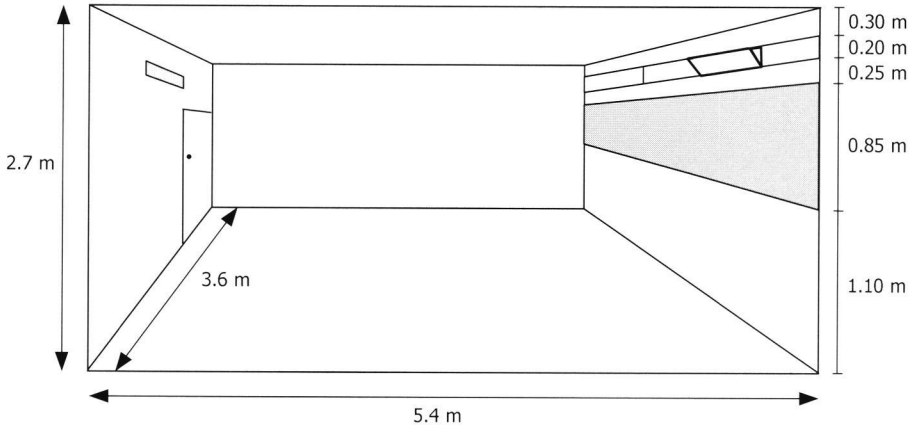

Figure 2.5 The office space under study with dimensions ($l \times w \times h$) 5.4 m × 3.6 m × 2.7 m. Cross-ventilation of the space takes place through a cantilever window in the façade and a rectangular vent in the opposite wall. The furnishing to accommodate two people is not shown.

The outline of the design specifications is:
- Concrete floor with unspecified floor-covering
- Concrete roof slab, 120 mm insulation outside, false ceiling
- Heavy interior walls (sand-lime brick)
- Double-glazing, standard glass, 12 mm cavity
- Parapet with 240 mm insulation
- External sunblinds
- A single ventilation opening in the separation wall with the corridor, just below the ceiling.
- An openable cantilever window in the façade, just below the ceiling.
- Air-tightness of the façade in accordance with the Dutch building code.

Throughout this study variations on a scenario with the following outline have been used:
- Office hours are from 8.00 – 18.00, 7 days a week.
- The total internal heat production from people, lighting and equipment amounts to 20 W/m^2 during office hours[1].
- The (hourly) outdoor climate conditions are as specified in the Test Reference Year for De Bilt, The Netherlands (see Section 2.3.1).
- The internal office doors are assumed to be closed at all times[2].
- The (fire-)doors to the staircases at both sides of the corridor are closed at all times.
- No cooling plant is installed.
- All offices are operated identically.

Further details can be found in Appendix A.

2.3 Thermal building simulation

2.3.1 Introduction

The term *thermal building simulation* covers a wide range of simulation and modeling activities related to buildings. In the context of this thesis we reduce the scope to the calculation of the temperature field in a building in response to given time-variant external conditions. Assessment of this temperature field, starting from building (design) specifications involves the following steps:
1. demarcation of the system to be modeled
2. specification of the required model output
3. modeling of the system
4. specification of the external conditions, i.e. the model inputs
5. simulation

We will briefly discuss these steps in the following paragraphs.

[1] Specified as heat load per m^2 floor area in the space.
[2] This originates from the idea that the operation of internal doors should not be driven by thermal comfort. In other words, it should be possible to maintain an acceptable indoor climate in the offices even with closed internal doors.

System demarcation

Although the term 'building' simulation suggests that the system to be modeled is the building itself, the scope of the model may vary from case to case. Dependent on the application the system may be smaller and represent only a part of the building, or larger and encompass elements of the building environment. In this case we will extend the system somewhat beyond the building boundaries to account for the influence of the direct environment.

Model output

Obviously, the required model output is determined by the purpose of the simulation. In this case we need a dynamic assessment of the indoor climate in a single space. On the basis of this information the occupants' comfort ratings can be estimated. All comfort models that can be used for this purpose require temperature information, i.e. air temperature and wall surface temperatures. Some models take also humidity and air velocity as input. In this study we confine ourselves to the simulation of temperatures; humidity and air velocity are not calculated.

System modeling

In the modeling of the system the following procedure may be followed:

- subdivision of the system into subsystems or components
- modeling of each component
- connection and assembly of the component models

This modular approach toward building modeling is advantageous in various respects. One of the most important benefits is that it paves the way for the deployment of building modeling tools. We will come back to that later.

After subdivision of the system into components, the modeling of each component involves the following aspects:

- conceptual modeling
- physical modeling
- numerical modeling
- quantification of model parameters

In the conceptual modeling stage, the model inputs and outputs are defined. Moreover, the required granularity of the model is chosen, i.e. the resolution of inputs, outputs, and internal states. The physical modeling stage covers the formulation of the actual expressions, which constitute the relationship between the inputs and the outputs. These expressions are subsequently implemented as numerical models. This modeling stage often involves discretization of the model.

These three steps fix the structure of the model. The component model is completed by the quantification of the parameters, which often have case-specific values.

In most practical situations, system models are developed in a building modeling and simulation environment. In such an environment, component models can be developed or picked from a library of standard models and assembled into a building model. The functionality and architecture of these modeling environments varies significantly (see

e.g. Sahlin, 1996). However, the conceptual and physical models for most of the components that are of interest in this study are very similar among modeling platforms. Hence, Section 2.3.2 through 2.3.5 address the mainstream physical modeling of these components and the physical basis for their assembly into a building model.

Specifications of the external conditions (inputs)

The external conditions can be subdivided into two categories:

1. outdoor climate
2. operation of the building (including occupant behavior)

An outline of the scenario has been presented in Section 2.2. More detailed information can be found in Appendix A.

In comfort performance evaluations in the design stage of a building, historical time series of (hourly) climate data, measured at a nearby meteorological station are used in current practice in The Netherlands (see e.g. ISSO, 1994). Commonly these data are either taken from 1964/1965[3] or from a Test Reference Year (Lund, 1985). As a result of this de facto standardization of the climate component in the scenario a broad frame of reference has been developed to which simulation results for new buildings can be compared.
In this thesis we will consider the measured climate data from the TRY for De Bilt. Related quantities such as the sky radiant temperature or the sky radiance distribution, which can be estimated on the basis of these data without knowledge of the building under study or its direct environment, will also be considered as pertaining to the scenario (see also Section 2.3.6).

The part of the scenario concerning the operation of the building specifies issues such as internal heat gains from people, equipment and lighting in the spaces as a function of time, and the control of e.g. solar shadings, windows and internal doors. It is one of the main tasks in the preparation of the simulation to tune the specification of this part of the scenario to the intended use of the building (in close consultation with the client). For standard buildings such as offices, guidelines can be found in e.g. ISSO (1994). Another effort to assist the selection of appropriate scenario elements by means of PAM's (Performance Assessment Method) can be found in Wijsman (1994).

Simulation

Most environments for building modeling also offer simulation functionality. We will not discuss the specifics of this process. For an exposé on this matter see e.g. Sahlin (1996).

In the following sections the physical models of the relevant subsystems are addressed. First the subsystem 'building space' is covered, followed by the subsystem 'external sunblind'. Subsequently, Section 2.3.4 is dedicated to the modeling of ventilation flows through the office spaces. In Section 2.3.5 physical considerations are given for the assembly of the subsystems into a building model. Then, Section 2.3.6 discusses the

[3] The actual period is 27 April 1964 – 27 April 1965.

quantification of model parameters and Section 2.3.7 concludes with a brief discussion on the simulation tools that have been used to build and implement the models for this study.

2.3.2 Building space

Figure 2.6 shows a schematic view of the office space under study. The position of the external sunblind below the cantilever window is clearly marked.

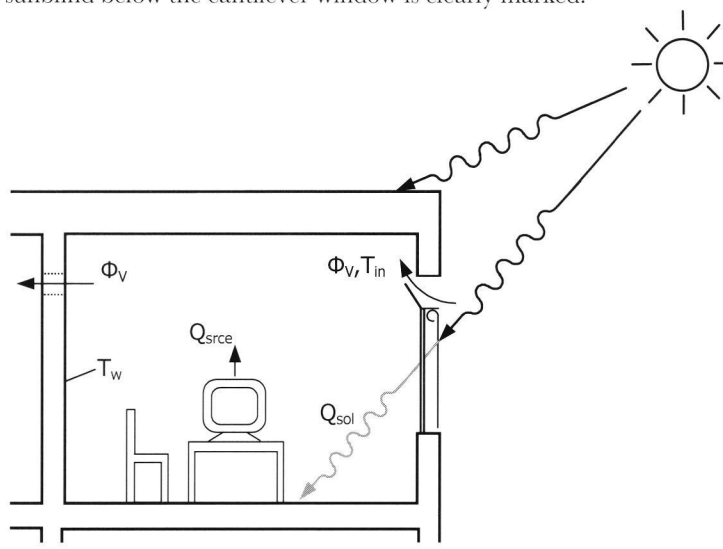

Figure 2.6 Schematic view of the office space with several of the variables acting in the model.

The subsystem 'building space' itself can further be subdivided into two (types of) components, i.e. the walls[4] and the volume they enclose. These subsystems will be discussed in the next subsections.

Volume enclosed by the walls

To assess the temperature in the enclosed volume, we assume that the air in the space is perfectly mixed. Under that assumption the uniform air temperature T_{air} can be assessed from the heat balance equation for the subsystem, which is given by (2.1).

$$C\frac{\partial}{\partial t}T_{air} = \rho\Phi_V c_p (T_{in} - T_{air}) + \\ + \sum_{j=1}^{N} \alpha_{c_{\text{int}},j}\left(T_{w_{\text{int}},j} - T_{air}\right)A_j + \\ + Q_{sol,c} + Q_{srce,c} \tag{2.1}$$

[4] The term *wall* in this thesis refers to any part of the enclosure of the space including floor and ceiling.

where

C	total heat capacity of the air and (a part of) the furniture
T_{air}	indoor air temperature
ρ, c_p	density and specific heat of air
Φ_V	air volume flow rate through the space
T_{in}	temperature of the incoming air
$\alpha_{c_{int},j}$	convective heat transfer coefficient at the internal surface of wall component j
$T_{w_{int},j}$	internal surface temperature of wall component j
A_j	area of wall component j
N	the number of wall components in the enclosure
$Q_{sol,c}$	convective part of solar gain
$Q_{srce,c}$	convective part of internal heat production by people lighting and equipment

The term on the left-hand side is the heat accumulation in the subsystem. As it is generally much smaller than the individual terms at the right hand side, it is often omitted in which case (2.1) becomes a stationary heat balance.
The first term on the right hand side (rhs) models the heat flow into the system by a single input single output flow scheme as in the current case. The total heat flow into the space by convective heat exchange with the space enclosure is represented by the second term. This enclosure is considered as consisting of N wall components, each with a uniform temperature field in the plane of the component. Term 3 in (2.1) is the heat, which is gained from absorption of solar radiation (by furniture) in the space, while the rhs closes with the (convectively emitted) sensible heat from internal sources, such as people, lighting and equipment.

Wall components

As mentioned in the previous subsection, the temperature field in each of the N wall components is assumed to be uniform in the plane of the component. In the direction normal to this plane the field T_w is described by the 1-dimensional Fourier-equation:

$$\frac{\partial}{\partial t}\rho_w c_w T_w = -\frac{\partial}{\partial x}\left(\lambda_w \frac{\partial T_w}{\partial x}\right) \tag{2.2}$$

where ρ_w, c_w and λ_w, the density, specific heat and conductivity of the wall component respectively, are commonly a function of x. If the wall component contains an air layer (e.g. in a cavity wall or a multiple glazed window) the heat transport at either side of the layer is in principle modeled by (2.2), while the air layer itself is simply modeled as a heat resistance:

$$q_{air} = \alpha_{tot}\,\Delta T \tag{2.3}$$

where

q_{air}	heat flux through the air layer
ΔT	temperature difference over the layer
α_{tot}	total heat transfer coefficient of the layer

Equations (2.1) through (2.3) form the basis of the thermal model for the space. Solution of these equations for $T_w(x)$ in each of the wall components and T_{air} (i.e. the *state* variables) requires additional specification of the boundary conditions for (2.2) and initial conditions for both (2.1) and (2.2).
For common buildings the effect of the initial conditions vanishes after a simulation period of one to two weeks. Hence, arbitrary initial conditions can be used if the simulated time span starts at least two weeks ahead of the period of interest.

The boundary conditions for (2.2) may differ from surface to surface. At the internal surface of a wall component j, i.e. the surface facing the space under study, the boundary condition for (2.2) is formulated as:

$$-\lambda_w \left.\frac{\partial T_{w,j}}{\partial n}\right|_{int} = \alpha_{c_{int},j}\left(T_{air} - T_{w_{int},j}\right) + q_{sol,r,j} + q_{srce,r,j} + \sum_{k,k\neq j} q_{r,jk} \qquad (2.4)$$

where

n	outward surface normal
$q_{sol,r,j}$	solar heat flux, absorbed at internal surface of wall component j
$q_{srce,r,j}$	radiant heat fluxes from heat sources absorbed at int. surface of component j
$q_{r,jk}$	net radiant heat flux from surface of component k irradiating this surface j

The first term on the rhs is the convective heat flux from the wall component to the air, which also occurs in (2.1). The absorption of solar radiation entering the space, absorption of radiant heat fluxes from internal sources and radiant heat exchange between wall components are accounted for in the second, third and fourth term respectively.

At the external surface of a wall component two possibilities are considered. The surface is either a part of the building envelope or it borders another space in the building.

In the first case, the boundary condition for the heat conduction in wall component j is modeled analogously[5] to (2.4) as:

$$-\lambda_w \left.\frac{\partial T_{w,j}}{\partial n}\right|_{ext} = \alpha_{c_{ext},j}\left(T_a - T_{w_{ext},j}\right) + q_{sol,r,j} + q_{env,r,j} \qquad (2.5)$$

where

$\alpha_{c_{ext},j}$	convective heat transfer coefficient at the external surface j
T_a	outdoor air temperature
$q_{sol,r,j}$	solar heat flux absorbed at external surface of wall component j
$q_{env,r,j}$	radiant heat exchange of surface j with the external environment.

[5] Note that despite the similarity in their notation, the second terms in the rhs of (2.4) and (2.5) do not relate to the same quantities.

In the second case, the boundary condition connects the sub-model of the space to the model of the rest of the building. Hence the choice for this boundary condition depends on the way the rest of the building is modeled.

2.3.3 External sunblind

Although an external sunblind reduces the amount of solar irradiation on the window, it also creates a sheltered climate in the space between the blind and the window. Due to this shelter effect the temperature of the external windowpane will generally be higher (and thus the effectiveness of the sunblind lower) than what would be expected on the basis of the sunblind's optical characteristics alone.

A common, but crude approach to account for this reduced efficiency is to apply a *solar factor* instead of the optical transmittance as a reduction factor for the incident solar irradiance. Estimates of this factor for several types of window systems (sunblind + window) can be found in e.g. ISSO (1975, 1994). In this thesis, however, a more explicit approach has been used, in which the sunblind and the cavity it forms in combination with the window, are treated as a separate component. This approach connects well to the modeling scheme presented in the previous sections.

The sunblind and the window form a ventilated cavity. Figure 2.7 shows a schematic view of this cavity.

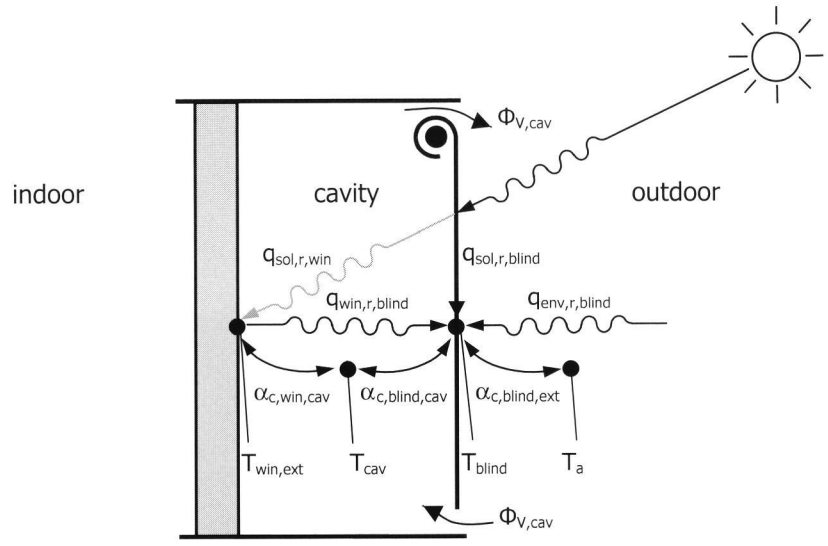

Figure 2.7 Schematic view of the cavity between external window pane and sunblind. The main parameters and variables in the thermal model are indicated. The horizontal dimensions of the cavity are exaggerated for illustrative purpose.

As soon as the sunblind is in operation (for details on the operation of the sunblind see the scenario specification in Appendix A.2), the external boundary condition for the temperature field in the external windowpane becomes slightly different from (2.5):

$$-\lambda_w \left.\frac{\partial T_{win}}{\partial n}\right|_{ext} = \alpha_{c,cav}\left(T_{cav} - T_{win,ext}\right) + q_{sol,r,win} + q_{blind,r,win} \tag{2.6}$$

where

T_{win}	the temperature field in the windowpane
$\alpha_{c,win,cav}$	the convective heat transfer coefficient at the window surface in the cavity
T_{cav}	the air temperature in the cavity
$q_{sol,r,win}$	the (reduced) absorbed solar irradiance at the window
$q_{blind,r,win}$	the radiant heat flux from the sunblind to the window pane

To close the model, two additional expressions are used, i.e. simplified heat balances for the air temperature in the cavity and the temperature of the sunblind. In these equations the assumptions are used that the heat capacity of the sunblind is negligible, as is the temperature difference between inside and outside of the blind.

$$0 = \alpha_{c,win,cav}\left(T_{win,ext} - T_{cav}\right)A_{win} + \alpha_{c,blind,cav}\left(T_{blind} - T_{cav}\right)A_{win} + \rho c \Phi_{V,cav}\left(T_a - T_{cav}\right) \tag{2.7}$$

$$0 = \alpha_{c,blind,cav}\left(T_{cav} - T_{blind}\right) + \alpha_{c,blind,ext}\left(T_a - T_{blind}\right) + q_{sol,r,blind} + q_{env,r,blind} + q_{win,r,blind} \tag{2.8}$$

where

$\alpha_{c,blind,cav}$	the convective heat transfer coefficient at the blind in the cavity
$\alpha_{c,blind,ext}$	the convective heat transfer coefficient at exterior of the blind
T_{blind}	the temperature of the sunblind
$\Phi_{V,cav}$	ventilation rate of the cavity with ambient air
$q_{sol,r,blind}$	solar heat flux absorbed at the blind
$q_{env,r,blind}$	the radiant heat flux from the building environment to the blind
$q_{win,r,blind}$	the radiant heat flux from the window pane to the sunblind

2.3.4 Ventilation modeling

Introduction

As discussed in section 2.3.1, the simulation approach is chosen such that the scenario specifies the experimental conditions the building is considered to be exposed to, whereas the model captures the response of the building[6] to these conditions. In practice, this distinction is commonly not preserved in the quantification of the airflow through the building. Indeed, airflow rates are often specified as model parameters with

[6] Strictly speaking, the model covers a system, which is substantially larger than the building itself. To connect the building to the (climate) data available in the scenario, part of the building environment is included in the model. Despite this, we will continue to use the term *building* model.

a more or less fixed value throughout the simulation (see e.g. ISSO, 1994, Wapenaar, 1992).

In a naturally ventilated building, however, airflows are either wind or buoyancy driven and can possibly be controlled by the occupants via the operation of windows. A consistent approach would require a separate modeling of the physical mechanisms driving the airflows on the one hand and the control of these flows by the occupants or other control systems on the other.
Moreover, current practice to specify (almost) stationary values for the airflow rate is in contrast with the dynamic character of the rest of the model. For evaluations of a building with respect to thermal comfort a proper representation of the dynamics in the temperature field is especially important (see Section 2.4). On these grounds it was decided in this study to model the ventilation in more detail.

In general, airflow through a building is driven by a combination of wind, thermal buoyancy and mechanically induced pressures. In the case under study we do not consider mechanical ventilation. Thermally induced pressures (stack effects) only occur when openings are located at different levels or if these openings have considerable vertical dimensions. In this case the airflows at different floors are fully separated by the airtight fire doors at both ends of the corridors. Within each floor all openings are located at the same level when the internal doors are closed, which is indeed assumed in the scenario. Moreover, the vertical dimensions of the openings are small. As a result, a stack effect need not be considered. By exclusion of thermally driven flow and mechanical ventilation, the only remaining driving force is wind.

Airflow model

To model the hourly averaged flow rate through the offices under study, a basic network approach has been used (e.g. Feustel, 1990, Liddament 1986). The network[7] is shown in Figure 2.8. The only driving mechanism is wind.

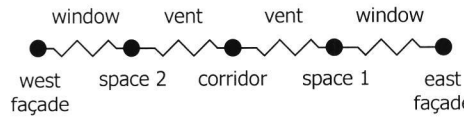

Figure 2.8 Network used to assess the airflow rate through the office space under study.

The spaces (zones) are characterized by pressure 'nodes', whereas the orifices, i.e. windows and vents, in the façades and partition walls are shown as flow 'resistances'. In addition to the zonal nodes two external nodes are indicated. The pressures in these

[7] This network is based on the assumption in Section 2.3.2 that no airflow occurs through the margins of the system, i.e. the building section in Figure 2.4. Even under identical operation of all offices, this will not generally be the case as for several wind angles significant horizontal pressure gradients will occur over the building facades. To keep the model transparent, the network as shown in Figure 2.8 will be used nonetheless.

nodes are the wind induced pressures on the west and east façades at the location of the windows. Leakage flows through cracks and joints are ignored.

The air mass flow Φ_j through an orifice j (j = 1,…,4) is modeled as a function of the pressure difference Δp_j over the orifice by the semi-empirical relation (Liddament, 1986, ASHRAE, 1993):

$$\Phi_j = C_{d,j} A_j \sqrt{2\rho \Delta p_j} \tag{2.9}$$

with ρ the density of air, A_j the area of the orifice, and $C_{d,j}$ the discharge coefficient.

By requesting that the net mass flow into each space (node) equals zero and that the sum of the pressure differences over all orifices (resistances) equals the total wind pressure drop between the west and east façade, the air mass flow through the spaces can be assessed.

Wind induced pressure differences

As discussed in Section 2.3.1, the climatic data in the scenario are based on measurements at a meteorological station. Commonly used climatic data sets contain information on the hourly averaged values of wind direction and wind speed. These data are measured at 10 m above ground level and converted to *potential* values by correcting them for imperfections at the meteorological observation site (Wieringa and Rijkoort, 1983).

The relation between the pressure p on a certain position $\underline{x}$ at the building envelope and the potential wind speed at the meteorological station is modeled by:

$$p(\underline{x}) = \tfrac{1}{2}\rho C_p(\underline{x})(\gamma U_{pot})^2 \tag{2.10}$$

where

ρ	density of air
U_{pot}	potential wind speed, i.e. (hourly averaged) wind speed measured at an ideal meteorological station at 10 m above ground level
$C_p(\underline{x})$	wind pressure coefficient or shape coefficient for position $\underline{x}$ at building envelope
γ	wind reduction (or amplification) factor

This equation expresses that the pressures at the building envelope are proportional to the dynamic wind pressure at the meteorological observation site (at 10 m height), i.e. $\frac{1}{2}\rho U^2_{pot}$. The wind reduction factor γ captures the effect of the far field, whereas the pressure coefficient covers the effects of the near-field and the building geometry (see Figure 2.9).

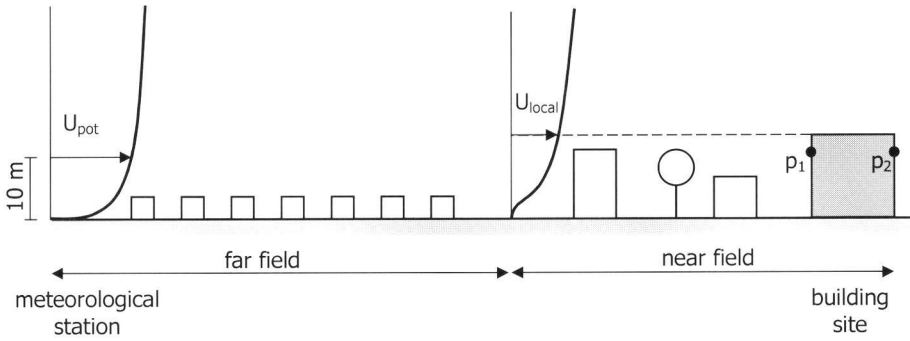

Figure 2.9 From a potential wind speed, measured at the meteorological station to the pressure distribution over the building. The figure schematically shows the mean wind velocity profile at the meteorological observation station with the potential wind speed and the local profile with the local wind speed at building ridge height, a common reference height for wind pressure coefficients.

The near field is the area around the building where individual obstacles of the scale of a building affect the pressure distribution. In wind tunnel experiments this area is modeled in detail and usually starts 300 – 1000 m upstream of the building (see e.g. ASCE, 1999). Upstream of the near field the effect of obstacles is parameterized in terms of a surface roughness (see e.g. Wieringa, 1993).

2.3.5 From component models to building model

In principle it is possible to describe the temperature field in all spaces in the building by a set of equations of the type (2.1) through (2.8) with additional expressions for the ventilation flow from Section 2.3.4. The boundary conditions at all interior wall surfaces are then of the form of (2.4). In practical applications this approach requires much time to build the model and to perform the simulations. The model can commonly be reduced without much loss of accuracy by taking account of symmetry.

As, according to the scenario, the space under study and the spaces left and right of it are operated identically, it is natural to assume that the temperature fields in those spaces will be similar. Hence we only introduce a small error if we apply the internal surface temperature of each component in the left partition wall as the boundary condition at the external surface of the corresponding component in the right partition wall. This approach is used here.
The space under study is located at the top floor (see Section 2.2), which means that even when identically operated, the temperature fields in the space under study and the space directly below it will not be identical. Nevertheless, to keep the model transparent we will assume that the temperature of the ceiling in the space under study is identical to the temperature of the ceiling in the space underneath. Application of this approach to the current case leads to a building section of three spaces that is modeled in detail with equations of the type (2.1) through (2.8) as shown in Figure 2.4.

Part of the system boundaries of the middle space, a part of the corridor, do not coincide with physical walls. At these boundaries, adiabatic conditions are assumed, i.e. both airflow and heat flow equal to zero.

The following sections elaborate the terms in (2.1) through (2.8) and discuss how they can be fleshed out from the design specifications and the scenario.

2.3.6 Quantification of model parameters

In the previous section the outline of the thermal model for a building space was laid out. The current section aims to clarify how this model can be given concrete form on the basis of given design specifications and scenario. This explanation subsequently addresses each of the terms in equations (2.1) through (2.10).

Space ventilation heat flow

Figure 2.5 shows that the space under study only has two vents in opposite walls of the space. Both infiltration through cracks and joints and single sided ventilation are considered to be insignificant. Hence, the first term in (2.1) fully covers the net heat flow carried into the space by an airflow rate Φ_V through the space. Considering c_p and ρ as known constants, quantification of this term requires assessment of Φ_V and T_{in}.

If the air flows in from outside the building, its temperature T_{in} is taken equal to the outdoor ambient temperature, which is specified in the scenario. Otherwise T_{in} is assigned the air temperature of another space in the system, which is a state variable in the model.

The air flow rate Φ_V can be calculated from equations (2.9) and (2.10). The potential wind speed is retrieved from the scenario. The areas of the window openings is found in the design specifications. This leaves the discharge coefficients, the pressure coefficients and the wind reduction factor to be quantified.

Discharge coefficient

The discharge coefficients $C_{d,j}$ mainly depend on the shape of the orifice, the direction of the flow and the degree of turbulence in the flow. For suitable values see e.g. Boulard and Baille (1995).

Wind pressure coefficients

Pressure coefficients relate the pressures on the building envelope to the dynamic (local) wind pressure at a given reference level. A common reference level is ridge height of the building of interest. In ventilation studies, mean (i.e. time-averaged) values of the pressure coefficients are generally used. The value of these coefficients depends on the position on the building envelope, the building geometry, the wind angle, the near field geometry and the shape of the wind profile.

Several tools have been developed to assist the assessment of mean wind pressure coefficients on the basis of existing experimental data from prior wind tunnel studies and

full-scale measurements. Examples of such tools can be found in e.g. Allen (1984), Liddament (1986), Swami and Chandra (1988), Grosso (1992, 1995), Walker and Wilson (1996) and Knoll, Phaff and De Gids (1995, 1996).

Wind reduction factor
The wind reduction factor is the ratio between the local mean wind speed (at a given reference height) and the potential wind speed reported at the meteorological station. The modeling of this factor belongs to the domain of boundary layer meteorology. Methods to assess it can be found in e.g. Wieringa and Rijkoort (1983), Bottema (1993), Geurts (1997) and Liddament (1986).

Internal convective heat transfer

The second terms in both (2.1) and (2.4) model convective heat transfer from the surface of the enclosure to the air in the space. All temperatures in these terms are state variables. Reviews of literature on internal heat transfer coefficients can be found in e.g. Halcrow (1987), Pernot (1989), Khalifa (1989, 1990) and Awbi and Hatton (1999).

Solar heat loads

Heat loads due to the absorption of solar radiation are represented by term 3 in (2.1), term 2 in (2.4), term 2 in (2.5) and term 3 in (2.8). These three terms can be quantified from information about the solar irradiation specified in the scenario. This information usually consists of the hourly averaged values of the direct irradiation on a normal plane and the diffuse irradiation on a horizontal plane. With models for the solar position, the radiance distribution over the sky and the effective reflection coefficient of the surroundings (albedo), the total solar irradiation on each part of the building envelope can be calculated from these data. Models for solar position and sky radiance distribution can be found in e.g. Velds (1992) and Gonçalves (1989).

Given the total irradiation distribution over the building envelope, the solar heat flux that is absorbed only depends on the solar absorptance. Tables with solar absorptance values for various materials (and surface conditions) can be found in e.g. ASHRAE (1993).

The solar radiant flux entering the space can also be calculated from this total irradiation for given geometry and optical characteristics of the window and sunblinds. The issue how the absorption of this flux is distributed over the furniture (convective fraction) and the wall surfaces (radiant fraction) is generally addressed pragmatically. A fixed fraction is attributed to the furniture and the remaining part is evenly distributed over an appropriate part of the space enclosure.

Loads from internal heat sources

Loads from heat sources in the space like occupants, lighting and equipment enter the model as inputs through term 4 in (2.1) (convective part) and term 3 in (2.4) (radiant part). The scenario commonly specifies the total internal heat load. To obtain separate

values for the radiant and the convective parts, ASHRAE (1993) and ISSO (1994) tabulate ratios between those parts for a range of heat sources.

Radiant heat exchange between internal wall surfaces

Term 4 in (2.4) represents the radiant heat exchange between internal wall surfaces. Under the assumption that these surfaces are gray radiators, the net radiant heat exchange between them is completely defined by the surface temperatures, emittances and mutual view factors. The surface temperatures are state variables in the model. Emittances for a variety of materials and surface conditions can be found in handbooks (e.g. ASHRAE, 1993, Siegel and Howell, 1981). As the geometry of the space is known, all necessary view factors in an empty space can be assessed by straightforward calculation. The effect of furniture is neglected.

External convective heat transfer

In some approaches both convective and radiant heat transfer from the building envelope are modeled by an expression similar to the first term in (2.5), but with an overall heat transfer coefficient. In this study, convective and radiant components are modeled separately, consistent with the approach at internal surfaces.

Convective heat transfer from the building envelope to the ambient (outdoor) air is expressed by the first term in (2.5). If the sunblinds are up, the convective heat transfer at the window surface is also covered by (2.5). Otherwise this heat transfer takes place at the sunblind as described by the second term in (2.8). The surface temperatures in these equations are state variables in the model. The outdoor ambient temperature is either taken from the scenario either directly or after correction for the effects of the building environment (urban heat islands, see e.g. Plate (1995), Kimani (1998)). Reviews of the literature on external heat transfer coefficients can be found in e.g. Allen (1987) and Strachan and Martin (1989).

The convective heat transfer in the cavity between window and sunblind is governed by the rate of ventilation with ambient air and the convective heat transfer coefficients at the surfaces of window and blind. In ISSO (1991) guidelines for these values can be found.

External radiant heat transfer

Term 3 in (2.5) and term 4 in (2.8) capture the net radiant heat exchange between the building (envelope) and its environment. As in the building simulation tool ESP-r (ESRU, 1995b), three different emitters are distinguished in this environment, i.e. the sky, the surrounding buildings and the ground. Both the building envelope and the environmental emitters are considered as gray radiators. Hence, the radiant heat exchange between an emitter and a wall component can be expressed in terms of their temperatures, emittances and a mutual viewfactor. The viewfactor can be calculated from the available geometrical (design) information, emittances are tabulated in handbooks and the temperature of the wall component is the state variable of interest. This leaves the temperatures of the environmental emitters to be specified.

Phenomenological models for the radiant sky temperature are reported in the literature (e.g. Stanzel, 1989). These models relate the radiant sky temperature to the outdoor air

temperature, the cloud cover factor and the humidity, which are available from the scenario.
Furthermore, it is assumed that the façades of surrounding buildings have the same average surface temperature as the façades of the building under study with the same orientation.
Finally, the ground is modeled as a horizontal wall of 1.2 m thick. Temperatures at 1.2 m depth are assumed to be known from the scenario, as are the material properties of the various ground layers. Heat conduction in the ground is modeled according to (2.2) with (2.5) as surface boundary condition.
If the sunblind is activated, there will be radiant heat exchange between the window surface and the sunblind. In modeling this heat transport, these surfaces are considered to be gray radiators with a mutual view factor of 1.

Heat transfer through air layer

The double-glazed window contains an air-filled cavity. Suitable values for the total heat transfer coefficient α_{tot} (see equation (2.3) can be found in e.g. the built-in library with window properties in ESP-r (ESRU, 1995b).

2.3.7 Implementation and verification

The previous sections outline the physical building model, which has been used in this study. To carry out actual simulations with this model, it had to be implemented as a computer model. As mentioned in Chapter 1 and in Section 2.3.1, several commercially available tools exist that facilitate this implementation. In this study, two of these tools for thermal building modeling and simulation have been used.
The first tool is BFEP (Augenbroe, 1986). BFEP is a toolbox rather than a program. Its inherent flexibility and versatility enable the development and use of non-standard model components, and the construction of a computer model that is suited for sample-based sensitivity and uncertainty analyses. Hence, all uncertainty and sensitivity analyses reported in this thesis were done with BFEP.
The second tool is ESP-r (ESRU, 1995a). ESP-r is a closed building simulation program. It has been involved in a substantial validation study (Jensen, 1990, 1994). This simulation program has been used to verify the BFEP-models by comparing the outputs (temperature traces) for a range of base-cases. It has not been deployed in the sensitivity and uncertainty analyses.

2.4 Performance criteria for thermal comfort

2.4.1 Introduction

The previous sections focused on the simulation of the thermal conditions in the building and more particularly on the indoor climate in the space under study. The output of this simulation serves as input to assessment of building performance with respect to the indoor climate.

As Figure 2.1 shows, performance assessment requires two elements:

- a comfort model to estimate occupant comfort ratings
- a definition of the performance indicator to carry out the post-processing

Both issues are addressed in the following sections. Before going into detail, however, a brief outline is given here.

Basically, two definitions of performance indicators for thermal comfort are encountered in The Netherlands. They both start from the notion that an indoor climate, which is causes dissatisfaction among 10% of the people or more, is unacceptable. The indicator according to the first definition is simply the relative fraction of time that the indoor climate is unacceptable. In the other definition the performance indicator also counts the number of hours with an unacceptable climate, but in the summation each hour is attributed a weight that is proportional to the percentage of people that would be dissatisfied with the climate in that hour. This approach incorporates the idea that the indoor climate deteriorates as more people would consider it unacceptable. Performance indicators of this type are commonly addressed as 'weighed' indicators. A more comprehensive discussion on these performance indicators can be found in 2.4.3.

In the comfort models, used to relate occupant (dis)satisfaction to the actual indoor climate, two main schools of thought can be identified. Loosely stated, the 'static' school uses models in which the thermal preferences of the occupants are considered to be fixed. In the 'adaptive' school, on the other hand, thermal preferences are modeled as a function of contextual factors and recent thermal history. The two types of comfort models are more elaborately discussed in 2.4.2.

Table 2.1 shows a classification of Dutch performance indicators along these two dimensions, i.e. 'weighed' or not, and based on a static or an adaptive comfort model.

Table 2.1 Classification of performance indicators for thermal comfort.

		weighed	
		no	yes
comfort model	static	TO	GTO
	adaptive	(TO*)	-

Both the TO –indicator (Dutch abbreviation for temperature excess) and the GTO-indicator (Dutch abbreviation for weighed temperature excess) are commonly used in The Netherlands (see e.g. De Wit et al., 1999b). In accordance with current international standards (ISO-7730, 1994, ASHRAE 55/55a, 1992) these indicators are based on static comfort models. However, growing discomfort with static models among practicing engineers, especially in connection with naturally ventilated buildings, has caused an upturn of the interest in adaptive comfort models (De Wit et al., 1999b). Hence an adaptive version of the TO-indicator, denoted here by TO*, is presented in this thesis as a possible alternative to the TO. An adaptive alternative of the GTO

cannot be given, as the output of the current adaptive comfort models do not enable calculation of the required weights.

In Dutch design practice, the TO and GTO are commonly assessed over a period of 1 year on the basis of representative outdoor climate data (see Sections 2.2 and 2.3.1). In that context, the TO (and TO*) performance indicator are simply expressed as the number of hours that more than 10% of the people would be dissatisfied. A common target value for the TO in offices (related to warm discomfort only) is 100 hours, based on 2000 office hours per year (RGD, 1979).
The dimension of the GTO is commonly referred to as 'weigh-hours'. A frequently used target value is 150 weigh-hours (Brouwers en Van der Linden, 1989), again related to a simulation period of 1 year with the representative outdoor climate data.

This thesis focuses on the TO and TO* indicators. The GTO-indicator is not considered. First, the TO-indicator is more transparent in communication between various actors in the design process. It's meaning can be understood without detailed knowledge of how it is calculated. Moreover, the question of whether performance control on the basis of GTO leads to better buildings than control on the basis of TO is still a subject of debate (Schalkoort, 1994, De Wit et al., 1999b).

The next two subsections address, respectively, the comfort models and the performance indicators.

2.4.2 Thermal comfort models

Introduction

Various global comfort models can be found in the literature (e.g. Fanger, 1970, Gagge et al., 1971, Humphreys, 1978, Auliciems, 1981, 1989, De Dear and Brager, 1998). They model the response distribution, which would be obtained if a large sample of people are exposed[8] to a certain thermal environment and asked to rate their sensations on a given scale. An example of such a scale is shown in Figure 2.10.

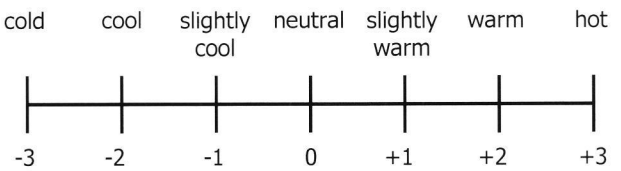

Figure 2.10 The 7-point ASHRAE sensation scale.

[8] Several of these models relate to long exposure times and do not account for climatic transients. Moreover, most of them are based on global climatic conditions and do not account for local effects such as e.g. draught at head level or cold feet.

The model output commonly consists of only a few characteristics of the response distribution, e.g. the mean response and/or the fraction of the responses that will exceed a certain critical value.

Thermal comfort models can be subdivided in *static* and an *adaptive* types. The static models, also referred to as 'heat-balance models', consider the occupants as passive recipients with static preferences, which are entirely driven by autonomic physical and physiological mechanisms. The adaptive models on the other hand, acknowledge the fact that psychological factors such as expectation based on recent experience may affect people's preferences. This allows them to adapt to a certain extent to the ruling climatic conditions.

Current international standards (ISO-7730, 1994, ASHRAE 55/55a, 1992) are based on static comfort models. The RGD, a Dutch government building agency, has developed models, which are compliant with ISO-7730. However, growing discomfort with static models among practicing engineers, especially in connection with naturally ventilated buildings, has caused an upturn of the interest in adaptive comfort models (De Wit et al., 1999b). Hence, a representative of this class of models has been used in this study. The next section give a brief exposé on static comfort models, whereas the subsequent section is dedicated to adaptive models.

Static approach

The most commonly used comfort performance criterion in The Netherlands, which has been proposed by a Dutch government building agency, the RGD (RGD, 1979, Brouwers and Van der Linden, 1989) is based on ISO-7730. The ISO-standard incorporates the comfort model developed by Fanger (1970), which is a representative of the class of 'static' comfort models. This model requires 6 input variables, i.e. air temperature, (mean) radiant temperature[9], (relative) humidity, air velocity, mean thermal resistance of the clothing and metabolic rate. On the basis of this input, a physical/physiological state variable is calculated, which Fanger refers to as the 'thermal load'. The response distribution is modeled in terms of this thermal load[10].

Fanger's relation between responses and thermal load is based on the results of climate chamber experiments with approximately 1300 subjects. For the various (stationary) thermal loads which these subjects were exposed to, they were asked to rate their thermal sensation on the ASHRAE-scale, which distinguishes 7 levels from 'cold' through 'neutral' to 'hot' (see Figure 2.10).

On the basis of the response distributions from these experiments, Fanger derived a relation between the thermal load and the mean response or mean 'vote'. He called the output of this relation the 'Predicted Mean Vote' or PMV.

---

[9] The mean radiant temperature is the uniform temperature of an imaginary black enclosure in which the radiant heat transfer from the human body equals the radiant heat transfer in the actual nonuniform enclosure (ASHRAE, 1993).

[10] In fact, the response distribution is also a function of the metabolism (see Fanger, 1970)

Moreover, he deduced an expression for the fraction of the subjects stating a vote with 2 or more in absolute value on the ASHRAE-scale. As he had concluded from earlier research (Gagge et al., 1967) that these vote indicate dissatisfaction, he denoted the result of this expression the 'Predicted Percentage Dissatisfied' or PPD.
In his experiments, Fanger found that the factors outdoor climate, sex, body build and age did not significantly change the relation between thermal load and the PMV and PPD. Hence, he concluded that thermal preference is a fixed, static function of the thermal load.

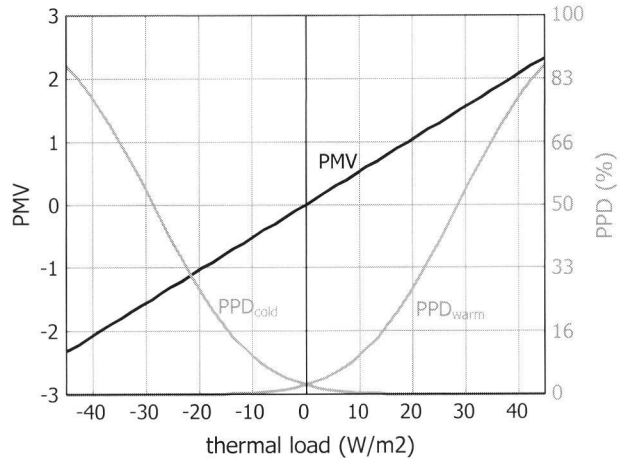

Figure 2.11 Relation between thermal load, PMV and PPD (at an office-level metabolism of 70 W/m²) according to the comfort model by Fanger (1970).

The two relations for PMV and PPD as a function of the thermal load and the physical/physiological model for this load constitute the Fanger-model in its basic form. Despite extensive criticism (see e.g. Schalkoort, 1994) it is one of the most widely used thermal comfort models.

One of the problems with the application of this model in a building simulation context is the input data it requires. Building simulation only provides the requested temperatures, which leaves air velocity, humidity, clothing level and metabolism to be specified from other sources. The latter two variables would most naturally be specified in the scenario along with the other occupancy-related variables. The first two environmental variables however, are part of the building's response to the conditions in the scenario and should, in a consistent approach, be simulated along with the temperature field.
For lack of good models for these variables, the performance indicators proposed by the RGD are based on default values for these variables, which are kept fixed throughout the simulated period (see 'Comparison of static and adaptive approaches'). The Fanger-model together with these defaults constitutes the static thermal comfort model that we will refer to as the RGD-model.

Adaptive approach

Examples of adaptive comfort models can be found in e.g. Humphreys (1978), Auliciems (1981) and De Dear and Brager (1998). Here we will focus on the most recently developed adaptive model by De Dear and Brager.

Adaptive comfort models start from the notion that thermal preferences are not static, but depend on contextual factors and recent thermal history. Research by Auliciems (1981, 1989), De Dear (1994) and Nicol (1993) suggests that satisfaction with indoor climate results from matching the actual thermal conditions in a given context with the expectations of what the indoor climate should be like in that context. In other words, satisfaction occurs through appropriate adaptation to the indoor climatic environment.

Three forms of adaptation may be distinguished (Folk, 1981, Prosser, 1958, Clark and Edholm, 1985):

- behavioral
- physiological
- psychological

Behavioral adjustment refers to all modifications, which influence the heat and mass fluxes governing the body's heat balance. This form of adaptation falls outside the scope of the static models, as it predominantly affects the inputs of these models.

Physiological adjustment is defined by De Dear and Brager as 'all of the changes in the physiological responses, which result from exposure to thermal environmental factors and which lead to a gradual diminution in the strain induced by such exposure.' A review of the literature (Brager and De Dear, 1997) shows that this form of adaptation is not likely to be a significant factor for the moderate range of conditions found in most buildings.

Psychological adaptation refers to changes of thermal preferences in reaction to past experience and expectation. De Dear and Brager carried out a meta-analysis of well-documented field studies in more than 160 buildings. They concluded that a significant correlation exists between thermal preferences and the outdoor climatic conditions in the preceding month. Apparently, thermal preferences are not static, but indeed depend on recent experience. In buildings with a centralized HVAC system, with fairly constant indoor climatic conditions and limited adaptive opportunities, this correlation can fully be explained from behavioral adjustments. In naturally ventilated buildings, however, behavioral adaptation only partially explains the observed changes in preferences, which suggests a contribution of psychological adjustment. This is supported by the work of Paciuk (1990) among others.

On the basis of a statistical meta-analysis of the field studies, De Dear and Brager developed two different models; one for buildings with centralized HVAC and one for

naturally ventilated buildings. As a function of the mean outdoor effective temperature[11] over the preceding month, they predict (see Figure 2.12):

- The optimum operative temperature. This is the operative temperature[12], which will expectedly be accepted by the greatest possible number of people.
- Acceptability ranges. A first range captures the operative temperatures, which will be acceptable to 80% of the people or more, whereas temperatures in a second range will satisfy at least 90%.

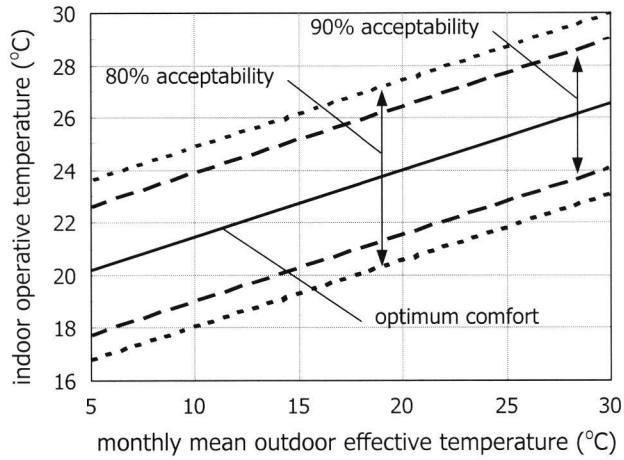

Figure 2.12 Acceptability ranges according to the adaptive model by De Dear and Brager (1998).

The information in Figure 2.12 provides a means of evaluating the acceptability of the indoor climate in naturally ventilated buildings in terms of the indoor operative temperature and the mean monthly outdoor effective temperature. The operative temperatures can readily be obtained from a building simulation, whereas all the information to calculate the outdoor effective temperature is available in the scenario.

Comparison of static and adaptive approaches

In the previous sections the main features of a static and an adaptive comfort model were discussed. In this section we will illustrate how these features express themselves in the context of building simulation. Figure 2.13 shows lines of equal acceptability for both the static RGD-model and the adaptive model for naturally ventilated buildings

[11] The effective temperature (ET*) is the (operative) temperature of an environment at 50% relative humidity that results in the same total heat loss from the skin as in the actual environment (ASHRAE, 1992). People at the same ET* value would be expected to have the same thermal sensation (see Gonzalez et al., 1978). The official ASHRAE algorithm for the ET*, which was used in the study by De Dear and Brager, is implemented in the ASHRAE RP-781 software package (Fountain and Huizenga, 1996).

[12] The operative temperature is the uniform temperature of an imaginary environment in which the heat transfer from the human body, both by radiation and convection, equals the total heat transfer in the actual nonuniform environment (NEN-ISO 7726, 1989). In this study, the operative temperature is approximated as the arithmetic mean of the (dry bulb) air temperature and the mean radiant temperature.

from De Dear and Brager. These lines are plotted as a function of time in the Test Reference Year (TRY, see Section 2.3.1) for De Bilt, The Netherlands.

To express the acceptability predicted by the static model in terms of operative temperature, it was assumed that air temperature and radiant temperature do not differ too much. Moreover, for the variables air velocity, relative humidity, clothing insulation and metabolism the respective default values of 0.1 m/s, 50%, 0.7 clo (0.11 m^2 K/W) and 1.2 met (70 W/m^2) were used (ISSO, 1994).

The neutral temperature (PMV = 0) according to the static model and the optimum comfort temperature from the adaptive model may be compared without the risk of overlooking semantic effects. Indeed, the research by De Dear and Brager (1998) shows that in naturally ventilated buildings there is no systematic deviation between thermal neutrality and optimum comfort or preferred temperature. Moreover, the margins of the 90%-acceptability ranges from the adaptive model can be interpreted as the analogon of those thermal conditions to which the static RGD-model attributes a PPD-value of 10%.

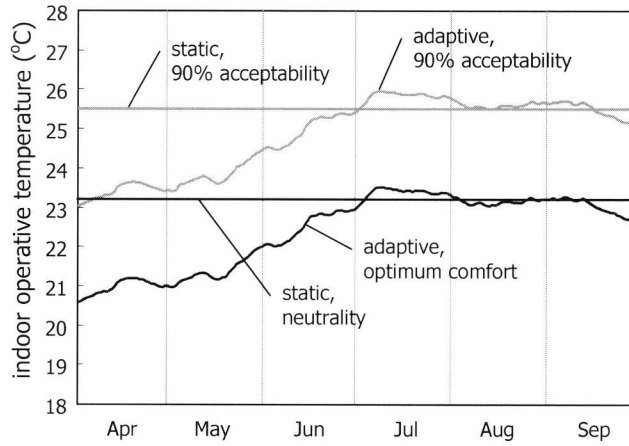

Figure 2.13 Iso-acceptability lines for the Test Reference Year in De Bilt according to the static RGD-model and the adaptive model from De Dear and Brager.

By definition, the preferences from the static model do not change with time, while the iso-acceptability lines according to the adaptive model show a preference for higher temperatures in summer. It is interesting that the interval between the neutral/optimum comfort temperature and the 90% acceptability line is almost identical for both models. Besides, the 90%-acceptability lines indicate that according to the adaptive model people will be slightly more tolerant to high temperatures in July, August and the first half of September (in this Test Reference Year) than predicted by the RGD-model. However, in the rest of the year the RGD-model conjectures significantly more tolerance.

2.4.3 Performance indicators

For office buildings, two types of performance indicators have been proposed by the Dutch Rijksgebouwendienst. These are the TO-indicator and the GTO-indicator, which are commonly used in The Netherlands (De Wit et al., 1999b). These indicators are based on the idea that an indoor climate in which less than 10% of the people would feel dissatisfied is acceptable. Conditions in which more people are uncomfortable should occur infrequently. Hence, the performance indicators are formulated as penalty functions on the frequency (fraction of time) that these conditions occur[13]. The threshold level of 10% is not arbitrarily chosen, but rests on a reference in appendix D of ISO-7730 (1994) that 'it is recommended as acceptable that the PPD be lower than 10%', where the PPD is the percentage dissatisfied as predicted by Fanger's comfort model.

As already discussed in Section 2.4.1, only the TO-indicator will be used in this study. This indicator is simply the number of (office) hours per year that the critical PPD-level is exceeded (RGD, 1979). With the RGD-defaults for clothing level, metabolism, air humidity and air velocity, and the assumption that air temperature and mean radiant temperature do not differ too much, the critical PPD-value can be converted to a critical operative temperature of 25.5 °C with Fanger's comfort model. To this temperature threshold the indicator owes its name: TO (Temperatuur Overschrijding, Dutch for temperature exceeding). A common target value is 100 hours, related to a simulation period of 1 year with the representative outdoor climate data mentioned in Section 2.3.1.
The TO-indicator is often used in combination with a second one of the same type, i.e. the number of hours that the (operative) temperature exceeds the level of 28°C.

When we return to the original idea that was proposed in the RGD-guideline, but quantify the percentage of dissatisfied on the basis of the adaptive model and not in terms of Fanger's PPD, we find an adaptive analogon for the TO-indicator. In this analogon, the fixed threshold of 25.5 °C is replaced by a critical temperature, which is a function of the outdoor effective temperature (see Figure 2.13). We will refer to this indicator as the TO*.

2.5 Discussion

The current chapter describes an approach, in which the indoor climate in the building is simulated under an a-priori fixed scenario. This scenario includes the specification of occupant behavior. Subsequently, a comfort model is used to predict how people would rate this indoor climate. Hence, the indoor climate in the building is assumed to be unaffected by the sensations of the occupants. For a centrally conditioned building, this may be a justifiable approach, but for a building with adaptive opportunities such as operable windows and sunblinds, this seems unrealistic.

[13] These indicators would more accurately be referred to as non-performance indicators, but this subtlety is ignored in this thesis.

The adaptive comfort model (De Dear and Brager, 1998) acknowledges behavioral adjustments of e.g. clothing level and metabolism in response to the indoor climate, and takes them into account. If the behavioral adjustments extend to operating windows and sunblinds, though, these cannot be accounted for in the comfort model alone. Indeed, these adjustments affect the indoor climate itself.
As none of the currently available comfort models provide insight into the behavioral aspects of occupant response, the occupant control over the building in response to the indoor climate cannot be modeled. Further research on this issue could contribute to more adequate performance evaluations and enable an evaluation of the effects of adaptive opportunities on occupant satisfaction. It is widely recognized that these opportunities are important, but with present day knowledge and in the present modeling approach there is no room for these facets.

2.6 Summary

In this chapter, two issues have been addressed. Firstly, the specific building, which will be used throughout this thesis, has been described. It is a four-story, naturally ventilated office building in the Netherlands. The description concerns the building itself, its environment and the occupancy scenario to be considered.
Secondly, an approach is described to evaluating the thermal comfort performance of the building. The performance evaluation approach consists of three steps. Initially, a building model is used to dynamically simulate the temperatures in the building in response to a particular scenario (i.e. a time series of the outdoor climate conditions and occupant behavior). Subsequently, a comfort performance indicator is calculated on the basis of the predicted indoor temperature time series. This calculation involves a thermal comfort model, which predicts how occupants will rate the indoor temperatures.
The building simulation model, the thermal comfort model(s) and the performance indicator(s) are described.

3 Crude uncertainty analysis

3.1 Introduction

In the previous chapter, it has been described how, in a specific case, building performance with respect to the indoor climate is assessed on the basis of a building model and a model for thermal comfort. This chapter analyses which uncertainty should be attributed to the resulting building performance.

Uncertainty may enter the assessment from various sources. The next paragraphs give a brief discussion. Slightly different classifications of the sources of uncertainty can be found in Pinney et al. (1991) and MacDonald et al. (1999).
Firstly, the design specifications do not completely specify all relevant properties of the building and the relevant installations. Instead of material properties, for instance, material types will commonly be specified, leaving uncertainty in the exact properties. Moreover, during the construction of the building, deviations from the design specifications may occur.
The uncertainty, arising from incomplete specification of the system to be modeled will be referred to as *specification* uncertainty.
Secondly, the physical model development itself introduces uncertainty, which we will refer to as *modeling* uncertainty. Indeed, even if a model is developed on the basis of a complete description of all relevant building properties, the introduction of assumptions and the simplified modeling of (complex) physical processes introduces uncertainty in the model.
Thirdly, numerical errors will be introduced in the discretization and simulation of the model. We assume that this *numerical* uncertainty can be made arbitrarily small by choosing appropriate discretizations and time steps. Hence, this uncertainty will not be addressed here.
Finally, uncertainty may be present in the *scenario*, which specifies the external conditions imposed on the building, including e.g. outdoor climate conditions and occupant behavior. The scenario basically describes the experiment, in which we aim to determine the building performance.

In current practice, it has become customary to use standardized scenario elements in comfort performance evaluations. The most striking example concerns the 'reference' time series of outdoor climate data (see Section 2.3.1). From the experience with performance evaluations, in which these standardized experimental conditions were used, a broad frame of reference has developed to which performance calculations for new buildings can be compared. If such comparisons are indeed meaningful to a decision maker, who aims to use a performance evaluation to measure the level of achievement on his objectives, there is no scenario uncertainty. If, however, a decision maker is actually interested in a performance assessment, based on a *prediction* of the

comfort sensations of the future occupants of the building, the scenario should be considered as a reflection of the future external conditions, which are uncertain.
As a systematic exploration of a decision-maker's objectives, and their translation into building performances is commonly not undertaken in building design, it is difficult to decide in general how to deal with scenario uncertainty. In this study, we will not address scenario uncertainty and defer a qualitative discussion of the consequences to Chapter 6.

To analyze these uncertainties and their impact on building performance, we start from a process scheme of building performance assessment as shown in Figure 3.1.

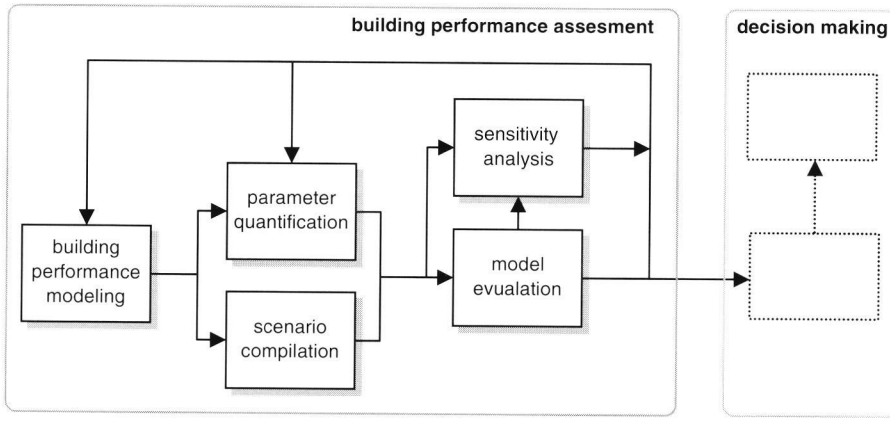

Figure 3.1 Process scheme of building performance assessment as input to decision making.

All process elements have been discussed in the previous chapter, except the sensitivity analysis. This is not a necessary ingredient for building performance assessment. It is a very useful tool, though, to gain insight into the model. This insight can be used e.g. to take specific measures to further develop the model or to effectively improve the building design with respect to the performance at hand.

The figure is also a process scheme for uncertainty analysis. The difference with the deterministic case is that model parameters may now be uncertain variables. This implies that the process elements are more complex. For instance, parameter quantification now requires not (only) an assessment of a point estimate, but (also) an assessment of the uncertainty. Moreover, in the presence of uncertainty, model evaluation is a process, which propagates uncertainty in scenario and parameters through the model into the model output. Furthermore, the scope of the sensitivity analysis is extended. Besides the sensitivities, the importances of the variables can also be assessed now. The term 'importance' is used here to express the relative contribution of a variable (or set of variables) to the uncertainty in the model output.

By accounting for uncertainty, richer information is generated, which can be used, not only for improved decision support, but also for more effective feedback to parameter quantification and performance modeling. First, if the uncertainty in the model output, i.e. the building performance, is found to be significant in some sense, the importance information from the sensitivity analysis may be used to reassess the most important parameters to gain more confidence in their uncertainty estimates and/ or to reduce the uncertainty in those parameters.
Moreover, the model developer (e.g. the building physics consultant) may use (prior) information on the uncertainties to build models, in which the crudeness of simplifying assumptions is balanced against the uncertainty, either in the process to be modeled or in other parts of the model.

Especially in the presence of uncertainty, it is better to assess performance in a cyclic rather than a linear approach. Proper assessment of uncertainties in parameters and inputs may be a formidable task. By starting with crude estimates, and deciding on selective refinement to those variables that really matter, the problem becomes tractable.

To be studied quantitatively, uncertainty must be provided with a mathematical representation. In this study, uncertainty is expressed in terms of probability. This representation is adequate for the applications of concern in this work and it has been studied, challenged and refined in all its aspects.

Moreover, in interpreting probability, we will follow the subjective school. In the subjective view, probability expresses a degree of belief of a single person and can, in principle, be measured by observing choice behavior. It is a philosophically sound interpretation, which fulfills our needs in decision analysis.
It should be mentioned, however, that in the context of rational decision making, one subjective probability is as good as another. There is no rational mechanism for persuading individuals to adopt the same degree of belief. Only when observations become available, subjective probabilities will converge in the long run. However, the aim of uncertainty analysis is not to obtain agreement on uncertainties. Rather, its purpose is to explore the consequences of uncertainty in quantitative models.

For more information on uncertainty analysis the reader is referred to Benjamin and Cornell (1970), Iman and Helton (1985), Janssen et al. (1990), and McKay (1995) among others. Discussions and background on the interpretation of probability can be found in e.g. Savage (1954), Cooke (1991), French (1993).

This chapter reports on a first cycle in the process of uncertainty analysis, i.e. crude quantification of uncertainties (Section 3.2), propagation through the model to obtain estimate of uncertainty in building performance (Section 3.3), and sensitivity analysis to identify the important parameters (Section 3.4). The chapter concludes in Section 3.5 with discussion and conclusions.

3.2 Uncertainty in model parameters

3.2.1 Introduction

As a first step in this crude uncertainty analysis, we will assess plausible ranges for the model parameters, globally expressing the uncertainty in their values. In future steps of the analysis, these ranges will be interpreted as central 95% confidence intervals. As mentioned in the introduction of the chapter, the parameter uncertainty may arise from two sources, viz. specification uncertainty and modeling uncertainty.

The specification uncertainty relates to a lack of information on the exact properties of the building. In the case at hand, this mainly concerns the building geometry and the properties of the various materials and (prefabricated) components.

Modeling uncertainty arises from simplifications and assumptions that have been introduced in the development of the model. As a result, the building model contains several (semi-) empirical parameters, for which a range of values can be found in the literature. Moreover, the model ignores certain physical phenomena.

Table 3.1 Uncertain model parameters

Description	Range (central 95% confidence interval)
Physical properties of materials and components	See Appendix B
Space dimensions[14]	[-0.02, 0.02] m
Wind reduction factor	[0.65, 0.85]
Wind pressure coefficients	See Figure 3.2
Discharge coefficients	[0.6, 0.75]
Internal convective heat transfer coefficients	See Figure 3.3, Figure 3.4
External convective heat transfer coefficients	See Figure 3.5
Albedo	[0.15, 0.30]
Convective heat transfer at sunblind and window[15]	[0.3, 3.0]
Distribution of incident solar gain:	
¬ fraction lost	[0.08, 0.12]
¬ fraction via furniture to air	[0.05, 0.15]
¬ fraction to floor	[0.22, 1.0]
¬ fraction to remainder of enclosure	rest
Air temperature stratification[16]	[0, 3] °C
Radiant temperature of surrounding buildings[17]	[-5, 5] °C
Local outdoor temperature[18]	[0, 1] °C

[14] The indicated range denotes the deviations from the nominal values

[15] The indicated range refers to an additional model parameter, introduced in Section 3.2.10.

[16] This is the air temperature difference over the height of the space.

[17] More precisely, this is the *deviation* of the actual radiant temperature of the surrounding buildings from the assumed temperature. The assumption entails that any façade of the surrounding buildings has the same average surface temperature as the façade of the building under study with corresponding orientation.

[18] The range in the column at the right relates to the *difference* between the local ambient temperature at the building site and the value reported at the meteorological station.

Table 3.1 shows the list of parameters, which have been considered as uncertain. Not all sources of (modeling) uncertainty could straightforwardly be attributed to one or more parameters in the existing model. In those cases additional parameters have been introduced in the model to make sure that in the uncertainty analysis only parameters need to be considered.
The uncertainties will be discussed in the following sections.

3.2.2 Physical properties of materials and components

As the (long) list of the various material and (prefabricated) component properties would blur the overview in Table 3.1, it has been referred to the Appendix (B). In the quantification of the uncertainties in the various parameters, which mainly result from *specification* uncertainty, extensive use has been made of the data collected for two previous sensitivity analyses in the field of building thermal modeling (Pinney et al. (1991), Jensen (1994)) and the underlying sources for these studies (CIBSE (1986), Clarke et al. (1990), Lomas and Bowman (1988)). Additional data have been obtained from ASHRAE (1997), ISSO (1994) and the Polytechnic Almanac (1995). For a few parameters a range was assumed for lack of data.

To estimate the correlations between the properties of different components and materials, each property x has been considered as the output of the hierarchical model:

$$x = \mu_x + \Delta x_1 + \Delta x_2 + \Delta x_3$$

where

μ_x general mean over the whole population
Δx_1 variation between types, which satisfy the description in the design specifications
Δx_2 variation between production batches within a type
Δx_3 variation between individual components within a batch

It has been assumed that the variation in the material and component properties predominantly arises from the first variation component Δx_1. Hence, complete correlation has been considered between properties of the same name, if they belong to components and materials of the same name. Dependencies between different properties or between unlike components or materials have not been considered.

3.2.3 Space dimensions

Due to irregularities in the construction process, the realized space geometry may deviate slightly from the geometry given in the design specifications. In this study we restrict the scope to deviations of the actual space dimensions (length, width and height) from the nominal values. The range of possible deviations has been estimated at [-0.02, 0.02] m.

3.2.4 Wind reduction factor

The wind reduction factor enters the model in (2.7), Section 2.3.4.3. It is the ratio between the wind speed, measured at 10 m above ground level at the meteorological station, and the local wind speed at a given reference level, to which the pressure coefficients are related. This reference level is usually chosen equal to the building roof height, in this case 14 m.

Approaches to assess the wind reduction factor γ are commonly based on the following scheme:

$$\begin{aligned} U_1 &= f_1(z_1, U_{c,1}) \\ U_{c,2} &= g(U_{c,1}) \\ U_2 &= f_2(z_2, U_{c,2}) \\ \gamma &= U_2 / U_1 \end{aligned} \tag{3.1}$$

where z is the height above the ground, U_c is a characteristic wind velocity and the indices refer to the locations of interest, i.e. the meteorological observation site (1) and the building site (2). For a known function f_1 and a given pair of values at the meteorological observation site (z_1, U_1) = (10 m, U_{pot})[19], the characteristic value $U_{c,1}$ can be calculated. With function g the value of $U_{c,2}$ is assessed, which serves as input to function f_2 to calculate the value of U_2 at the building site for a given height z_2. The wind amplification factor is the ratio of U_2 to U_1.

For neutral conditions, Wieringa and Rijkoort (1983) propose an implementation of this scheme, in which f_1 and f_2 are logarithmic wind velocity profiles at a (nearby) meteorological observation site and the building site respectively. These profiles are a function of the terrain parameters z_0 (characteristic roughness length) and d (displacement height). The characteristic velocity is the *meso* wind speed, defined as the (mean) wind speed at 60 m height. Wieringa and Rijkoort assume the difference between the meso wind speeds at both sites to be negligible. Application of this technique with standard terrain parameters for the meteorological observation site ($z_{0,1}$ = 0.03 m and d_1 = 0 m, see Wieringa and Rijkoort, 1983) and terrain parameters for the urban building environment $z_{0,2}$ = 0.75 m and d_2 = 2 m, yields a wind reduction factor of 0.85.

The algorithm described in Biétry et al. (1978) also starts from logarithmic wind velocity profiles. The friction velocities $u*$ are used as characteristic wind speeds:

$$\gamma = \frac{u_{*2}}{u_{*1}} \frac{\ln(z_2 / z_{0,2})}{\ln(z_1 / z_{0,1})} \tag{3.2}$$

[19] For the definition of U_{pot} see Section 2.3.4.

Based on the analysis of a large number of measurements, Biétry et al. propose the following values for $u*/(u*)_{ref}$, where $u*$ is the friction velocity at a site with roughness length z_0 and $(u*)_{ref}$ is the friction velocity at a reference site with roughness length $(z_0)_{ref} = 0.07$ m:

z_0	0.005	0.07	0.30	1.00	2.50
$u*/(u*)_{ref}$	0.83	1.00	1.15	1.33	1.46

We write $u*_2/u*_1 = (u*_2/(u*)_{ref}) * (u*_1/(u*)_{ref})^{-1}$, and calculate $u*_2/u*_1$ from interpolations of the values in the above table for $z_{0,2} = 0.75$ m and $z_{0,1} = 0.03$ m respectively. Substitution of this ratio into equation (3.2) with $z_2 = 14$ m and $z_1 = 10$ m yields a wind reduction factor of 0.65.

Liddament (1986) describes a technique in which the logarithmic wind velocity profiles are replaced by power laws. For *urban* terrain (this method does not use terrain characterization in terms of z_0 and d) a value of approximately 0.65 is obtained.

The observed scatter between different model outcomes arises from lack of knowledge about the value of the wind reduction factor, given that:

- neutral conditions apply, i.e. thermal buoyancy effects are insignificant
- the wind profile at the building site can be expressed in terms of terrain roughness parameters only
- the terrain roughness upstream of the building site is uniform

In most practical situations these conditions will not apply (Bottema, 1993). For instance, thermal buoyancy effects are commonly important for lower wind velocities (e.g. Holtslag, 1984), which are likely to occur at the warm days that are of particular interest to this study.

Moreover, the wind velocity profile can only be properly expressed in terms of terrain roughness above a height $z_{min} > 20z_0 + d$ (e.g. Wieringa and Rijkoort, 1983). Below this height, individual obstacles mark the profile. With the current choice of $z_{0,2} = 0.75$ m and $d_2 = 2$ m the minimal height $z_{min} = 17$ m, which exceeds the selected reference height of 14 m.

Finally, uniform terrain conditions are the exception rather than the rule.

Nevertheless, in this first exploration of the effects of the various uncertainties, we will stay close to the observed inter-model scatter and use the range [0.65, 0.85] for the wind reduction factor in the uncertainty analysis.

3.2.5 Wind pressure coefficients

As explained in Section 2.3.4.3, pressure coefficients relate the pressures on the building envelope to the dynamic local wind pressure at a given reference level. In this study the local wind velocity is defined as the velocity directly upstream of the area shown in Figure 2.3, whereas the ridge height of the building of interest (14 m) is chosen as the

reference level. In ventilation studies, mean (i.e. time-averaged) values of the pressure coefficients are generally used.

Several tools have been developed to assist the assessment of mean wind pressure coefficients on the basis of existing experimental data from prior wind tunnel studies and full-scale measurements. The tools from Allen (1984), Grosso (1992, 1995), and Knoll, Phaff and De Gids (1995, 1996) have been applied to the current case (see Figure 2.3) to assess the required wind pressure difference coefficients[20]. The results are shown in Figure 3.2. A more detailed analysis of the wind pressure difference coefficients can be found in Chapter 4.

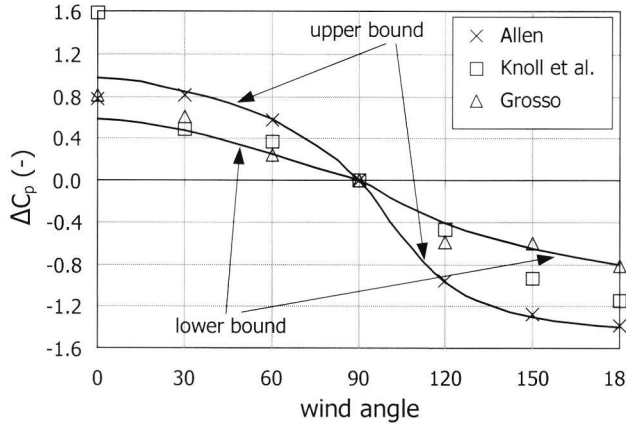

Figure 3.2 Wind pressure difference coefficients from three different models as a function of wind angle (for the definition of the wind angles see Figure 2.3 in chapter 2). The figure is symmetric with respect to wind angle 180°, so only the values between 0° and 180° are shown. The drawn lines indicate the upper and lower bounds, which have been used in the uncertainty analysis.

As already mentioned in the previous section, inter-model scatter does not commonly give a good idea of the uncertainty. However, it provides a convenient first estimate for a crude uncertainty analysis. Hence, lower and upper bounds have been used, which are closely tied to the various model results as shown in Figure 3.2. In the analysis, the absolute values of the mean pressure difference coefficients for different wind angles have been considered to be completely and positively correlated. Loosely stated, this means that if the magnitude of the wind pressure difference coefficient for a given wind angle has a high value (relative to its range in Figure 3.2), the pressure differences for all other angles are also large, and vice versa.

[20] The wind pressure difference coefficient is the difference between the pressure coefficient for the window of modeled building section (see Section 2.2) in the west façade and the one for the window in the east façade.

3.2.6 Discharge coefficients

Discharge coefficients have been introduced in the model in (2.6), Section 2.3.4.2. Bot (1983) reports on experimentally observed flow characteristics of window openings in greenhouses. His results indicate that a discharge coefficient of 0.65 would be an appropriate value for both the windows and vents in the current case. In a review of discharge coefficients for vertical rectangular openings, Boulard and Baille (1995) report values between 0.60 and 0.74. Straw et al. (1999) refer to unpublished full-scale measurements of wind-induced discharges through rectangular openings in a cubic structure. In these experiments values up to 0.75 were found for flows skimming along the cube face containing the opening.
In this study we will use the range [0.6, 0.75] to reflect the uncertainty in the discharge coefficients. The coefficients for the four openings of interest will be considered as uncorrelated.

3.2.7 Internal convective heat transfer coefficients

Internal heat transfer coefficients act in (2.1) and (2.4) in Section 2.3.2. Reviews on literature reporting semi-empirical models for internal heat transfer coefficients from experiments can be found in e.g. Halcrow (1987), Khalifa (1989), Pernot (1989) and Awbi and Hatton (1999). The majority of these models have been obtained under free convection conditions at isolated flat plates, while only a few experiments in real-sized spaces have been conducted. The studies generally report relations that can be written in the form:

$$\alpha_{c,\mathrm{int}} = C(\Delta T)^n \tag{3.3}$$

where ΔT is the temperature difference over the air boundary layer and C and n are (semi-) empirical coefficients. Different values for (C, n) are found depending on the direction of the heat flow (horizontal, upward or downward), the flow regime (laminar or turbulent) and the dimension of the surface.

Figure 3.3 shows semi-empirical models as they were obtained for horizontal heat flow (vertical surfaces) in six different studies. The studies by Li et al. (1987), Khalifa and Marshall (1990), Min et al. (1956) and Awbi and Hatton (1999) concern experiments on surfaces in spaces with typical office dimensions. The widely used models found in Alamdari and Hammond (1983) and ASHRAE (1997) are advocated for use in building simulation models.
In agreement with the experimentally observed values, heat transfer coefficients dependent on the temperature difference ΔT have been used in the uncertainty analysis. For vertical walls, the minimum and maximum values at each temperature difference are marked by the bold lines in Figure 3.3. These bounds correspond to the curves from Alamdari and Hammond (1983) and Li et al. (1987) respectively.
Heat transfer coefficients at horizontal surfaces are commonly found to be different from those at vertical walls. For upward (buoyant) heat flow slightly higher values are found, whereas for downward (stagnant) heat flow the values are much lower.

The selected range for the heat transfer coefficients related to upward heat flow is shown in Figure 3.4. The bounds correspond to those in Figure 3.3, multiplied by 1.2. Indeed, analysis of coefficients found in a large number of studies (mostly isolated plate experiments) shows that the values of heat transfer coefficients for upward flow are commonly 0-30% higher than the coefficients for horizontal heat flow (at similar temperature differences).

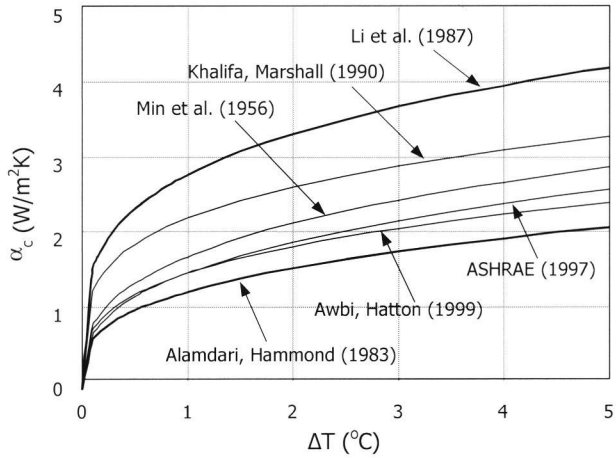

Figure 3.3 Models for the internal convective heat transfer coefficient at a vertical wall as a function of the temperature difference over the air-wall boundary layer. Where necessary, characteristic wall dimensions have been used in accordance with the dimensions of the space under study (see Figure 2.5). The bold lines indicate the values that are used as lower and upper bounds in the uncertainty analysis.

The range for coefficients related to downward heat flow are also shown in Figure 3.4. The upper bound corresponds to the ASHRAE (1997) model, whereas the lower bound originates from the experiments by Min et al. (1956).

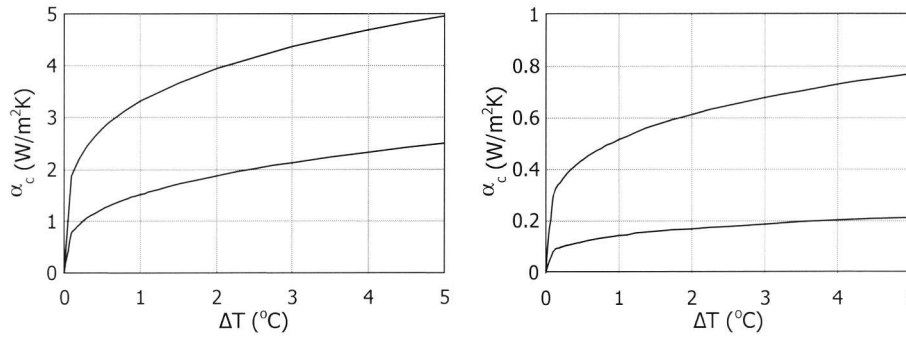

Figure 3.4 Lower and upper bounds for internal convective heat transfer coefficients. The graph at the left shows the values for upward (buoyant) heat flow, whereas the one at the right is related to downward (stagnant) heat flow.

In the analysis, the heat transfer coefficients within a single space have been considered as completely correlated: positive correlation between the coefficients for horizontal and upward heat flow, negative correlation between coefficients corresponding to heat flows with upward and downward directions. The analysis of coefficients from various studies mentioned earlier strongly supports the positive correlation. The negative correlation is present, but less pronounced.
Coefficients in separate spaces have been considered independent.

3.2.8 External convective heat transfer coefficients

These coefficients enter the model in (2.5) in Section 2.3.2. Reviews of literature on external heat transfer coefficients can be found in e.g. Strachan and Martin (1989) and Allen (1987). They report relations for the heat transfer coefficients, determined from experiments, of the general form:

$$\alpha_{c,ext} = A + B u^{C} \tag{3.4}$$

where u is the surface-parallel flow velocity, and A, B and C are semi-empirical constants.

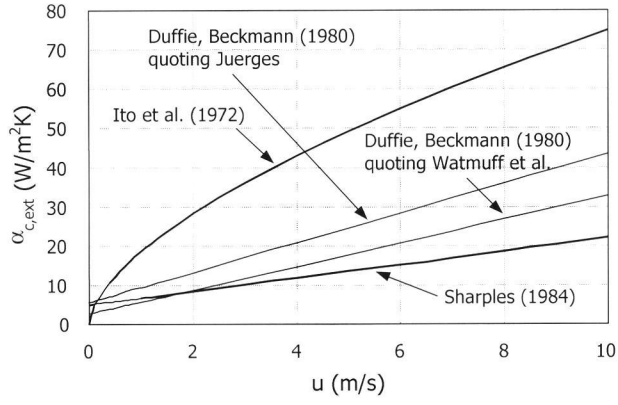

Figure 3.5 Models for the external convective heat transfer coefficient as a function of the wind velocity along the surface. The bold lines indicate the values that are used as lower and upper bounds in the uncertainty analysis.

Uncertainty in the value of the external heat transfer coefficients arises from two sources. First, the value of the surface flow velocity has to be determined from the available meteorological data. This process is hampered with similar uncertainty as already mentioned in relation to the assessment of the wind reduction factor and the wind pressure coefficients.
Second, the value of (A, B, C) is uncertain. This is illustrated by the large scatter between semi-empirical models reported in the literature (see Figure 3.5). Strachan and Martin

hypothesize that this scatter is mainly due to different definitions of the surface wind speed and to different measurement positions on the buildings.

The extreme curves from Ito (1972) and Sharples (1984) were obtained in measurements on real buildings . The results quoted by Duffie and Beckman (1980) are derived from older experiments in wind tunnels.

In the analysis, external heat transfer coefficients dependent on the wind speed have been used. The uncertainty estimate for the external convective heat transfer coefficients is based entirely on the uncertainty in (*A*, *B*, *C*) given the local surface wind speed. This wind speed was calculated from the local wind speed (which is also uncertain as a result of the wind reduction factor γ) with the ESP-r algorithm (ESRU, 1995b). A range for the heat transfer coefficient was used as shown in Figure 3.5 as a function of the local surface wind speed. Heat transfer coefficients at the various external wall components have been treated as fully dependent.

3.2.9 Albedo

The albedo is the overall reflection coefficient of the environment for short-wave radiation. This variable was introduced in Section 2.3.3. Reflection coefficients for various surfaces can be found in e.g. Iqbal (1983), Fröhlich and London (1986) and Velds (1992). These sources show that reflection coefficients depend on the condition of the surface (and the solar angle). For instance, the albedo of (dark) sand may vary from 0.10 to 0.20 dependent on the surface roughness and the water content. The reflectance of concrete ranges from 0.22 to 0.37 dependent on age and specific composition. Based on these relative variations, in the uncertainty analysis albedo values in the range [0.15, 0.30] have been used. This range is comparable to the one used in the PASSYS-sensitivity analysis ([0.2, 0.3], Jensen (1994)), but narrower than the interval that Lomas and Bowman (1988) used in their analysis, i.e. [0.1, 0.4]. This latter interval was based on extreme values for asphalt on the one hand to light sand on the other.

3.2.10 Convective heat transfer at sunblind and window

In section 2.3.3 the thermal modeling of the sunblinds has been addressed. As expressed by equations (2.6) through (2.8) In case the sunblind is activated, the convective heat transfer at sunblind and window is governed by four quantities:

$\alpha_{c,blind,ext}$ convective heat transfer coefficient at external surface of blind

$\alpha_{c,blind,cav}$ convective heat transfer coefficient at surface of blind bordering the cavity between window and blind

$\alpha_{c,win,ext}$ convective heat transfer coefficient at window surface bordering the cavity between window and blind

$\Phi_{V,cav}$ ventilation rate of the cavity with ambient air

ISSO (1993, 1994) proposes guidelines from which the following tentative values can be derived for the current case:

$\alpha_{c,blind,ext}$ 30 W/m^2 K

$\alpha_{c,blind,cav}$ 12 W/m^2 K

$\alpha_{c,win,ext}$ 8 W/m^2 K

$\Phi_{V,cav}$ 0.5 m^3/s

Consistent with the discussion in Section 3.2.8, we will use a wind velocity dependent value for the external heat transfer coefficient here rather than a fixed value. Although at a sunblind, which is commonly permeable to some degree, the value of this coefficient may be different from the value at a regular building surface, it is questionable whether this difference will be significant compared to the uncertainty we assume in the heat transfer coefficients (see Figure 3.4). Hence we will also apply the ranges in Figure 3.4 to $\alpha_{c,blind,ext}$.

It is rational to assume that besides the external heat transfer coefficient, the ventilation rate and the coefficients at the surfaces in the cavity increase with the wind velocity too. As a straightforward model for the variation of these quantities with wind velocity we will assume that their values change proportionally to the external heat transfer coefficient.

The proportionality constants in this model, though, are quite uncertain. The numbers from ISSO (1993, 1994) provide some guidance, but certainly cannot be accepted without further ado. Let us assume that the dominant uncertainty lies in the (forced) ventilation rate with ambient air. This means that the uncertainty in the heat transfer coefficients in the cavity, given this ventilation rate, is considered to be (much) smaller than the uncertainty in the ventilation rate itself. We now write:

$$\Phi_{V,cav} = \beta \times (\alpha_{c,ext} / 30) \times 0.5 \quad \text{m}^3/\text{s}$$

$$\alpha_{c,blind,cav} = \beta \times (\alpha_{c,ext} / 30) \times 12 \quad \text{W/m}^2\,\text{K}$$

$$\alpha_{c,win,cav} = \beta \times (\alpha_{c,ext} / 30) \times 8 \quad \text{W/m}^2\,\text{K}$$

$$\alpha_{c,blind,ext} = \alpha_{c,ext}$$

where $\alpha_{c,ext}$ is calculated as discussed in Section 3.2.8, the numbers in brackets are adopted from ISSO (1993, 1994) and β is an uncertain parameter. For $\beta = 1$ and $\alpha_{c,ext} = 30$ W/m^{2}K, the values suggested by ISSO are retrieved. In the uncertainty analysis we will take values for β from the range [0.3, 3]. Values of β for different sunblinds are considered to be completely and positively correlated.

3.2.11 Distribution of absorption of the incident solar radiation

Solar radiation entering a space through the window may be subdivided into three components:

- fraction lost
- fraction via furniture to air
- fraction absorbed at walls

The first component is light, which is reflected out of the space again without being absorbed. Based on calculations for a space of similar geometry as the one under study, Pinney et al. (1991) propose the range [0.05, 0.14] for this fraction. This range is based on the extreme optical characteristics of a variety of materials. As in the current case the materialization of the space is known, we will use the narrower range [0.08, 0.12].

The second component represents the heat, which is generated by the absorption of a part of the incident solar radiation by furniture in the space and convectively transferred to the indoor air. For this convective fraction of the total solar gain, ISSO (1994) recommends the value 0.1. In their choice of uncertainty limits for a sensitivity analysis, Pinney et al. (1991) use the range [0.05, 0.15]. This interval properly includes the value proposed by ISSO and will be adopted in the current analysis.

The remaining part of the solar radiation is absorbed by the enclosure of the space. In most current simulation tools the absorption of the solar gain is assumed to be evenly distributed over an appropriate part of the space enclosure. In the uncertainty analysis four ways to distribute this gain will be considered. One extreme assumption is that all solar radiation is directly absorbed at the floor (fraction absorbed by floor is 1.0), whereas in the other extreme it is considered to be evenly absorbed over the entire enclosure as a result of internal reflections (fraction to floor is 0.22). In the two intermediate schemes we will assume that 40% and 70% respectively is directly absorbed at the floor and the rest is evenly distributed over the enclosure.

The factions 'lost' and 'via furniture to air' have been assumed to be independent from each other and from the scheme, which regulates the distribution of the remaining solar gain over the walls. Distributions in different spaces are also treated as independent.

3.2.12 Air temperature stratification

As explained in Section 2.3.2, it has been assumed that the air temperature in building spaces is uniform. However, this will generally not be the case. In naturally ventilated buildings there is limited control over either ventilation rates or convective internal heat loads. This results in flow regimes varying from predominantly forced convection to fully buoyancy driven flow. In the case of buoyancy driven flow, plumes from both heat sources and warm walls rise in the relatively cool ambient air, entraining air from their environment in the process, and create a stratified temperature profile. Cold plumes from heat sinks and cool walls may contribute to this stratification. Forced convection flow elements, like jets, may either enhance the stratification effect or reduce it, dependent on their location, direction, temperature, and momentum flow.

If we consider the current approach as a zero-order approximation of the spatial temperature distribution, then it is a logical step to refine the model by incorporating first order terms. As vertical temperature gradients in a space are commonly dominant, we will use the following model:

$$T_{air}(z) = \overline{T}_{air} + \xi\left(z - \tfrac{1}{2}H\right) \tag{3.5}$$

where

T_{air}	air temperature
$\overline{T}_{air}$	mean air temperature
z	height above the floor
H	ceiling height of the space
ξ	stratification parameter

Dropping the assumption of uniform air temperature has the following consequences:

- the temperature of the outgoing air is no longer equal to the mean air temperature as the ventilation openings in the spaces are close to the ceiling (see Figure 2.5)
- the (mean) temperature differences over the air boundary layers at the ceiling and floor, driving the convective heat exchange between the air and those wall components, are no longer equal to the difference between the surface temperature and the mean air temperature
- the occupants, which are assumed to be sitting while doing their office work, are residing in the lower half of the space and hence experience an air temperature, which is different from the mean air temperature

With (3.5) we can quantify these changes. As the ventilation openings are near the ceiling, we take that the temperature of the outgoing air is:

$$T_{out} = T_{air}(H) \tag{3.6}$$

Moreover, the convective heat fluxes from the floor and the ceiling to the air are described by respectively:

$$q_{floor} = \alpha_{c_{int,floor}}(T_{int,\,floor} - T_{air}(0)) \;,\; q_{ceil} = \alpha_{c_{int,ceil}}(T_{int,\,ceil} - T_{air}(H)) \tag{3.7}$$

Finally, the (mean) air temperature experienced by the occupants, T_{occ}, is estimated with:

$$T_{occ} = T_{air}(1/4\,H) \tag{3.8}$$

These changes modify the model presented in the previous chapter.

In the analysis we will assume that ξ in equation (3.5) is a fixed, but uncertain parameter. This means that we randomize over a wide variety of flow conditions in the space that may occur over the simulated period.
In e.g. Loomans (1998, full-scale experiments and flow field calculations) and Chen et al. (1992, flow field calculations) vertical temperature differences over the height of an

office space are reported between 0 and 2 °C for mixing ventilation conditions and from 1 °C up to 6 °C for displacement ventilation configurations. These numbers suggest that vertical temperature differences of several degrees may not be uncommon. Hence, we will choose ξ in the range [0, 1] °C/m in this study.
The temperature stratification in separate spaces has been considered as independent. No stratification has been assumed in the corridor between the office spaces in the case at hand.

3.2.13 Radiant temperature of surrounding buildings

In modeling the radiant heat exchange with other buildings in the environment, it has been assumed that any façade of the surrounding buildings has the same average surface temperature as the façade with corresponding orientation of the building under study (see Section 2.3.3). In general however, these facade temperatures may not be exactly identical e.g. as a result of dissimilar environmental conditions (shading, wind shelter). The temperature difference is tentatively modeled as an uncertain parameter with a range of [-5.0, 5.0] °C.

3.2.14 Outdoor ambient temperature

In chapter 2, the outdoor ambient temperature was introduced as an element of the scenario, which is not considered in the uncertainty analysis in the current chapter. However, this scenario temperature is assumed to be observed at a meteorological station, whereas the local temperature at the building site would be a more suitable input to the building model. In the local thermal field, generated by an urban area, the temperature is usually higher than that of its surroundings. Plate (1995) reports heat island temperatures in large cities, which in wintertime may differ up to 10 – 12 °C with temperatures observed in suburban areas. A survey by Kimani (1998) of algorithms for converting meteorological weather data to urban locations shows that there is a lack of generally applicable engineering models due to the complexity of the processes involved. Considering that the current case addresses summer conditions in a moderate climate, we will attribute a modest, but again tentative range of values to the difference between local and meteo ambient temperature: [0, 1] °C.

3.2.15 Discussion and summary

The approach laid out in the previous subsections results in a total number of 89 independent[21] uncertain parameters. It is likely that this set of parameters is incomplete. First, some sources of uncertainty may have been overlooked. This is always a risk when uncertainty is investigated from the angle of a given modeling approach.
Moreover, several assumptions and simplifications have not been addressed intentionally. For example, the symmetry assumptions, which were used to keep the model transparent (Section 2.3.3), have not been considered. The one-dimensional approximation of heat conduction in wall-components is another example. These

[21] Actually, the number of uncertain parameters is greater than 89, but parameters which are treated as completely dependent, such as the wind pressure coefficients, are counted as a single parameter.

simplifications have been considered as conscious choices, which are deemed to be justified in the case at hand. One of the ideas behind an uncertainty analysis is to obtain a reference for this kind of modeling choices. If a deliberate simplification has an effect on the model output, which turns out to be insignificant compared to the uncertainty in that output, the choice is obviously justified. If not so, the justification of the choice should be judged on the effect it may have on the decision that is to be made on the basis of the model output.
Obviously there is no clear-cut boundary between necessary and freely chosen model simplifications. This depends among other things upon the possibilities of the modeling tools at hand. Hence, the choice of such a boundary in this thesis is arbitrary to some degree.

Finally, no uncertainty has been considered in either of the two comfort models. The thermal simulation model does not specify all input variables of the static comfort model. Hence, the remaining input variables have to be estimated heuristically, introducing uncertainty. This type of uncertainty is not introduced when the adaptive comfort model is used. This model, based on field experiments, relates the observed occupants' response distributions only to the operative temperature in these experiments, which can be assessed by thermal simulation. Hence, the effects of the variability in all other variables are automatically included. In this way, however, uncertainty is introduced to which degree the variation of these variables (especially air velocity and humidity) in the building under study will be similar to the variation that occurred in the field studies.

3.3 Propagation of uncertainty

On the basis of the parameter uncertainties identified in the previous section, the uncertainty in the model output, i.e. the building performance was calculated by propagation of the parameter uncertainties through the model.
For lack of explicit information on the parameter distributions, normal distributions were assumed for all parameters from which samples were drawn. The parameter ranges, established in the previous sections, were interpreted as central 95% confidence intervals. Where necessary, the normal distributions were truncated to avoid physically infeasible values.

Technique

For the propagation, a Monte Carlo simulation technique was used, i.e. Latin Hypercube Sampling. This is a form of stratified sampling. The domain of each parameter is subdivided into N disjoint intervals (strata) with equal probability mass. In each interval a single sample is randomly drawn from the associated probability distribution. If desired, the resulting samples for the individual parameters can be combined to obtain a given dependency structure. Application of this technique provides a good coverage of the parameter space with relatively few samples compared to simple random sampling (crude Monte Carlo). It yields an unbiased and often more efficient estimator of the mean, but the estimator of the variance is biased. The bias is

unknown, but commonly small. More information can be found in e.g. McKay et al. (1979), Iman and Conover (1980) and Iman and Helton (1985).

Implementation

In this study the algorithm for Latin Hypercube sampling from UNCSAM (Janssen et al., 1992) was applied. A total of 250 samples were propagated, which is well above the value of $4k/3$ (k = 89 being the number of parameters) that Iman and Helton (1985) recommend as a minimum.

For each sample of parameter values, a dynamic temperature simulation was carried out with the BFEP-implementation of the building model (see Section 2.3.7). From the resulting temperature time series, both the static (TO) and adaptive (TO*) performance indicator were calculated.

In all simulations, a single, deterministic scenario was used as described in Appendix A2. This scenario covers a period of 6 months from April through September.

Results

The results of the propagation of 250 samples are shown in Figure 3.6, both for the static (TO) and the adaptive (TO*) performance indicator.

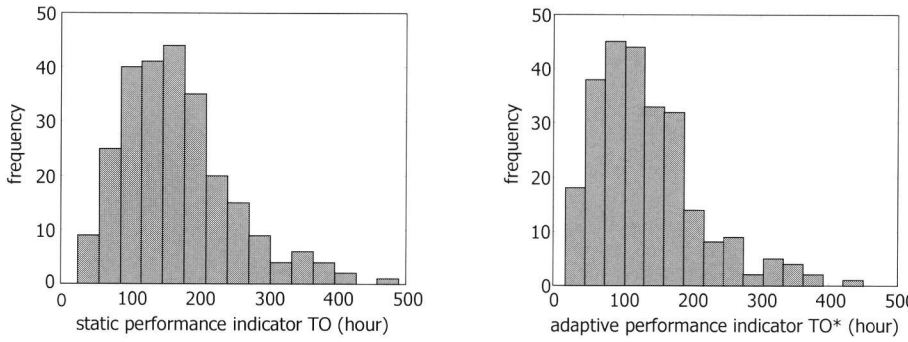

Figure 3.6 Histograms of the static (left) and adaptive (right) performance indicator, obtained from the propagation of the Latin Hypercube sample of size 250. Note that uncertainty in the scenario has not been taken into account. A common target value for TO is 100 hours (see Section 2.4.1).

The variability in the comfort performance, observed in the Monte Carlo exercise is significant. For both the static and the adaptive performance indicator the coefficient of variation, i.e. the standard deviation divided by the mean value, is about 0.5.

3.4 Sensitivity analysis

3.4.1 Introduction

The aim of the sensitivity analysis is to find a limited set of parameters, which accounts for most of the uncertainty in the model output. In this study an approach is used that consists of two steps:

1. Parameter screening to rank parameters in the order of their importance, i.e. their individual contribution to the uncertainty in the model output.
2. Validation to verify that the set of parameters identified as most important in the screening, do indeed jointly account for the majority of the uncertainty in the model output.

These two components of the analysis are subsequently discussed.

3.4.2 Technique

Screening technique

An investigation of methods for sensitivity analysis and parameter screening can be found in e.g. Janssen (1990), Saltelli et al. (1993), McKay (1995) and Kleijnen (1997). In the analysis in this study the factorial sampling technique as proposed by Morris (1991) has been used.

In an earlier analysis (De Wit, 1997c) this technique was found to be suitable for application with building models. It is economical for models with a large number of parameters, it does not depend on any assumptions about the relationship between parameters and model output (such as linearity) and the results are easily interpreted in a lucid, graphical way. Moreover, it provides a global impression of parameter importance instead of a local value. Thus, the effect of a parameter on the model output is assessed in multiple regions of the parameter space rather than in a fixed (base case) point in that space. This feature allows for exploration of non-linearity and interaction effects in the model.

A possible drawback of the method is that it does not consider dependencies between parameters. In situations where a lot of information on the uncertainty or variability of the parameters is available this might be restrictive, but in the current study this is hardly the case.

In this method the sensitivity of the model output for a given parameter is related to the *elementary effects* of that parameter. An elementary effect of a parameter is the change in the model output as a result of a change Δ in that parameter, while all other parameters are kept at a fixed value. By choosing the variation Δ for each parameter as a fixed fraction of its central 95% confidence interval, the elementary effects become a measure of parameter importance.

Clearly, if the model is non-linear in the parameters or if parameters interact, the value of the elementary effect of a parameter may vary with the point in the parameter space where it is calculated. Hence, to obtain an impression of this variation, a number of elementary effects are calculated at randomly sampled points in the parameter space.

A large sample mean of the elementary effects for a given parameter indicates an important "overall" influence on the output. A large standard deviation indicates an input whose influence is highly dependent on the values of the parameters, i.e. one involved in interactions or whose effect is nonlinear.

Hence, an overview of the output of the sensitivity analysis can be obtained from a figure in which sample mean and standard deviation of the elementary effects are plotted for each of the parameters.

Technically, the procedure is implemented as follows. Each of the k model parameters is scaled to have a region of interest equal to [0,1]. The scaled k-dimensional parameter vector is denoted by $\underline{x}$. For each parameter, the region of interest is discretized in a p-level grid, where each x_i may take on values from {0, 1/(p-1), 2/(p-1), ... ,1}.
The elementary effect d of the i-th input is then defined by:

$$d_i(\underline{x}) = \frac{y(x_1,...,x_i+\Delta,...,x_k) - y(\underline{x})}{\Delta}$$

where y is the model output, i.e. the performance indicator TO or TO*, $x_i \leq 1-\Delta$ and Δ is a predetermined multiple of 1/(p-1).

The estimates for the mean and standard deviation of the elementary effects are based on independent random samples of the elementary effects. The samples are obtained by application of carefully constructed sampling plans.
The general procedure to assess one single sample for the elementary effect of each parameter is as follows. Initially, the parameter vector is assigned a random base value (on the discretized grid). An observation of the model output is made. Then a 'path' of k orthogonal steps through the k-dimensional parameter space is followed. The order of the steps is randomized. After each step an observation is made and the elementary effect associated with that step is assessed.
With this procedure a set of r independent samples for the elementary effects can be obtained by repeating this procedure r times. An illustration for a 3-dimensional parameter space is presented in Figure 3.7.

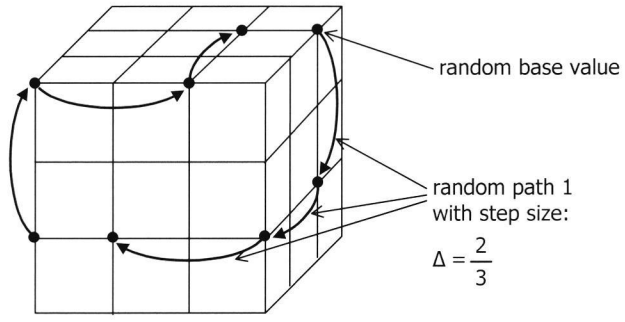

Figure 3.7 Illustration of the procedure to assess two samples of the elementary effect of each parameter. The illustration is for a 3-dimensional parameter space with a 4 level grid (k = 3, p = 4, r = 2).

Validation technique

The screening method enables a comparison of the importance of individual parameters on the basis of their elementary effects. With this comparison, a limited set of parameters can be identified, which probably accounts for the bulk of the uncertainty in the model output. However, in case of strong interaction effects in the model, individual parameter importance may not provide reliable guidance. Although the selected screening technique is designed to incorporate parameter interactions into the

individual parameter effects to some degree, it is sensible to validate that the allegedly important set of parameters is indeed the set that was aimed for.

The validation is implemented as a Monte Carlo simulation study. Three sample matrices were used. The first sample matrix contained the Latin Hypercube sample that was used in the propagation (see Section 3.3). The second sample matrix was identical to the first one for the allegedly important parameters, but contained base case values (mean values) for the other parameters. The last sample matrix was a 'mirror' of the second one: mean values for the candidate important parameters, while identical to the first sample matrix for the other parameters.

By comparison of the variances in the model output resulting from the three sample matrices, the fraction of the total variance explained by the important parameters can be assessed as well as the fraction that is explained by the remaining parameters.

3.4.3 Results

Screening results

In this study, the 89 parameters ($k = 89$) were discretized on a 4-level grid ($p = 4$). The elementary step Δ was chosen to be 2/3, as shown in Figure 3.7. For each parameter 5 independent samples ($r = 5$) of the elementary effects on both the static comfort performance indicator TO and the adaptive indicator TO* were assessed in 450 simulation runs with the BFEP-implementation of the building model (see Section 2.3.7). The mean values of TO and TO* over these runs were 170 hours and 140 hours respectively. Figure 3.8 shows for each parameter the sample mean m_d and the standard deviation S_d of the observed elementary effects on the static performance TO. Similarly, Figure 3.9 shows these statistics of the elementary effects on the adaptive indicator TO*.

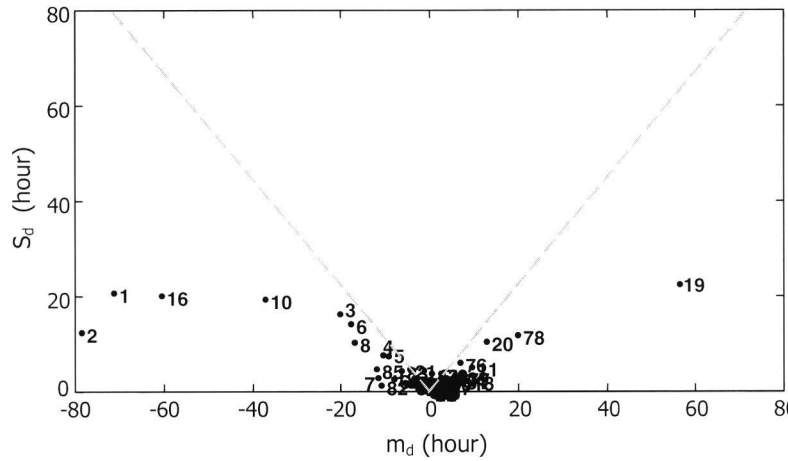

Figure 3.8 Sample mean m_d and standard deviation S_d of the elementary effects on the static comfort performance indicator TO obtained in the parameter screening. The numbers in the plot are the parameter indices (see Table 3.2). The dotted lines constituting the wedge are described by $m_d = \pm 2\ S_d/\sqrt{r}$. Points above this wedge indicate significant non-linear effects or parameter interactions.

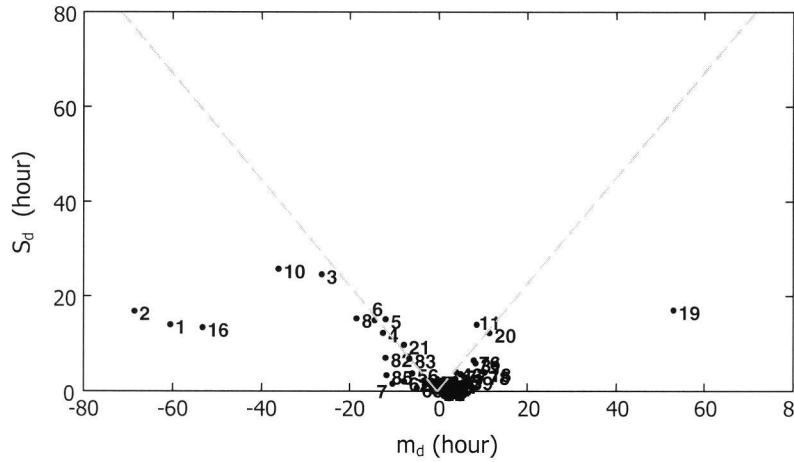

Figure 3.9 Sample mean m_d and standard deviation S_d of the elementary effects on the adaptive comfort performance indicator TO obtained in the parameter screening. The numbers in the plot are the parameter indices (see Table 3.2). The dotted lines constituting the wedge are described by $m_d = \pm 2\ S_d/\sqrt{r}$. Points above this wedge indicate significant non-linear effects or parameter interactions.*

The dotted lines, constituting a wedge, are described by $m_d = \pm 2\ S_d/\sqrt{r}$, where $S_d/\sqrt{r}$ is the standard deviation of the mean elementary effect. If a parameter has coordinates (m_d, S_d) below the wedge, i.e. $|m_d| > 2\ S_d/\sqrt{r}$, this is a strong indication that the mean elementary effect of the parameter is non-zero. A location of the parameter coordinates above the wedge indicates that interaction effects with other parameters or non-linear effects are dominant.

Table 3.2 shows the 13 most important parameters found in the screening process in decreasing order of importance. The importance ranking for static and adaptive performance indicators is similar.

Table 3.2 Parameters, which emerge from the parameter screening as most important. The ranking is in decreasing order of importance. The importance ranking for static and adaptive performance indicators is similar.

index	description
2	wind pressure difference coefficients
1	wind reduction factor
16	temperature stratification in space under study
19	local outdoor temperature
10	external heat transfer coefficients
3,4,5,6	discharge coefficients of windows and vents
8	internal heat transfer coefficients in space under study
11	albedo
78	solar transmission of windows
20	solar transmission of sunblinds

Validation results

With all parameters in Table 3.2 included in the set of important parameters, this set explains about 94% of the total variance. The remaining parameters account for 3%, which leaves 3% of the variance unexplained. This 3% of the variance that cannot be attributed to the separate parameter sets apparently originates from interactions between parameters in the individual sets.
When only the top 5 parameters in Table 3.2 are included in the important set, this set still explains 85% of the total variance, leaving 10% for the remaining parameters and another 5% for interactions.

These numbers were found for the static and the adaptive comfort performance alike. They confirm that the parameters in Table 3.2 are the parameters of interest, of which the first five deserve primary focus.

3.5 Discussion and conclusions

Three immediate conclusions can be drawn from the results in the previous sections. First, top 5 parameters in Table 3.2, i.e. the wind pressure difference coefficients, the wind reduction factor, temperature stratification, local outdoor temperature and the model for the external heat transfer coefficients are the parameters which account for the majority of the uncertainty in the model output.
Second, although several parameters of secondary importance line up along the wedges in Figure 3.8 and Figure 3.9, indicating the presence of parameter interactions or non-linearity of the model output in the parameters, these effects do not seem to play a significant role. Lomas and Eppel (1992) report similar findings in their sensitivity studies on thermal building models. These studies concerned different model outputs (air temperature and plant power) though, and considered a slighly different set of uncertain parameters.
Finally, the variability in the comfort performance assessments, obtained in the Monte Carlo propagation exercise is significant. This is expressed by the coefficient of variation of 0.5 and the histogram in Figure 3.6. In current practice the simulated value of the performance indicator is commonly compared with a maximum value between 100 - 200 hours (see Section 2.4.4) to evaluate if the design is satisfactory or not under the selected scenario. Figure 3.6 shows that a simulated point value of the performance does not give much basis for such an evaluation. Indeed, simulation results may depict the design as highly satisfactory or as quite the contrary by just changing the values of the model parameters over plausible ranges.

However, the observed spread in the comfort performance values is based on crudely assessed 95% confidence intervals for the model parameters. An improved quantification of the uncertainty in the building performance could be obtained via a more thorough assessment of the parameter uncertainties. Clearly, those parameters, which have been ranked as the most important ones, deserve primary focus.
The ranges for the most important set of parameters, i.e. the wind pressure difference coefficients, have been based on the scatter between various models. Proper use of these

models, though, requires wind-engineering expertise, both to provide reliable inputs to the models and to assess the impact of features in the case under study, which are not covered in the models (see also Chapter 4).
The uncertainty in parameter number 1 in Table 3.2, the wind reduction factor, has been addressed in a similar way. Only two models have been considered here, which both assume neutral stability conditions among other things. For strong winds this assumption is commonly justified, but as the wind velocity decreases, the effect of thermal buoyancy on the wind velocity profile becomes more important. Hence, the range that was selected for this parameter in the sensitivity analysis may be considered as modest. Despite this fact the parameter turns out to be important.
The uncertainty estimate for the thermal stratification in a space has been based on hardly more than the notion that a temperature difference between ceiling and floor of a couple of degrees is not unusual. A fairly crude parameterization of the stratification has been used with an equally crude assumption about the uncertainty in the parameter. As this parameter turns out to be important, the phenomenon deserves further attention, but more merit cannot be attributed to the current uncertainty range or to its contribution to the uncertainty in the building performance.
A similar argument holds for the difference between the local outdoor temperature and the air temperature measured at the meteorological station. The range assumed in this study seems modest when compared to the ranges of values that are reported from measurements. However, due to the complexity of the underlying processes it is difficult to straightforwardly extrapolate the findings in these experiments to the current case. Again, more study is required.
The last of the top 5 important parameters relates to the external heat transfer coefficients. Here, we quantified the ranges on the basis of inter-model scatter, conditional on the surface-parallel wind velocity, which was calculated with the ESP-r algorithm. The assessment of this velocity is however hampered by similar problems to the assessment of wind pressure coefficients, which give reason to believe that an additional contribution to the uncertainty in heat transfer coefficients may be expected from this source.

Summarizing, it is desirable to further investigate the uncertainty in the model parameters, especially the ones identified as most important. The next chapter addresses the uncertainty in the wind pressure difference coefficients. Chapter 5 deals with quantification of the uncertainty in the air temperature distribution in a space. The internal heat transfer coefficients are also addressed in this chapter.

4 Uncertainty in wind pressure coefficients

4.1 Introduction

To simulate natural ventilation flows in buildings, the wind pressure distribution over the building envelope is required. In the design of low-rise buildings, wind tunnel experiments are scarcely employed to measure these wind pressures. Instead, techniques are used which predominantly rely on inter- or extrapolation of generic knowledge and data, e.g. wind pressure coefficients, previously measured in wind tunnel studies and full-scale experiments. Due to the complexity of the underlying physics, this is a process, which may introduce considerable uncertainty. None of the existing techniques, however, accounts for this uncertainty.

In the sensitivity analysis reported in Chapter 3, the effect of the uncertainty in wind pressure coefficients on the output of a building simulation model was compared to the effect of other uncertainties. The output in this study was the building performance with respect to thermal comfort. It was found that the contribution of the wind pressure (difference) coefficients to the overall uncertainty was potentially significant.
The quantification of the uncertainty in the sensitivity analysis, however, did not go beyond the appraisal of the analyst performing the study. The main aim of this chapter is to evaluate the uncertainty in wind pressure coefficients, assessed on the basis of existing data, in a more rigorous way.
To quantify uncertainty, structured elicitation of expert judgment was used. A method to acquire and process the experts' assessments was selected, which has a solid methodological and mathematical foundation. It has been developed in the framework of the joint CEC/USNRC Consequence Code Uncertainty Analysis (Cooke and Goossens, 2000).

As in the previous chapters, this study was carried out in the context of a specific case. The case was designed to tentatively explore the effect of the immediate surroundings of the building on the uncertainty as well as the effect of the pressure tap positions on the building façade. A description of the case has been presented Section 4.2.
Section 4.3 evaluates the option to assess the requested uncertainty from the spread in the output of various models, which have been developed to assess wind pressure coefficients on the basis of a parametric analysis of existing data. The assessment of this uncertainty by means of expert judgment is the subject of Section 4.4. To obtain empirical reference material for the experts' judgments, two wind tunnel experiments were carried out to obtain empirical reference material for the experts' judgments. The set-up of these experiments is briefly addressed in Section 4.4.7. Section 4.5 presents the

results of both wind tunnel and expert judgment studies, followed by the analysis of the acquired data in Section 4.6. The sections with discussion and conclusions conclude the chapter.

4.2 Case definition

4.2.1 Introduction

A widely accepted method to assess wind pressure coefficients in the design stage of a building, is a wind tunnel study. In a wind tunnel, a scale model of the building and its surroundings is immersed in a simulated boundary layer flow. From measurements of both surface pressures and wind velocities or dynamic pressures, pressure coefficients can be assessed.
These wind tunnel values do not fix the required full-scale values without uncertainty. Due to scaling effects and simplifications in both the simulated boundary layer and the wind tunnel model, the acquired pressure coefficients only approximately capture the relation between wind velocities and surface pressures on the full scale building in an actual wind field. For instance, buoyancy effects, which may significantly affect the boundary layer flow at low wind speeds, are absent in a typical wind tunnel flow.

Although potentially important, uncertainties resulting from these effects are not addressed in this chapter. We consider a wind tunnel study as a first step in the assessment of wind pressure coefficients. As mentioned earlier, even this step is not frequently made in the design stage of low-rise buildings. Therefore we aim to answer the question: 'Given the specification of a wind tunnel experiment on a building under design, what is the uncertainty in the requested wind pressure coefficients if these coefficients are assessed on the basis of existing data and generic knowledge, rather than in a specific wind tunnel experiment?' Consequently, the case in this study is defined as a scale model of a building and its surroundings, immersed in a simulated boundary layer in a wind tunnel.

4.2.2 Building and its surroundings

A description of the building and its surroundings has already been given in Section 2.2. The essential elements are recalled here for the sake of convenience.
The case concerns a scale 1:250 wind tunnel model of a four-story office building situated at the outskirts of a town. Figure 4.1 shows the turntable layout with the office building (framed building in the center) and a schematic representation of the obstacles within a radius of 300 m around it. The upper half of the area shows a typical urban setting, which was modeled after a part of the Dutch town Delft to ensure realistic conditions. The lower half is left void, with exception of the embankment of the roadway. This mimics a large open space in an otherwise urban environment.

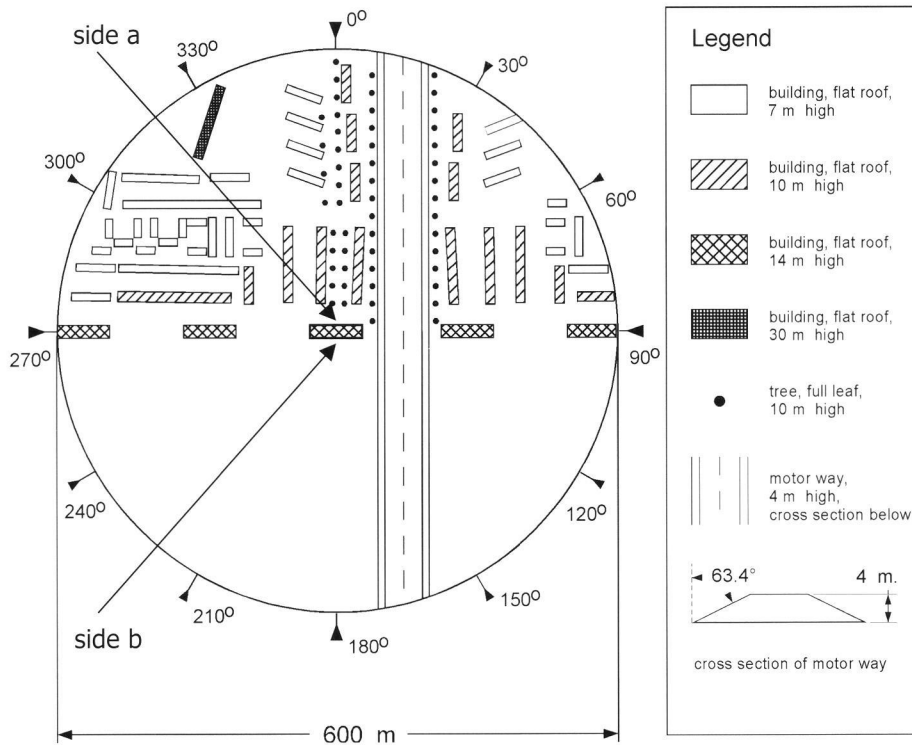

Figure 4.1 Schematic layout of the turntable model. The dimensions refer to full-scale. The model scale is 1:250. The building in the center is the office building under study. Side a and side b are indicated.

4.2.3 Simulated boundary layer

The building group in Figure 4.1 is immersed in a simulated 'urban' boundary layer. In this study we characterize the boundary layer by the profile of the mean horizontal wind speed only. This profile, representing the situation at the center of the empty turntable is shown in Figure 4.2 (scale 1:250). The upper part of the profile approximately matches a log-law profile with roughness length $z_o \approx 3.10^{-3}$ m. This corresponds to a full-scale z_o value of 0.75 m, which reflects urban upstream conditions (e.g. Wieringa, 1993).
This velocity profile corresponds to the 'urban' profile that can be routinely generated in the low speed German-Dutch wind tunnel (DNW-LST). This wind tunnel is located at the facility of the Dutch Aerospace Laboratory (NLR) in the Noordoostpolder in The Netherlands (NLR, 1993).

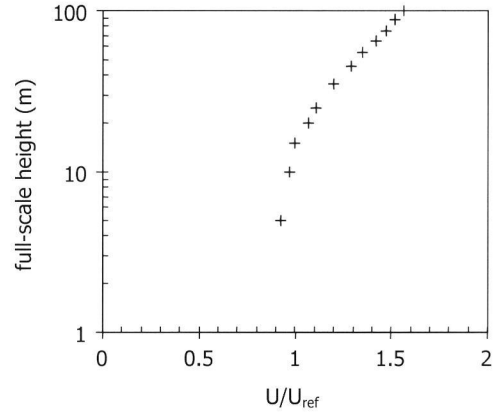

Figure 4.2 Mean velocity profile in the wind tunnel at the center of the empty turntable with 'urban' roughness upstream of the turntable. The reference wind speed U_{ref} is the mean value at 14 m height (full scale, i.e. the roof height of the office building under study) on the empty turntable.

4.2.4 Wind pressure difference coefficients

Figure 4.3 shows the full-scale dimensions of the office building together with the locations of two pairs of pressure taps. The position of the pair of taps at level 1 coincides with the location of two windows at the top-level floor of the building. The other pressure taps 2a and 2b have positions corresponding to the location of windows at the second floor.

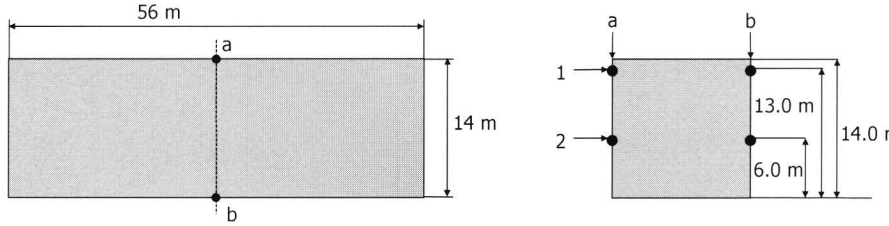

Figure 4.3 Top view of the central building (left) and vertical cross-section (right). Side a is directed to the built-up half of the turntable, whereas side b is directed to the void half. At the center of each side a set of 2 pressure sensors is placed in a vertical line. The positions of the 4 pressure sensors (1a, 1b, 2a, 2b) are marked (●).

The floors are cross-ventilated, so the pressure differences between positions 1a and 1b, and between 2a and 2b are of particular interest as they drive ventilation flows through the offices. These pressure differences are related to the mean reference wind speed U_{ref} by the pressure difference coefficients ΔC_{p1} and ΔC_{p2}, where ΔC_{pi} is defined as:

$$\Delta C_{p_i} = \frac{p_{ia} - p_{ib}}{\frac{1}{2}\rho U_{ref}^2} \tag{4.1}$$

where U_{ref} is the mean horizontal wind speed at building roof height on the empty turntable (see Figure 4.2) and ρ is the density of air.
The ventilation models considered in this thesis take time-averaged pressures as their input. Consequently, (4.1) relates to time-averaged values of both the pressures and the pressure difference coefficients.

4.3 Calculation models for wind pressure coefficients

4.3.1 Introduction

Several models are reported in the literature to assist the assessment of wind pressure coefficients on the basis of existing experimental data. These models are based on parametric analyses of selected data from both wind tunnel and full-scale experiments. As a first step in the exploration of the requested uncertainty, four of these models were used to estimate the wind pressure (difference) coefficients in the case at hand and the spread in their outcomes was analyzed.
A detailed description of these four models can be found in Allen (1984), Swami and Chandra (1988), Grosso (1992, 1995) and Knoll, Phaff and De Gids (1995). A brief summary of the main features of these models is presented in the next section. Subsequently, the model outputs are compared for the current case.

4.3.2 Summary of model features

Allen (1984)

Allen presents a model to assess surface averaged pressure coefficients on rectangular buildings for ventilation purposes. For specific building configurations, and a limited number of locations on the façades, expressions for local pressure coefficients are given. The expressions are based on data from Bowen (1976), Akins, Peterka and Cermak (1975) and Tieleman and Gold (1976).
To assess the local wind pressure coefficients for a specific façade, related to the dynamic pressure at roof height, the model requires the following input:

- wind field:
  - ¬ wind angle relative to the outward normal on the building façade
  - ¬ wind velocity profile, e.g. parameterized by α, the wind velocity profile exponent
- measuring location:
  - ¬ horizontal and vertical position on the façade
- building geometry:
  - ¬ aspect ratio of building plan, i.e. ratio of the depth of the building to the width of the facade under study
- near field geometry:
  - ¬ shelter factor, i.e. ratio of building height to the height of the surrounding buildings

The range of application is restricted to rectangular buildings, i.e. buildings with a rectangular floor plan and a flat roof.

Swami and Chandra (1988)

Swami and Chandra developed a model to assess surface averaged pressure coefficients on low-rise buildings for application in ventilation calculations. The values are related to the dynamic pressure at roof level.

Eight different data sets were used in the parametric analysis underlying the model, i.e. Akins, Peterka and Cermak (1979), Ashley (1984), Cermak et al. (1981), Hamilton (1962), Jensen and Franck (1965), Lusch and Truckenbrodt (1964), Vickery, Baddour and Karakatsanis (1983) and Wiren (1985). The data were aggregated to obtain surface-averaged pressure coefficients, if necessary.

The expressions to calculate the pressure coefficient for a specific façade contain the following variables:

- wind field:
  - ¬ wind angle, relative to the outward normal of the façade
- building geometry:
  - ¬ aspect ratio of building plan, i.e. ratio of the depth of the building to the width of the facade under study

The building geometry is parameterized by the side ratio only in this model, whereas the influence of the velocity profile on the pressure coefficients is ignored in absence of systematic data. Effects of near field are not accounted for in the value of the pressure coefficient, but in a shielding factor on the wind induced ventilation flows. These shielding factors are based on the 5 shielding classes of Sherman and Grimsrud (1982).

As in the current case the (purely wind driven) cross ventilation flows are approximately proportional to the square root of the wind pressure differences (see Chapter 2), the squared shielding factors are assimilated in the pressure difference coefficients in this study.

The range of application is restricted to a building geometry, compliant with:

- aspect ratio of building plan between 1/8 and 1
- eaves height to short wall ratio between 0.1 and 0.4
- ratio of overhang to eaves height between 0 and 0.2
- roof slope between 0° and 60°

Grosso et al. (1992, 1995)

The package CPCALC (Grosso, 1992) was developed at the Lawrence Berkeley Laboratory, University of California, as a component of the multizone air-flow model COMIS (Feustel, 1990). In the framework of the CEC-DGXII PASCOOL programme (Santamouris et Argiriou, 1995) the model was reviewed and the underlying data set enhanced, which resulted in CPCALC$^+$ (Grosso et al., 1995). CPCALC$^+$ models local pressure coefficients on the envelope of buildings with rectangular floor plans. The reference height for these coefficients is building roof height.

It is based on 3 sources of wind tunnel data, i.e. Hussain and Lee (1980), Akins and Cermak (1976) and Da Silva and Saraiva (1993, 1994).

The expressions to calculate the pressure coefficients take the following variables as input:

- wind field:
  - ¬ wind velocity profile exponent α
  - ¬ wind angle relative to outward normal of façade
- measuring location:
  - ¬ horizontal and vertical position on the façade
- building geometry:
  - ¬ frontal aspect ratio, viz. ratio of building length to building height
  - ¬ side aspect ratio, viz. ratio of building width to building height
- near field geometry:
  - ¬ plan area density of upstream terrain
  - ¬ relative building height, viz. ratio of building height to height of surroundings

Valid output of the model is *not* warranted in conditions with:

- wind field:
  - ¬ $\alpha > 0.33$
- building geometry:
  - ¬ irregular shape or overhangs
  - ¬ aspect ratios (side or frontal) less than 0.5 or greater than 4
- near field geometry:
  - ¬ plan area density > 50%
  - ¬ plan area density > 12.5% if building of interest has a different height from its surroundings or a different shape from a cube
  - ¬ staggered or irregular pattern layout
  - ¬ height of building under study more than 4 times height of surrounding buildings or less than half their height.

Knoll, Phaff and De Gids (1995)

The Cp-generator, a computer tool, was developed at TNO, Delft, to predict local pressure coefficients on building surfaces as input to ventilation simulations (Knoll, Phaff, De Gids, 1995, Knoll and Phaff, 1996). The default reference height for these coefficients is building roof height.

The Cp-generator is based on both wind tunnel measurements (Phaff, 1977, 1979) and full scale experimental data (Lugtenburg, Den Ouden and De Gids, 1972, Eaton, Mayne and Cook, 1975, Wells and Hoxey, 1980).

The basis of the model is a formula, describing the general relation of wind pressure and wind direction for an unshielded object. This relation, presented in Phaff (1977) and Walker and Wilson (1994), is fitted to data from wind tunnel experiments (Phaff, 1977, 1979). With a set of additional formulas, in terms of the building dimensions and azimuth, the locations of the pressure taps and the terrain roughness, the wind pressures on different locations on the roof and each façade can be predicted.

The expressions for the pressures on sloped roofs are derived from an analysis of full scale data (Lugtenburg, Den Ouden and De Gids, 1972, Wells and Hoxey, 1980). The

effect of repeating roof slopes (e.g. greenhouses) was modeled on the basis of experimental results from Eaton, Mayne and Cook (1975).
Shielding by nearby obstacles is taken into account as a correction on the unshielded pressures, based on both the distance and angle between the building and the obstacle and the pressure at the leeward surface of the obstacle. This leeward pressure is calculated analogously to the leeward pressures on the building under study.

The output of the program should be handled with caution for:
- buildings with non-rectangular floor plans
- complex surroundings (non-block shaped obstacles, strong flow-interaction effects between obstacles and/or obstacles and building under study)

4.3.3 Comparison of model outputs

To obtain a first impression of the uncertainties in pressure difference coefficients derived from existing data, these models were used to estimate the pressure difference coefficients in the current case for 7 equidistant wind angles between 0° and 180° as indicated in Figure 4.1. The models by Allen, Knoll et al. and Grosso allow for the assessment of the local coefficients ΔC_{p1} and ΔC_{p2}. Their output is shown in Figure 4.4 and Figure 4.5. Swami & Chandra developed a model, which calculates façade averaged pressure coefficients. Figure 4.6 shows the results of Swami & Chandra's model together with those of Allen and Grosso, which also allow for the assessment of façade averaged coefficients.
The figures show that whereas the spread in the outputs from the different models for ΔC_{p1} is considerable, they agree rather well on ΔC_{p2} except for 0°. The degree of consensus on the façade-averaged coefficients strongly depends on the wind angle.

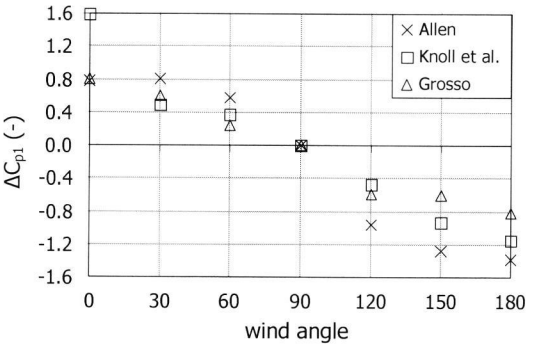

Figure 4.4 Wind pressure difference coefficients ΔC_{p1}, assessed on the basis of existing data according to three different models. The data points are identical to those shown in Figure 3.2.

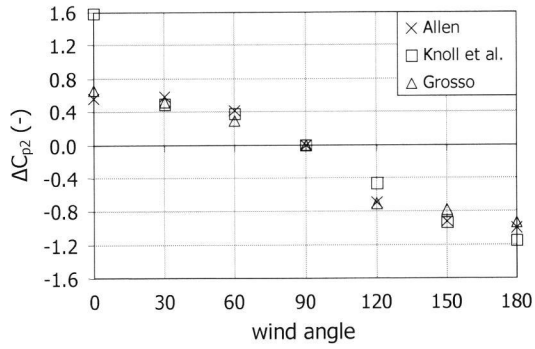

Figure 4.5 Wind pressure difference coefficients ΔC_{p2}, assessed on the basis of existing data according to three different models.

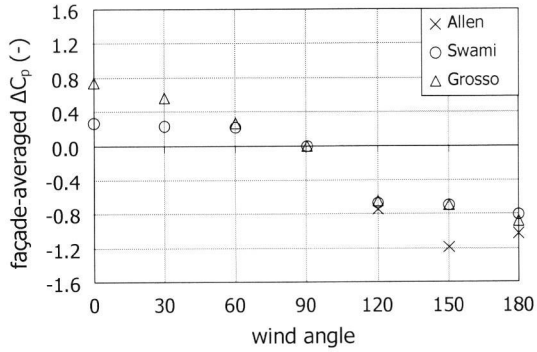

Figure 4.6 Façade averaged wind pressure difference coefficients, assessed on the basis of existing data according to three different models.

If we would consider adopting the scatter in the model outcomes as a measure of the uncertainty, it is important to contemplate which factors contribute to that scatter and, more importantly, which do not.

First, the model outcomes depend on the choices of the analyst:

- Several models require a characterization of the velocity profile in terms of α or z_0. Which values most adequately represent the profile in Figure 4.2?
- The case at hand is out of the range of application of some of the models. Are the outcomes still appropriate?
- If the surroundings of the central building have to be classified in a 'shielding' class, which class description best fits the current case?

Moreover, not all uncertainty is captured in the variation of the model outcomes:

- The scatter in the experimental data on which the models are based is eliminated by regression or averaging. Part of this scatter may be measurement error, but part of it results from effects unexplained by the model. Models sharing the same parameters most likely ignore the same effects.

- There is overlap in the data sets underpinning the different models. This overlap introduces a dependency between the model predictions.
- The majority of the data underlying the models that assess the effect of the near field were obtained in (wind tunnel) experiments with regularly arranged near field layouts. The near field in this case is irregular and consists of buildings of different heights.

Although the results of this exercise support the assumption that significant uncertainty exists in wind pressure coefficients, predicted on the basis of existing data, they do not provide a proper basis to assess this uncertainty. Wind-engineering expertise is required, both to provide reliable inputs to the models and to assess the impact of features in the case under study, which are not covered in the existing models.

Hence, the uncertainty in these pressure coefficient assessments can best be quantified by experts in the field. These experts are acquainted with the complexity of the underlying physics and hence best suited to interpolate and extrapolate the data they have available on the subject and assess the uncertainties involved. The next section reports on an experiment in which expert judgment was used to quantify the uncertainties in the wind pressure difference coefficients in the case at hand.

4.4 Expert judgment study

4.4.1 Introduction

In an expert judgment study, uncertainty in a variable is considered as an observable quantity. Measurement of this quantity is carried out through the elicitation of experts, viz. people with expertise in the field and context to which the variable belongs. These experts are best suited to filter and synthesize the body of existing knowledge and to appreciate the effects of incomplete or even contradictory experimental data.
The uncertain variables are presented to the experts as outcomes of (hypothetical[22]) experiments, preferably of a type the experts are familiar with. They are asked to give their assessments for the variables in terms of subjective probability distributions, expressing their uncertainty with respect to the outcome of the experiment. Combination of the experts' assessments aims to obtain a joint probability distribution over the variables for a (hypothetical) decision-maker (DM), who could use the result in his/her decision problem. This resulting distribution, which is referred to as the DM, can be interpreted as a 'snapshot' of the state-of-the-knowledge, expressing both what is known and what is not known.

To meet possible objections of a rational decision maker to adopt the conclusions of an expert judgment study, which are based on subjective assessments, it is important that a number of basic principles are observed. These include:

[22] The hypothetical experiments are physically meaningful, though possibly infeasible for practical reasons.

- Scrutability/accountability: all data, including experts' names and assessments, and all processing tools are open to peer review.
- Fairness: the experts have no interest in a specific outcome of the study.
- Neutrality: the methods of elicitation and processing must not bias the results.
- Empirical control: quantitative assessments are subjected to empirical quality controls.

Cooke and Goossens (2000) present a procedure for structured elicitation and processing of expert judgment, which takes proper account of these principles. The main features of this procedure are:

- The experts are elicited on experimentally observable quantities only.
- The experts' rationales, underpinning their assessments, are documented.
- The combination of the experts' assessments is based on their performance, which is obtained from a statistical comparison of their assessments on so-called *seed* variables with measured realizations of these variables.

This procedure was closely followed here. The case described in section 4.2 was presented to six experts, renowned for their expertise in the field of wind pressure measurements on low-rise buildings. For each of the twelve wind angles in Figure 4.1 they were individually asked to assess the values of ΔC_{p1} and ΔC_{p2}, which would be found if this model would be examined in a wind tunnel with the velocity profile shown in Figure 4.2. Each expert's assessment of a coefficient did not consist in a 'best estimate', but in a median value plus a central 90% confidence interval expressing his uncertainty. Probability distributions were constructed for each expert from his assessments on the basis of the principle of minimal information (see Appendix C.1, Cooke, 1991).
The values of ΔC_{p1} and ΔC_{p2} for the 12 wind angles were also measured in two separate wind tunnel experiments. On the basis of a statistical comparison of the experts' assessments with the measured data, the experts' performances could be scored.
For each pressure difference coefficient and each wind angle a single (marginal) probability distribution (DM) was constructed by taking a weighted average of the individual experts' probability distributions. The experts' weights were determined on from their performances.

It is an unusual situation that the variables on which the experts are elicited can also be measured. Indeed, in a regular setting expert judgment is used to quantify (the uncertainty in) variables, which cannot be measured. In that case, separate *seed* variables are added to the questionnaire. These variables can be measured and are used to determine the performances of the experts.
In this study, it is possible to measure the variables of interest, but in a practical building design context this is never done. Hence, the question is what the uncertainties in the wind pressure difference coefficients are, when only generic knowledge and data are used to assess these coefficients. This creates a comfortable situation, in which no separate seed variables have to be included in the questionnaire. Instead, the variables of interest can be measured and used to score the experts' performances.

The next sections discuss the implementation of the procedure in this study. If necessary, concise background information is provided. The most important notions involved in the combination of the experts' judgments are briefly clarified in Appendix C.1. For further reading see Cooke (1991) and Cooke and Goossens (2000). Similar approaches in civil engineering applications can be found in Elst (1997) and Haar et al. (1998).

4.4.2 Questionnaire

In the approach according to Cooke and Goossens, each question is posed to the experts in the context of a case. The case describes a hypothetical experiment and requests the experts to assess the outcome of this experiment in a specific format.
In this study, all cases referred to the same hypothetical wind tunnel test as described in Section 4.2. The only difference between the cases was the wind angle, which took values from 0°, 30°, ..., 330° (see Figure 4.1). In each case, the experts were asked to state three quantile values of their subjective distributions over the wind pressure differences $\Delta C_{p,1}$ and $\Delta C_{p,2}$. Moreover, they were requested to quantify the statistical dependencies between a number of the wind pressure difference coefficients in different cases.

Quantile assessments

For each of the twelve wind angles shown in Figure 4.1, the experts were asked to fill out a table similar to Table 4.1.

Table 4.1 Quantile values of the wind pressure difference coefficients to be assessed by the experts for each of the twelve wind angles.

wind angle	variable	quantile values		
		5%	50%	95%
0°	ΔC_{p1}			
	ΔC_{p2}			

In making their assessments, the experts were requested to assume all information, presented in the context of the case definition, without uncertainty. All information not specified in the case definition should be considered as uncertain. This uncertainty should be accounted for in their assessments if deemed significant.

The choice between direct elicitation of the difference coefficients and the obvious alternative to calculate the differences from expert assessments of the individual pressure coefficients for both façades was made deliberately. The latter approach would require that the experts not only assess the quantile values for the pressure coefficients, but also the statistical dependency between these coefficients. This would burden the elicitation and draw heavily on the ability of the experts to assess their subjective dependencies. Of course, the experts were free to use this approach if they preferred to, but it was not imposed by the structure of the questionnaire.

Dependencies

The ΔC_{p1}'s and ΔC_{p2}'s, assessed by the experts, are considered to pertain to two different building simulation models. The ΔC_{p1}'s are parameters in a thermal simulation model for spaces at the top floor, whereas the ΔC_{p2}'s act in a similar model for spaces at the second floor. Due to the building layout, these simulations can be carried out independently and statistical dependencies between ΔC_{p1}'s and ΔC_{p2}'s need not be considered.
However, as pressure difference coefficients for different wind angles are parameters of the same model, dependencies between these variables are potentially important. Hence, it was decided to elicit these dependencies from the experts.

A common way to represent dependencies between variables is in the form of a (rank) correlation matrix. Clearly, it would have been impossible to elicit all elements of the correlation matrices for both the $\Delta C_{p,1}$'s and $\Delta C_{p,2}$'s. The experts should have constructed 2 positive definite matrices by assessing a total of 132 off-diagonal terms.
As an alternative, a technique for representing dependence called 'dependence trees' was used (Meeuwissen and Cooke, 1994). Between the variables, a tree (an acyclic undirected graph) of dependence relations is defined. This tree counts n-1 arcs, n being the number of variables, and each arc is assigned a rank correlation value. On the basis of these n-1 values a rank correlation matrix can be constructed, which together with the marginal distributions represents a distribution that has minimal information relative to the independent joint distribution (the product of the marginals).

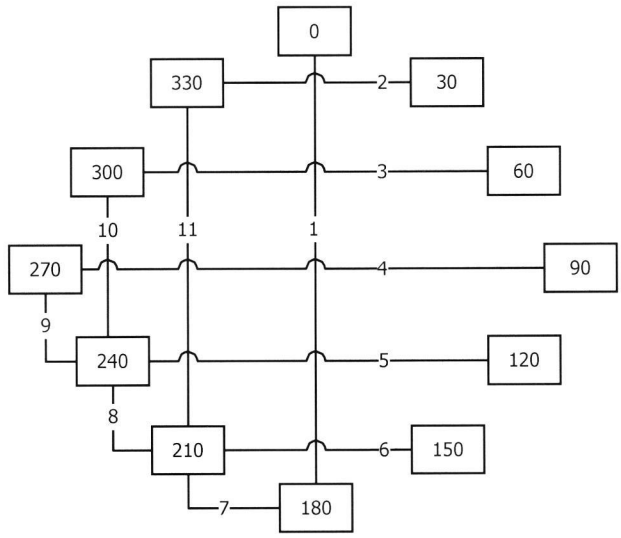

Figure 4.7 Dependence tree presented to the experts in the final questionnaire. The numbers in the boxes are the wind angles. The connecting lines are the arcs of the tree, which are numbered for reference.

A further reduction of the number of dependencies to be elicited was suggested in discussions with the experts, mainly in the dry-run stage. They indicated that the

dependencies between $\Delta C_{p,1}$'s and $\Delta C_{p,2}$'s would be very similar. Hence, it was decided to ask the experts to assess the dependency values between the $\Delta C_{p,2}$'s only and use the result for the $\Delta C_{p,1}$'s as well (see Figure 4.7). In this approach, the experts would have to elicit 11 dependencies only, which was deemed viable.

The 11 rank correlations were not elicited directly. Even trained statisticians have difficulty assessing rank correlations (Gokhale and Press, 1982). Therefore an alternative approach was used, which has been successfully deployed in the joint CEC/USNRC accident consequence uncertainty analysis (Harper et al., 1994). For each couple of wind angles (arc) in Figure 4.7, the experts were asked to state the following conditional probability:

Suppose one of the two pressure difference coefficients in the couple is observed in an experiment and its value is found to exceed your median assessment. What is your (subjective) probability that, in the same experiment, the other pressure difference coefficient in the couple will also fall above your median value?

Under suitable assumptions (among which minimal information), this conditional probability can be uniquely transformed to a rank correlation (Cooke and Kraan, 1996).

4.4.3 Selection of the experts

A pool of candidates for the expert panel was established by screening the literature on relevant issues like wind-induced pressures on low-rise buildings in complex environments and wind-induced ventilation of buildings. Main sources were the Journal of Wind Engineering and Industrial Aerodynamics and AIRBASE, the Bibliographic Database of the International Energy Agency's Air Infiltration and Ventilation Centre. A selection of internal reports from several Dutch institutes was also included in the screening process.

Table 4.2 List of experts in the experiment

Willem de Gids, Bas Knoll, Hans Phaff	The Netherlands Organization for Applied Scientific Research (TNO), Delft, The Netherlands
Jacques-André Hertig	Laboratoire de Systèmes Energétiques EPFL, Lausanne, Switzerland
Brian Lee	University of Portsmouth, Portsmouth, UK
David Surry	The University of Western Ontario, London, Canada
Ton Vrouwenvelder	Technische Universiteit Delft, Delft, The Netherlands
Eddy Willemsen	Duits-Nederlandse Windtunnel, Noordoostpolder, The Netherlands

Seven experts were selected on the basis of the following criteria:

- access to relevant knowledge
- recognition in the field
- impartiality with respect to the outcome of the experiment
- familiarity with the concepts of uncertainty
- diversity of background among multiple experts
- willingness to participate

One of the experts withdrew in the training stage, as he did not appreciate the concept of subjective probability. The final panel consisted of the experts listed in Table 4.2 (in alphabetical order). The team of Willem de Gids, Bas Knoll and Hans Phaff from TNO worked together and produced one single set of assessments. They will be referred to as a single expert. Ton Vrouwenvelder and Eddy Willemsen also acted as experts in the dry run (see section 4.4.5).

4.4.4 Expert training

It would have been unwise to confront the experts with the questionnaire without giving them some training on beforehand. None of the experts but one had ever participated in an experiment involving structured elicitation of expert judgment, so they were unacquainted with the motions and underlying concepts of such an experiment. Moreover, acting as an expert entails the assessment subjective quantile values and subjective probabilities, a task the experts are not familiar with. Extensive psychological research (Kahneman et al, 1982, Cooke, 1991) has revealed that untrained assessors of subjective probabilities often display severe systematic errors or biases in their assessments.

Hence, a concise training program for the experts was developed (Wit, 1997a) to:
- provide an overview of the process
- develop confidence
- introduce the experts to the task they must perform
- instill awareness and control of biases
- practice making probabilistic judgments

The training consisted of two parts:
- Self-study by the experts before making their assessments (3 hours).
- Consolidation during the meeting with each expert individually, prior to the actual elicitation (1 hour).

The training included two miniature expert judgment experiments, one with 'almanac questions' and one similar to the actual experiment. In both experiments, the experts received quantitative feedback on their performance and biases, if any.

4.4.5 Dry-run

The aim of the dry-run was to obtain feedback on the issues:
- are the questions clear and unambiguous?
- can the training material be studied in the allocated time and are the training goals achieved?
- can the elicitation be completed within the allocated time?

The dry-run meetings proceeded exactly as the actual elicitation meetings were planned: a brief consolidation of the expert training followed by the elicitation, in which the expert explicated his assessments to the analyst. However, some extra time was reserved to discuss the issues mentioned above.

The dry run revealed that the required time to complete the training and the elicitation was estimated reasonably well. Furthermore, the design of the dependence tree was completed in this stage (see Section 4.4.2).

4.4.6 Elicitation

The experts were contracted to spend 2 days on their assessments, of which about 1.5 days were allotted to the elicitation. In this stage, the core of the experiment, the experts make their judgments available to the analyst. Individual meetings with each expert were arranged. Moreover, the experts were specifically asked not to discuss the experiment among each other. In this way, the diversity of viewpoints would be minimally suppressed.
The elicitation took place in three parts. Prior to the elicitation meeting, each expert prepared his assessments e.g. by looking up relevant literature and making calculations. During the meeting, these assessments were discussed with the analyst, who avoided giving any comments regarding content, but merely pursued clarity, consistency and probabilistic soundness in the expert's reasoning. On the basis of the discussion, the expert revised and completed his assessments if necessary.
Completion of the elicitation coincided with the writing of the rationale, a report documenting the reasoning underlying the assessments of the expert. During the writing of this rationale, which was done by the analyst to limit the time expenditure of the expert to a minimum, issues that had not been identified in the meeting were discussed with the expert by correspondence.

Several of the experts chose to separately assess the wind pressure coefficients on side *a* and side *b* plus their dependency and calculated the assessments for the pressure difference coefficients from those numbers. These calculations were generally carried out with rather crude statistical techniques. In those cases, the analyst proposed to carry out the calculations on behalf of the expert in concordance with the mathematical framework underlying the selected procedure for elicitation and processing of expert judgment. All experts in question agreed, but did no longer take the responsibility for the resulting pressure difference coefficients[23].
The experts' rationales can be found in Wit (1999a).

4.4.7 Wind tunnel experiments

Introduction

A single probability distribution (DM) for each wind pressure difference coefficient is calculated as a weighted average of the individual experts' distributions. An expert's weight is basically his performance, which is determined by comparing his assessments

[23] This introduces an interesting conceptual problem. Technically speaking, the assessment of the pressure coefficients and their dependencies is the domain of the expert, whereas the calculation of the resulting pressure differences is a statistical manipulation, which is the expertise of the analyst. Therefore, the pursued course of action is a natural one. But on the other hand, the expert will now be scored on the basis of assessments for which he does not take full responsibility.

on so-called seed variables with measured realizations of these variables (see Section 4.6). In this way empirical control is implemented.

Commonly, the seed variables form a separate set of variables in the questionnaire, of which (measured) realizations are known or become available to the analyst (not to the experts). It is assumed that the performance of the experts on these seed variables is representative for their performance on the actual variables of interest, for which no observations can be made. To make this assumption plausible, the seed variables must pertain to the experts' domain.
In this particular research situation it was possible to actually measure the variables of interest in a wind tunnel study. Hence, no additional seed variables had to be selected and the performance of the experts could directly be scored on the variables of interest.

To obtain the realizations on the variables, two wind tunnel experiments were carried out once the experts' assessments had been compiled. The first experiment took place in the DNW-LST, the wind tunnel the case was tailored to. The other experiment was conducted in the boundary layer wind tunnel BLWT1 of the University of Western Ontario, London, Canada. In both tests, the same model elements were used.

The turntable model is shown in Figure 4.1. In addition to the 4 taps presented to the experts, pressures were also measured on neighboring positions as shown in Figure 4.8. The purpose of the extra taps was to gather more information on the pressure distribution around the primary taps for possible diagnostic use.

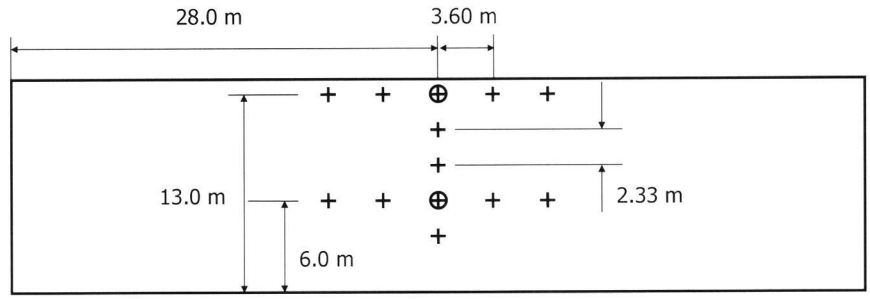

Figure 4.8 Positions of the taps on both long facades (full-scale values). The taps under study in the expert judgment experiment are marked with a circle.

The experimental conditions in both wind tunnels are briefly discussed here. For more details see Willemsen (1998) for the experiment in the DNW-LST, Soerensen (1998) for the UWO test.

Low speed wind tunnel DNW-LST

The DNW-LST has a closed return circuit at atmospheric pressure. The test section has a length of 8.75 m and a cross-section at the position of the turntable of 3.0 m x 2.25 m (width x height).

To generate the requested urban boundary layer, 3 spires and a trip were installed at the entrance of the test section. The floor of the test-section was covered with a staggered array of cubical roughness elements with an edge of 50 mm. The roughness elements extended up to the edge of the turntable. The resulting profiles of both mean velocity and turbulence intensity are shown in Figure 4.9.

From a number of pre-runs, it became clear that pressure coefficients, obtained from 10 s averaged observations with a stationary turntable, agreed well with those, measured in a continuous mode. In this mode, the turntable rotates at an angular velocity of approximately 1°/s and the pressures are sampled at a frequency of 2 Hz. As the continuous mode is faster, this mode was used in the actual tests.
A free stream velocity of 20 m/s was used in the experiments.

The wind tunnel study was carried out by DNW-LST-staff. Further details of the experiment can be found in Willemsen (1998).

Boundary layer wind tunnel UWO-BLWT1

The BLWT1 at the University of Western Ontario is an open-return tunnel. The test section has a length of 28.7 m and a cross-section at the position of the turntable of 2.4 m x 2.1 m (width x height).

To obtain pressure difference coefficients, which could be used as realizations of the seed variables in the expert judgment experiment, the mean velocity profile had to match the 'urban' DNW-LST profile as closely as possible. Indeed, experts had made their assessments on the basis of the DNW-LST profile (see Section 4.4.1).
The best match was acquired with 3 spires and a 0.35 m trip at the entrance of the test section, approximately 19 m upstream of the center of the turntable. The floor of the test-section was covered with roughly square, soft foam blocks about 20 to 25 mm high. They were mounted on 3 to 4 mm thick masonite boards with 2 or 3 block heights between in a random array. The roughness elements extended up to the edge of the turntable. An additional trip of 0.1 m height was mounted 2.5 m upstream of the turntable center to get a better match with the lower part of the DNW-LST profile.
Pressure data on the building were collected as 30 s averages for 40 wind angles at a free stream wind speed of 13 m/s.

The wind tunnel study was carried out by Lars Soerensen in cooperation with UWO-staff. Further details of the experiment can be found in Soerensen (1998).

Velocity profiles

The profiles, used in the tests are shown in Figure 4.9.

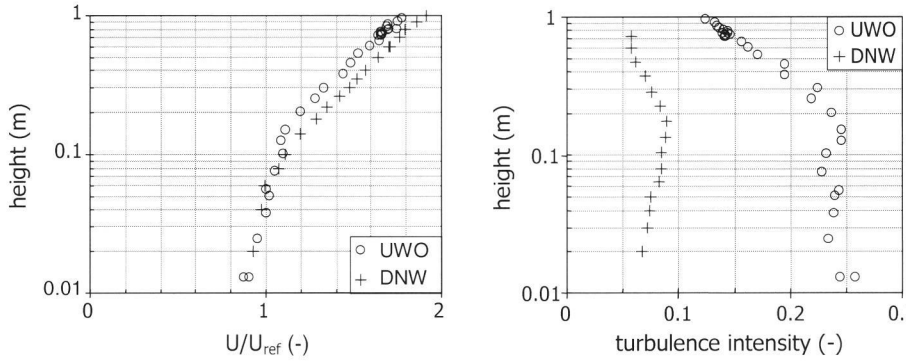

Figure 4.9 Mean horizontal velocity profile (left) and turbulence intensity profile (right) of the boundary layers in the two wind tunnels. The profiles were measured at the center of a void turntable. The reference velocity U_{ref} is the mean horizontal wind velocity at building roof height.

4.5 Results

4.5.1 Wind tunnel results

Figure 4.10 shows the results from both wind tunnel tests. As the purpose of the wind tunnel tests was primarily to obtain empirical reference material for the expert judgment study, only the wind pressure difference coefficients are shown here. The wind tunnel results are covered in more detail in appendix C.3.

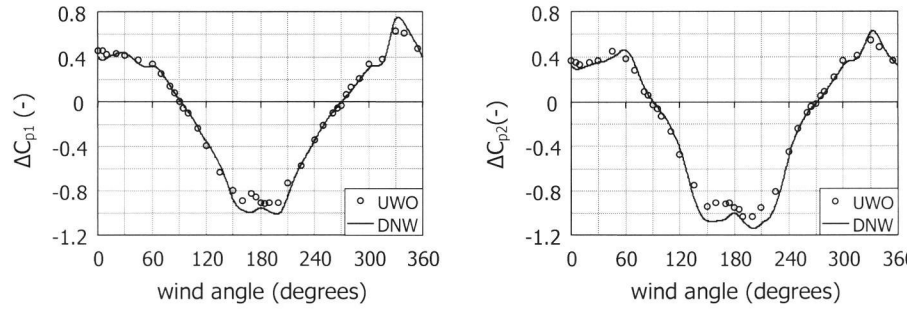

Figure 4.10 Wind tunnel results from both DNW-LST and UWO-BLWT1 tunnels. The symbols are the 30s averages, measured in the UWO tunnel. The drawn lines show moving averages of the DNW-results. The realizations, used to score the experts were taken from these moving average curves.

The results from both wind tunnels are in good agreement, except for the 'isolated' wind angles, where the pressure differences are most sensitive to the characteristics of the simulated boundary layer.

4.5.2 Experts' assessments

Figure 4.11 and Figure 4.12 give an itemwise presentation of the results of both the experts' assessments and the wind tunnel results.

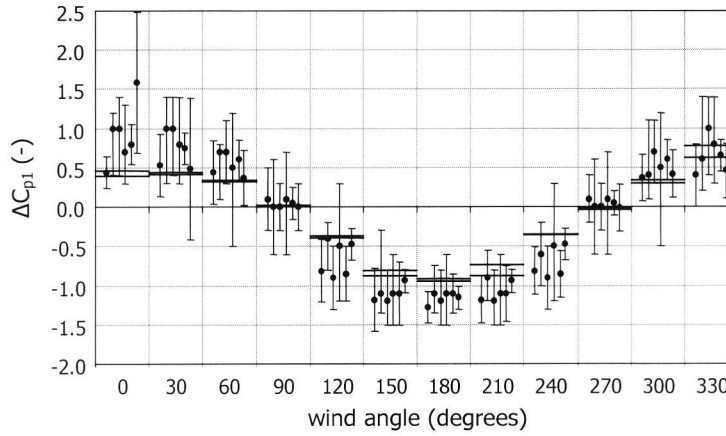

Figure 4.11 Assessments of the 6 experts for the $\Delta C_{p,1}$'s. The dots are their median values, the error bars their central 90% confidence intervals. The drawn horizontal lines show the realizations from the two wind tunnel tests. For each wind angle, the results of experts 1 through 6 are shown from left to right.

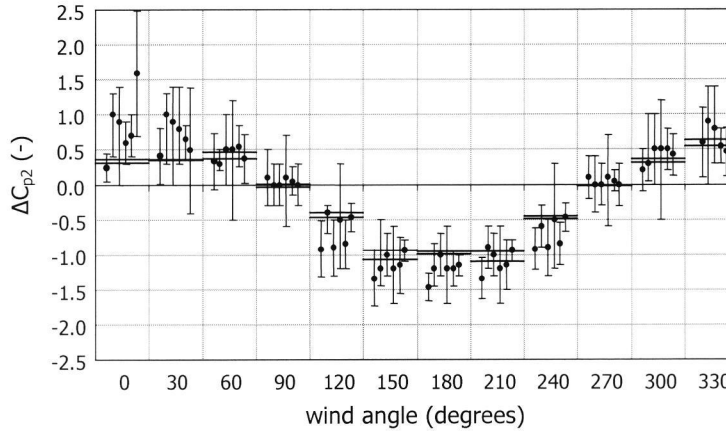

Figure 4.12 Assessments of the 6 experts for the $\Delta C_{p,2}$'s. The dots are their median values, the error bars their central 90% confidence intervals. The drawn horizontal lines show the realizations from the two wind tunnel tests. For each wind angle, the results of experts 1 through 6 are shown from left to right.

Figure 4.11 and Figure 4.12 refer to the experts by number. These numbers were randomly attributed to the experts in Table 4.2 and will be used throughout this chapter.

In Figure 4.13 and Figure 4.14 the assessments are shown expertwise.

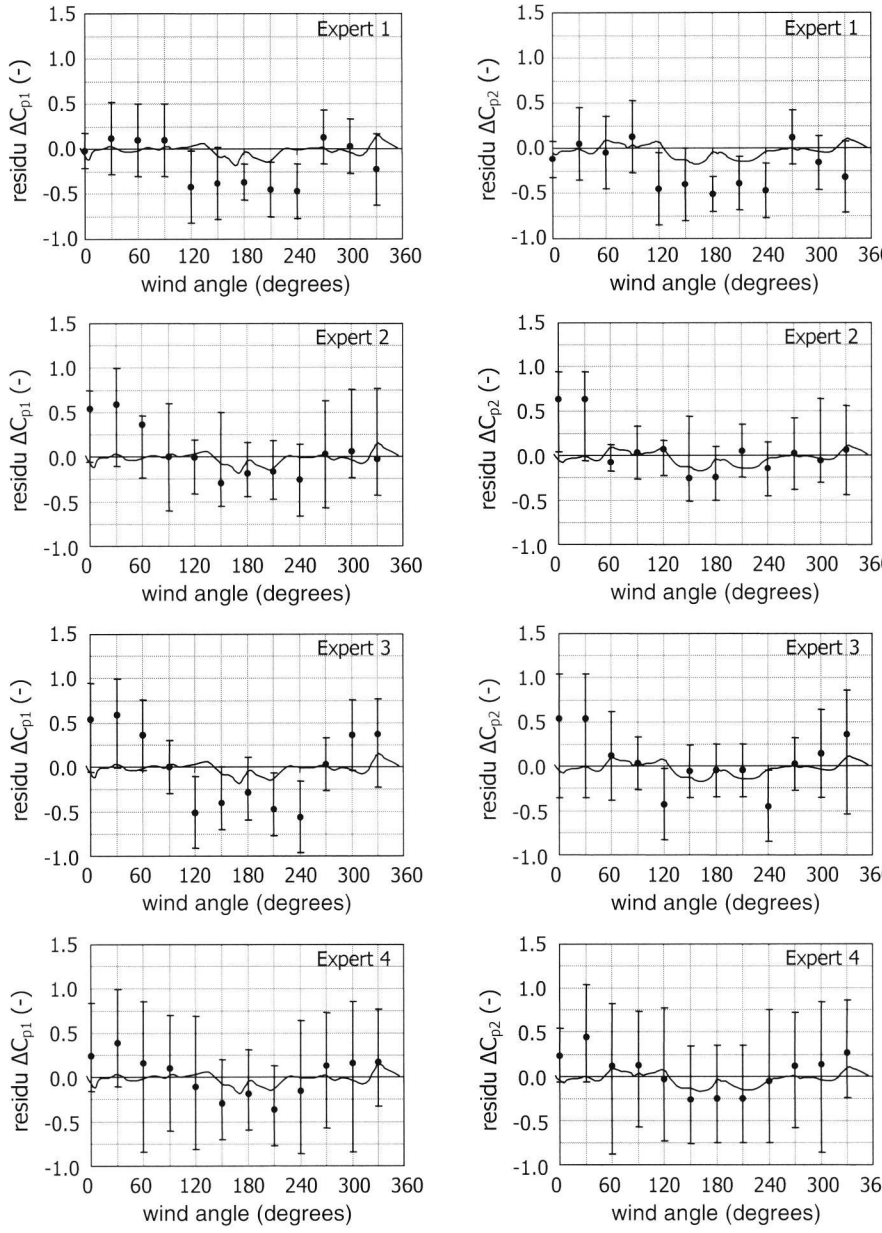

Figure 4.13 Expertwise presentation of the assessments of experts 1 through 4. The graphs show all data relative to the realizations of the UWO-BLWT1 experiment. The dots are the median estimates of the experts, the error bars represent their 90% confidence intervals. The drawn lines show the moving averages of the DNW-LST results relative to the UWO- BLWT1 data.

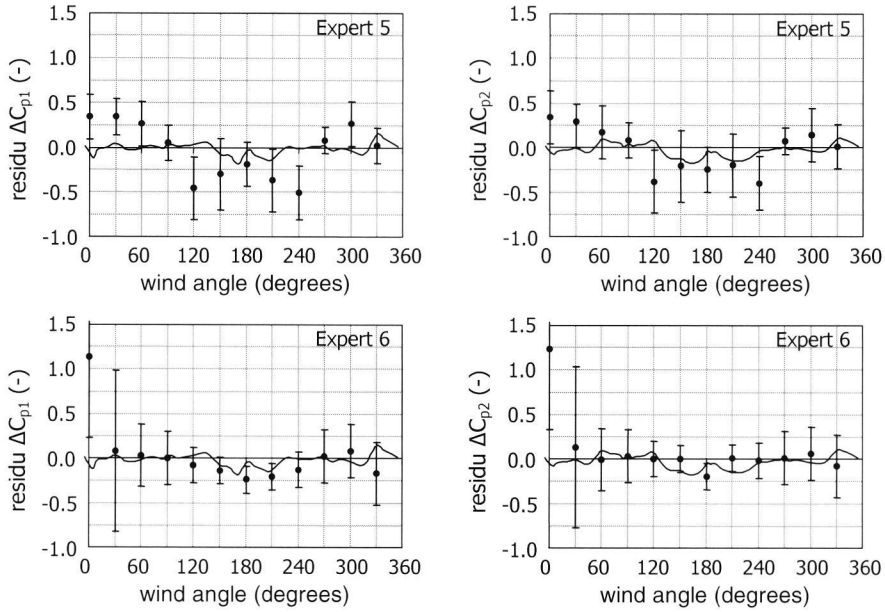

Figure 4.14 Expertwise presentation of the assessments of experts 5 and 6. The graphs show all data relative to the realizations of the UWO-BLWT1 experiment. The dots are the median estimates of the experts, the error bars represent their 90% confidence intervals. The drawn lines show the moving averages of the DNW-LST results relative to the UWO- BLWT1 data.

Tables with all results can be found in Appendix C.2. The experts' dependency assessments are also listed in this appendix.

4.6 Analysis of the expert data

4.6.1 Introduction

To obtain a single (joint) distribution for the decision-maker (DM) over all variables, the experts' assessments must be combined. This involves three issues:

1. Construction of a (marginal) probability distribution from the three elicited quantile values for each variable and each expert.
2. Combination of the resulting marginal distributions for each variable.
3. Combination of the experts' dependency assessments.

The first issue is briefly addressed in Section 4.6.2. To deal with steps 2 and 3 the classical model (Cooke, 1991) is adopted in this study. The classical model uses weighted averaging of the experts' marginal distributions and dependency assessments to obtain the distribution for the decision-maker (DM). This reduces the combination problem to determining the weights. The experts' weights are based on their performances, which are scored on the basis of a statistical comparison between their assessments and the measured realizations on the seed variables.

Section 4.6.3 gives a brief introduction to performance, a central notion in the classical model, and reviews the performance scores of the experts in this study. The subsequent section addresses the performance-based combination of the experts' marginal distributions, whereas Section 4.6.5 discusses the combination of their dependencies. Finally, Section 4.6.6 is dedicated to a robustness analysis of the resulting DM. Additional information on the classical model can be found in Cooke (1991) or (in summary) in Appendix C.1.

4.6.2 From quantile values to a marginal distribution

For each variable, three values are elicited from the experts. These values correspond to the 5%, 50% and 95% quantiles of their subjective probability distribution. Many probability distributions can be constructed, which satisfy these quantiles. In this study we use the distribution, which has minimum information relative to the uniform distribution on a suitably chosen intrinsic range. A discussion on the choice of the intrinsic range and the distribution of probability mass between the given quantile values can be found in Appendix C.1.

4.6.3 Performance

Introduction

An expert's performance can be scored per variable (or item), or globally. The item performance $w_{e,i}$ of expert e on variable i is defined as the product of two measures, calibration C_e and information score $I_{e,i}$ (Cooke, 1991):

$$w_{e,i} = C_e I_{e,i}$$

Analogously, the global performance w_e of expert e is calculated from:

$$w_e = C_e I_e$$

where his global informativeness I_e is his average information score over all variables.

Roughly, calibration measures the degree to which the observed realizations support the expert's assessments. In scoring calibration, an expert is regarded as a statistical hypothesis: 'the realizations are samples, drawn independently from distributions corresponding to the expert's quantile assessments'. The calibration score can be interpreted as the minimum significance level at which this hypothesis would not be rejected. Ergo, a calibration score has a value between 0 and 1 and higher scores are better.

The information score indicates how 'tight' the expert's distributions are. It is calculated per variable as the information of the expert's distribution relative to the uniform distribution on the intrinsic range for that variable. It expresses what we learn from the expert's assessments if we initially believe that the variable is uniformly distributed on the intrinsic range. Information scores are always positive and higher scores are preferred.

The fact that an expert's performance is the product of two scores, calibration and information, suggests that he could compensate a low calibration by being highly informative. This is only possible to a limited extent. An expert's performance is dominated by his calibration, as this score may range over five orders of magnitude, whereas the information score rarely varies more than a factor five between experts. Hence, the information score serves to modulate between more or less equally calibrated experts.

It can be shown that this method of scoring experts is 'asymptotically strictly proper', which means that experts on the long run receive the highest weights if they state assessments according to their true beliefs (Cooke, 1991).

Application in this study

Commonly, the experts' performances are calculated on the basis of seed variables, a separate set of variables in the questionnaire, for which observations become available to the analyst in within the duration of the study. In this specific research setting, no separate seed variables were needed, as the variables of interest, on which the experts were elicited, could also be measured. Hence, the experts' performance scores could be calculated on the basis of the actual variables of interest.

For each of the 24 elicited pressure difference coefficients, 2 realizations were obtained in 2 independent wind tunnel experiments. Global calibration and information scores were calculated on the basis of all realizations on all 24 variables[24]. The results are shown in Table 4.3.

Table 4.3 Experts' performance scores, calculated with the classical model on the basis of all 24 ΔC_p's and scaled to an effective number of 10 variables by adjusting the power of the test to 10/24 = 0.42. Details on the calculation of the performance scores can be found in Appendix C.1.

Expert	Calibration C_e	Information I_e	Performance w_e
1	$3.0\ 10^{-2}$	0.65	$2.0\ 10^{-2}$
2	$7.6\ 10^{-1}$	0.55	$4.2\ 10^{-1}$
3	$2.9\ 10^{-1}$	0.46	$1.3\ 10^{-1}$
4	$4.9\ 10^{-1}$	0.17	$8.3\ 10^{-2}$
5	$7.0\ 10^{-2}$	0.81	$5.7\ 10^{-2}$
6	$7.8\ 10^{-1}$	0.73	$5.7\ 10^{-1}$

The first column lists the experts by number. These are the same randomly attributed numbers, which were used in Figure 4.11 through Figure 4.14. In the remainder of this document, the experts will be addressed by their number only. The second column shows the calibration scores for each expert. The global information scores, based on

[24] The sample distribution (see Appendix B.1) was calculated as the average of the two sample distributions for each set of realizations.

the default intrinsic ranges (see Appendix C.1), are in column 3. Finally, the performance, product of calibration and information, is displayed in the last column.

Calibration scores can only be interpreted in relation to the number of seed variables from which they were calculated. The expert scores in Table 4.3 are based on 24 seed variables. However, they have been scaled to an effective number of 10 seed variables, a common number in expert judgment studies, by adjusting the power of the test to 10/24=0.42 (see Appendix C.1).

The high calibration scores in Table 4.3 suggest that the results of the wind tunnel studies are credible as realizations, which are independently drawn from the experts' distributions. However, a closer inspection of the assessments of e.g. expert 4, who has a fair calibration score of 0.49, shows that the realizations are clearly not randomly distributed around his median assessments. Instead, there appears to be a pattern: items with negative realizations tend to be under-estimated, whereas items with positive realizations are over-estimated. This pattern might be the result of a bias, which is accidentally not filtered out as the same number of positively valued and negatively valued quantities are used in the scoring.

To investigate this hypothesis, the rationales of all experts were consulted to find out which approach they had used to assess the requested pressure differences $\Delta C_{p,ab}$ between face a and face b of the building. It turned out that, for each wind angle, the experts first assessed the pressure difference coefficients $\Delta C_{p,wl}$ between windward and leeward side. Subsequently they adjusted the signs to obtain the requested pressure differences between side a and side b. Hence, it was considered more appropriate to score the experts on their initial assessments of the pressure difference coefficients between windward and leeward side. In this way, possible systematic tendencies of any of the experts to over- or underestimate would not be masked. This resulted in the performance scores in Table 4.4[25].

Compared to the calibration scores in Table 4.3, Table 4.4 shows a deterioration of the calibration scores of several of the experts. These experts apparently show a systematic bias in their assessments of the pressure differences between windward and leeward faces. This supported by Table 4.5. This table lists, for each of the experts, whether he shows a tendency to overestimate (median values to high) or underestimate (median

[25] The classical model assumes that the variables on which the experts are scored are statistically independent. Under this assumption, the calibration score can be interpreted as the likelihood of the realizations under the hypothesis that the variables are distributed concordant with the expert's assessments. Clearly it is difficult to uphold this assumption here. Indeed, the experts explicitly state their subjective dependencies between the ΔC_p's for various wind angles. Their assessments reveal notable dependencies.
Dependency decreases the effective number of independent variables. This is most clear when complete dependency exists between the variables. In that case, the experts basically assess one single variable. As the experts were scored on 24 variables in this study, some reduction does not immediately pose a problem as long as the scores only serve to compare experts in the same experiment. However, in a comparison with other expert judgment studies, the effective number of independent variables would be required. No method exists to assess this number though.

values to low). Moreover, each expert's tendency for overconfidence (90% confidence intervals too narrow) or underconfidence (90% confidence intervals too wide) is shown. A tendency is observed if a comparison of the expert's assessments with the measured data shows that the null-hypothesis 'the expert does not show the bias' is rejected at a significance level of 0.05. It turns out that all experts show a tendency to overestimate. Moreover, 4 of the 6 are apparently overconfident.

Table 4.4 Experts' performance scores, based on their assessments of the pressure difference coefficients $\Delta C_{p,rel}$ between windward and leeward faces, instead between face a and face b.

Expert	Calibration C_e	Information I_e	Performance w_e
1	$3.0\ 10^{-2}$	0.65	$2.0\ 10^{-2}$
2	$3.6\ 10^{-1}$	0.55	$2.0\ 10^{-1}$
3	$1.0\ 10^{-2}$	0.46	$4.6\ 10^{-3}$
4	$1.0\ 10^{-3}$	0.17	$1.7\ 10^{-4}$
5	$1.0\ 10^{-4}$	0.81	$8.1\ 10^{-5}$
6	$3.0\ 10^{-1}$	0.73	$2.2\ 10^{-1}$

The scores in Table 4.4 show an almost equal calibration score for experts 2 and 6. The calibration scores of the other experts are lower by an order of magnitude or more, which is significant.

Table 4.5 Overview of the systematic biases the experts display in their quantile assessments of the pressure difference coefficients between windward and leeward faces. A '+' refers to 'over' in the column heading, '-' relates to 'under' and a '0' means that the tendency is not observed.

Expert	Tendency to over/under-estimate	Tendency for over/under-confidence
1	+	+
2	+	0
3	+	+
4	+	0/-
5	+	+
6	+	+

4.6.4 Combination of the experts' marginal distributions

Introduction

For each variable, the experts' assessments must be combined to obtain the DM for that variable. Combination of the experts' assessments according to the classical model uses linear pooling, which means that the DM is a weighted average of the experts'

distributions. Two types of weights are considered, equal weights and performance-based weights.
The decision-maker based on equal weights, or the 'equal weight DM', is simply the arithmetic average of the experts' probability distributions. In the assessment of the performance-based decision-makers on the other hand, each expert receives a weight that is basically his normalized performance. The normalization serves to ascertain that the sum of weights for each variable equals 1.
However, if an expert's calibration score is below a suitably chosen value of the significance level α_{opt}, the expert, considered as a hypothesis, is 'rejected' and his weight is set to zero. The significance level receives the value that optimizes the performance of the DM, which is calculated in the same way as the performance of individual experts.

Two performance-based decision-makers can be distinguished, viz. the global weight DM and the item weight DM. In assembling the item weight DM, the experts' weights are calculated per variable as their (normalized) item performances. Analogously, the global weight DM uses each expert's global performance as a single weight for all variables.

Application in this study

Table 4.6 shows the performance scores for four different decision-makers.

Table 4.6 Comparison of performances of different decision-makers. The 'best' expert is the expert with the highest overall performance.

DM	Significance level α	Calibration C_{DM}	Information I_{DM}	Performance w_{DM}	Contributing experts
Equal weight	-	$2.0.10^{-2}$	0.14	$2.8.10^{-3}$	1,...,6
Global weight	0.36	$3.6.10^{-1}$	0.55	$2.0\ 10^{-1}$	2
Item weight	0.30	$4.2.10^{-1}$	0.47	$2.0.10^{-1}$	2, 6
'Best' expert	-	$3.0.10^{-1}$	0.73	$2.0\ 10^{-1}$	6

It is clear that all DM's outperform the equal weight decision-maker. The only expert contributing to the optimized DM on the basis of global weights is expert 2. The optimized DM's do not outperform the 'best' expert in the study. This might be due to the fact that all experts show the same bias, i.e. overestimation. Indeed, in that case any combination of experts shows this tendency.
The differences in performance scores of the best expert, the item weight DM and the global weight DM are negligible. Either of them is equally eligible as the 'optimal' combination of the experts' assessments. In this study we will use the global weight DM. The 5%, 50% and 95% quantile assessments of this DM are shown in Figure 4.15. These values are tabulated in Appendix C.2.

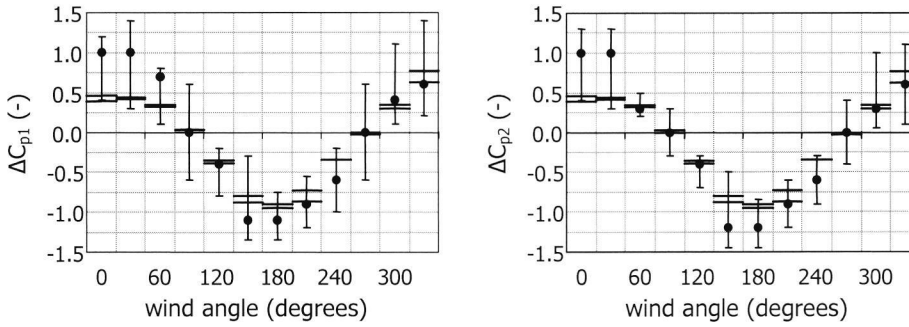

Figure 4.15 Quantile values of the global weight DM. The dots are the median values, the error bars represent the 90% confidence intervals. For reference the wind tunnel results are also shown as horizontal bars.

4.6.5 Combination of the experts' dependencies

Introduction

Each of the experts assessed the dependencies associated with the 11 arcs in the dependence tree in Figure 4.7. Their assessments are tabulated in Appendix C.2 in the form they were elicited, viz. as conditional probabilities (see section 4.4.2). In principle, the combined conditional probabilities for the DM can be calculated by linear pooling, using the expert weights as discussed in the previous section. A discussion on the mathematical subtleties involved can be found in Cooke and Kraan (1996).

However, as only one expert (no. 2) participates in the global weight DM, which will be used in the remainder of this study, the combination of dependencies is trivial. The rank correlation matrix for the pressure difference coefficients can directly be determined from the 11 conditional probabilities, which were elicited from expert 2. This involves two steps:

1. Calculation of the rank correlation corresponding to the elicited conditional probability for each arc of the dependence tree.
2. Assessment of the full correlation matrix from these rank correlations for the 11 arcs.

Step 1

Cooke and Kraan (1996) argue that given arbitrary continuous marginal distributions for two variables, the rank correlation between these variables is uniquely determined by the elicited conditional probability under the assumption that the joint distribution over the variables is minimally informative relative to the joint distribution with independent marginals (the product of the marginals). They also provide numerically computed values of the rank correlations as a function of the conditional probability in question for the case of multiple experts.

Step 2

Meeuwissen and Cooke (1994) show that for every rank correlation dependence tree there exists a unique joint distribution having minimal information relative to the

product distribution with the specified univariate marginals. With the uncertainty analysis tool UNICORN (Cooke, 1995) the rank correlation matrix of this joint distribution can be simulated from the specified rank correlations for the dependence tree on a random sampling basis.

Application in this study

Table 4.7 shows the rank correlation matrix for the pressure difference coefficients, simulated with UNICORN on the basis of 10 000 samples. The boxed values show the rank correlation values corresponding to the conditional probabilities that were elicited from the experts.

Table 4.7 Rank correlation matrix for the pressure difference coefficients. The matrix quantifies the dependencies between both the ΔC_{p1}'s and the ΔC_{p2}'s. Dependencies between ΔC_{p1} and the ΔC_{p2} were not elicited. The boxed cells show the rank correlations corresponding to the conditional probabilities that were directly elicited from the experts.

wind angle	0°	30°	60°	90°	120°	150°	180°	210°	240°	270°	300°	330°
0°	1	0.52	0.43	-0.07	-0.56	-0.58	-0.93	-0.91	-0.89	-0.13	0.69	0.68
30°	0.52	1	0.26	-0.05	-0.34	-0.37	-0.55	-0.56	-0.55	-0.09	0.41	0.74
60°	0.43	0.26	1	-0.03	-0.29	-0.3	-0.45	-0.46	-0.47	-0.08	0.62	0.36
90°	-0.07	-0.05	-0.03	1	0.04	0.04	0.07	0.07	0.07	0.38	-0.04	-0.06
120°	-0.56	-0.34	-0.29	0.04	1	0.4	0.6	0.61	0.62	0.09	-0.47	-0.46
150°	-0.58	-0.37	-0.3	0.04	0.4	1	0.62	0.63	0.62	0.08	-0.47	-0.48
180°	-0.93	-0.55	-0.45	0.07	0.6	0.62	1	0.98	0.96	0.13	-0.73	-0.73
210°	-0.91	-0.56	-0.46	0.07	0.61	0.63	0.98	1	0.98	0.14	-0.74	-0.75
240°	-0.89	-0.55	-0.47	0.07	0.62	0.62	0.96	0.98	1	0.14	-0.75	-0.73
270°	-0.13	-0.09	-0.08	0.38	0.09	0.08	0.13	0.14	0.14	1	-0.1	-0.11
300°	0.69	0.41	0.62	-0.04	-0.47	-0.47	-0.73	-0.74	-0.75	-0.1	1	0.55
330°	0.68	0.74	0.36	-0.06	-0.46	-0.48	-0.73	-0.75	-0.73	-0.11	0.55	1

4.6.6 Robustness analysis

Introduction

Confidence in the conclusions of the study benefits by robust results, i.e. a DM that is relatively insensitive to the exclusion of one single expert or one single realization in the analysis. In a robustness study, the sensitivity of the DM to a certain perturbation is related to the information score of the perturbed DM relative to the original DM. As an anchoring value for this information discrepancy, the relative information of the experts' distributions to the equal weight DM (average expert) is used, which is in the order of 0.5 on average.

Robustness for experts

Not surprisingly, the DM only changes if expert 2 is removed from the expert panel. Recalculation in that case yields a DM with an information score of 0.63 relative to the

original DM. This is comparable to the anchoring value, which indicates a moderate sensitivity.

Robustness for items

If the measured realizations are removed one at a time and the global DM recalculated, the maximum information relative to the original DM is 0.2. Comparison with the anchoring value indicates that the DM is fairly robust for items.

4.7 Discussion

4.7.1 Introduction

Basically, Figure 4.15 and Table 4.7 together with the assumption of minimal information (see Cooke, 1991, Appendix C.1) specify the joint probability distributions over both ΔC_{p1}'s and ΔC_{p2}'s for the decision-maker. Considering the fair calibration score of the DM, this information provides an answer to the principal question in this chapter, i.e. 'what is the uncertainty that should be considered in wind pressure difference coefficients assessed from existing data and generic knowledge?'.

However, two other issues deserve notice. First, the case structure was designed in such a way that a distinction can be made between:

- measuring location near the center of the façade versus close to the roof edge.
- approach flow over open terrain versus over built-up terrain

It is interesting to investigate to what extent the experts distinguish between these situations in their uncertainty assessments and how this affects their performance scores. These issues are discussed in section 4.7.2.

Moreover, in section 4.7.3 we discuss the question under what provisions expert judgment could develop as an alternative for a wind tunnel study.

4.7.2 Disaggregation

The case structure enables distinction between:

- measuring location near the center of the façade versus close to the roof edge.
- approach flow over open terrain versus over built-up terrain

In this section the experts' assessments are disaggregated to study whether they distinguish between these situations and how this affects their performance scores.

First, the experts' assessments on $\Delta C_{p,1}$ and $\Delta C_{p,2}$, the pressure difference coefficients at measuring positions 1 (close to the roof edge) and 2 (near the center of the façade) respectively, will be compared. Subsequently, separate evaluations of the subsets $\Delta C_{p,exposed}$ (wind angles 120°, 150°, 180°, 210° and 240°, approach flow over open terrain) and $\Delta C_{p,built\text{-}up}$ (wind angles 300°, 330°, 0°, 30° and 60°, approach flow over built-up terrain) will be carried out.

Measuring position 1 versus 2

Table 4.8 and Table 4.9 list the experts' performance scores for the $\Delta C_{p,1}$'s and $\Delta C_{p,2}$'s respectively. In each of these tables, the second column shows the calibration scores, which are scaled to 10 items to allow comparison with the other calibration scores presented in this chapter. The third column presents the mean relative information scores of the experts on the items the tables refer to. The information scores relate to intrinsic ranges, which are identical for $\Delta C_{p,1}$ and $\Delta C_{p,2}$ for each wind angle. These ranges are the smallest intervals, comprising the default intrinsic ranges for both the $\Delta C_{p,1}$ and the $\Delta C_{p,2}$ involved (see Appendix C.1). Equation of the intrinsic ranges enables comparison of these information and performance scores between Table 4.8 and Table 4.9. The fourth column shows the overall expert performance, i.e. the product of the calibration score and the information score. The last column shows the normalized weights of the experts.

Table 4.8 $\Delta C_{p,1}$, 12 items, calibration power 0.83 (10 effective items), $\alpha_{opt}=8.1\ 10^{-2}$

Expert	Calibration C_e	Information $I_{e,common}$	Performance w_e	weight
1	$9.6\ 10^{-3}$	0.66	$6.3\ 10^{-3}$	0
2	$7.5\ 10^{-2}$	0.49	$3.7\ 10^{-2}$	0
3	$2.1\ 10^{-3}$	0.52	$1.1\ 10^{-3}$	0
4	$1.2\ 10^{-3}$	0.19	$2.3\ 10^{-4}$	0
5	$1.0\ 10^{-4}$	0.87	$8.7\ 10^{-5}$	0
6	$8.1\ 10^{-2}$	0.76	$6.2\ 10^{-2}$	1.0
DM (global)	$8.1\ 10^{-2}$	0.76	$6.2\ 10^{-2}$	

Table 4.9 $\Delta C_{p,2}$, 12 items, calibration power 0.83 (10 effective items), $\alpha_{opt}=6.9\ 10^{-1}$.

Expert	Calibration C_e	Information $I_{e,common}$	Performance w_e	weight
1	$4.7\ 10^{-2}$	0.68	$3.2\ 10^{-2}$	0
2	$6.9\ 10^{-1}$	0.67	$4.6\ 10^{-1}$	1.0
3	$6.6\ 10^{-2}$	0.46	$3.0\ 10^{-2}$	0
4	$1.2\ 10^{-3}$	0.19	$2.3\ 10^{-4}$	0
5	$2.0\ 10^{-3}$	0.80	$1.6\ 10^{-3}$	0
6	$5.7\ 10^{-1}$	0.76	$4.3\ 10^{-1}$	0
DM (global)	$6.9\ 10^{-1}$	0.67	$4.6\ 10^{-1}$	

The information scores on common intrinsic ranges do not differ much between $\Delta C_{p,1}$ and $\Delta C_{p,2}$, which indicates that the experts were about equally informative, i.e. uncertain, in their assessments of $\Delta C_{p,1}$ and $\Delta C_{p,2}$. However, most experts perform significantly less on $\Delta C_{p,1}$ than on $\Delta C_{p,2}$. The difference between the performance scores for the optimized DM is approximately a factor 7. Further analysis shows that the DM for the $\Delta C_{p,1}$'s has both a significant tendency to overestimate and a significant tendency

for overconfidence, whereas both tendencies are absent in the DM for the $\Delta C_{p,2}$'s. This is valuable feedback information, which may help to improve expert performance in future expert judgment studies in this field.

Exposed versus built-up

To study the effect of the buildings and trees on the experts' assessments, the set of assessments on the $\Delta C_{p,exposed}$'s for approach flow over the 'southern', void half (wind angles $\theta \in \{120^o, 150^o, 180^o, 210^o \text{ and } 240^o\}$) are compared to their mirror set on the $\Delta C_{p,built\text{-}up}$'s for approach flow over the 'northern', built-up half (approach flow angles $180^o\text{-}\theta$).

The numbers in columns 2, 4 and 5 were calculated analogously to their counterparts in the previous sub-section. To obtain the information scores in the third column, the intrinsic range for each variable in the exposed set and its 'mirror' in the built-up set was set to the smallest interval comprising the default intrinsic ranges for each of the two variables.

Table 4.10 $\Delta C_{p,exposed}$, 10 items, calibration power 1.0, (10 effective items), $\alpha_{opt}=7.3\ 10^{-2}$.

Expert	Calibration C_e	Information $I_{e,common}$	Performance w_e	weight
1	$1.0\ 10^{-4}$	0.91	$9.1\ 10^{-5}$	0
2	$5.8\ 10^{-2}$	0.87	$5.0\ 10^{-2}$	0
3	$2.7\ 10^{-4}$	0.79	$2.1\ 10^{-4}$	0
4	$1.2\ 10^{-3}$	0.37	$4.4\ 10^{-5}$	0
5	$1.0\ 10^{-4}$	0.85	$8.5\ 10^{-5}$	0
6	$7.3\ 10^{-2}$	1.41	$1.0\ 10^{-1}$	1.0
DM (global)	$7.3\ 10^{-2}$	1.41	$1.0\ 10^{-1}$	

Table 4.11 $\Delta C_{p,built\text{-}up}$, 10 items, calibration power 1.0, (10 effective items), $\alpha_{opt}=7.9\ 10^{-1}$.

Expert	Calibration C_e	Information $I_{e,common}$	Performance w_e	weight
1	$7.9\ 10^{-1}$	0.84	$6.6\ 10^{-1}$	1.0
2	$4.6\ 10^{-1}$	0.71	$3.3\ 10^{-1}$	0
3	$3.1\ 10^{-3}$	0.45	$1.4\ 10^{-3}$	0
4	$1.2\ 10^{-3}$	0.35	$4.2\ 10^{-4}$	0
5	$1.0\ 10^{-4}$	1.06	$1.1\ 10^{-4}$	0
6	$2.5\ 10^{-1}$	0.50	$1.3\ 10^{-1}$	0
DM (global)	$7.9\ 10^{-1}$	0.84	$6.6\ 10^{-1}$	

Leaving aside expert 5, the information scores of the experts and the DM for the southern, 'exposed' wind angles are higher (less uncertainty) than for the northern angles. This is in accordance with expectations as a relative abundance of experimental data is available on pressure coefficients for exposed buildings.

However, all experts and the DM receive a lower performance score for the 'exposed' wind angles. Further analysis shows that the DM for the $\Delta C_{p,exposed}$'s is significantly overconfident and has a significant tendency to overestimate. Both biases are absent in the DM for the $\Delta C_{p,built\text{-}up}$'s. Apparently, the relatively high informativeness (reduced uncertainty) in the assessments for the exposed wind angles is unjustified.
As in the previous sub-section, this information may be valuable to improve expert performance in future expert judgment studies in this field.

4.7.3 Expert judgment compared to wind tunnel

It is interesting to compare the uncertainty in the DM's assessments, shown in Figure 4.15, with the uncertainties in pressure difference coefficients, obtained from a wind tunnel experiment. This reveals the extra information we gain by doing a specific wind tunnel experiment instead of an assessment on the basis of existing data.
As each sound wind tunnel test, compliant with the case description in section 4.2 yields valid realizations of the wind pressure difference coefficients, the spread in the outcomes of such tests would be a suitable estimator for the uncertainty. In a recently completed study (Hoelscher, 1997), twelve wind tunnel laboratories measured the surface pressures at a floor-mounted cube, corresponding to 50m height in full-scale. They were asked to perform the measurements in a simulated boundary layer flow at neutral stratification corresponding to urban terrain with a profile exponent of α = 0.22 +/- 0.02. Apart from a few basic constraints, the participants were free to perform the tasks according to their own judgment and standards.

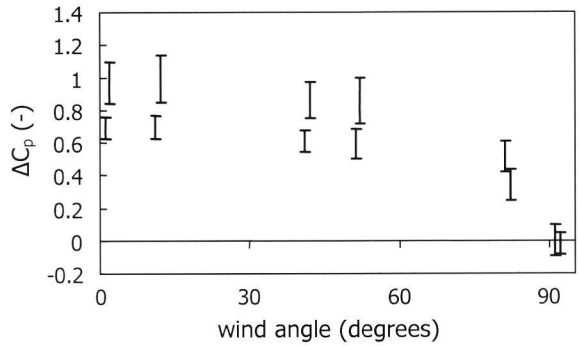

Figure 4.16 Spread in wind pressure difference coefficients, measured in twelve different wind tunnels on an isolated cube (Hoelscher, 1997). The error bars represent the 90% confidence intervals. The upper error bars are obtained the façade centerline at a level of 0.5 of the cube height, the lower bars were found at 0.93 of the cube height also at the façade centerline.

Figure 4.16 shows the 90% confidence intervals for pressure difference coefficients between front and back of the cube, measured at the façade centerline at 0.93H and 0.5H respectively, where H is the obstacle height. These measuring locations are comparable to those of ΔC_{p1} (0.93H) and ΔC_{p2} (0.43H) respectively. Figure 4.16 shows that the width of the confidence intervals is on average 0.2 and does not significantly depend on the wind angle.

To explore if these results obtained for an isolated cube of 50m full-scale height make sense in the current case, a virtual expert was created. His median values were chosen equal to the outcomes of the UWO wind tunnel test. The 95% and 5% quantile values were set to the median value +/- 0.1 to obtain 90% confidence intervals of width 0.2. Subsequently, the performance of this virtual expert was scored on the results of the test in the DNW tunnel along with the other experts. Table 4.12 lists the performance score of this virtual expert. For comparison, the scores of the DM based on the experts' assessments is also shown.

Table 4.12 Performance of a virtual expert, created on the basis of the data from the UWO-test and scored on the results of the experiment in the DNW-tunnel, calibration power 0.42 (10 effective items). For comparison, the scores of the DM based on the experts' assessments are recalled from Table 4.6.

	C_e	I_e	w_e
Virtual expert	$3.8\ 10^{-1}$	1.65	$5.2\ 10^{-1}$
DM (global)	$3.6.10^{-1}$	0.55	$2.0\ 10^{-1}$

Comparison of both sets of scores in Table 4.12 shows that the virtual expert, created on the basis of wind tunnel data, has a calibration score, which is similar to that of the DM, calculated from the expert judgments. However, the information score of the virtual expert is 3 times higher than the information score of the DM. Or, alternatively, the confidence intervals of the virtual expert are 3-6 times narrower than the confidence intervals of the DM. This can be interpreted as the extra information, which is gained by doing a wind tunnel experiment in this case.

Wind pressure coefficients, assessed on the basis of existing data in this study have an uncertainty, which is large compared to both their median values, and to the (estimated) uncertainty in wind tunnel results. This suggests that the output of models and tools, based on a parametric analysis of prior wind tunnel and full-scale data, have little meaning unless the uncertainty in this output is quantified. This study shows that an expert judgment study is an adequate method to perform this quantification. In the form it was implemented here though, it is also a very expensive approach, far more expensive than a wind tunnel study.

The most obvious measure to cut back the costs, i.e. by reducing the number of experts in the panel to e.g. 1 or 2, is not an attractive one at this stage. Indeed, the experts in this study show little agreement in their assessments. This is expressed in their rationales, which underpin their assessments with different and sometimes even conflicting arguments. Moreover, the experts' calibration scores show a large scatter and only two out of six experts receive a fair calibration score.

Thus, at this stage it should be concluded that an expert judgment study is not an attractive alternative for a wind tunnel experiment. However, this tentative conclusion is moderated by the following consideration. If expert judgment studies would be as common as wind tunnel studies are today, experts would be better trained to make subjective probability assessments, which might allow for a reduction of the number of experts in the study (see e.g. Cooke, 1991). Moreover, experts would probably be better equipped to estimate wind pressure coefficients on the basis of available data, which might lead to a reduction of their uncertainty without a loss of calibration.

Hence, it seems worthwhile to dedicate further research efforts to the exploration of the perspectives of expert judgment in this field.

4.8 Conclusions and recommendations

Expert judgment was successfully employed to quantify the uncertainty in wind pressure difference coefficients for a flat-roofed low-rise building (l x w x h: 56 m x 14 m x 14 m) in an urban environment. The uncertainty was measured in the situation that the coefficients are assessed on the basis of existing experimental data and knowledge rather than with a specific (wind tunnel) experiment. The observed uncertainty is large, both compared to the median values of the coefficients, and compared to the (estimated) uncertainty in wind tunnel results. This suggests that point estimates on the basis of existing data do not give useful information. Instead, probability distributions for the coefficients as obtained from an expert judgment study, might be valuable for certain applications.

Moreover, valuable feedback information was obtained to assist experts in improving their assessments in possible expert judgment studies in the future. Firstly, it was observed that the experts showed a significant tendency to overestimate and a significant tendency for overconfidence in their assessments of the pressure difference coefficients near the roof edge (pressure taps located at the centerlines of the long facades and 1m below the roof edge). These tendencies were absent in their assessments of the coefficients at approximately half the building height.
Secondly, the experts were found to display similar biases for wind angles with flow approaching the building over an exposed near field, whereas these biases were absent for situations with flow approaching over irregularly built-up, urban terrain.

In the form it was implemented in this study, elicitation and processing of expert judgments is much more expensive than a wind tunnel experiment. Further study is required to investigate to which extent the costs (and possibly the uncertainties) would be reduced if experts would become more familiar with and skilled in the assessment of subjective probabilities.

5 Uncertainty in the indoor air temperature distribution

5.1 Introduction

A central component of simulation models which assess thermal comfort in a building space is the energy balance for the indoor air. In current simulation tools, the air volume is lumped into one single node, to which a single temperature, i.e. the mean air temperature is assigned. Under the assumption that the air temperature is uniform, this air node temperature can be used in the calculation of the ventilation heat flows and the heat flows from the air to the room enclosure on the basis of (semi-) empirical models for the convective heat transfer coefficients. Moreover, the uniform temperature assumption is adopted in the assessment of the average thermal sensation of an occupant in the room. This approach was used in Chapter 3.

However, the temperature distribution in the air will generally not be uniform. Indeed, in naturally ventilated buildings, which are used as an example throughout this thesis, there is limited control over either ventilation rates or convective internal heat loads. This results in flow regimes varying from predominantly forced convection to fully buoyancy driven flow. In the case of buoyancy driven flow, plumes from both heat sources and warm walls rise in the relatively cool ambient air, entraining air from their environment in the process, and create a stratified temperature profile. Cold plumes from heat sinks and cool walls may contribute to this stratification. Forced convection flow elements, like jets, may either enhance the stratification effect or reduce it, dependent on their location, direction, temperature, and momentum flow.

Non-uniformity of the temperature profile distribution affects the energy balance for the air volume. Moreover, it may cause the local air temperature, experienced by an occupant, to deviate from the mean air temperature. These effects may result in a bias of the simulation output, i.e. the building performance with respect to thermal comfort. In the sensitivity analysis, reported in Chapter 3, the effect of an alternative assumption for the air temperature distribution in building spaces was explored. The analysis revealed that the effect ranks among the more important modeling uncertainties investigated in that same study. Consequently, it was felt that additional study would be appropriate to investigate how air temperature distributions can be more thoroughly assessed in building simulation.

In theory, the flow field in a space is fully determined by the Navier-Stokes equations plus the equation for energy conservation with their boundary and initial conditions. When these equations for the flow are solved simultaneously with the other equations in

the building simulation model, the two sets of equations supply each other's boundary conditions and the temperature field is dynamically calculated. Unfortunately this process is hampered by two problems:

1. Straightforward solution of the flow equations is not possible in cases of practical interest.
2. As a result of approximations in the structure and incompleteness of the input of building simulation models, the boundary conditions for the flow are not uniquely specified. This results in uncertainty in the flow field.

Substantial research efforts have been dedicated to the first problem, which has common features in all areas of flow modeling. The second problem, which is building simulation specific, has received negligible attention. It is interesting to address both problems in tandem though. Indeed, it seems pointless to use a sophisticated model for the air temperature distribution in a building simulation if the input to this model is highly uncertain. Hence this study explores a way to model the relevant aspects of the air temperature distribution with their inherent uncertainties rather than to focus on a method to produce the 'best' values for given boundary conditions without uncertainty.

The study is tailored to a specific space, which is similar to the one in the crude uncertainty analysis in Chapter 3. It is described in section 5.2. Section 5.3 gives a brief overview of existing approaches to model temperature distributions in building spaces. The subsequent section elaborates on the uncertainties in the boundary conditions for the flow in a typical building simulation context. A strategy to come to a model for the relevant features of the air temperature distribution with their uncertainty, which can be implemented in a building simulation model to assess the effects on building performance, is proposed in section 5.5. This strategy is explored step by step in the subsequent sections.
In Section 5.6 a heuristic model for the air temperature distribution is formulated. Section 5.7 reports on the assessment of the uncertainty in this temperature distribution in a number of carefully selected cases. As in Chapter 4, expert judgment is used in this stage. Then, in Section 5.8, the uncertainties in the temperature distributions from Section 5.7 are mapped to the parameters in the heuristic model from Section 5.6. When this mapping process, which is referred to as 'probabilistic inversion', is successful, it results in a (joint) probability distribution over the model parameters, expressing their uncertainty, which can be used in combination with the heuristic model in building simulation.

The aim of the study is to assess the feasibility of the approach, to identify problem areas, and, if possible, to come up with a workable model for the space to be used in an uncertainty analysis. The final section is used for discussion and conclusions. In addition to an evaluation of the case study, generalization to other spaces will be discussed as a step in the development towards a general tool for engineering practice.

5.2 Description of the space

The space addressed in this chapter closely resembles the spaces which were considered in the crude uncertainty analysis in Chapter 3. A sketch of the space is given in Figure 5.1. It is part of a low-rise office building.

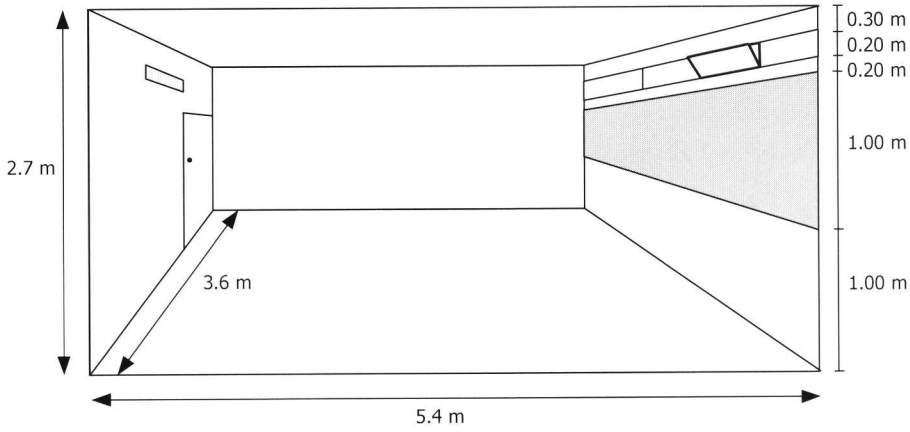

Figure 5.1 The office space under study with internal dimensions (l × w × h) 5.4 m × 3.6 m × 2.7 m. The height of the fixed window is 1.0 m. Cross-ventilation of the space takes place through a cantilever window in the façade and a rectangular vent in the opposite wall. The furnishing to accommodate two people is not shown.

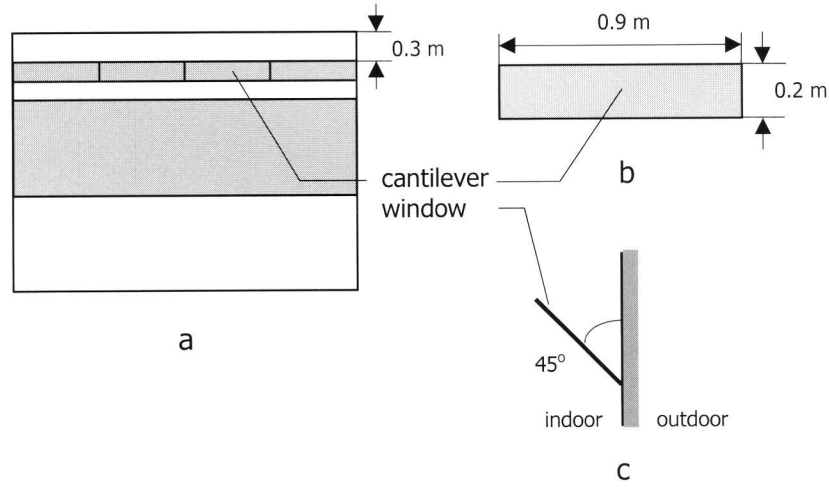

Figure 5.2 Layout of the facade (a), the cantilever window (b) and a side view of the opened cantilever window (c).

The building is situated in a moderate climate, like in The Netherlands. The period of interest is the spring/summer (April-September), during which the indoor climate in the building depends on natural ventilation supported by mechanical ventiation if required. The space is cross-ventilated through a cantilever window in the façade (see Figure 5.2) and a vent at the same level in the opposite wall. The door in this facade is closed.
The space has a concrete floor. The interior walls between the spaces are constructed of sand-lime bricks and the ceiling is false. The facade is well-insulated and the windows in the facade consist of double-glazing. A moveable external solar shading device is mounted.
The space is furnished to accommodate 2 office workers. The bordering spaces are similar in design and operation.

5.3 Modeling of the air temperature distribution

5.3.1 Introduction

This section starts with a recapitulation of the way the air temperature distribution in spaces is modeled in the current building simulation models. Subsequently, a brief overview is presented of alternative modeling approaches.

5.3.2 Current modeling approach

Current building simulation models start from the energy balance for the indoor air volume of the entire space (see also Figure 5.3 and Section 2.3.2.

$$\rho c_p V \frac{dT_{air}}{dt} = Q_{vent} + \sum_i Q_{wall,i} + Q_c \tag{5.1}$$

$$Q_c = Q_{srce,c} + Q_{sol,c} \tag{5.2}$$

$$Q_{vent} = \rho c \Phi_V (T_{in} - T_{out}) \tag{5.3}$$

where

ρ, c_p, V	density and specific heat of air, air volume
$Q_{srce,c}$	convective part of internal heat production
$Q_{sol,c}$	convective part of solar gain
T_{in}	temperature of the incoming air
Φ_V	air volume flow through the space[26]

[26] In general, multiple flows may enter and leave the space and the volume flows will be state variables in a coupled mass and heat transport problem (see Chapter 2). The space, specified in section 5.2, however, has only two openings and the prevailing ventilation mechanism will be cross-ventilation. As both openings are located at the same height, the temperature field in the space will have a negligible effect on the volume flows through the openings. Hence, these volume flows can be assessed separately and imposed as boundary conditions on the airflow in the space.

$Q_{wall,i}$ heat flows from wall component[27] i to the air
T_{air} mean air temperature
T_{out} temperature of the air leaving the space

An illustration of the main variables in these equations is shown in Figure 5.3. As $Q_{wall,i}$, T_{air} and T_{out} are unknown, (5.1) and (5.3) do not form a closed set. To settle this, the following additional equations are used in current building simulation practice (see also Chapter 2):

$$T_{out} = T_{air} \tag{5.4}$$

$$Q_{wall,i} = \alpha_{c,i}\left(T_{wall,i} - T_{air}\right)A_{wall,i} \tag{5.5}$$

where

$A_{wall,i}$ the surface area of wall component i
$T_{wall,i}$ the surface temperature of wall component i, a boundary condition provided by the rest of the building simulation model
$\alpha_{c,i}$ convective heat transfer coefficient for wall component i, a (semi) empirical parameter

Equation (5.4) is satisfied by the assumption of uniform air temperature. Moreover, under this assumption, the temperature difference over each wall boundary layer is adequately modeled by $T_{wall,i} - T_{air}$. This means that literature values for the heat transfer coefficients, which are commonly related to the temperature difference over the wall boundary layer, can be used to quantify $\alpha_{c,i}$ (see e.g. Khalifa, 1989). Finally no separate evaluation of the local air temperature, experienced by an occupant of the space, is required as this occupant is immersed in a uniform temperature field.

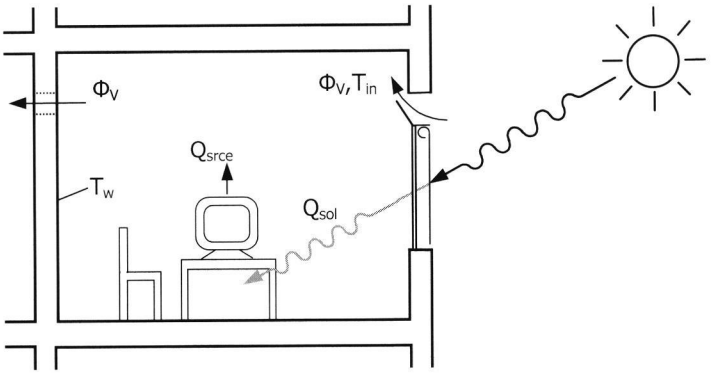

Figure 5.3 Illustration of the variables acting in the heat balance of the space.

[27] As explained in chapter 2, in a building simulation model, the enclosure of a space is sub-divided in enclosure- or wall-components with different materials and/or orientation.

However, as discussed in the introduction, uniform air temperature is actually the exception rather than the rule. This implies that (5.4) no longer holds, straightforward application of the literature values for the heat transfer coefficients is questionable, and an occupant may sense an air temperature different from the mean value. To assess these effects, more detailed modeling of the air temperature distribution is required. The next section gives an overview of approaches to model the flow field in building spaces. The section mainly focuses on their applicability to naturally ventilated spaces in the context of a building simulation.

5.3.3 Alternative modeling approaches

This section presents a concise overview of existing methods to assess the flow field in building spaces. The methods range from universal approaches to problem specific solutions. The methods are addressed in descending order of universality. More detailed overviews can be found in e.g. Loomans (1998) and Heiselberg et al. (1998).

Computational fluid dynamics (CFD)

Computational fluid dynamics is a generic term for a rapidly developing collective of models and numerical techniques to simulate flow fields in a variety of applications. All CFD-approaches are based on the equations for energy, momentum and mass conservation. A recent investigation on the application of CFD to simulate the airflow in building spaces can be found in Loomans (1998). Loomans demonstrates that calculation of these flow fields involves a delicate balance between computational load and accuracy. Several approximate methods have been developed to allow coarser discretization of the equations, both in space and in time. However, the universality of several of these methods is limited and calibration against measurements is recommended. Moreover, there are no general rules to determine the structure and resolution of a spatial discretization grid, which produce sufficiently accurate solutions. Finally, convergence of the numerical solution is often controlled by a number of relaxation factors, which have to be set on the basis of experience.

These complications cause the necessity to validate CFD-models against measurements (Chen, 1997, Baker et al., 1997). Of special concern is the assessment of the heat transfer at the walls. Niu (1994) concludes that an accurate simulation of this heat transfer in building spaces is very difficult to obtain.

Moreover, application of CFD in a building simulation context requires simultaneous solution of the flow equations and the other equations in the building simulation model. Negrão (1995) reports on an attempt to integrate a dynamic CFD-model into a building simulation model. Although extremely computationally intensive, the approach was successful for relatively uncomplicated cases, but in cases of practical interest it appeared difficult or even impossible to achieve convergence.

Zonal models

To alleviate the computational loads inherent in CFD-calculations, the zonal model approach was developed (see e.g. Inard et al., 1996, Rodríguez et al., 1993, Peng, 1996). As CFD, this approach spatially partitions the space, but the resulting cells (or *zones*) are much larger. For each zone, equations of energy and mass conservation are formulated. However, as conservation of momentum is not explicitly considered, the resulting set of equations is not closed.

To close the problem, additional information about the flow pattern has to be added. Two methods to obtain this information can be found in literature. First, the flow pattern can be obtained from a dedicated experiment (measurements or CFD-calculations). The resulting zonal-model can then be applied to situations, where the flow pattern is expected to be similar to that in the experiment. Examples of this approach can be found in Howarth (1985), Chen (1988) and Peng (1996).
Alternatively, the additional information can be based on assumptions about the flow pattern, e.g. based on semi-empirical behavioral laws for individual flow components (Inard et al., 1996). Reliable application of both types of zonal models requires a profound knowledge of fluid dynamics.

Gagneau et al. (1997) propose a method to overcome this problem, but their approach is still in its infancy and its merits cannot be assessed yet.

Semi-empirical approaches

For various controlled ventilation strategies, semi-empirical 'engineering' models have been developed to assess the temperature distribution. Examples can be found in e.g. Krühne (1995) and Mundt (1996) for displacement ventilation. Another example is reported in Chen et al. (1992). They present a database with pre-computed (stationary) flow fields (temperature, velocity and contaminant concentration) for various air conditioning strategies, as a function of space geometry, heat load, ventilation rate etc.
All these approaches concern spaces with controlled ventilation or air conditioning. This implies that supply air temperature, supply flow rate and space heat gain are fully coupled. In naturally ventilated spaces, these variables may vary almost independently of each other, constituting a much larger set of conditions to be covered by a model.

Conclusion

The more universal approaches (CFD and zonal models) to calculate flow fields in building spaces require expert knowledge, i.e. a thorough understanding of fluid dynamics and the subtleties involved in numerical flow simulation. Moreover, reliable and flexible integration of either of these approaches in a dynamic building simulation model is still subject of research. Application of the semi-empirical models requires much less expert judgment. However, for a naturally ventilated space, as described in section 5.2, no models are available to date.

5.4 Uncertainty

The typical building simulation context, addressed throughout in this thesis, is the design context, in which building performance is to be assessed on the basis of the design and specifications and a scenario, specifying the conditions during operation of the building (see Chapter 2). In this context, not all boundary conditions for the airflow are available. In the current building simulation models, the air temperature is calculated from (5.1) through (5.5) with the following information on the boundary conditions:

Table 5.1 Information on the boundary conditions for the airflow, available in the given building simulation context.

$\underline{T}_{wall}$	the area averaged surface temperatures of all wall components
Φ_V	the air volume flow rate
T_{in}	the supply air temperature
$Q_{srce,c}$	the sum of the convective heat gains from all internal heat sources
$Q_{sol,c}$	the convective part of the solar gain entering the space

These variables are quantified either directly from the scenario or by the other equations in the simulation model. However, a dynamical assessment of the flow field in a building space requires more detailed information, e.g. the spatial distribution of $Q_{srce,c}$, i.e. specification of the heat sources and their position in the space, and the degree of furnishing and the location of the furniture. Moreover, the outdoor climate is usually represented (in the scenario) as a time series of hourly averaged data. However, the indoor air flow field is likely to be sensitive to sub-hourly fluctuations in e.g. the air flow rate and the solar gain, which are highly variable processes. Finally, determination of air temperature experienced by an occupant requires knowledge of the location of the occupant in the space, which is not available.

5.5 Modeling under uncertainty

As discussed in the previous section, we start from the assumption that, apart from the geometry of the space, the information in Table 5.1 is available on the boundary conditions of the flow field. We will address these variables as the vector $\underline{x}$:

$$\underline{x} \equiv (\underline{T}_{wall}, \Phi_V, T_{in}, Q_{srce,c}, Q_{sol,c})$$

As discussed in section 5.3, we drop the common assumption that the air temperature is uniform. Hence, we replace (5.4) with:

$$T_{out} = T_{air} + \Delta T_{out} \tag{5.6}$$

and add an equation for the air temperature T_{occ}, experienced by an occupant:

$$T_{occ} = T_{air} + \Delta T_{occ} \tag{5.7}$$

Under the uniform air temperature assumption, no separate definition of the occupant air temperature T_{occ} was required. Here, we define T_{occ} as the mean air temperature of an air volume, located at an unknown position on the floor, with a horizontal cross section of 1 m^2, extending from the floor up to 1.35 m (the top level of a sitting person).

With (5.6) and (5.7), the air temperature in the space is no longer modeled in terms of T_{air} only, but with the triplet T_{air}, ΔT_{out} and ΔT_{occ}. These three variables are combined in the vector $\underline{y}$:

$$\underline{y} \equiv (T_{air}, \Delta T_{out}, \Delta T_{occ})$$

Uncertainty in $\underline{y}$ results from the sources discussed in the previous section. We seek to find a model in terms of $\underline{x}$, which can be implemented in a building simulation model to quantify $\underline{y}$ with its uncertainty for the space in section 5.2.

First, we assume that a (quasi-) stationary model of the flow field in terms of $\underline{x}$ suffices. In a typical building simulation context, the boundary conditions and inputs of the model are hourly averaged climate data. Hence, processes with a characteristic time scale that is significantly smaller than one hour may be considered to respond instantaneously to a change in the boundary conditions and/or inputs. Loomans (1998) reports on measurements of the time required by the air in an office space to adapt from a fully mixed flow to a stationary displacement flow at 0.75 air changes per hour. This process takes only a couple of minutes, which corroborates that quasi-stationary modeling of the flow field in a building simulation context is a sensible approach.

Under this assumption, we can write $\underline{y}$ as a function of $\underline{x}$:

$$\underline{y} = M(\underline{x}, \underline{d}) \tag{5.8}$$

where M is the requested model and $\underline{d}$ is a vector with model parameters.

To find a combination of M and $\underline{d}$, which quantifies the uncertainty in $\underline{y}$, the following strategy was explored in this study:

1. Postulate a heuristic model M
2. For each $\underline{x}_i$ in a suitably chosen set X of values for $\underline{x}$, measure the uncertainty in $\underline{y}_i$.
3. Find a joint probability distribution over $\underline{d}$ such that for each $\underline{x}_i$ in X the model outcome $M(\underline{x}_i, \underline{d})$ reproduces the observed uncertainty in $\underline{y}_i$ (probabilistic inversion).

The three steps of the strategy are subsequently addressed in the following sections.

5.6 Heuristic model

5.6.1 Introduction

As already discussed in section 5.3, no general models for $\underline{y}$ of the form (5.8) are available from literature to implement in a building simulation model. Hence it was decided to postulate such a model, based on heuristics on the one hand and results from

several experimental and computational experiments, documented in the literature, on the other hand.
As mentioned in the introduction, the flow regime in naturally ventilated spaces may vary from buoyancy dominated flow, through mixed convection to fully forced convection. Hence, the model should describe $\underline{y}$ as a function of $\underline{x}$ throughout this range of flow regimes.
The required level of adequacy depends on the uncertainty in $\underline{y}$. As long as the errors in $\underline{y}$ due to inadequacies in the model structure M are small compared to the observed uncertainty in $\underline{y}$, the model satisfies the need. As at this stage the uncertainty in $\underline{y}$ is yet to be investigated, the level of model sophistication is determined intuitively.

The modeling of each of the three elements of $\underline{y}$ will be discussed separately.

5.6.2 Modeling of the difference between exhaust air temperature and mean air temperature

The difference between the mean air temperature and the exhaust air temperature is ΔT_{out}. Under the assumption that vertical temperature differences in spaces are generally dominant, we will consider a one-dimensional air temperature profile $T(z)$ where z is the height above the floor. In this approximation, ΔT_{out} can be interpreted as the temperature difference between two different levels above the floor.

First, several systematic studies are reviewed, which concern predominantly buoyancy driven flows in spaces. Subsequently the influence of forced ventilation flows is studied.

Buoyancy driven flow regime (natural convection)

In situations without forced ventilation flow (in the space under study this means that the supply air flow rate Φ_V is small and does not significantly affect the flow pattern), we seek to find a model for ΔT_{out} in terms of $Q_{src,c}$, $Q_{sol,c}$, and $\underline{T}_{wall}$.

Two types of configurations are frequently used to study the effect of convective heat sources on the temperature profile in buoyancy driven flows:

1. Spaces with displacement ventilation
2. Radiator heated spaces

A concise literature review of studies on these configurations suggests that the air temperature difference ΔT between two vertically separated locations in the space varies with the convective heat load Q_c as:

$$\Delta T \sim Q_c^n \tag{5.9}$$

for given type and location of the heat source(s). The heat sources addressed in the studies include window surfaces, heated by solar irradiation. Reported values of the exponent n are between 0.5 and 2. A more detailed report on the literature sources and their analysis can be found in appendix D.

Equation (5.9) does not explicitly take account of the information in $\underline{T}_{iwall}$ about the surface temperature distribution over the walls. Differences in surface temperature between parts of the enclosure can drive thermal stratification. Those differences may e.g. result from an uneven distribution of incident solar irradiation over the enclosure and/or persistent thermal stratification in the preceding period. In the case under study however, which concerns a well-insulated building with heavy internal walls, double glazing with external solar shading, operated in the summer season, deviations of the surface temperatures from the mean value T_{iwall} will be strongly reduced by radiant heat exchange. It is assumed that the contribution of a possible non-uniform temperature distribution over the space enclosure to differences in air temperature will be small. Hence, this contribution will be added to the model for ΔT_{out} as an error term.

On the basis of these considerations, the following model is proposed for ΔT_{out} in a buoyancy driven flow regime in the space:

$$\Delta T_{out} = a_0 + a_1 Q_c^n \tag{5.10}$$

where a_0 is the error term, a_1 is a constant of proportionality, Q_c is the sum of the convective parts of the internal and solar heat gains, and n is an exponent between 0.5 and 2.

Mixed and forced convection

As the forced ventilation flow rate grows, the influence of the supply jet on the flow pattern and thermal stratification will increase accordingly. The available information to characterize the jet consists of the flow rate Φ_V and the supply air temperature T_{in}. It is attempted to extend the model for ΔT_{out}, formulated for a buoyancy-driven regime in the space, to take account of Φ_V and T_{in}.

In the literature, a considerable amount of studies can be found on how to obtain certain desired flow field characteristics by controlling the velocity and temperature of the supply jet in air conditioned spaces. However, systematic investigations on the effect of an uncontrolled supply jet on the flow field are few and far between. Hence, it was decided to postulate a heuristic model and verify it against the few data available from the literature. This is discussed in the following subsections.

Warm jet

At moderate flow rates, a relatively warm jet ($T_{in} \geq T_{air}$) will rise in the ambient air and transport warm air to the upper regions of the space, thus sustaining a stratified temperature profile in the air. The warmer the supply air at a given flow rate, the stronger this effect will be.

If, at a given supply air temperature, the flow rate reduces to zero, the flow regime will become fully buoyancy driven. On the other hand, if the flow rate increases beyond a

certain point, the mixing effect of the jet grows dominant and thermal stratification will be suppressed.
A basic model for ΔT_{out}, which complies with these notions, is given in the following equation:

$$\Delta T_{out} = \frac{a_0 + a_1 Q_c + a_2 \rho c_p \Phi_V (T_{in} - T_{air})}{1 + a_3 \Phi_V^2} \quad (T_{in} \geq T_{air}) \tag{5.11}$$

where (a_0, a_1, a_2, a_3) is a vector with model parameters. If the flow rate $\Phi_V = 0$, (5.10) is recovered, except for the exponent n. Considering the heuristic nature of the rest of the model and the fact that experimentally observed values for n are in the order of 1, a linear approximation of (5.10) is deemed satisfactory.

The amount of experimental data in literature to validate the model is scarce. A systematic study in which the vertical temperature profile in an office space is measured as a function of ventilation flow rate and supply air temperature for locations of supply and exhaust comparable to those the case study, was found in Sandberg (1986). A primary validation of the heuristic model in (5.11) was carried out on the basis these data. Three experiments in the study by Sandberg concern configurations comparable to the space described in section 5.2. The room dimensions in his study were 4.2 m x 3.6 m x 2.5 m (l × w × h), diffusers supplied the air horizontally just below the ceiling and exhausts were located near the ceiling.

In each configuration, stationary measurements were carried out for three ventilation rates, 1 air change per hour (ACH), 2 ACH and 4 ACH, corresponding to 0.011, 0.021 and 0.042 m^3/s respectively. At each of these ventilation rates, the vertical temperature profile was determined for two or three values of the supply air temperature, which we will refer to as a 'low', 'moderate' and 'high' value. These supply air temperatures were consequently higher than the exhaust temperature.

The symbols in Figure 5.4 show the experimental data for T_{out}-T_{1m} (difference between the extract air temperature and the air temperature at 1 m above the floor) as a function of the airflow rate and the supply air temperature. The drawn lines show the best fits of (5.11) to the data. As Sandberg does not report the mean air temperature, T_{air} was estimated with the measured value of T_{1m}.

As the internal heat load was kept at a fixed value in all three configurations, only one single value for $a_0 + a_1 Q_c$ was used in all model fits (0.15 °C). The values of a_2 and a_3 were optimized for each configuration separately.

Although model predictions and experimentally observed values do not perfectly coincide, the relevant trends are present and the model rarely deviates more than 0.5 °C from the measured data. Considering the fact that the model is to be used under uncertainty in the parameter vector $\underline{d}$, it is deemed useful.

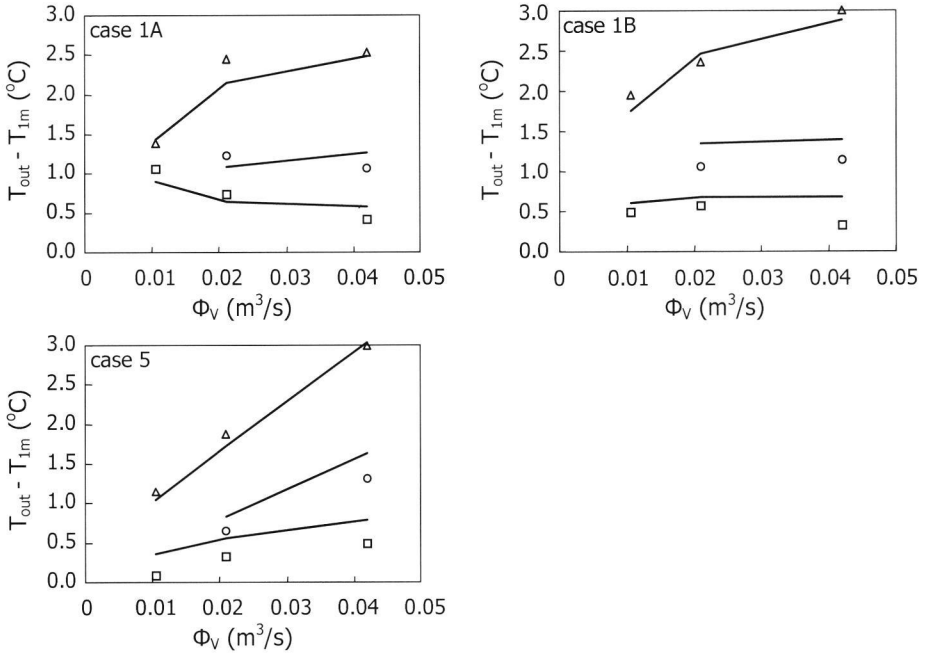

Figure 5.4 Comparison between measured values (symbols) and fitted model values (lines) for T_{out}-T_{1m} (difference between the extract air temperature and the air temperature at 1m above the floor). At each flow rate Φ_V, this temperature difference was measured for two or three values of T_{in}. The symbols □, O and Δ represent data associated with the lower, moderate and higher values of T_{in} respectively. The three lines in each graph accordingly connect model predictions associated with the lower, moderate and higher values of T_{in}. In configurations 1A and 1B the supply is a circular diffuser, located in the center of the ceiling, and the extract is positioned in a wall just below the ceiling. The diffuser types differ between these configurations. Configuration 5 has the supply in the short wall and the extract in a long wall. Both are located just below the ceiling.

Cool jet

For a cool jet, the situation is different. If the temperature difference between the supply air and the air in the space is large and the flow rate sufficiently small, the cool air in the jet will drop and predominantly mix up with air in the lower regions of the space, thereby sustaining thermal stratification. This is typically a winter situation and we assume here that in summer conditions this situation will not occur too often.

If the cool jet mixes up with air in the upper regions of the space, it will reduce or even inverse thermal stratification. At a fixed flow rate, this effect increases for a growing difference between supply air temperature and ambient room temperature. The dependence on the flow rate is expected to be qualitatively similar to that for warm jets.

Sandberg reports the effects of cool jets on the vertical temperature profile in three configurations with supply and exhaust located just below the ceiling. These measurements show small, positive vertical temperature gradients. However, as only one

observation with a cool jet is performed in each configuration, no information is available about the temperature profile as a function of the supply air temperature or the airflow rate.

In absence of information to suggest otherwise, the model structure in (5.11) is also adopted for supply air temperatures below room air temperature. Under that model, Sandberg's data indicate that the coefficient a_2 will not have the same value for warm and cool jets.

Resulting model
Hence the model is formulated as:

$$\Delta T_{out} = \begin{cases} \dfrac{a_0 + a_1 Q_c + a_2 \rho c_p \Phi_V (T_{in} - T_{air})}{1 + a_3 \Phi_V^2} & (T_{in} \geq T_{air}) \\ \dfrac{a_0 + a_1 Q_c + a_4 \rho c_p \Phi_V (T_{in} - T_{air})}{1 + a_3 \Phi_V^2} & (T_{in} < T_{air}) \end{cases} \tag{5.12}$$

In the expression for $T_{in} < T_{air}$, the coefficient a_4 appears in stead of a_2.

5.6.3 Modeling of the difference between temperature experienced by an occupant and mean air temperature

The difference between the temperature experienced by an occupant and the mean air temperature is ΔT_{occ}. In the development of its model, ΔT_{out} has been considered as a temperature difference between two vertically separated positions in the air. As this consideration also applies for ΔT_{occ}, an analogous line of reasoning can be followed to come to an expression in terms of $\underline{x}$. Hence, the proposed model for ΔT_{occ} is:

$$\Delta T_{occ} = \begin{cases} \dfrac{b_0 + b_1 Q_c + b_2 \rho c_p \Phi_V (T_{in} - T_{air})}{1 + b_3 \Phi_V^2} & (T_{in} \geq T_{air}) \\ \dfrac{b_0 + b_1 Q_c + b_4 \rho c_p \Phi_V (T_{in} - T_{air})}{1 + b_3 \Phi_V^2} & (T_{in} < T_{air}) \end{cases} \tag{5.13}$$

The structure of the model for ΔT_{occ} is identical to that for ΔT_{out}, but a different set of coefficients is used.

5.6.4 Modeling of the mean air temperature

A model for the mean air temperature T_{air} is already used in the current building simulation models in the form of the heat balance for the air volume:

$$0 = \rho c_p \Phi_V (T_{in} - T_{air} - \Delta T_{out}) + \sum_i \alpha_{c,i} (T_{wall,i} - T_{air}) A_{wall,i} + Q_c \tag{5.14}$$

This equation follows after combining (5.1), (5.3), (5.5), and (5.6), omitting the dynamic term in the left hand side of (5.1) (assumption of quasi-stationarity). The model parameters are the convective heat transfer coefficients $\alpha_{c,i}$.

In this study, we will use an average heat transfer coefficient α_c, which modifies (5.14) to:

$$0 = \rho c_p \Phi_V (T_{in} - T_{air} - \Delta T_{out}) + \alpha_c \sum_i (T_{wall,i} - T_{air}) A_{wall,i} + Q_c \qquad (5.15)$$

The values of heat transfer coefficients in the literature depend on the direction of the heat flow they modulate (horizontal, upward or downward) and hence on the orientation of the wall component they relate to. Especially the value for downward (stagnant) heat flow, which may occur at either a relatively cold floor or a warm ceiling, is much lower than the values for horizontal and upward flows (see Figure 3.3 and Figure 3.4). Hence, by the assumption of a single value for the heat transfer coefficient at all walls, the stagnant heat flows will be relatively overestimated. Considering the radiant heat exchange between wall components and the uncertainty in the value of the heat transfer coefficient, this is not deemed to be a significant obstacle.

Equations (5.12), (5.13) and (5.15) together form a closed set, forming a model for $\underline{y}$ as a function of $\underline{x}$ of the form (5.8) with parameter vector $\underline{d} = (a_0, \ldots, a_4, \alpha_c, b_0, \ldots, b_4)$.

5.6.5 Discussion

The model for $\underline{y}$, postulated in the previous sections, has a highly tentative character. It is predominantly based on heuristics and qualitative reasoning. It has no solid basis in first principles, nor is it sufficiently validated against measurements. The question arises what merit can be attributed to the model.

First, it is important to realize that the current approach in building simulation is a special case of the model in (5.12), (5.13) and (5.15), except for the use of a single value for the convective heat transfer coefficient instead of a separate value for each wall component.

Second, the aim of the study is to model the uncertainty in $\underline{y}$ rather than to produce accurate point estimates of $\underline{y}$. This makes the required accuracy of the model dependent of the (yet unknown) uncertainty in $\underline{y}$. Hence, it is worthwhile to complete the study with this model to investigate to what extent it succeeds to represent the observed uncertainty. Based on the results of this investigation, efficient steps can be planned to either improve the model if it is found inadequate, or to give it a more solid basis if it proves to meet the purpose.

5.7 Expert judgment study

5.7.1 Introduction

In section 5.4, the uncertainty in the relevant characteristics of the air temperature field, summarized in the three-element vector $\underline{y}$, was discussed in qualitative terms. This section addresses the assessment of this uncertainty.

Ideally, assessment of the uncertainties would be based on a statistical analysis of experimental data, obtained in a space matching the description in section 5.2. The design of experiment underlying such a data set should sufficiently cover the values of $\underline{x}$ that may occur in the (naturally ventilated) space under study. Moreover, it should display sufficient variation over those aspects of the boundary conditions, which are uncertain in a building simulation context. Such a data set is not available. A specific experiment to obtain such results would be a complicated, expensive and time-consuming exercise.

Besides, it is not evident that an experiment is the only way to obtain the required uncertainties. Indeed, advanced simulation tools are available, such as CFD and zonal model techniques (see section 5.3.3), as well as experimental results, obtained in different configurations. Before embarking on a sophisticated experimental study, it would be interesting to investigate to what extent the uncertainties can be quantified on the basis of these existing sources of information.

As mentioned in section 5.3.3, reliable flow field simulation requires expertise in both fluid dynamics and the numerical techniques to solve the governing equations. Interpretation of existing experimental results, often obtained under dissimilar conditions, to the case at hand, also requires knowledge of fluid dynamics as well as experience with measurements on flow fields. Hence it was decided to use expert judgment to quantify the requested uncertainties.

5.7.2 Main features of the expert judgment study

Expert judgment was also used in Chapter 4 to quantify uncertainties. The approach that was followed in that study, is also adopted here. For the sake of convenience, the main features of the method are recalled in this section.

More information can be found in Chapter 4 and Appendix C.1 in this thesis, or in Cooke (1991) and Cooke and Goossens (2000). Issues that are specific for the current study are addressed in the subsequent sections.

In an expert judgment study, uncertainty in a variable is considered as an observable quantity. Measurement of this quantity is carried out through the elicitation of experts, viz. people with expertise in the field and context to which the variable belongs. These experts are best suited to filter and synthesize the body of existing knowledge and to appreciate the effects of incomplete or even contradictory experimental data.

The uncertain variables of interest, also referred to as *elicitation* variables (in this study ΔT_{out}, T_{air} and ΔT_{occ}), are presented to the experts as outcomes of (hypothetical[28]) experiments, preferably of a type the experts are familiar with. They are asked to give their assessments for the variables in terms of subjective probability distributions, expressing their uncertainty with respect to the outcome of the experiment. Combination of the experts' assessments aims to obtain a joint probability distribution over the variables for a (hypothetical) decision-maker (DM), who could use the result in his/her decision problem. This resulting distribution, which is referred to as the DM, can be interpreted as a 'snapshot' of the state-of-the-knowledge.

To meet possible objections of a rational decision maker to adopt the conclusions of an expert judgment study, which are based on subjective assessments, it is important that a number of basic principles are observed. First, the results should be verifiable and accountable. In other words, all data including the experts' names and assessments, and all processing tools should be open to peer review. Second, the experts should have no interest in a specific outcome of the study (fairness). Third, the method should warrant neutrality, i.e. the methods of elicitation and processing must not bias the results. Finally, it is important that the experts' assessments are subjected to empirical control.

Cooke and Goossens (2000) present a procedure for structured elicitation and processing of expert judgment, which takes proper account of these principles. We mention the main features of this procedure here. First, the experts are elicited on experimentally observable quantities only. Besides, the experts are trained in the assessment of subjective probabilities prior to the elicitation (De Wit, 1998). Moreover, the experts' rationales, underpinning their assessments, are documented. Finally, the combination of the experts' assessments is based on their performance, which is obtained from a comparison of their assessments on so-called *seed* variables with measured realizations of these variables.

This procedure was closely followed here. In this study 5 experts were selected on the basis of their expertise in simulation or measurement of flow fields in building spaces. They were asked to assess the elicitation variables ΔT_{out}, T_{air} and ΔT_{occ}, in the space described in section 5.2 for a number of specified values of the *case* variables $\underline{T}_{iwall}$, Φ_V, T_{in}, $Q_{srce,c}$ and $Q_{sol,c}$.
The seed variables were related to similar characteristics of the air temperature distribution in another space for specified stationary boundary conditions. Realizations of these characteristics were available to the analyst (i.e. the author) from unpublished prior climate chamber measurements.

5.7.3 Questionnaire

The questions presented to the experts are referred to as cases. All cases together form the case structure. The case structure consisted of two parts. One part concerned the

[28] The hypothetical experiments are physically meaningful, though possibly infeasible for practical reasons.

elicitation variables ΔT_{out}, T_{air} and ΔT_{occ}, which had to be assessed in the context of the space in section 5.2. The other part addressed the seed variables.

5.7.3.1 Elicitation variables

First, we will address the constitution of one single case. Subsequently, the considerations on the number of cases will be addressed. Finally, the composition of the total case structure for the elicitation variables is discussed.

Single case

Strictly speaking, assessment of the uncertainty in the elicitation variables on the basis of the available information in a building simulation context would require that the experts are given the value of $\underline{x}$ in each case (see Section 5.5). However, the model that will be used in the probabilistic inversion, only takes a selection of $\underline{x}$ as input. First, $\underline{x}$ contains the surface temperatures of all wall components, whereas the model uses only the area-averaged surface temperature. Moreover, the individual contributions of convective internal and solar gains are combined in a single model variable representing the sum of both gains.

In this situation it would be most efficient to specify the case structure in terms of the model variables only. However, the experts may not agree with the assumptions underlying the model and omission of information from $\underline{x}$ could lead to spurious uncertainty in the experts' assessments. On the other hand, a systematic investigation into the effects of the surface temperature distribution would be beyond the scope of this work. Hence, a middle course was taken.

It was decided to include extra information on the surface temperature distribution in the case definitions in addition to the area-averaged value. If this information would bear significantly upon their rationales, the assumption that the information is superfluous would be disputed. As one of the more important mechanisms causing surface temperature differences between wall components is the uneven absorption of solar radiation, the additional information the experts received consisted of the total solar gain Q_{sol} entering the space. They were also given the part of this gain that is convectively emitted to the air to enable the evaluation of the total convective heat gain in the space. The vector of case variables $\underline{x}^*$ thus consisted of:

$$\underline{x}^* = (T_{wall}, \mathbf{\Phi}_V, T_{in}, Q_{int,c}, Q_{sol}, Q_{sol,c})$$

where T_{wall} is the area averaged surface temperature, Q_{sol} is the total incident solar gain and $Q_{sol,c}$ the part of Q_{sol} that is emitted convectively to the air.

Each case requested the experts to assess $\underline{y}$ as the outcome of the following hypothetical experiment. From a large population of spaces matching the description in section 5.2, one space is randomly selected. At some arbitrary moment in the spring/summer period (April-September), measuring equipment is installed in the space. The variables T_{wall}, $\mathbf{\Phi}_V$, T_{in}, $Q_{int,c}$, Q_{sol} and $Q_{sol,c}$ are monitored for a period of 1 hour. Given the observed hourly averaged values of these variables, what would have been the hourly averaged values of ΔT_{out}, T_{air} and ΔT_{occ} if they had been measured in the same experiment?

The information on the experimental conditions did not include the initial conditions. This is consistent with the assumption, discussed in section 5.6 that a quasi-stationary approach suffices. However, the experts may not share this point of view and attribute uncertainty to $\underline{y}$ due to a lack of knowledge on the initial conditions. A large contribution of this uncertainty to the overall acquired uncertainty is undesirable, as information on the time history is actually available in a building simulation, but was assumed to be insignificant. In the discussion in Section 5.9, the experts' rationales are scrutinized to reveal the composition of their uncertainty at this point.

Number of cases

The costs of probabilistic inversion (computational effort) and, to a lesser extent, of expert elicitation impose constraints on the maximum number of cases. Whereas the experts develop skills to deal with each next question more efficiently, the computational demands of the probabilistic inversion grow more or less exponentially with the number of cases (see section 5.8). To keep computation times at an acceptable level, a maximum of 9 cases, i.e. 27 elicited variables, was used in this study.

Within this limitation on the number of cases, it was deemed infeasible to study the temperature field in the space for two directions of the airflow. For a given flow rate, the effect of the supply jet on the flow field strongly depends on the geometry of the supply aperture. As shown in Figure 5.2, the orifices in the opposite walls are differently shaped. Hence, a ventilation flow entering the space through the window in the façade will have a different impact on the flow field than a flow at the same rate in the opposite direction. In the context of this pilot study it was decided to only consider cases with ventilation flows entering through the window.

Resulting case structure

To design the 9 cases, values of $\underline{x}^*$ were selected to optimally cover the space, spanned by these variables. The selected values and ranges for the individual elements of $\underline{x}^*$ are discussed in appendix D. They were combined to form the case structure in Table 5.2. For values of A_{wall}, ρ, and c_p see Appendix A.

Table 5.2 Case structure for the elicitation variables.

		Case 1	Case 2	Case 3	Case 4	Case 5	Case 6	Case 7	Case 8	Case 9
Φ_V	m^3/s	$2.8.10^{-2}$	$2.8.10^{-2}$	$2.8.10^{-2}$	$7.0\ 10^{-2}$	$7.0\ 10^{-2}$	$7.0\ 10^{-2}$	$2.1\ 10^{-1}$	$2.1\ 10^{-1}$	$2.1\ 10^{-1}$
$Q_{int,c}$	W	0	620	0	0	620	620	620	620	0
Q_{sol}	W	0	0	490	510	500	470	0	480	0
$Q_{sol,c}$	W	0	0	49	51	50	47	0	48	0
T_{in}	°C	23.0	26.7	23.5	15.1	30.8	20.3	17.2	28.1	14.5
T_{wall}	°C	23.0	23.0	23.0	23.0	23.0	23.0	23.0	23.0	23.0

Questions

For each case, the experts were asked to fill out the following two tables:

Table 5.3 Quantile values of the elicitation variables to be assessed by the experts for each case.

variable	quantiles			
	5%	50%	95%	
T_{air}				°C
T_{out} - T_{air}				°C
T_{occ} - T_{air}				°C

Table 5.4 Dependencies to be assessed by the experts for each case.

variable 1	variable 2	dependency
T_{air}	T_{out} - T_{air}	
T_{occ} - T_{air}	T_{out} - T_{air}	

Table 5.3 requests the experts to specify their median estimate, or 50% quantile value, and their central 90% confidence intervals, bounded by the 5% and 95% quantile values, for each of the elicitation variables ΔT_{out}, T_{air} and ΔT_{occ}. These data provide information about the experts' marginal distributions, but they do not reveal information about the dependencies between the variables. Hence, Table 5.4 asks for a separate specification of the dependencies between the elicitation variables within a single case.

A common way to represent dependencies between variables is in the form of rank correlations. However, these rank correlations cannot be elicited directly. Therefore an alternative approach was used, as already illustrated in Chapter 4. The experts, having assessed their marginal distributions over variables 1 and 2, were asked to answer the following question: 'Imagine that variable 1 has been measured in the case (experiment) at hand. Its value is found to exceed your median (50% quantile) value. What is your subjective probability that a measurement of variable 2 would also have exceeded your median assessment, if it had been measured in the same experiment?'

Under suitable assumptions (among which minimal information), this conditional probability can be uniquely transformed to a rank correlation (Cooke and Kraan, 1996).

5.7.3.2 Seed variables

To implement empirical control, the experts were also asked to assess a number of variables of which experimental realizations were available to the analyst, but not to the experts. The realizations were taken from an internal CSTB-report, which describes experiments in a climate chamber carried out by François et al. (1993). These experiments were described to the experts in the questionnaire and the experts were asked to assess the outcomes, again in the form of three quantile values. The seed variables were chosen to resemble the elicitation variables as closely as possible. A description of these experiments as they were presented to the experts, is given below.

Description of the hypothetical experiments

The experiments are carried out in another office space (office space 2) with dimensions as shown in Figure 5.5. The space is mechanically ventilated with outdoor air. The interior surface temperatures of the enclosure of the space are monitored. A hot water radiator is mounted below the window. During the experiments the space is empty.
Airflow into the space can be mechanically induced through a horizontal slit in the facade just below the ceiling as shown in Figure 5.5. The geometry of the slit is unknown. The air flows out through cracks and joints, mainly in the wall opposite to the facade. The door in this wall is closed during the experiments.

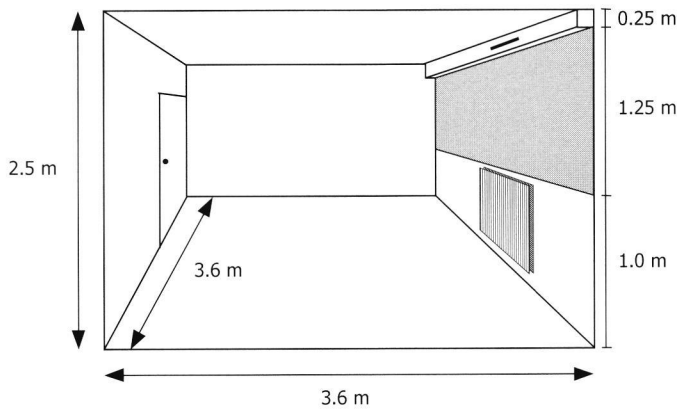

Figure 5.5 Office space 2. Internal dimensions (l x w x h) 3.6 m x 3.6 m x 2.5 m. Height of the window 1.25 m. Ventilation inlet is located above the window, 18 cm below the ceiling. The space is not furnished (empty). A hot water radiator is located below the window.

The seed variables to be assessed by the experts were:

1. $T_{2.4\,m}$ - $T_{0.1\,m}$, the air temperature difference between 0.1 m below the ceiling and 0.1 m above floor level in the center of the space
2. $T_{1.5\,m}$, the air temperature at 1.5 m above floor level in the center of the space

In each case, these variables were considered to be the outcomes of the following experiment:
Prior to the experiment, a stationary situation is created. No solar radiation enters the space and no internal heat sources are in operation, except for the hot water radiator. The following variables are measured, while maintaining the stationary conditions:

Φ_V air volume flow through the space
T_{in} temperature of the incoming air
T_{win} interior surface temperature of the window
T_{floor} average surface temperature of the floor
T_{ceil} average surface temperature of the ceiling
T_{wall} area-averaged interior surface temperature of the walls (floor, ceiling and window surface excluded)

$Q_{h,c}$ convective heat production by hot water radiator
T_p surface temperature of the parapet just behind the radiator

For each case, what would have been the values of the seed variables, had they been measured in the same experiment? All unspecified experimental conditions should be considered uncertain.

Five of these experiments were presented to the experts. The conditions in these experiments are shown in Table 5.5.

Table 5.5 Case structure for the seed variables.

		Case A	Case B	Case C	Case D	Case E
Φ_V	m^3/s	$4.7.10^{-3}$	$4.7.10^{-3}$	0	$4.7.10^{-3}$	0
T_{in}	°C	4.0	4.0	-	4.5	-
T_{win}	°C	15.0	6.0	6.0	5.8	9.0
T_{floor}	°C	20.1	20.2	19.9	27.2	21.2
T_{ceil}	°C	20.3	21.1	21.3	20.6	31.0
T_{wall}	°C	19.8	20.2	20.2	19.5	20.6
$Q_{h,c}$	W	220	440	330	0	0
T_p	°C	34.5	45.2	39.2	17.3	18.0

Questions

For each case, the experts were asked to fill out the following table:

Table 5.6 Quantile values of the seed variables to be assessed by the experts for each case.

variable	quantiles			
	5%	50%	95%	
$T_{2.4\,m}$ - $T_{0.1\,m}$				°C
$T_{1.5\,m}$				°C

5.7.4 Selection of the experts

A pool of candidates for the expert panel was established by screening recent literature on relevant issues. Additional sources were the membership lists of IEA Annex 20 (Lemaire, 1993) and Annex 26 (Heiselberg et al., 1998). From the many candidates resulting from the screening, 5 were selected. Table 5.7 shows the names of the participating experts in alphabetical order. To select the experts, the same criteria as in Chapter 4 were applied.

Table 5.7 List of experts in the experiment in alphabetical order.

Qingyan Chen	Massachusetts Institute of Technology (MIT), Boston, USA
Tony Lemaire	The Netherlands Organization for Applied Scientific Research (TNO), Delft, The Netherlands
Alfred Moser	Eidgenössische Technische Hochschule (ETH), Zürich, Switzerland
Peter Nielsen	Aalborg University, Aalborg, Denmark
Mats Sandberg	Royal Institute of Technology (KTH), Gävle, Sweden

Peter Nielsen and Tony Lemaire also acted as experts in the dry-run.

One of the experts initially misunderstood the questions in the questionnaire. When this came to light, there was insufficient time left to revise his assessments and he withdrew from the expert panel.

5.7.5 Dry-run

The aim of the dry-run was to obtain feedback on the issues:

- are the questions clear and well-posed?
- can the training material be studied in the allocated time and are the training goals achieved?
- can the elicitation be completed within the allocated time?

The dry-run meetings proceeded in a similar way as the actual elicitation meetings were planned: a brief consolidation of the expert training followed by the elicitation, in which the expert explicated his assessments to the analyst. However, only two cases were presented to the experts and considerable time was reserved to discuss the issues mentioned above.
On the basis of the dry-run, the case-structure was adjusted and the questionnaire was improved on a few points.

5.7.6 Elicitation

The experts were contracted to spend 3 days on their assessments, of which about 2.5 days were allotted to the elicitation. In the elicitation stage, the core of the experiment, the experts made their judgments, both quantile values and dependency assessments, available to the analyst. Each expert was elicited individually. They were specifically asked not to discuss the experiment with each other. In this way, the diversity of viewpoints would be minimally suppressed. Moreover, any overconfidence resulting from the (partial) consensus that is often reached among experts in a group elicitation session would be avoided (Cooke, 1991).

The elicitation stage took place in three parts. Prior to the elicitation meeting, each expert prepared his assessments e.g. by looking up relevant literature and making calculations. During the meeting, these assessments were discussed with the analyst, who avoided giving any comments regarding content, but merely pursued clarity, consistency and probabilistic soundness in the expert's reasoning. On the basis of the discussion, the expert revised and completed his assessments if necessary. The experts were not informed which of the elicited variables were the seed variables.
Completion of the elicitation coincided with the writing of the rationale, a report documenting the reasoning underlying the assessments of the expert. During the writing of this rationale, which was done by the analyst to limit the time expenditure of the expert to a minimum, issues that had not been identified in the meeting were discussed with the expert by correspondence.

The rationales of the experts can be found in De Wit (2001).

5.7.7 Results

This section presents the experts' quantile assessments in a graphical form. Table with both the quantile and dependency assessments can be found in Appendix D.
Each expert is referred to by a number. These numbers were randomly attributed to the experts in Table 5.7 and will be used throughout the study. No results are shown for expert number 5 for reasons discussed in section 0.

Figure 5.6 shows an itemwise comparison of the quantile assessments of the four experts on the seed variables with the measured realizations (François et al., 1993). The assessments of the item weight decision-maker (see section 5.7.8) are also shown.

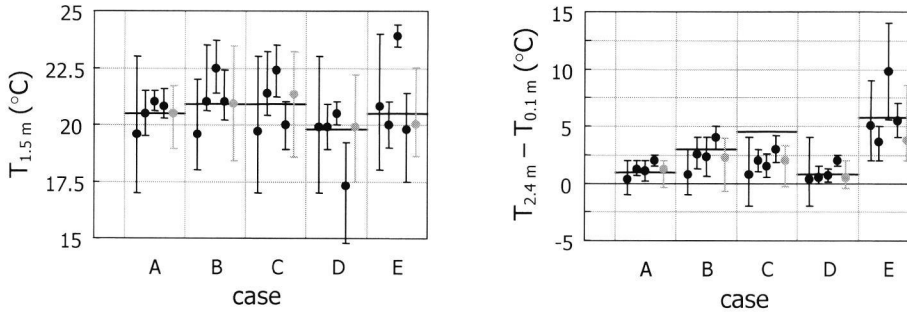

Figure 5.6 Itemwise presentation of the experts' assessment on the seed variables. The dots are their median values, the error bars show their central 90% confidence intervals. The drawn lines indicate the realizations, which were measured in a study by François et al. (1993). For each case, the results of experts 1 through 4 are shown from left to right. The rightmost, gray results show the quantile values of the item weight DM (see section 5.7.8).

The experts' assessments on the elicitation variables are shown in Figure 5.7 through Figure 5.9.

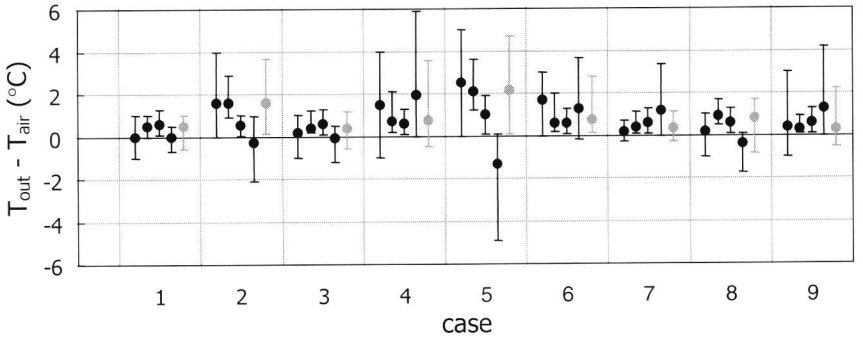

Figure 5.7 The experts' assessment on T_{out}-T_{air}. The dots are their median values, the error bars show their central 90% confidence intervals. For each case, the results of experts 1 through 4 are shown from left to right. The rightmost, gray results show the quantile values of the item weight DM (see section 5.7.8).

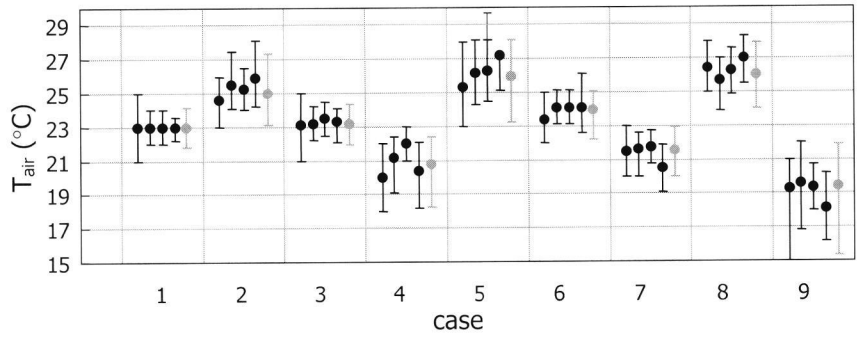

Figure 5.8 The experts' assessment on T_{air}. The dots are their median values, the error bars show their central 90% confidence intervals. For each case, the results of experts 1 through 4 are shown from left to right. The rightmost, gray results show the quantile values of the item weight DM (see section 5.7.8).

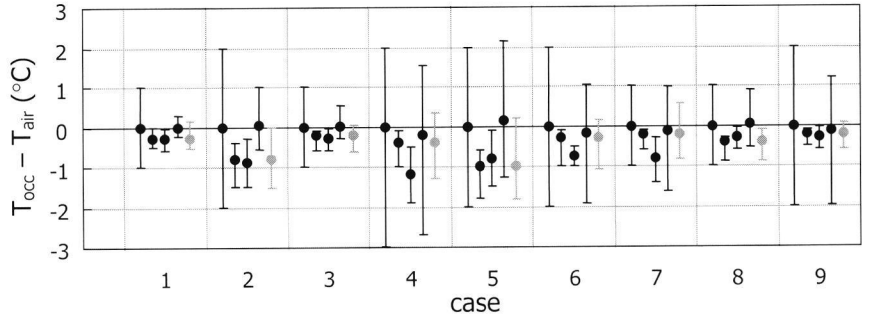

Figure 5.9 The experts' assessment on T_{occ}-T_{air}. The dots are their median values, the error bars show their central 90% confidence intervals. For each case, the results of experts 1 through 4 are shown from left to right. The rightmost, gray results show the quantile values of the item weight DM (see section 5.7.8).

5.7.8 Analysis and combination of the experts' assessments

The experts' assessments were scored and combined according to the classical model, as developed by Cooke (1991). An outline of this model is given in Chapter 4 and Appendix C.1.

Table 5.8 shows the experts' performance scores, calculated from a comparison of their assessments on the 10 seed variables with the observed realizations. Experts 1 and 2 receive a fair calibration score, comparable to the calibration scores of the best calibrated experts in the study in Chapter 4. The other experts are significantly less calibrated. Expert 1, however, is on average a factor 4-5 less informative than expert 2.

Table 5.8 Experts' performance scores as calculated with the classical model.

Expert no.	Calibration C_e	Global information score I_e		Performance w_e
		all items	seed items	
1	$2.2\ 10^{-1}$	0.24	0.17	$3.6\ 10^{-2}$
2	$2.4\ 10^{-1}$	0.91	0.92	$2.2\ 10^{-1}$
3	$1.0\ 10^{-4}$	0.88	1.00	$1.0\ 10^{-4}$
4	$1.0\ 10^{-2}$	0.48	0.92	$9.2\ 10^{-3}$

The first column lists the experts by number. These are the same randomly attributed numbers, which were used in Figure 5.6 through Figure 5.9. In the remainder of this document, the experts will be addressed by their number only. The second column shows the calibration scores for each expert. The global information scores, based on the default intrinsic ranges (see appendix C.1), are in column 3. Finally, the performance, product of calibration and information, is displayed in the last column.

From the experts' assessments, four different decision-makers were calculated. Their scores are shown in Table 5.9.

Table 5.9 Performance scores of four different decision-makers.

Decision maker	C_e	I_e all items	I_e seed items	w_e	Significance level	Participating experts
Equal weight	$2.2\ 10^{-1}$	0.12	0.12	$2.7\ 10^{-2}$	-	1, 2, 3, 4
Global weight	$2.4\ 10^{-1}$	0.91	0.92	$2.2\ 10^{-1}$	$2.4\ 10^{-1}$	2
Item weight	$6.8\ 10^{-1}$	0.47	0.41	$2.8\ 10^{-1}$	$2.2\ 10^{-1}$	1, 2
'Best' expert	$2.4\ 10^{-1}$	0.91	0.92	$2.2\ 10^{-1}$	-	2

The first 4 columns in this table are similar to those in Table 5.8. The significance levels in column 5 refer to the interpretation of each expert as a hypothesis. If an expert's calibration score is below this significance level, he is 'rejected' and hence does not participate in the DM (column 6). More information can be found in Appendix C.1.

The equal weight DM has a fair calibration score, but its performance is low as a result of a low information score. The global weight DM has an optimal performance for a significance level, at which all experts but expert 2 are rejected. Hence this DM and the

'best' expert have equal scores. The item weight DM is less informative than the global weight DM, but due to a better calibration score, it outperforms all other decision-makers.
Hence, the item weight DM will be used in the remainder of this chapter as the optimal combination of the experts' assessments. The quantile values of this decision-maker are shown in Figure 5.6 through Figure 5.9 in a graphical form and tabulated in Appendix D.

In the elicitation sessions, highest priority was given to the quantile assessments. It turned out that these assessments demanded the bulk of the available time and concentration. Having completed their assignment on the quantile values, most experts were reluctant to embark upon the assessment of the dependencies, which required familiarizing with the concept of conditional probability and developing a strategy to quantify these probabilities.
It was felt that the acquired dependency values have insufficient basis to be analyzed on equal terms with the quantile assessments. Hence, it was decided not to use the experts' dependency assessments in the probabilistic inversion.

5.8 Probabilistic inversion

5.8.1 Introduction

The aim of probabilistic inversion is to map the uncertainties that were assessed in the expert judgment study to the parameters in the heuristic model from Section 5.6. When successful, this mapping process results in a (joint) probability distribution over the model parameters, expressing their uncertainty, which can be used in combination with the heuristic model in building simulation.
The success of the probabilistic inversion is measured by the degree to which the expert assessments (DM) in the 9 cases can be reproduced on the basis of the resulting probability distribution over the model parameters.

Technically, the expert judgment study in section 5.7 resulted in probability distributions over $\underline{y} \equiv (\Delta T_{out}, T_{air}, \Delta T_{occ})$ for 9 cases, specified[29] by the value of $\underline{x} \equiv (\underline{T}_{wall}, \Phi_V, T_{in}, \underline{Q}_{srce,c}, \underline{Q}_{sol,c})$. We will refer to $\underline{x}$ and $\underline{y}$ in each of these cases as $\underline{x}_j$ and $\underline{y}_j, j = 1,\ldots,9$.

In section 5.6, a model M for $\underline{y}$ as a function of $\underline{x}$ was proposed:

$$\underline{y} = M(\underline{x}, \underline{d}) \tag{5.8}$$

Equations (5.12), (5.13) and (5.15) define the model M with parameter vector $\underline{d} = (a_0, \ldots, a_4, \alpha_c, b_0, \ldots, b_4)$. For a given value of $\underline{d}$, M can be used in each case to obtain an estimate $\underline{\hat{y}}_j$ for $\underline{y}_j$:

[29] In fact, only partial information on $\underline{x}$ was used to specify the cases, but this is immaterial to the discussion in this section.

$$\underline{\hat{y}}_j = M\left(\underline{x}_j, \underline{d}\right) \;, j = 1,\ldots,9 \tag{5.16}$$

The aim of the probabilistic inversion is to find a probability distribution over $\underline{d}$ such that

$$\underline{\hat{y}}_j \sim \underline{y}_j \;, j = 1,\ldots,9 \tag{5.17}$$

where ~ means ' has the same distribution as'. As already mentioned in section 5.7.7, the experts' assessments on the dependencies between the elements of $\underline{y}$ will not be used in the probabilistic inversion, which implies that (5.17) is equivalent to:

$$\hat{y}_{ij} \sim y_{ij} \;, \quad i = 1\ (\Delta T_{out})\ ,\ 2\ (T_{air})\ \text{or}\ 3\ (\Delta T_{occ}) \quad \text{and} \quad j = 1,\ldots,9$$

In the jargon of probabilistic inversion, the elicitation variables y_{ij} assessed by the experts are called 'observables' and the space they span is analogously referred to as the 'observable space'. The elements of the parameter vector are the 'target variables' or 'targets' forming the 'target variable space'. In this study, the dimensions of observable space and target variable space are 27 and 11 respectively.

Methods for probabilistic inversion problems with more than one target variable were developed by Cooke (1994), Hora and Young (see Harper et al., 1994), and Kraan and Cooke (Kraan and Cooke, 1996, 1997, 1999 and Kraan, 1999). The PARFUM-method by Cooke (PARameter Fitting for Uncertain Models) was designed for small problems with e.g. two target variables, and is unfit for the problem in this study. The PREJUDICE-method by Kraan and Cooke (PRocessing Expert JUDgment Into Code paramEters) is based on the technique by Hora and Young. As it can deal with large problems (more than 2 or 3 targets), it is used in this study.

5.8.2 Solution scheme

The PREJUDICE-method for probabilistic inversion is based on the following solution scheme:

1. Sampling from the target variable space (model parameter space).
2. Propagation of the samples through the model to obtain corresponding samples in the observable space.
3. Distribution of the probability mass over the samples in the observable space to match the given quantile values for each observable. As each sample in the observable space uniquely corresponds to a sample in the target variable space, this step also yields a distribution of the probability mass over the target variable space.
4. Representation of this joint probability distribution over the target variables in terms of marginal distributions and (rank-) correlations.

Each of the steps in the scheme will be briefly discussed here.

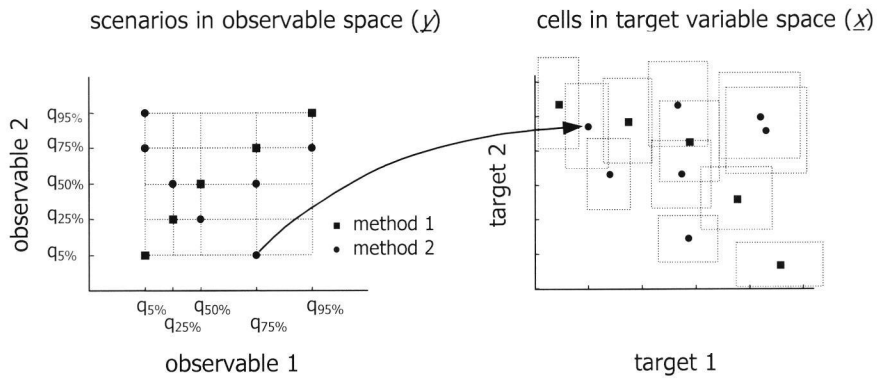

Figure 5.10 Illustration of the steps in the heuristic algorithm to identify a region of the target variable space from which samples will be drawn. To enable a graphical representation, both the observable space and the target variable space are chosen 2-dimensional. The left figure shows the scenarios as points in the observable space with an indication of the method that has been used to generate them. From an optimal model fit to each scenario in the sense of (5.18), corresponding points are generated in the target variable space, as shown in the right figure. Around each of these points a cell is defined from which samples are taken.

Sampling from the target variable space and propagation (Step 1, 2)

In most practical applications, the target variable space is so large that sampling has to be heuristically guided to obtain good results with a tractable number of samples and hence an acceptable amount of computational effort. These heuristic algorithms basically seek a suitable region in the target variable space, over which the probability mass will be distributed. An illustration is shown in Figure 5.10.

First, a set of K 'scenarios', i.e. combinations of realizations for the observables, is defined. Two methods to generate scenarios were applied here:

1. For a given value of $q \in [0\%, 100\%]$, this method generates a scenario by combining the DM's q quantile values of all elicitation variables. Common choices for q are 5%, 25%, 50%, 75% and 95%.
2. For each elicitation variable, one of the DM's 5%, 25%, 50%, 75% or 95% quantile values is randomly selected. These independently selected quantile values are combined to form a scenario.

For the scenario with index k, $k = 1,\ldots,K$, 'best' estimates for the target variables in $\underline{d}_k$ are calculated as the solution of:

$$\min \max_{i,j} \left(\hat{y}_{ij}(\underline{d}_k) - y_{ij,k} \right)^2 \tag{5.18}$$

where $y_{ij,k}$ is the value of y_{ij} in scenario k.

The idea is that in step 1 of the scheme samples are only drawn from sections of the target variable space in the vicinity of the values $\underline{d}_k$, obtained from the fits of the model

to the selected scenarios. To enable this, PREJUDICE defines hypercubes or cells in the target variable space around the $\underline{d}_k$'s. Sampling only takes place from those cells.
There are no rules for an optimal size or configuration of the cells in the target variable space. Hence, this configuration is determined by trial and error. Further research is ongoing in this area (Kraan, 2000).

From each of the cells in the target variable space, a suitable number of samples is drawn to generate a feasible optimization problem (see step 3) and ascertain a sufficiently smooth distribution of the probability mass over the target variable space at acceptable computational loads. As samples may be generated in physically inadmissible areas of the observable space, each sample has to be checked after being propagated and rejected if physically unrealistic.

Distribution of the probability mass over the samples (Step 3)

The aim of this step is to distribute the probability mass over the samples in the observable space to match the DM's quantile assessments. Figure 5.11 shows a two-dimensional observable space. The DM's quantile assessments define a grid in the space, which is shown by the dotted lines. The crosses represent the propagated samples. The total probability mass of all samples in the consecutive columns of cells in the grid should equal 0.05, 0.45, 0.45 and 0.05 respectively. For variable 2, the probability masses should be likewise distributed over the consecutive rows in the grid. Generalization to observable spaces of larger dimension is straightforward.

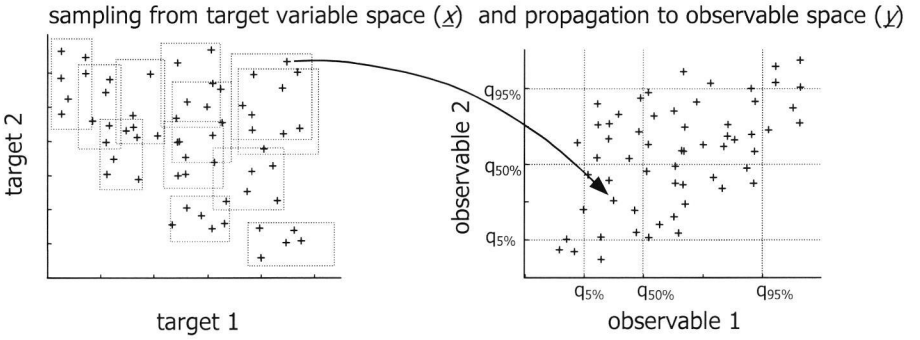

Figure 5.11 Illustration how samples are drawn from cells in the target variable space and subsequently propagated to the observable space. In this example, 5 samples are taken from each cell. The grid in the observable space is defined by the DM's quantile assessments.

In general, there may be many distributions matching the DM's quantile assessments. If more than one solution exists, the distribution is chosen, which has minimum information (Appendix C.1) with respect to a uniform background measure. This distribution can be interpreted as the solution of a constrained Non-Linear Programming (NLP) problem (see Kraan and Cooke, 1999).

If no solution is found, this may have two causes.

1. The samples do not provide sufficient coverage of the observable space. This may be resolved by either drawing more samples from each cell, generated by the heuristic algorithm, or by enhancing the number of scenarios to enlarge the region in the target variable space from which samples can be drawn.
2. No solution exists (problem is infeasible). In this case, reduction of the dimension of the observable space may be an option. If the original observable space has dimension n, n sub-spaces of dimension n-1 can be defined. If a solution is found in each of these n spaces of lower dimension, an approximation to the requested distribution over the target variables can be obtained by averaging the n distributions[30], found from the solutions in the sub-spaces. If the problem is still infeasible in one or more of the sub-spaces, further dimension reduction can be applied.

Joint probability distribution over the target variables (step 4)

Step 3 assigns a probability mass to the samples in the observable space. As each sample in the observable space corresponds to a sample in the target variable space, step 3 implicitly provides a joint sample distribution over the target variables. To make the distribution practicable as input to further analyses, it is necessary to represent it in a more amenable format. A common representation of joint distributions is in the form of marginal distributions and a (rank-) correlation matrix.

5.8.3 Implementation in the study

The implementation of the solution scheme in the current study is step-wise discussed in this section.

Sampling from the target variable space

By means of the methods, described in the previous section, 230 scenarios were generated. For each scenario a corresponding point $\underline{d}_k$, k = 1,...230, in the target variable space was found as a solution of (5.18). Around each of these points a separate hypercube was constructed, with extreme corner points 0.5 $\underline{d}_k$ and 1.5 $\underline{d}_k$. From each of these 230 hypercubes, 1000 samples were drawn and propagated through the model.

Propagation of the samples

The observable space in this study has 27 dimensions. This is too large to enable sufficient coverage with a tractable number of samples. A computational compromise was found by dividing the observable space in three separate observable spaces of dimension 9 each. This division was performed along natural boundaries: one observable space of dimension 9 was created for the ΔT_{out}'s in all 9 cases, one for the T_{air}'s and one for the ΔT_{occ}'s. The 230 000 samples, drawn from the target variable space were propagated to each of these observable spaces.

---

[30] Averaging yields a combined distribution with respect to which the n distributions are minimally informative (see Kraan and Cooke, 1997).

To filter out physically inadmissible samples, intrinsic ranges were defined for each observable on a heuristic basis. Samples with a value outside the intrinsic range for one or more of the observables were rejected. No restrictions were imposed on combinations of values for the various observables. About 112 000 of the 230 000 samples were rejected.

Actually, about 5 10^6 different observable spaces of dimension 9 can be created from an original observable space with 27 dimensions. Strict application of the solution scheme would have required solution of the NLP-problem in each of these observable spaces and subsequent averaging of the acquired probability distributions over the target variable space. Theoretically, this is possible, but to keep the problem computationally tractable, only three 9-dimensional observable spaces were considered here.

Distribution of the probability mass over the samples

In two of the observable spaces, i.e. for the ΔT_{out}'s and the ΔT_{occ}'s, the NLP-problem was feasible and a distribution of the probability mass over the samples was established, which matched the experts' assessments. In the observable space, spanned by the T_{air}'s, no solution could be found. As attempts to augment the number and selection of scenarios and the number of samples did not alleviate the problem, it was decided to consider the problem infeasible. Consequently, a probability distribution over the target variables was calculated as the average of the distributions obtained from the NLP-solutions obtained in the two other observable spaces.

5.8.4 Results

Figure 5.12 through Figure 5.16 and Table 5.10 show the results of the probabilistic inversion.

Elicitation variables

When the joint probability distribution over the model parameters, obtained in the probabilistic inversion, is propagated through the model in the 9 cases that were presented to the experts, distributions over the elicitation variables (observables) are obtained as shown in the following three sets of figures. As a reference, the 5%, 50% and 95% quantiles from the DM are also shown.

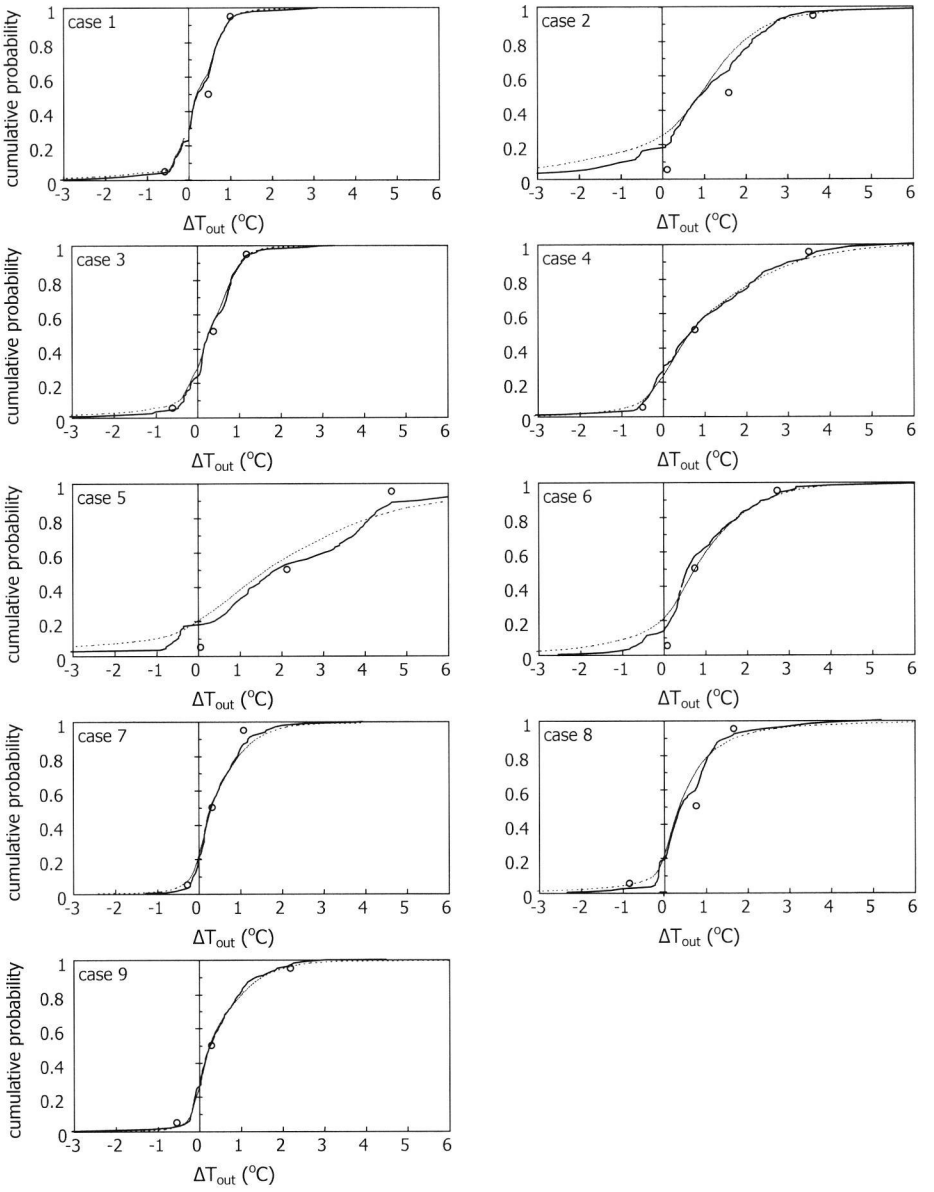

Figure 5.12 The marginal distributions for ΔT_{out}, resulting from the probabilistic inversion (bold, drawn lines) compared with the 5%, 50% and 95% quantile values from the item weight DM (circles). The thin, dotted lines result from the propagation of 10^5 samples, drawn from the reduced joint distribution over the target variables, i.e. the distribution represented by marginals and rank correlations only.

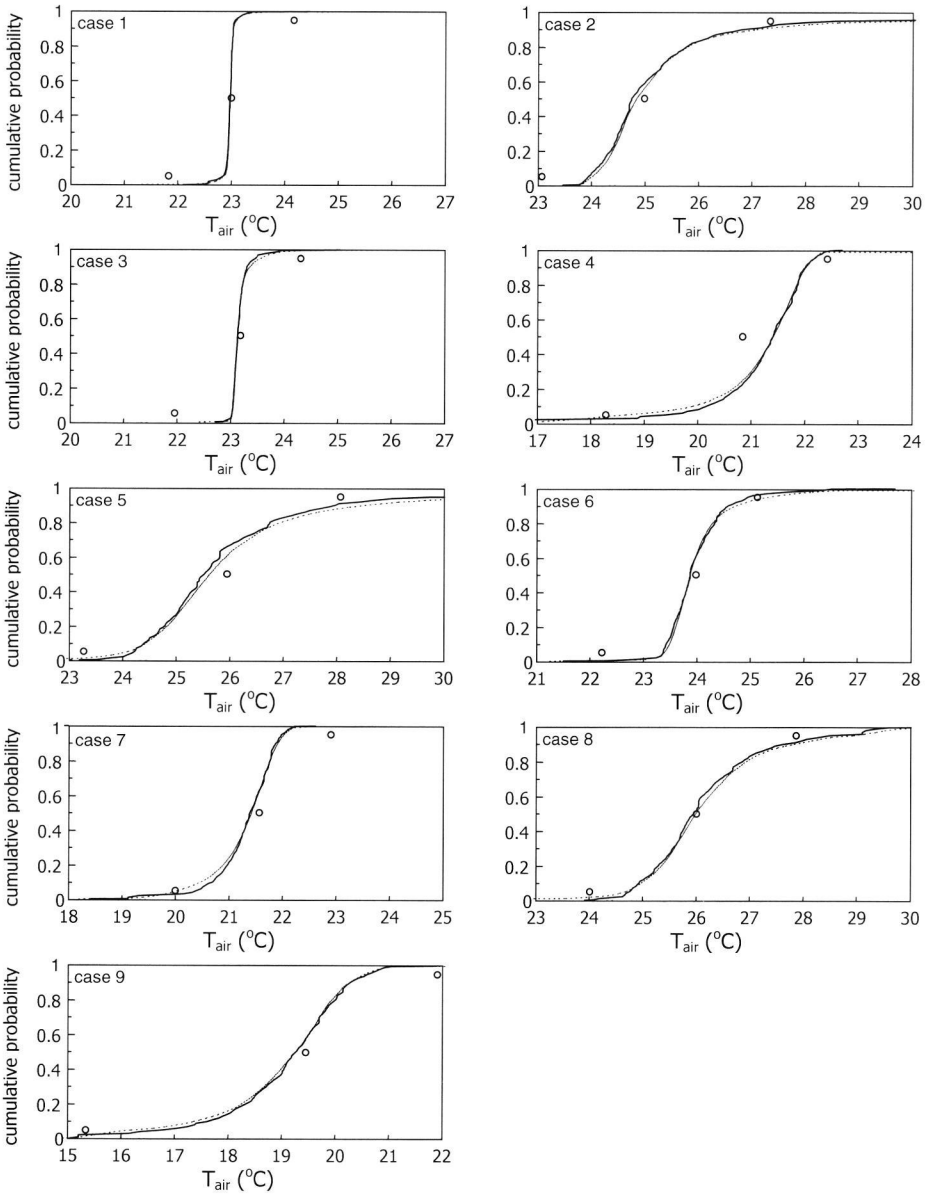

Figure 5.13 The marginal distributions for T_{air}, resulting from the probabilistic inversion (drawn lines) compared with the 5%, 50% and 95% quantile values from the item weight DM (circles). The thin, dotted lines result from the propagation of 10^5 samples, drawn from the reduced joint distribution over the target variables, i.e. the distribution represented by marginals and rank correlations only.

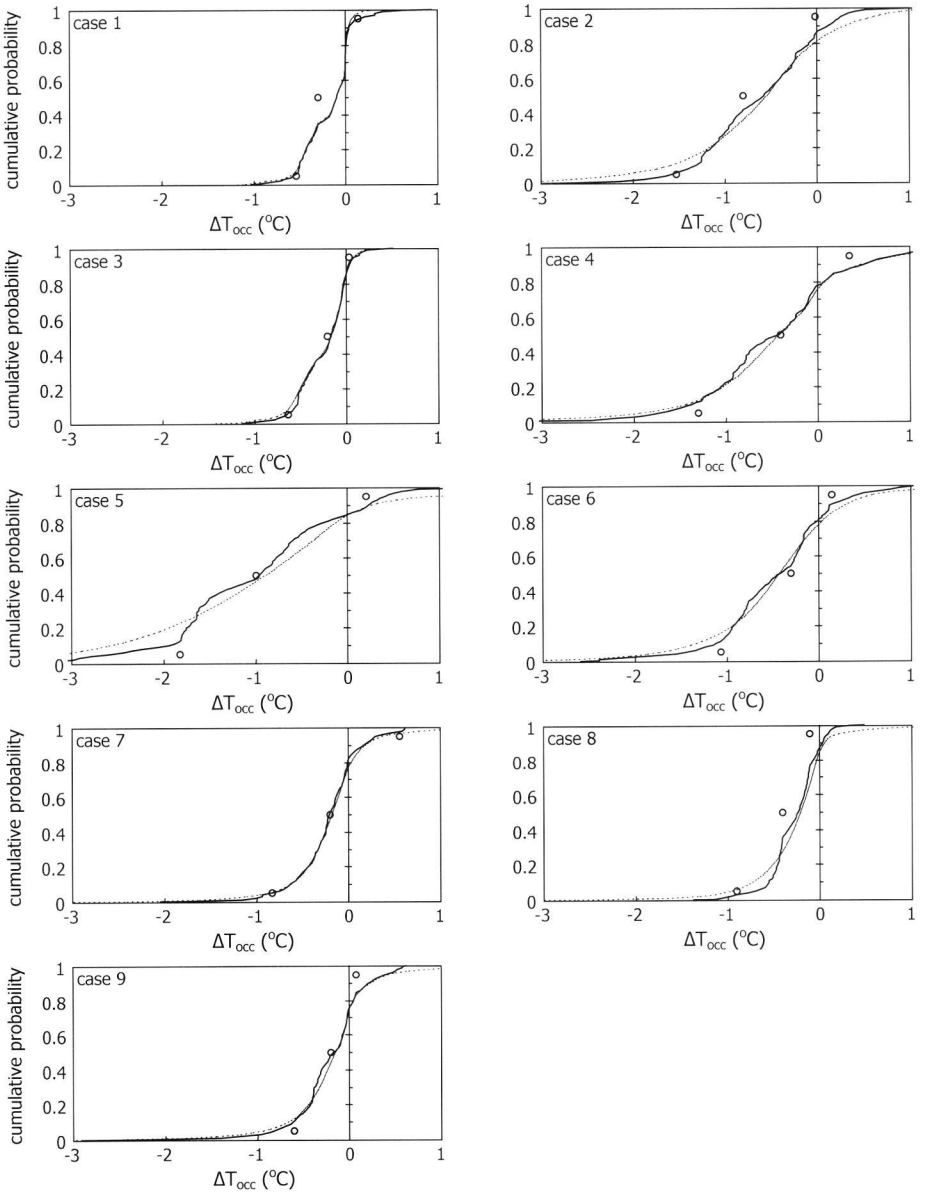

Figure 5.14 The marginal distributions for ΔT_{occ}, resulting from the probabilistic inversion (drawn lines) compared with the 5%, 50% and 95% quantile values from the item weight DM (circles). The thin, dotted lines result from the propagation of 10^5 samples, drawn from the reduced joint distribution over the target variables, i.e. the distribution represented by marginals and rank correlations only.

To use the joint sample distribution over the target variables, resulting from the probabilistic inversion, in further analyses, it must be cast in a more amenable, yet approximate representation. A common representation in terms of marginal distributions and rank correlation matrix is shown in Figure 5.15, Figure 5.16, and Table 5.10.

The information that is lost in this representation is estimated by a comparison of the marginal distributions over the elicitation variables, calculated from the approximate distribution over the targets, with the original marginals from the probabilistic inversion. For each case and each elicitation variable, both marginals are shown in Figure 5.12 through Figure 5.14. The approximated marginals are based on the propagation of 10^5 samples, drawn from a minimally informative joint distribution over the targets satisfying the specified marginals and rank correlation matrix.

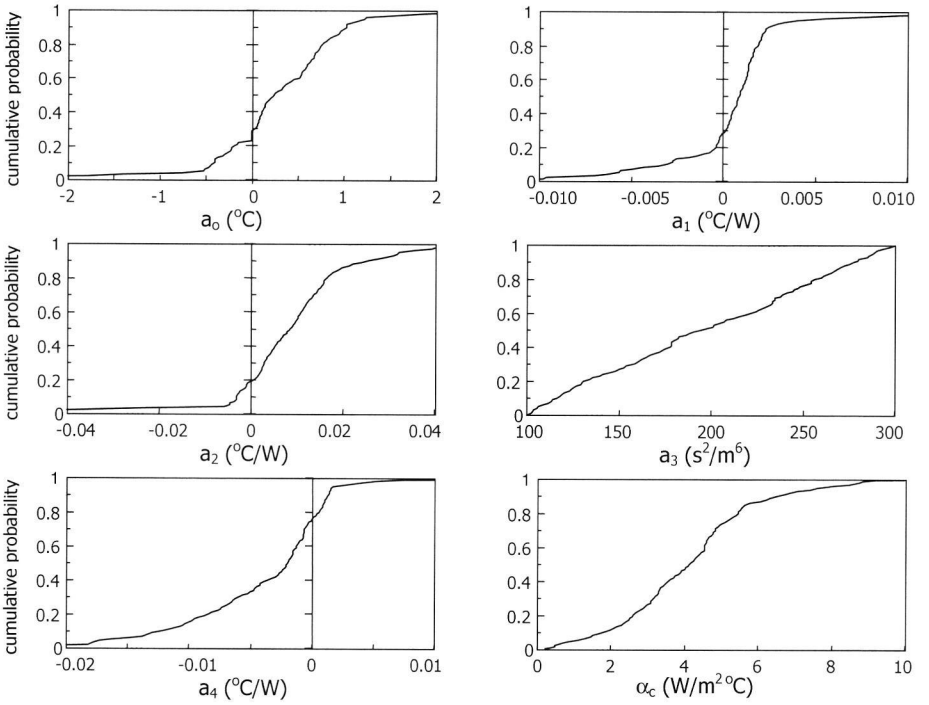

Figure 5.15 The marginal distributions for the coefficients of (5.12) and (5.15), resulting from the probabilistic inversion.

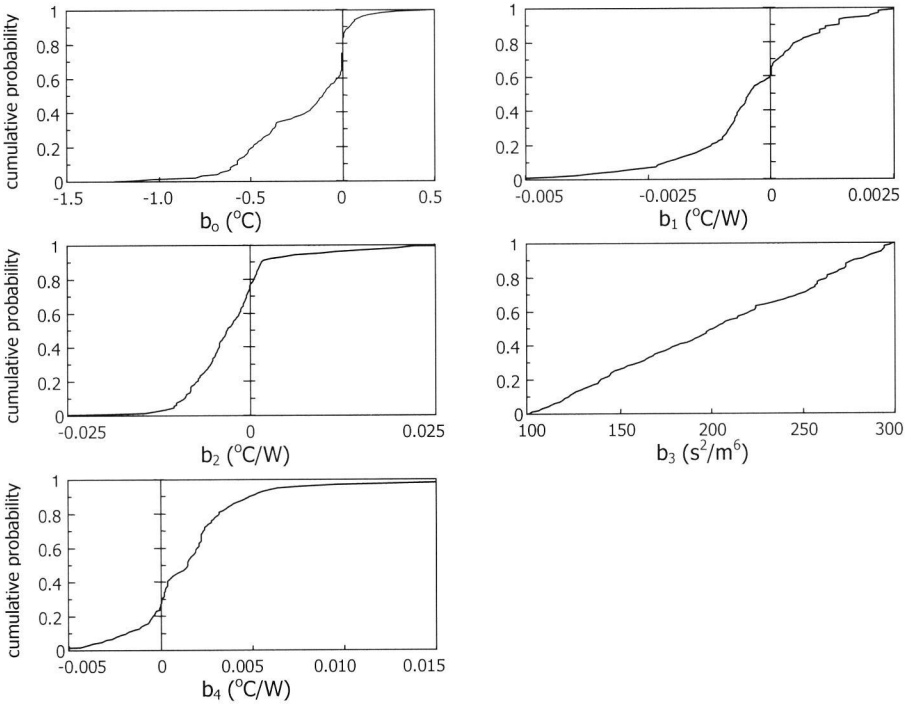

Figure 5.16 The marginal distributions for the coefficients of (5.13), resulting from the probabilistic inversion.

Table 5.10 Rank correlation matrix of the target variables.

	a_0	a_1	a_2	a_3	a_4	α_c	b_0	b_1	b_2	b_3	b_4
a_0	1	-0.12	0.54	0.00	-0.57	0.09	0.20	-0.11	0.25	-0.08	0.00
a_1	-0.12	1	-0.36	0.02	0.16	0.30	-0.21	0.04	-0.16	0.00	0.20
a_2	0.54	-0.36	1	0.07	-0.59	-0.15	0.17	-0.35	0.29	-0.14	-0.31
a_3	0.00	0.02	0.07	1	0.04	0.03	0.03	-0.07	-0.08	-0.01	-0.02
a_4	-0.57	0.16	-0.59	0.04	1	-0.01	-0.13	0.07	-0.20	0.04	0.12
α_c	0.09	0.30	-0.15	0.03	-0.01	1	-0.33	0.07	-0.30	0.00	0.08
b_0	0.20	-0.21	0.17	0.03	-0.13	-0.33	1	-0.28	0.60	-0.05	-0.35
b_1	-0.11	0.04	-0.35	-0.07	0.07	0.07	-0.28	1	-0.31	0.14	0.36
b_2	0.25	-0.16	0.29	-0.08	-0.20	-0.30	0.60	-0.31	1	-0.05	-0.48
b_3	-0.08	0.00	-0.14	-0.01	0.04	0.00	-0.05	0.14	-0.05	1	0.06
b_4	0.00	0.20	-0.31	-0.02	0.12	0.08	-0.35	0.36	-0.48	0.06	1

5.9 Discussion and conclusions

The study reported in this chapter consists of three main elements, i.e. the postulation of a (heuristic) model, assessment of the uncertainty by means of expert judgment, and probabilistic inversion. In section 5.6.5 a brief discussion was devoted to the modeling. We will come back to this subject at the end of this section. First, the expert judgment study and the probabilistic inversion will be addressed.

Expert judgment study

As mentioned in section 5.7.3.1, some potentially relevant information, which is available in a building simulation context, was omitted in the specification of cases 1-9 for practical reasons. This information concerns:

- the initial conditions
- the surface temperature distribution over the enclosure of the space

The rationales of the experts, participating in the item weight DM, show that this lack of knowledge causes only a small contribution to their uncertainty. Exceptions are cases 1 and 3, in which other sources of uncertainty are virtually absent. This corroborates the assumption that this information was not essential for the assessment of $\underline{y}$.

The fair calibration score of the optimal decision-maker indicates that his uncertainty is a suitable measure of the uncertainty, which has to be considered in values of $\underline{y}$ assessed on the basis of existing/generic data in the available time (about 2.5 days for all cases). However for the cases 1-9, the experts' rationales show that results from experiments directly comparable to the cases at hand could hardly be found. Moreover, the experts had difficulty in finding suitable quantitative data and models to guide or back up their intuition on the impact of several unknown factors. This forced them to increase the uncertainty in their assessments.
Most of them felt more familiar with the assessment of the seed variables (cases A-E), which they could back up with a relative abundance of available experimental data and/or models.

Hence, it is likely that the observed uncertainty in cases 1-9 would have been smaller if more experimental data would have been available on similar configurations. Whether extension of the available time would have had a similar effect is unclear. One of the experts claimed that if he had had the time and resources to carry out a set of systematic CFD-experiments, this would have significantly reduced his uncertainty. It would require another expert judgment study, though, to establish the size of this reduction and investigate its effect on the calibration score. Such a study would cost a multiple of the resources that were disposable in this experiment.

Probabilistic inversion

For several of the cases Figure 5.12 and Figure 5.14 show deviations between the DM's quantile assessments on the one hand and the marginal distributions over the elicitation variables resulting from the probabilistic inversion on the other hand. These deviations occur despite the fact that in the observable spaces both for the ΔT_{out}'s and the ΔT_{occ}'s

probability distributions were found, which exactly match the DM's quantile assessments. However, these distributions were obtained in two separate NLP-problems and hence correspond with two different probability distributions over the target variables. The final probability distribution over the target variables was calculated as the average of those two distributions. Apparently, the probability distributions over the elicitation variables, calculated with the averaged distribution over the targets, do not exactly match the DM's quantiles, although the agreement is fair.

In establishing the probability distribution over the samples, the DM's assessments on T_{air} were not used, as the NLP-problem appeared infeasible in the observable space for the T_{air}'s. Nevertheless, for most cases the match between the marginals resulting from the probabilistic inversion and the DM's assessments on T_{air} are acceptable. The two salient exceptions are cases 1 and 3, where the model completely fails to explain the uncertainty of the DM. This can (partly) be explained from a combination of two effects. First, in situations as in cases 1 and 3, where both the ventilation heat flow and the convective heat gain is insignificant, the model structure results in an air temperature T_{air}, which is highly insensitive for any of the parameters. Hence it is hardly possible to model the uncertainty in T_{air} in those cases in terms of parameter uncertainties.
Second, the rationales show that expert 2, participating in the item weight DM, explicitly included measuring uncertainty in his assessments (see Wit, 2001). This is a logical step in view of the fact that the experts were not informed which of the variables were the seed variables. Consequently, expert 2 considered each of the variables in the questionnaire as a possible seed variable, which might be used to score him on the basis of a measured value. As this measured value would most likely be affected by measurement uncertainty, he included this uncertainty in his assessments.
Consequently, the uncertainties in the elicitation variables were augmented as a result of an artifact in the elicitation. For most cases, this 'parasitic' contribution to the uncertainties could be folded into the parameter uncertainty to a fair degree, but, as a result of the model structure, this did not work for cases 1 and 3.

Figure 5.12 through Figure 5.14 enable a comparison of the original marginals for the observables and the marginals obtained from propagation of the approximate joint distribution over the target variables, i.e. the distribution represented by the marginals and rank correlations only. The latter marginal distributions are generally less informative (broader) than the original ones. The main deviations occur for cases 2, 5 and 6. These deviations are the price for the (inevitable) data reduction in the joint distribution over the target variables.

For most of the model parameters no values from the literature are available, which can be used as a reference for the values obtained from the probabilistic inversion. An exception is the heat transfer coefficient α_c. For α_c, the 5%, 50% and 95% quantile values are 1.1, 4.1 and 7.6 W/m^2K respectively. The median value is quite realistic in view of the available experimental data (see e.g. Section 3.2.7). However, the central 90% confidence interval, i.e. the difference between 95% quantile and 5% quantile is

quite large, compared to the range that was estimated in the crude uncertainty analysis in Chapter 3 on the basis of the literature.

For future application of probabilistic inversion with the PREJUDICE-method in similar problems, it is recommended that a better method is developed to filter out physically unrealistic samples. In this study, the uncertainty/consequence analyst created this filter. However, the design of such a filter actually belongs to the domain of the experts. A first step could be to ask the experts to give additional 0% and 100% quantile values for the elicitation variables. Experience in other expert judgment studies however shows that experts are often reluctant to state these values. This is understandable as a single realization outside their [0%, 100%] range for only one of the elicited variables implies a calibration score of 0. Moreover, these intervals would not enable detection of physically unrealistic *combinations* of values for the observables. Giving more attention to the dependencies between the variables in the elicitation stage could reduce the likelihood that such combinations are taken along in the probabilistic inversion. These dependencies could be used in the heuristic algorithm to generate scenarios, which are physically more meaningful than the random combinations of quantile values, which were used in this study.

Finally, with the exception of T_{air} in cases 1 and 3, the DM's uncertainty has been captured in the model parameters quite fairly. Although improvements can be made (see comments mentioned above), the PREJUDICE-method proved to be a practicable approach to the probabilistic inversion of the uncertainty in the observables to parameter uncertainty in this study.

Conclusions

The study has resulted in a model with an associated joint probability distribution over the model parameters, which sufficiently captures the uncertainty in the relevant aspects of the air temperature distribution, which was elicited from a panel of experts. This leads to the following conclusions:

- The selected approach, outlined in section 5.5, has proven to be feasible, although improvements can be made in various aspects as discussed above.
- The model can be used to account for the uncertainty in the air temperature distribution in the uncertainty analysis of building performance. The model has been specifically developed for the building space described in Section 5.2.
- In the study, a prior appraisal of the uncertainty in the phenomena to be modeled was used to estimate the required level of sophistication and detail in the modeling. The expert judgement study, in which the uncertainty in the model output was established in carefully selected cases, combined with the probabilistic inversion showed that the resulting model was sufficiently detailed. Indeed, the uncertainty in the model output could acceptably be represented by uncertainty in the model parameters.

However, two things should not be overlooked. Firstly, the only solid empirical control on the model resulting from this study, apart from the fragmentary experimental data

that were used in the development of the heuristic model, was obtained through the seed variables in the expert judgment study. The fact that the model to a fair degree reproduces the experts' assessments, which were given without prior knowledge of the model structure, is encouraging. However, an underlying model structure with more empirical (or theoretical) underpinning would increase the confidence that the model also adequately captures the uncertainty in cases over which the experts were not elicited. Moreover, the concomitant experimental data would give experts more grip in possible future expert judgment studies.

Secondly, this study provides us with a model to assess the uncertainty in $\underline{y}$ for a given $\underline{x}$. This is the uncertainty in $\underline{y}$ without knowledge of previous values of $\underline{y}$. However, in a simulation we are actually interested in the uncertainty in $\underline{y}$ conditional on the history of $\underline{y}$. In fact, $\underline{y}$ can be considered a stochastic process, driven by the uncertain boundary conditions, which are also stochastic processes. As a result of the (unknown) statistical dependencies between the boundary conditions in consecutive time-points, the successive $\underline{y}$'s are also dependent.
For example, the experts included uncertainty in their assessments due to the unknown configuration of the furniture in the building space. However, if this configuration becomes known at a certain time-point in the simulation, it is not likely to be much different at the next time-point. This introduces statistical dependency between the time-points.
The results of this study do not provide any information about this dependency. In sampling terms this implies that no information is available whether a single sample should be drawn from the distribution over the model parameters once and used throughout the simulation, or that the distribution should be re-sampled each hour, or anything in-between. For practical reasons, however, we will use fixed parameter values in the uncertainty propagation in the next chapter.

6 Propagation and implications of uncertainty

6.1 Introduction

The previous chapters in this thesis report on subsequent stages in an uncertainty analysis. The focus of the analysis is a specific aspect of the performance of office buildings, i.e. their performance with respect to thermal comfort in the office spaces. The assessment of this performance aspect in the design stage of a building, e.g. to support design decisions, is commonly based on (computer) simulations of the indoor climate in the building. As a result of incomplete information, both about the building and relevant external factors, these performance assessments are uncertain. The uncertainty analysis aims to quantify this uncertainty in the building performance and to identify those factors that contribute most importantly to this uncertainty.
The setting of the uncertainty analysis in this thesis is a single case study. The case, concerning a low-rise, naturally ventilated office building in the Netherlands, is described in detail in Chapter 2. This chapter also addresses the approach used to build the simulation model, and the definition of thermal comfort performance. In Chapter 3, a crude assessment has been made of the uncertainties in the model parameters. These uncertainties have been propagated through the model to obtain a first estimate of the uncertainty in the building performance. In a subsequent sensitivity analysis, the parameters have been ranked in the order of decreasing importance, viz. contribution to the overall uncertainty.
Two sets of parameters have been selected for further analysis from the top of the ordered parameter list resulting from Chapter 3. The uncertainty in the first set, consisting of the wind pressure (difference) coefficients, has been thoroughly quantified in Chapter 4. The assessment of the uncertainty in the other set of parameters, acting in the submodel for the temperature distribution in the indoor air, has been carried out in Chapter 5.

In the current chapter, Section 6.2, the uncertainties that have been identified and analyzed in the previous chapters, are propagated through the model to assess the resulting uncertainty in the building performance aspect of interest.
An evaluation of this uncertainty on its own merits may give an intuitive idea of its significance and the relevance to account for it in design decisions. The only way, however, to fully appreciate these issues is by evaluation of the impact of uncertainty information on, or rather its contribution to, a design decision analysis. Hence, in Section 6.3, the uncertainty in the building performance is introduced as input to a fictitious decision problem, in which a decision maker is facing the choice of whether or not to implement a cooling system into the design. The decision problem is analyzed

according to the principles of Bayesian decision theory and illustrates the role and significance of uncertainty in the decision problem.
In Section 6.4, particulars of both the propagation and the decision analysis are discussed. Furthermore, a discussion is included on the total uncertainty analysis, which has been used as a vehicle throughout this thesis. The chapter closes with a brief summary. Conclusions and recommendations are presented in the next chapter.

6.2 Propagation of the uncertainty

6.2.1 Introduction

The uncertainty in the model output, i.e. the thermal comfort performance, is investigated in three stages. Firstly, in Section 6.2.2 the uncertainty in the building performance resulting from only the wind pressure difference coefficients is studied. The uncertainty in the wind pressure coefficients has been studied thoroughly in Chapter 4 and it is worthwhile to study its effect on the building performance. Secondly, the effect of the uncertainty in the indoor air temperature distribution, which was explored in depth in Chapter 5, is addressed separately in Section 6.2.3. Finally, in Section 6.2.4, the uncertainty in all model parameters is propagated through the model.

In propagating the uncertainties through the model in order to assess the uncertainty in the model output, Monte Carlo simulation was used, based on simple random sampling. The parameters from the parameter sets, which were studied in Chapter 4 and 5, required specific attention, as these parameters are dependent. Their dependencies were modeled in terms of dependence trees of rank correlations. Sampling of these parameters was done with UNICORN (Cooke, 1995), an uncertainty analysis tool, which is particularly suitable for dealing with this type of dependency modeling.

6.2.2 Wind pressure difference coefficients

The uncertainty in the wind pressure coefficients was assessed by means of expert judgment in Chapter 4. It is quantified in terms of marginal distributions for 12 wind directions, each 30^0 apart, and their dependencies. The marginal distributions are shown in Figure 4.15. The dependencies are represented either in terms of a dependence tree with rank correlations (Appendix C) or a rank correlation matrix (Table 4.7). These marginal distributions, together with the dependencies, form the joint distribution over the wind pressure coefficients, which we will refer to as the distribution for the decision-maker or simply the DM.
In Chapter 4, two sets of wind pressure difference coefficients were assessed. The first set (coefficients ΔC_{p1}) is related to two openings in opposite facades at 1 m below roof level (see Figure 4.3). The second set pertains to two similar openings at a height of 6 m, which is about half the building height. In the propagation of the uncertainties through the model, we will use the data from the first set, which are relevant for an office space at the top floor of the building.

Figure 6.1 and Figure 6.2 show the propagation results. These figures are based on 500 random samples from the joint distribution over the ΔC_{pi}-coefficients. This is a sufficiently large number to obtain an accurate estimate of mean and standard deviation. All parameters other than the wind pressure difference coefficients were kept at fixed base values. For most of these parameters, the base value was set to the mean value. For the dependent parameters in the model for the air temperature distribution (see equations 5.11, 5.12 and 5.14), base case values were selected differently. For these parameters a set of values was assessed, which reproduced the DM's median values (see Figure 5.7 through Figure 5.9, or Appendix C.2) as closely as possible in the sense of equation 5.17. The uncertainty propagation was carried out with the BFEP-implementation of the building model (see Section 2.3.7), conditional on the scenario (weather data and occupant behavior) that was also used in Chapter 3 (see Appendix A2).

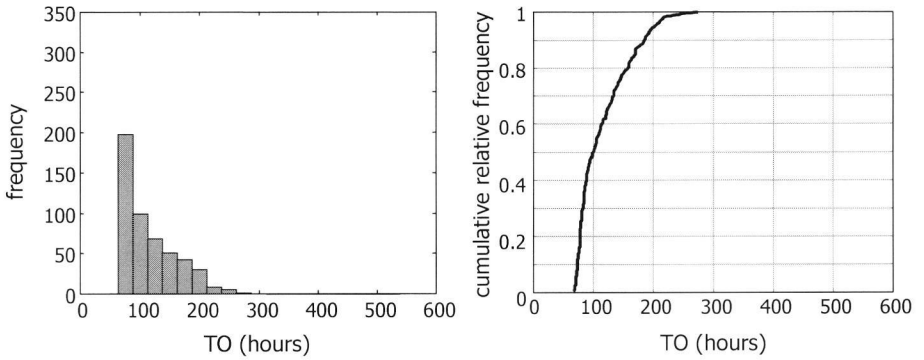

Figure 6.1 Frequency distributions of the ***static*** *comfort performance indicator TO on the basis of 500 samples. Only the uncertainty in the wind pressure difference coefficients was propagated, while the other parameters were kept at their base values. The left figure shows a histogram of the propagation results, whereas the right figure shows the cumulative relative frequency.*

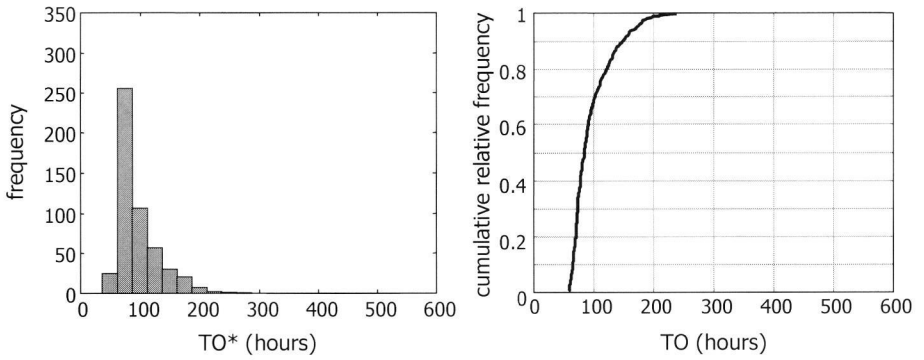

Figure 6.2 Frequency distributions of the ***adaptive*** *comfort performance indicator TO* on the basis of 500 samples. Only the uncertainty in the wind pressure difference coefficients was propagated, while the other parameters were kept at their base values. The left figure shows a histogram of the propagation results, whereas the right figure shows the cumulative relative frequency.*

A comparison of the figures shows that the results for the static and the adaptive comfort performance indicators are similar both in location of the distribution and in spread. For both indicators the coefficient of variation is about 0.4, indicating that the uncertainty resulting from only the wind pressure difference coefficients is already significant.

To get an idea of the dependencies between the wind pressure difference coefficients mutually and between these coefficients and the performance indicators, Cobweb-plots (Cooke and Kraan, 1996) were made. Two cobweb-plots for the model yielding the static TO-indicator as output are shown in Figure 6.3. Plots for the adaptive TO* are similar.
Each line in these Cobweb-plots connects the realizations of all wind pressure coefficients and the resulting TO-indicator within a single sample. All variables are scaled on the same interval [0, 1] by plotting their quantile-ranks rather than their actual values. By selecting only those lines, which pass through a narrow interval of quantile values for a single variable, a visual impression of the dependency between this variable and the other variables is obtained. In contrast to global dependency measures like (rank) correlation, this dependency has a local character as the Cobweb only focuses on a narrow range of values for a single variable. If values in another range are selected, a different dependency structure may show. For an illustration of this effect see the Cobweb-plots in the next subsection.

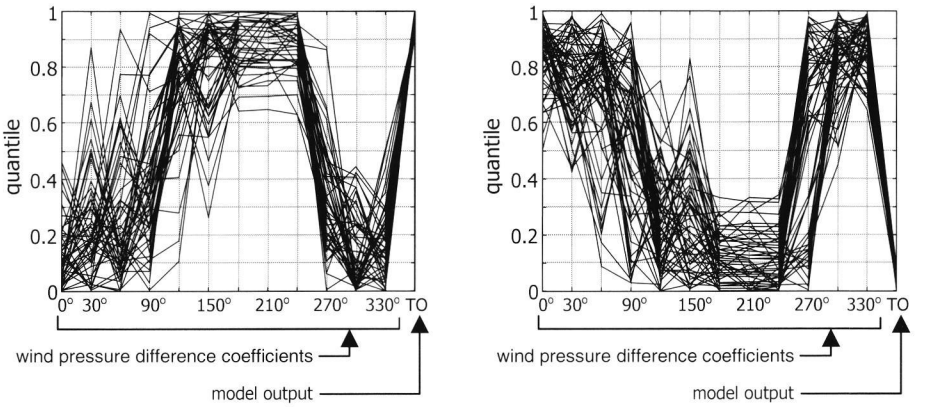

Figure 6.3 Cobweb-plots of the results from the propagation through the model for the static performance indicator TO. The left Cobweb only shows samples, which yield TO-values in excess of its 0.9 quantile, whereas the right Cobweb is conditional on TO-values below its 0.1 quantile.

The Cobwebs in Figure 6.3 show that low values for TO correspond to pressure difference coefficients that are high in absolute value and vice versa. This makes good sense as increasing (absolute) pressure coefficients correspond to increasing ventilation rates. Furthermore, the plots do not indicate an increased dependency between the performance indicator TO and the wind pressure coefficients for the prevailing wind directions in The Netherlands (southwest, corresponding to 300°-330° in Figure 6.3).

6.2.3 Indoor air temperature distribution

The uncertainty in the parameters of the model for both indoor air temperature distribution and the heat exchange between indoor air and the enclosing walls was assessed by means of expert judgment in Chapter 5. It is quantified in terms of marginal distributions for the 11 parameters and their dependencies. The marginal distributions are shown in Figure 5.15 through 5.17 and tabulated in Appendix D. The dependencies are represented in terms of a rank correlation matrix (Table 5.11).

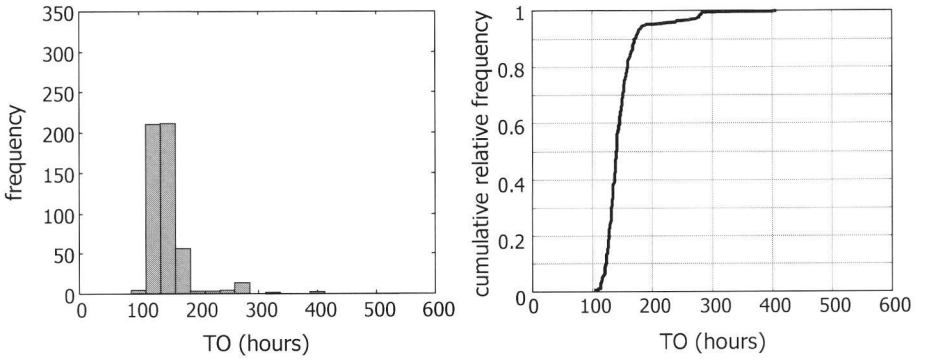

Figure 6.4 Frequency distributions of the ***static*** *comfort performance indicator TO on the basis of 500 samples. Only the uncertainty in the 11 parameters in the model for the indoor air temperature distribution was propagated, while all the other parameters were kept at their base values. The left figure shows a histogram of the propagation results, whereas the right figure shows the cumulative relative frequency.*

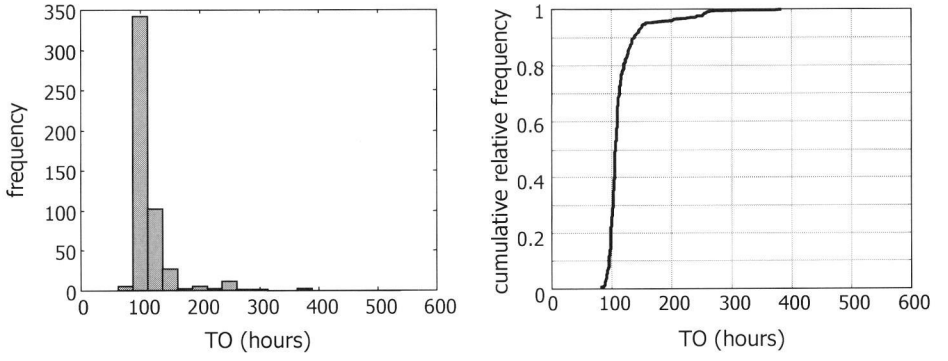

Figure 6.5 Frequency distributions of the ***static*** *comfort performance indicator TO on the basis of 500 samples. Only the uncertainty in the 11 parameters in the model for the indoor air temperature distribution was propagated, while all the other parameters were kept at their base values. The left figure shows a histogram of the propagation results, whereas the right figure shows the cumulative relative frequency.*

Figure 6.4 and Figure 6.5 show the results of the propagation of only the uncertainty in the parameters of the model for the air temperature distribution (see equations 5.11, 5.12 and 5.14). The figure is based on 500 random samples, which were drawn from the joint distribution over these parameters as identified in the probabilistic inversion in Chapter 5 (see Figure 5.15 and 5.16 or Appendix D for the marginal distributions and Table 5.11 for the rank correlation matrix). This is a sufficiently large number to obtain an accurate estimate of mean and standard deviation. All other parameters than these parameters in the model for the air temperature distribution were kept at base values. For the wind pressure difference coefficients, these were set to the median values of the distributions for the decision-maker (see Figure 4.15 or Appendix C). For the other parameters the mean value was chosen. Again, the scenario defined in Chapter 3 (see Appendix A2) was used. The simulations were carried out with the BFEP-implementation of the building model (see Section 2.3.7).

As in the previous subsection, the resulting distributions for the static TO-indicator and the adaptive TO*-indicator are quite similar, although the TO*-values are somewhat lower over the whole range. Figure 6.4 and Figure 6.5 show that most of samples yield indicator values in a relatively small range, but a limited number of outliers is found with very high values. To analyze the origin of this 'heavy tail' of the distributions, a cobweb plot was made to see if the high values for TO and TO* would show a pronounced dependency with one of the individual parameters in the model for the air temperature distribution. The result for the TO-indicator is shown in Figure 6.6 (left). It is clear that high values for TO (above 0.95 quantile) correspond exclusively with values of the heat transfer coefficient α_c below its 0.05-quantile value, while other parameters do not show a pronounced dependence. A similar result is found for the adaptive TO*.

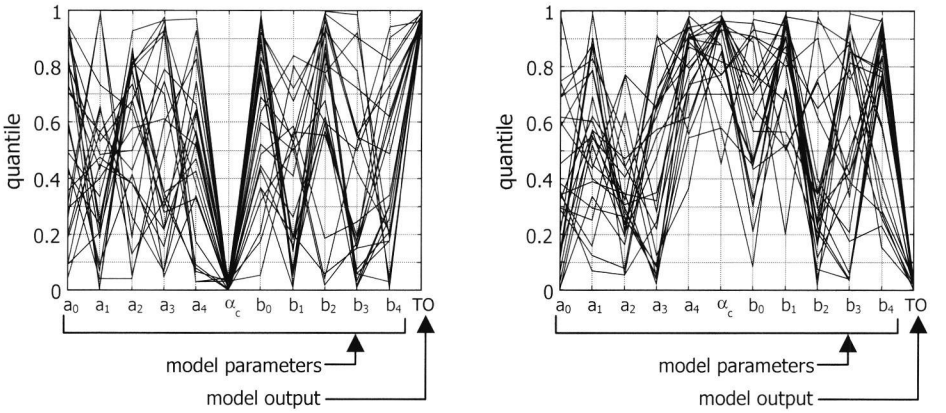

Figure 6.6 Cobweb-plots of the results from the propagation through the model for the static performance indicator TO. The left Cobweb only shows samples which yield TO-values in excess of its 0.95 quantile, whereas the right Cobweb is conditional on TO-values below its 0.05 quantile.

TO and α_c are not as closely tied up for all values of TO. Figure 6.6 (right) shows that for the lower end of the distribution of TO the dependency is much less pronounced.

This nature of the dependency between TO and the heat transfer coefficient also clearly shows from a scatter plot (see Figure 6.7).

It has already been mentioned and discussed in Chapter 5, that the range for the heat transfer coefficient resulting from the probabilistic inversion is quite large, compared to values that have been found from experimental observations. Figure 6.7 shows that especially values of $\alpha_c < 1.1$ W/m²K (its 5% quantile value) do have a large effect on the model output TO.

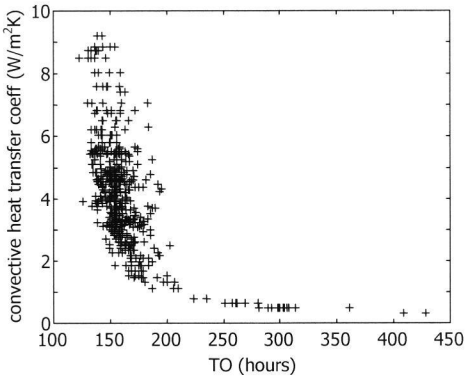

Figure 6.7 Scatter plot of the static TO-indicator against the value of the internal convective heat transfer coefficient (α_c).

6.2.4 All parameters

For the parameters, other than those addressed in the previous sections, we interpret the ranges identified in Chapter 3 as central 95% confidence intervals and assume that all parameters are normally distributed. Where necessary, these normal distributions are truncated to avoid physically infeasible values.
An exception is made for two parameters, i.e. the wind reduction coefficient and the correction of the meteo-value for the ambient temperature to the local ambient temperature. In the discussion of Chapter 3 it was mentioned that the ranges applied to these parameters, probably do not cover the uncertainty in their values to the same extent as for the other parameters. Hence it was decided to consider the ranges for these parameters as only central 70% confidence intervals.

Figure 6.8 and Figure 6.9 show the results of the propagation of the uncertainty in all parameters. The figures are based on 500 random samples and the scenario as specified in Chapter 3 (see Appendix A2).
It is clear from both figures that the uncertainty in the indicators for thermal comfort performance is quite pronounced. This finds expression in e.g. the coefficient of variation (standard deviation divided by the sample mean), which is 0.6 for both TO and TO*. This is a moderate increase compared to the value of 0.5 that was obtained

in the crude uncertainty analysis in Chapter 3. The implications of this uncertainty are the subject of the next section.

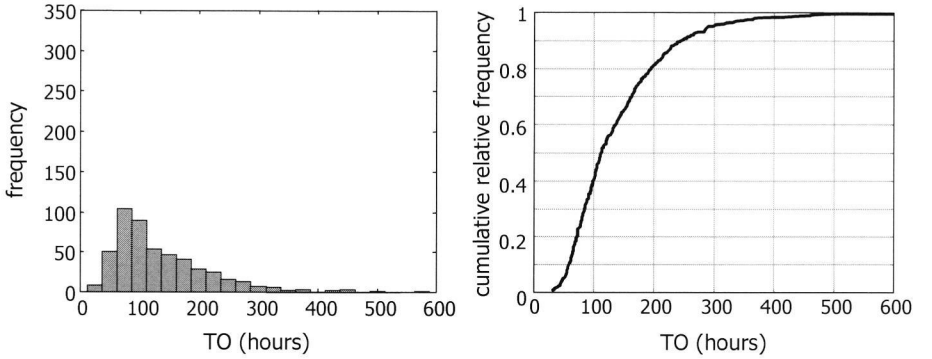

Figure 6.8 Frequency distributions of the ***static*** *comfort performance indicator TO on the basis of 500 samples. The uncertainty in all parameters is propagated. The left figure shows a histogram of the propagation results, whereas the right figure shows the cumulative relative frequency.*

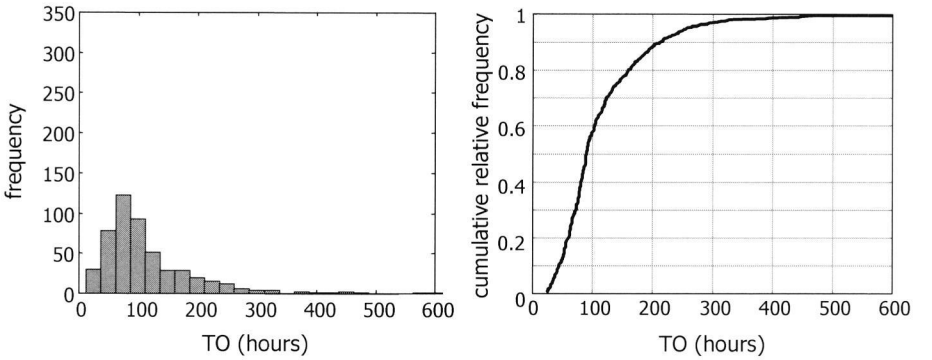

Figure 6.9 Frequency distributions of the ***adaptive*** *comfort performance indicator TO on the basis of 500 samples. The uncertainty in all parameters is propagated. The left figure shows a histogram of the propagation results, whereas the right figure shows the cumulative relative frequency.*

6.3 Implications for design decisions

6.3.1 Introduction

The previous section shows that significant uncertainty exists in the values of the performance indicators TO and TO*, which are assessed on the basis of information typically available in a design context. An important question is what the implications of this uncertainty are for design, or rather for building physics advice in design.

In Chapter 1 we stated that the building physics expert participates in the analysis of those decisions in the design process, which concern measures or consequences of a

building physics nature. His advice aims to improve the decision-maker's[31] understanding of the decision problem facing him. How could information on uncertainty contribute to this understanding? This question is addressed in the next two sections.

6.3.2 Advice on the basis of 'best' estimates

Within the paradigm of current advice practice 'best' point estimates of performance are delivered as basis for decisions. From our viewpoint about the aim of a decision analysis and the role of performance in such an analysis these approaches are questionable. Indeed, imagine a decision-maker, who is faced with the choice whether or not to integrate a cooling system in the design of the building that we have been studying throughout this thesis. In the particular context, he prefers to implement the cooling-system if the TO-performance value of the building (without cooling) will exceed, say, 150 hours. To assess the performance, he has a simulation study done. The building physics consultant performing the study uses one of the defaulting approaches discussed before, which happens to be successful in the sense that the simulation result is close to the most likely value according to Figure 6.8, i.e. 100 hours. This value is well below the threshold value of 150 hours and the decision-maker comfortably decides not to implement the cooling system.

Suppose now that the consultant had not just provided a point estimate, but the full information in Figure 6.8 or Figure 6.9. Then the decision-maker should have concluded that the performance is not at all *well below* the threshold of 150 hours. In fact, the probability of getting a building with TO in excess of 150 hours is about 1 in 3. In other words, his perception of the decision problem would have been quite different in the light of the extra information. This in itself is a clear indication that the uncertainty information is relevant for the decision analysis. Hence, the advice should convey this uncertainty in some form.

However, it may not be clear to the decision-maker how to decide in the presence of this extra information. It is no longer sufficient to simply compare the outcome of the performance assessment with a threshold value. To use the information constructively in his decision analysis, the decision maker needs to weigh his preferences over the possible outcomes (performance values) against the probability of their occurrence. This requires a more sophisticated approach.

A suitable framework is offered by Bayesian decision theory that we will discuss in the next section.

6.3.3 Bayesian decision analysis

This section aims to illustrate, in a simplified example related to the case that has been used throughout this thesis, how a greater and more explicit knowledge of uncertainty

[31] Note that the terms 'DM' and 'decision-maker' in Chapters 4 and 5 are often used in the sense of 'probability distribution for the decision-maker', i.e. the combination of the experts' assessments. In this chapter 'decision-maker' consequently refers to a (hypothetical) person.

could be sensibly incorporated in decision making. It will do so on the basis of Bayesian decision theory. Pioneering work underpinning this theory was done by De Finetti (1937), Ramsay (1931), Von Neumann and Morgenstern (1943) and Savage (1954) among others. A comprehensive introduction and bibliography can be found in e.g. French (1993).

In concordance with the point of view we adopted in Chapter 1 on the purpose of a decision analysis and the role of advice in such a process, Bayesian decision theory is a normative theory. It describes how a decision-maker *should* decide if he wishes to be consistent with certain axioms encoding rationalism. It is not a prescriptive tool, but rather an instrument to analyze and model the decision problem.

The theory embeds rationality in a set of axioms, ensuring consistency. We will assume that the decision-makers considered here in principle wish their choice behavior to display the rationality embodied in these axioms. If not, a decision analysis on Bayesian grounds is not useful: it will not bring more understanding. Moreover, we assume (as we have done implicitly throughout the thesis) that the decisions are made by a single decision-maker. Choice behavior by groups with members of multiform beliefs and or preferences can not be rational in a sense similar to that embedded in the axioms mentioned before.

First, in the next subsection, we will address the basic steps in a Bayesian analysis of a decision problem and briefly introduce the notions that come into play in such an analysis. Subsequently, the approach will be illustrated in a simple example of a decision problem involving thermal comfort performance. Qualifications and generalizations of the example to decision problems that may be encountered in real design contexts are discussed in Section 6.4 in broad terms. Section 6.5 closes the chapter with conclusions and recommendations.

Problem formulation

Suppose a decision-maker is concerned with the quality of the working environment in the office building under design. He may consider several alternative *actions*: leave the design as it is (say, as described in section 2.2), integrate a cooling system in the design, reduce the glass-area in the façade, improve the lighting system, etc. We shall not dwell on the process in which such a list of alternative actions is generated, we just assume that it exists.

Once the list of possible actions has been established, the central question in the decision problem is how to choose between these actions. In order to make this choice, the decision-maker evaluates the actions in terms of their achievements on his objectives. For a certain decision-maker, the list of resulting objectives might look like: minimize investment costs, maximize the occupants' content, maximize the building's architectural allure, minimize environmental impact, etceteras.

Now, for each of these objectives, it would be convenient to identify an *attribute* or *performance* with a quantitative *scale* to directly indicate the degree to which the corresponding objective is achieved. Let us attempt to do this for the objectives of our example decision-maker. A direct attribute for the first objective, i.e. 'minimize investment cost', would obviously be the investment cost itself, with a scale in units of e.g. one thousand Dutch guilders. For the second objective 'maximize occupants' content', however, there is no obvious scale on which to measure the degree of achievement. Two problems are evident. First, there are many factors that may affect the occupants' content, such as thermal aspects, visual aspects, ergonomic aspects etc. How can these factors be jointly captured in a single attribute? Second, for each factor there is still no self-evident scale. We shall address these problems subsequently.

The first problem, i.e. the selection of a single attribute or scale, which captures several factors underlying a single objective, is discussed in Keeney (1981). Basically, he describes two types of solutions. The first solution is a further decomposition of the objectives until all relations between objectives and attributes are one-to-one. An alternative solution is the construction of a scale, which combines all effects in some balanced way. An example of such a constructed scale to measure an occupant's satisfaction with the indoor environment[32] is presented in Cox and Rolloos (1995). We will adopt the first approach here and consider a sub-objective "maximize occupants' content with thermal aspects of indoor climate"; for a discussion on the implications and problems associated with both approaches see Keeney (1981).

The second problem concerns the absence of an obvious attribute with associated scale for a given objective. This is a difficulty encountered in many decision problems. In these circumstances it is common to use *proxy* or *indirect* attributes (see also Keeney, 1981). Examples of proxy attributes for the thermal aspects of the occupants' content with the building are the TO and TO* performance indicators, which were introduced in section 2.4.3 and have been used throughout this thesis. The validity of proxy attributes in a decision analysis rests on the decision-maker's *assumption* that such an attribute is highly correlated with the effect that is actually to be measured. We will come back to this in the discussion.

Along the same lines of reasoning, (proxy) attributes can be associated with the other (sub-) objectives that have been identified. The attribute scale related to the building's architectural allure could e.g. depend on the proportion of glazing in the façade, the energy consumption by HVAC-systems in the building might add to the attribute level for environmental impact, etceteras.

Assessment of the consequences

In this stage of the decision analysis, an assessment of the consequences of each action under consideration is carried out. These consequences are expressed as attribute levels (or performance values in the terminology we have been using in the previous chapters). The assessment of performances including their uncertainty has been the main topic of this thesis so we will not dwell on this subject here. It is important to note, though, that our earlier choice to represent of uncertainty in terms of subjective probability has been

[32] Note that this is not a scale to measure the occupant's satisfaction with a *building*.

based on the fact that this representation is one of the cornerstones of Bayesian decision theory (see e.g. Savage, 1954).

Modeling of preferences

Especially in complex decision problems involving multiple attributes with uncertainty in their value, it is commonly a difficult task to rank the various actions in order of preference without a systematic approach to deal with the problem bit by bit. Bayesian decision theory offers such an approach.

The crux of this theory is that if a decision maker adopts the rationality encoded in its axioms, it can be proven that the preferences of the decision maker can be numerically represented in terms of a function over the attribute levels, the *utility* function. In a case that each action leads to a set of attribute levels without uncertainty, the actions can be associated with a single value of the utility function, and the action with the highest utility is preferred. Moreover, if the attribute levels resulting from the actions are uncertain, an action with higher *expected* utility is preferred over one with a lower expected utility. Hence, the *optimal* action is the one with the highest expected utility.

Let us illustrate this with actions that can be expressed in terms of a single attribute X. Consider two actions a_1 and a_2. Action a_1 gives rise to attribute level $\boldsymbol{x_1}$, whereas action a_2 leads to attribute level $\boldsymbol{x_2}$. The consequences or attribute levels $\boldsymbol{x_1}$ and $\boldsymbol{x_2}$ are uncertain. The decision-maker associates probability distributions to these consequences, expressing his degrees of belief in their occurrences. The utility function represents the decision-makers preferences over the (uncertain) outcomes of the two actions and hence over the actions themselves:

$$a_1 \gtrsim a_2 \quad \text{if and only if} \quad E\{U(\boldsymbol{x_1})\} \geq E\{U(\boldsymbol{x_2})\}$$

where $\gtrsim$ means 'is at least as preferable as', $U(.)$ is the decision maker's utility function and $E\{.\}$ denotes 'the expected value of'.
The utility function is unique up to positive affine transformations. This basically means that we are free to choose the origin and the scale of the utility function without changing the preferences it reflects.

The practical importance of the utility function as a quantitative model for the decision-maker's preference is that the function can be assessed by observing the decision-maker's choice behavior in a number of simple reference decision problems. After this assessment, he can use the function to rank the actions in the actual decision problem in the order of expected utility. He may directly use this ranking as the basis for his decision or explore the problem further e.g. by doing a sensitivity analysis for assumptions made in the elicitation of either uncertainty or utility, or by a comparison of the expected utility ranking with an intuitive ranking he had made on beforehand.
Moreover, a systematic assessment of the utility functions helps the decision maker to clarify and straighten out his own preferences, including the elimination of possible inconsistencies.

The next section illustrates the use of the utility function in an example.

6.3.4 Example

Introduction

In this example we consider the situation that only two actions are of concern to the decision-maker, i.e. he either leaves the design as it is or he integrates a modest cooling system in the design:

Table 6.1 Overview of possible actions considered in the example decision problem.

action	symbol
leave design as it is (see description case in Section 2.2)	a_1
integrate cooling system in design	a_2

Furthermore, he has only two (conflicting) objectives, i.e. "minimize investment cost" and "maximize occupants' content with thermal aspects of indoor climate". To measure the achievement on the first objective he uses the investment cost itself, which, we assume, can be assessed with negligible uncertainty. The scale of the investment cost is in thousands of Dutch guilders. As proxy attribute for the second objective the TO is selected, the building performance indicator for thermal comfort as defined in Section 2.4.3. The TO is the number of office hours per year that the operative temperature in a carefully selected space exceeds 25.5 °C under a specific scenario. We will denote the attribute 'investment cost' by X and its level by x, whereas the symbol for the TO-indicator is Y with y as its value. So, summarizing:

Table 6.2 Objectives and attributes (performances) used by the decision maker.

objective	attribute	symbol	units
minimize investment cost	investment cost	X	10^3 Dfl
maximize occupant content	TO-indicator	Y	hours

Table 6.3 shows the consequences of the two actions:

Table 6.3 Consequences of the two possible actions in terms of the attributes.

action	x	y
a_1	0	see Figure 6.8
a_2	400	0

According to the table, the TO-indicator will have value $y = 0$ in case the cooling is installed as this system will be dimensioned to achieve this. The possibility of failure of

this system is not considered here. The investment cost of the system is set to 400 10^3 Dutch guilders (Dfl), based on the reasonable amount of 130 Dfl per m^2 floor area.
The question in this example is which of these actions the decision-maker should choose. According to the expected utility rule, the optimal choice for the decision-maker is the action with maximum expected utility. Assessment of the expected utility requires assessment of the subjective probabilities over the attribute levels and his utility function over these levels.

Assessment of subjective probability

The example decision-maker only considers uncertainty in Y under action a_1. The previous chapters and the preceding section have addressed the assessment of this uncertainty in a way that a rational decision-maker would have minimum objections to adopt these assessments as his own. So we will assume here that the sample distribution in Figure 6.8 reflects the decision-maker's subjective probability density function over Y under action a_1.

Elicitation of utility function

A first step in the actual elicitation of the utility function is the assessment of the (in)dependence structure of this function. The dependence structure indicates in which way the decision-maker's preferences on one attribute depend on the levels of the other attributes. Here we will assume that the decision-maker holds the attributes *additively independent*, which implies that his utility function can be written as:

$$U(x, y) = b_2\, U_X(x) + b_1\, U_Y(y) + b_0 \tag{6.1}$$

U_X and U_Y are called *marginal* utilities over X and Y. French (1993) briefly addresses the elicitation of (in)dependency structures and gives references. We will not go into that subject here: less strong assumptions about independence lead to similar lines of reasoning as we will follow here although more elaborate.

The next step is to assess the marginal utilities over X and Y. Like the elicitation of subjective probabilities discussed in Chapters 4 and 5, proper elicitation of (marginal) utilities requires some sophistication. It is however not the aim of this example to go into details and possible pitfalls of the elicitation; we only indicate its basics to illustrate the use of utility in decision analysis.
Let's start with attribute Y. As a first step, the decision-maker considers a choice between the two actions sketched in the decision tree in Figure 6.10. Action 1 yields a building with a TO-value $y = 100$ hours for sure. Action 2 results in a building with either $y = 300$ hours if the pointer of the wheel in Figure 6.10 ends up in the shaded area after a single spin, and in a building with $y = 0$ hours otherwise.

Both actions only differ in attribute Y and are identical on all other attributes. Which action would he prefer? The decision-maker considers the situation and concludes, say, that he would choose action 2. Subsequently he estimates how big the shaded area on the wheel should be to make him indifferent between action 1 and action 2. Let's say

that he would require the *expected* 'cost' of both actions to be approximately the same: the shaded area should cover about 1/3rd of the wheel.

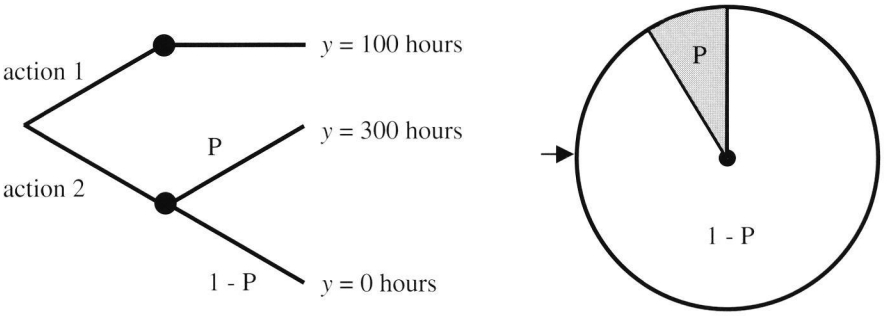

Figure 6.10 Simple decision tree (left) and probability wheel (right), both used in the elicitation of a decision maker's utility function.

With this information the decision-maker's utility for y = 100 hours can be calculated. As mentioned in the previous section we are free to choose both origin and scale of the utility function. We take:

$$U_1(0) = 0 \tag{6.2}$$

$$U_1(300) = -1 \tag{6.3}$$

From his indifference between actions 1 and 2 when the shaded proportion of the probability wheel is 1/3rd we can calculate with the expected utility rule that:

$$U_1(100) = 2/3 \times U_1(0) + 1/3 \times U_1(300) = 2/3 \times 0 + 1/3 \times -1 = -1/3 \tag{6.4}$$

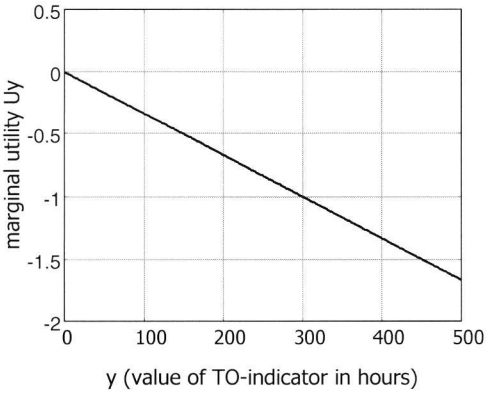

Figure 6.11 Marginal utility function of the example decision-maker over the level of attribute Y (value of TO – indicator in hours).

The utilities for a number of other values of Y can be assessed along a similar line of working. The result of the elicitation for the example decision-maker is a linear marginal utility function as sketched in Figure 6.11. A proper elicitation procedure could include cross-checking to incur and/or verify consistency in his preferences and the absence of various biases but we will not go into these issues here.

Elicitation of the decision-maker's marginal utility function over the investment costs could take a similar form. We assume in this example that this function is also linear.

Now that the marginal utility functions have been elicited, the joint utility function over X and Y can be assessed. Given the linearity of the two marginal utilities, equation (6.1) can be rewritten as:

$$U(x, y) = c_2\, x + c_1\, y + c_0 \tag{6.5}$$

Again we use the fact that we can arbitrarily set the origin and scale of the function and take:

$$U(0, 0) = 1 \tag{6.6}$$

$$U(400, 300) = 0 \tag{6.7}$$

To fix all three constants in equation (6.5) the decision-maker has to make a trade-off between X and Y. We assume here that he prefers to implement the cooling-system if and only if the TO-performance value of the building (without cooling) will exceed 150 hours. Hence, he holds:

$$U(400, 0) = U(0, 150) \tag{6.8}$$

expressing his indifference between an investment of 400 10^3 Dfl and a TO-indicator value of zero on the one hand, and a zero investment in combination with a TO value of 150 hours on the other. Note that this is a preference statement over a trade-off between attributes *in the absence of uncertainty*. It is exactly the type of statement the decision-maker will have to make in most current design situations, where each alternative action (design) is labeled with a single TO-value as if this value were known without uncertainty.

Equations (6.6), (6.7) and (6.8) enable the calculation of the constants in equation (6.5) and we obtain

$$U(x,y) = -8.3\ 10^{-4}\ x\ -\ 2.2\ 10^{-3}\ y + 1 \tag{6.9}$$

as the utility function of the decision maker.

Calculation of expected utilities

His expected utility is then:

$$E\{U(x,y)\} = -8.3\ 10^{-4}\ x\ -\ 2.2\ 10^{-3}\ E\{y\} + 1 \qquad (6.10)$$

as the investment cost x is considered to be known without uncertainty. As a result of the linearity of the utility function of this specific decision-maker, we need only limited information on the probability distribution over y, i.e. only the expected value, to calculate the decision-maker's expected utility.

On the basis of equation (6.10) we can calculate the expected utilities for both actions a_1 and a_2:

Expected utility of action 1: $-8.3\ 10^{-4} \times 0 - 2.2\ 10^{-3} \times 137 + 1 = 0.70$
Expected utility of action 2: $-8.3\ 10^{-4} \times 400 - 2.2\ 10^{-3} \times 0 + 1 = 0.67$

where we used the information from Table 6.3 and the mean of the values in Figure 6.8. These results suggest that action 1 is the most preferred action of this decision-maker, barring the result of any further analysis the decision-maker might consider.

A risk-averse decision maker

Before we go over to a discussion of several issues that were deferred in the previous sections, it is interesting to investigate the result of the analysis for another (imaginary) decision-maker. He not only has an identical perception of the decision problem, but also shares his preferences with the first decision-maker in the example, except for his marginal utility for attribute Y (TO-indicator).

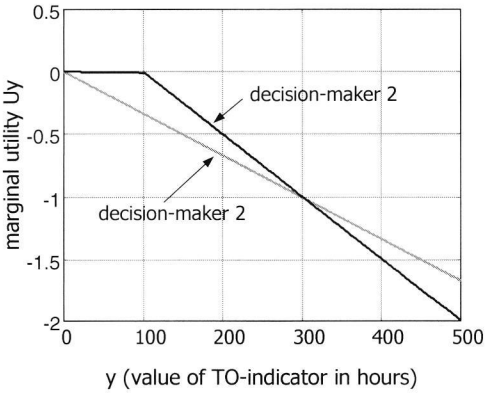

Figure 6.12 Marginal utility function of the second example decision-maker over the level of attribute Y (value of TO – indicator in hours). This decision-maker is risk averse. As a reference, the marginal utility function of the first decision maker is also shown. The lines cross at the coordinates (0,0) and (300,-1) as the marginal utility function is fixed at these points by equations (6.2) and (6.3).

To elicit his marginal utility over Y, he is also asked to consider the choice between the actions in Figure 6.10. Unlike his colleague, he prefers action 1. His line of reasoning might be that buildings with a value of the TO-indicator of 100 hours or less are reputedly good buildings with respect to thermal comfort and he is not willing to take

much risk that he would end up with a building with y = 300 hours. This decision-maker is *risk averse*.
Further elicitation of his marginal utilities yields the function shown in Figure 6.12.

Following the same approach as for the first decision maker we arrive at the utility function:

$$U(x,y)=\begin{cases}-1.25\,10^{-3}\,x+1.0 & 0\le y\le 100 \text{ hours}\\ -1.25\,10^{-3}\,x-1.0\,10^{-2}\,y+2.0 & y>100 \text{ hours}\end{cases} \qquad (6.11)$$

Calculating the expected utilities we get:

Expected utility of action 1: 0.47
Expected utility of action 2: 0.50

Hence, with a reservation for the output of a sensitivity analysis, this decision-maker would prefer action 1, whereas his colleague tends to action 2. In itself it is not surprising that two decision-makers with different preferences make different choices in the same situation. However, the two decision-makers in this example would have preferred the same decision in the absence of uncertainty. It is solely as a result of the introduction of uncertainty into the problem that they tend to different choices.

6.4 Discussion

Figure 6.8 and Figure 6.9 show the results of the propagation of the uncertainty in all parameters. As these results are subsequently used as input to a decision analysis, the suggestion might arise that this thesis satisfactorily covers all aspects of the uncertainty analysis that was initiated in Chapter 3. Many issues have not been addressed, though, or deserve further qualifications. We will discuss several of them in this section.

Assessment of parameter uncertainties

Firstly, in Chapter 3, five parameters (or rather parameter sets) were identified as important, i.e. their joint share in the overall uncertainty was estimated to be about 85%. The uncertainty in only two of these parameter sets has been thoroughly assessed in Chapters 4 and 5 by means of expert judgment. Through the same method as in Section 3.4.2 it can be estimated that the uncertainty in these two sets accounts for about 50% of the variances that can be calculated from Figure 6.8 and Figure 6.9. This implies that the author's crude assessment of the parameter uncertainties in Chapter 3 form an important, but non-calibrated contribution to the uncertainties displayed in these figures.

Moreover, the results from the expert judgment studies, reported in Chapters 4 and 5, deserve some qualifications. As these issues are discussed at length in the discussion sections of these chapters, we will not go into them here.

Uncertainty resulting from proxy attributes

In Dutch design practice, the performance indicator for thermal comfort TO and related indicators have developed as more or less standard attributes. In the section on problem formulation in Section 6.3.3, these performance indicators have been introduced as proxy or indirect attributes. Proxy attributes, in contrast to direct attributes, do not directly measure the achievement on the decision-maker's objectives, but are assumed to be strongly correlated with this achievement. They are used in cases where no direct attributes can be found.

The statement that the performance indicators and objectives are *correlated* implies uncertainty. As this uncertainty is not explicitly assessed or analyzed in a decision analysis, it clouds the decision-maker's preference assessments, which is at odds with the goal of a decision analysis. Hence, it is desirable to keep the attributes as direct as possible. To increase the 'directness' of the TO-indicator, the following three sources of uncertainty need to be reduced.

The first source of uncertainty is related to the choice of a scenario. Up until now we considered the performance indicators as a function of the occupant thermal sensation that will occur under a given scenario (specifying e.g. a time series of outdoor climate conditions and characteristics of occupant behavior). It is reasonable to assume though, that performance indicators observed under the *actual* outdoor climate and occupant behavior will correlate better to a decision maker's objectives than indicators calculated under a fictitious scenario. Hence, although the uncertainty in e.g. future climatic conditions and occupant behavior does not emerge as uncertainty in the value of the performance indicator (attribute) in the current approach, it adds to the uncertainty in the preferences of the decision-maker. It would contribute to the clarity of the decision problem, and thus further the goal of the decision analysis as a whole, if uncertainty in the variables and processes in the scenario would be explicitly addressed in the uncertainty analysis of the attribute levels.

A similar line of reasoning can be upheld for uncertainty in the thermal comfort models. Both the TO and the TO* performance indicators, quantifying the number of hours that the (operative) temperature exceeds some critical value, actually aim to model the time that more than 10% of the people will be dissatisfied as they conceive the indoor climate as 'too warm'. The relation between the indoor climate and the occupants' sensation is incorporated in the thermal comfort models underlying the indicators. Uncertainty in these models has not been considered in the uncertainty analysis (see discussion in section 3.2.4) and hence does not contribute to Figure 6.8 and Figure 6.9. Again, explicit account for this uncertainty in the decision analysis would contribute to clarity.

The last source of uncertainty arises from the relation between the actual achievement on the decision maker's (sub-)objective and the number of hours that 'more than 10% of the occupants will be dissatisfied' as a result of a too warm indoor climate. If, e.g. the decision-maker would also be the future user of the building, he might actually be

interested in maximizing the productivity of the future office workers. In that case, the (uncertainty in) loss of productivity given 'dissatisfaction' would be of special interest to him (for a recent review on the relation between indoor climate and productivity see e.g. Sensharma et al., 1998).
Another decision-maker, in another context, might be planning to let the building. His objective could be to maximize the rental income over a reference period. In his utility assessments, he experiences uncertainty in the relation between the degree to which the future users of the building can deduct rent and their dissatisfaction (for an example along this line of thinking in case of dissatisfaction with building vibrations see Vrouwenvelder and Van Oosterhout, 1996).
As a final example, consider a situation in which the decision-maker is under contractual obligation to surrender a building with a certain target performance. In that case, target performance, performance indicator, scenario and probably the method to measure the performance would be specified in the contract. Hence, the decision-maker would only have to consider modeling and specification uncertainties as mentioned in chapter 3, and possibly measurement uncertainty in the assessment of the actual performance of the building after completion.

Practical relevance

It has not been part of this thesis to study the decision making process in current building design. It is postulated that design evolution proceeds along iterative cycles of creative design generation, separated by instances of distinct design decision making, such as choosing between two design alternatives.
Although the previous sections only scratch the surface of (Bayesian) decision theory and its opportunities for decision analysis, many may already wonder whether an approach, which requires so much fuss for such a relatively simple decision problem, does have any practical relevance. Indeed, real-world decision problems will commonly be much more complex, while time and resources to do a decision analysis are limited. Yet, even in those situations, or rather *especially* in those situations, the principles of Bayesian decision making are valuable. Obviously more assumptions will have to be introduced and the assessments of e.g. uncertainties and utilities will be more crude. However, once a decision maker (or his consultants) gets acquainted with the notions and motions of a Bayesian decision analysis, he will be able to better prioritize those elements of the analysis, which resolve his most pressing vaguenesses in the decision problem and which check his most notorious intuitive biases and inconsistencies, in short: which most efficiently improve his confidence that he can make a well-considered, rational decision.

6.5 Summary

The current chapter concludes the uncertainty analysis that was initiated in Chapter 3. The propagation of all uncertainties through the model to obtain the uncertainty in the comfort performance indicators is reported and discussed. Subsequently, it is illustrated how the uncertainty in a comfort performance indicator can constructively be used in a design decision analysis. An example is elaborated, in which a decision-maker is confronted with a choice between two design alternatives.

7 Closure

7.1 Summary and conclusions

Evaluations of thermal building performance at a time that the building is still under design, implicate uncertainty. Quantitative appraisal of this uncertainty can contribute to more rational design decisions. Moreover, it gives guidance in the development and selection of methods to assess building performance.
In current design practice, uncertainties in performance assessments are not explicitly quantified. In the literature on building performance simulation these uncertainties have received some attention, but several questions have been left open. Firstly, it has been acknowledged that many of the uncertainties cannot be estimated by straightforward statistical analysis of available data. This raises the question by which method these uncertainties could be assessed and whether such a method would be applicable in design practice. Secondly, although intuitive arguments have been put forward to emphasize the relevance of quantitative uncertainty information for design decisions, no attempts have been made to show *how* a decision maker could use this information to improve his decision.
In this thesis, an uncertainty analysis is presented for a specific performance aspect of a specific building under design. Expert judgment is used to quantify uncertainty that cannot be estimated on a statistical basis. The integration of quantitative uncertainty assessments in a design decision analysis is illustrated in the context of Bayesian decision theory.

The building, which was selected for the analysis, is a low-rise, naturally ventilated office building in The Netherlands. Thermal comfort in the building in summer is the performance aspect that was investigated. To quantify this aspect of performance, two indicators, TO and TO*, were used. Both indicators aim to reflect the number of hours per year that more than 10% of the people would consider the indoor climate as uncomfortably warm. The two indicators differ in the underlying comfort models, though. The TO-indicator is based on the static comfort model by Fanger (1970) with default values for air velocity, humidity, clothing level and metabolism as recommended in ISSO (1994). The TO*-indicator starts from the adaptive comfort model by De Dear and Brager (1998).
The indicators were calculated on the basis of numerically simulated temperatures in the building. In the development of the building simulation model, a mainstream approach was applied with an extension for the air flow modeling.

In this thesis, uncertainty is represented in terms of subjective probabilities. Uncertainties from four sources are distinguished, i.e. specification uncertainty, scenario uncertainty, modeling uncertainty, and numerical uncertainty. Specification uncertainty arises from the lack of information in the design specifications about the building as it

will be delivered. Scenario uncertainty implies that the external factors, to which the building is exposed during the performance assessment, are not precisely known. Modeling uncertainty stems from assumptions and simplifications in the development of the physical building model. Numerical uncertainty may be introduced in the translation of the (physical) building model into a (numerical) computer model and in the simulations with this model.
Scenario uncertainty was not addressed in this thesis, nor was numerical uncertainty.
The uncertainties from the other two sources were assessed by the author on the basis of data in the literature, and propagated through the building simulation model. The resulting uncertainty in the indicators for comfort performance were found to be significant, as expressed by a coefficient of variation (ratio of standard deviation and mean) of 0.5. Both means and standard deviations of the two indicators TO and TO* were similar.

The research presented in the first part of this thesis concentrated on a crude uncertainty analysis. The uncertainties were assessed by the author on the basis of data from the literature. The uncertainty analysis revealed various model parameters for which the uncertainty had to be quantified on an ad-hoc basis. For these parameters insufficient data could be found, the available data were conflicting, or the validity and relevance of these data could not be established. The uncertainty in two sets of these parameters was further analyzed. These parameter sets were identified as significantly contributing to the uncertainty in building performance.

The first parameter set contains the wind pressure difference coefficients, relating the local wind velocity to pressures differences over the building façade. These pressure differences drive the ventilation flows through the building. The uncertainty in these coefficients was quantified in an expert judgment study with a method from Cooke and Goossens (2000). In this study, six experts assessed the uncertainty in 24 wind pressure difference coefficients on the basis of generic knowledge and data. For each coefficient, a weighted average of their assessments was calculated for use in the uncertainty analysis. Each expert's weight was determined from a statistical comparison of their assessments with measured values of the pressure difference coefficients, which had been obtained in two separate wind tunnel experiments.
The expert judgment study proved to be successful. The statistical comparison showed that the experts' combined assessments are well-calibrated, i.e. they are suitable measures of the uncertainty in predictions of the wind pressure difference coefficients.
Moreover, the expert judgment study pointed out to the participating experts that the amount of data in the literature, which can readily be used as a basis for the prediction of wind pressure coefficients, is limited. This was taken up as an incentive to improve this situation (Surry, 1999).
Finally, the expert judgment study turned out to be more expensive than a wind tunnel study, while the resulting uncertainties were larger. An obvious measure to cut back the costs through the reduction of the number of participating experts, is unattractive. Indeed, only two of the six experts turned out to be well-calibrated in the comparison of their assessments with the measured data.

Expert judgment was also applied to quantify the uncertainty in the indoor air temperature distribution in Chapter 5. An important difference with the expert judgment study on wind pressures was the lack of a suitable model for the indoor air temperature distribution. This created the opportunity to address the model development in tandem with the uncertainty analysis. Anticipating significant uncertainty in the air temperature distribution, given the information on boundary conditions in a building simulation context, a coarse heuristic model was proposed with a limited number of empirical parameters. The uncertainties in the relevant characteristics of the air temperature distribution were assessed for 9 different sets of boundary conditions, by means of expert judgment. The same method was used as for the wind pressure coefficients. Subsequently, probabilistic inversion was applied with the PREJUDICE technique developed by Kraan (2000). Probabilistic inversion attempts to find a joint probability distribution over the model parameters, such that the model produces uncertainty estimates, which comply with the experts' combined assessments.

The conclusions from this expert judgment study were very similar to those obtained from the previous one. Again the experts' combined assessments showed a good calibration score, when compared with measured data. Moreover, both the assessments and the calibration scores varied significantly between the experts. Furthermore, the experts experienced a lack of relevant data in the literature to underpin their assessments.
The results of the probabilistic inversion showed that a distribution over the 11 model parameters could be found, which reproduced the experts' assessments for 25 out of the 27 elicited variables with sufficient accuracy. The failure of the model to properly reflect the experts' uncertainties on the remaining 2 variables might, on the basis of the experts' rationales, be attributed to a flaw in the elicitation of the experts. This indicates that the level of detail of the proposed model for the air temperature distribution is well-chosen, or more precisely put: not too crude. It is possible that a simpler model would have performed equally well. This could be verified on the basis of the same expert data, as these were collected independently of the model.
Probabilistic inversion has been found to be a powerful tool to quantitatively verify whether the selected level of model refinement is adequate in view of uncertainty in the process, which the model aims to describe. However, it is costly in terms of computation time and in its current form it requires a skilled operator. Hence, the technique is not suitable in the context of design practice.

In the first part of Chapter 6, the uncertainties in all model parameters, including those obtained from the expert judgment studies, were propagated to find the resulting uncertainty in the thermal comfort performance. Both for the TO and the TO* indicator a coefficient of variation of 0.6 was obtained. This is a moderate increase compared to the value of 0.5, which was obtained in the initial uncertainty analysis in Chapter 3.
Finally, it is illustrated how Bayesian decision theory can be applied to constructively use the quantitative information about the uncertainty in a design decision analysis. An example is described, in which two (fictitious) decision makers face the same choice

whether or not to integrate a cooling system in the building design. The example shows how the decision makers, who would take the same action in the absence of uncertainty, tend to different actions in the presence of uncertainty as a result of their different attitudes toward risk. This underlines the importance of explicit uncertainty information to rational design decisions.

In conclusion, the work underlying this thesis analyzes how performance predictions can be deployed in design decision analyses in a rational way. The focus is on the uncertainties which are inherent in these predictions: which part should they play in a decision analysis, how can they be assessed, and are they significant enough to be considered at all? These questions are addressed in the context of a specific case, which concerns the performance of a four story, naturally ventilated office building with respect to the thermal comfort of its occupants. The study indicates that the uncertainty in the thermal comfort performance, assessed in the design stage of a building, can be significant. Furthermore, expert judgment, in combination with probabilistic inversion if necessary, has proven to be a sound instrument to quantify uncertainties in building model parameters, which cannot be assessed on the basis of a straightforward statistical analysis. The method is expensive though and, in its current form, requires users who are skilled in the elicitation and processing of subjective probabilities. Hence, it does not yet seem a useful tool for routine application in building design practice. Finally, it has been demonstrated how uncertainty in building performance assessments can be used in, and is essential to, rational design decisions.

7.2 Recommendations

The work in this thesis shows that uncertainties in building model parameters, which cannot be assessed by statistical analysis of generic data, can suitably be quantified by means of expert judgment. However, this method is too costly for frequent application in design practice. It may be a useful tool in specific, non-standard design-situations, but the question arises how regular building physics consultancy could profit from the results of this thesis.

Firstly, the bottom line of this work is that uncertainty in building performance should be taken into account. Hence, if 'crude' uncertainty analyses, in which the building physics consultant assesses all uncertainties, would become more common in building design practice, this would be a significant step forward. In this approach, a consultant may directly profit from the material that was collected on building model parameters in this study, both from the literature and the two expert judgment studies. A necessary requirement for the adoption of uncertainty analysis in practice would be the enhancement of the functionality of most building simulation tools to facilitate uncertainty and sensitivity analyses.

Secondly, a consultant's uncertainty assessments could gradually improve if he was occasionally scored in a similar way to the experts in this study: by statistical comparison of his assessments of *seed* variables with measured data. Hence it would be useful if libraries with suitable seed variables could be developed, e.g. by branch-organizations.

Thirdly, if in future research more expert judgment studies would be carried out on building model components, experts in the associated domains would become more skilled in the assessment of uncertainties and more involved in building simulation. Hence, their domain expertise would become more readily available to the building simulation community. Moreover, the information about the uncertainties that result could be used to review whether the level of refinement in the current mainstream modeling approach, which is implemented in most building simulation tools, is in accordance with the level of uncertainty.

Chapter 6 explained how an individual decision maker can use uncertainty information in a Bayesian decision analysis to make an optimal decision. This approach, however, requires a drastic change in design decision making. It would be desirable to find an intermediate way in which the essence of decision making under uncertainty is preserved, but with minimal changes to the current process of design decision making. The essence of decision making under uncertainty, is balancing consequences against the probability of their occurrence. Current design decisions are based on comparisons of single valued assessments against deterministic criteria. The limit state approach, as it is commonly applied in structural mechanics, combines these two worlds and might be an option to investigate.

In this thesis it has been assumed that the thermal comfort performance indicator TO (or TO*), possibly calculated on the basis of a standardized scenario, is one of the yardsticks for the decision makers objectives. Indeed, this indicator is commonly used in current design analyses. However, little research has been done to investigate how this comfort performance indicator or other indicators correlate with the actual objectives a decision maker might have. Research in this field could significantly contribute to the rationality in design decisions concerning issues of thermal comfort.

References

Akins, R.E., Cermak, J.E., *Wind pressures on buildings,* Report CER76-77REA-JEC15, Fluid Dynamic and Diffusion Laboratory, Colorado State University, USA, 1976.

Akins, R.E., Peterka, J.A., Cermak, J.E., *Average pressure coefficients for rectangular buildings,* Proc. of the Fifth International Conference on Wind Engineering, Fort Collins, Colorado, 1979.

Akins, R.E., Peterka, J.A., Cermak, J.E., *Pressure distributions in atmospheric shear flows,* Proc. 2nd U.S. National Conference on Wind Engineering Research, Colorado State University , 1975.

Alamdari, F., Hammond, G.P., *Improved data correlations for buoyancy-driven convection in rooms,* Building Services Engineering Research and Technology v4 n3 pp106-112, 1983.

Allen, C., *Wind pressure data requirements for air infiltration calculations,* Report AIC-TN-13-84 of the International Energy Agency-Air Infiltration and Ventilation Centre, UK, 1984.

Allen, J., *Convection coefficients for buildings: External surfaces,* in: An investigation into analytical and empirical validation techniques for dynamic thermal models of buildings" SERC/BRE, Vol.2, Ch.7, BRE, Watford, UK, 1987.

ASCE, Aerospace division, *Wind tunnel studies of buildings and structures,* ASCE Manuals and Reports on Engineering Practice No. 67, American Society of Civil Engineers – Aerospace Division, Reston, Virginia, September, 1999.

Ashley, S.K., *Field and wind tunnel testing on natural ventilation cooling effects on three Navy buildings,* Technical report R-912 of the Naval Civil Engineering Laboratory, Port Hueneme, Canada, 1984.

ASHRAE, *Handbook of fundamentals,* American Society of Heating Refrigerating and Air-Conditioning Engineers, Atlanta, Georgia, 1993.

ASHRAE , *Handbook of fundamentals,* American Society of Heating Refrigerating and Air-Conditioning Engineers, Atlanta, Georgia, 1997.

ASHRAE, *ANSI / ASHRAE Standard 55-1992, Thermal environmental conditions for human occupancy,* American Society of Heating Refrigerating and Air-Conditioning Engineers, Atlanta, Georgia, 1992.

Augenbroe, G.L.M., *Research-oriented tools for temperature calculations in buildings,* Proc. 2nd Int. Conf. on System Simulation in Buildings pp234-255, Liege, 1986.

Auliciems, A., *Thermal Comfort,* in: N. Ruck (ed.) 'Building design and Human Performance', pp71-88, Van Nostrand, NY, 1989.

Auliciems, A., *Towards a psychophysiological model of thermal perception,* Int. J. Biometeorology v25 pp109-122, 1981.

Awbi, H.B., Hatton, A., *Natural convection from heated room surfaces*, Energy and Buildings v30 n3 pp233-244, 1999.

Baker, A.J., Kelso, R.M., Gordon, E.B., Roy, S., Schaub, E.G., *Computational fluid dynamics: a two-edged sword*, ASHRAE Journal pp 51-58, August, 1997.

Bietry, J., Sacre, C., Simiu, E., *Mean wind profiles and change of terrain roughness*, J. Struct. Div., ASCE, v104 pp1585-1593, 1978.

Bot, G.P.A., *Greenhouse climate: from physical processes to a dynamic model*, Ph.D. Thesis Wageningen University, The Netherlands, 1983.

Bottema, M., *Wind climate and urban geometry*, Ph.D. Thesis, Eindhoven University of Technology, 1993.

Boulard, T., Baille, A., *Modeling of air exchange rate in a greenhouse equipped with continuous roof vents*, J. Agric. Engng. Res. V61 pp37-48, 1995.

Bowen, A.J., *A wind tunnel investigation using simple building models to obtain mean surface wind pressure coefficients for air infiltration estimates.*, Report LTR-LA-209 of the National Aeronautical Establishment, National Research Council Canada, 1976.

Brager, G.S., De Dear, R.J., *Thermal adaptation in the built environment: a literature review*, Energy and Buildings v27 pp83-96, 1998.

Brouwers, G.F.M., Linden, A.C. van der, *Evaluation of the thermal indoor climate (in Dutch)*, Klimaatbeheersing v18 n7 pp257-264, 1989.

Cermak, J.E., e.a., *Passive and hybrid cooling developments: Natural ventilation-A wind tunnel study*, DOE Contract no. DE-AC03-80C-S11510, Fluid Dynamics and Diffusion Laboratory, Colorado State University, Fort Collins, Colorado, 1981.

Chen, Q., *Computational fluid dynamics for HVAC: Successes and Failures*, ASHRAE Trans. v103 n1 pp178-187, 1997.

Chen, Q., *Indoor air flow, air quality and energy consumption of buildings*, Ph. D. thesis Delft University of Technology, Delft, Netherlands, 1988.

Chen, Q., Meyers, C.A., Kooi, J. van der, *Convective heat transfer in rooms with mixed convection*, Proc. Int. Seminar on Air Flow Patterns in Ventilated Spaces, pp69-82, National Fund of Scientific Research in Belgium, Liege, Belgium, February, 1989.

Chen, Q., Moser, A., Suter, P., *A database for assessing indoor air flow, air quality, and draught risk*, Report International Energy Agency, Energy Conservation in Buildings and Community Systems Programme, Annex 20: Air flow patterns within buildings, Subtask 1: Room air and contaminant flow, Swiss Federal Institute of Technology, Zurich, April 1992.

CIBSE, *Design data*, CIBSE Guide, Volume A, Chartered Institution of Building Services Engineers, London, UK, 1986.

Clark, R.P., Edholm, O.G., *Man and his thermal environment*, Arnold, London, 1985.

Clarke, J., Yaneske, P., Pinney, A., *The harmonisation of thermal properties of building materials*, Report CR59/90 of the Building Research Establishment, Watford, UK, 1990.

Cooke, R.M., *Experts in uncertainty*, Oxford University Press, NY, 1991.

Cooke, R.M., Goossens, L.H.J., *EUR 18820 - Procedures guide for uncertainty analysis using structured expert judgment*, Report prepared for the European Commission, ISBN 92-894-0111-7, Office for Official Publications of the European Communities, Luxembourg, 2000.

Cooke, R.M., Kraan, B., *Dealing with dependencies in uncertainty analysis*, in: P.C. Cacciabue and I.A. Papazoglou (eds.) 'Probabilistic Safety Assessment and Management (ESREL '96 - PSAM III, June 24-28, 1996, Crete, Greece), Volume 1, Springer, 1996.

Cooke, R.M., *Parameter fitting for uncertain models: modelling uncertainty in small models*, Reliability Engineering & System Safety v44 pp89-102, 1994.

Cooke, R.M., *Unicorn: methods and code for uncertainty analysis*, Report Unicorn r3.0, pre-release for students and reviewers, SSOR TUDelft, 1994.

Cooper, P., Linden, P.F., *Natural ventilation of an enclosure containing two buoyancy sources*, J. Fluid Mechanics v311 pp153-176, 1996.

Cox, C.W.J., Rolloos, M., *Indoor climate factors in offices (in Dutch)*, Stichting Bouwresearch (SBR), Rotterdam, Netherlands, 1995.

Da Silva, F.M., Saraiva, J.G., *Determination of pressure coefficients over simple shaped building models under different boundary layers*, Minutes of the PASCOOL-CLI meetings, Florence May 1993, Segovia, November 1993, Wind tunnel test reports, INETI, Lisbon, Januari, March, 1994.

De Dear, R.J., Brager, G.S., *Developing an adaptive model of thermal comfort and preference*, ASHRAE Trans. Technical paper for the Winter Meeting, San Francisco, January1998.

De Dear, R.J., *Outdoor climatic influences on indoor thermal comfort requirements*, in: N.A. Oseland, M.A. Humphreys (eds.) 'Thermal Comfort: past, present and future', Building Research Establishment, UK, 1995.

De Finetti, B. *Theory of probability*, Wiley, New York, 1974.

Duffie, J.A., Beckmann, W.A., *Solar engineering of thermal processes*, Wiley, New York, 1980.

Eaton, K.J., Mayne, J.R., Cook, N.J., *Wind loads on low-rise buildings - effects of roof geometry*, Proc. 4th Wind Conference, London, 1975.

Elst, N.P. van, *Reliability of movable water barriers (in Dutch)*. Delft: Delft University Press, WBBM report Series 35, 1997.

ESRU, *ESP-r, A building energy simulation environment*, User Guide Version 8 Series, ESRU Manual U95/1, Energy Systems Research Unit, University of Strathclyde, Glasgow, UK, 1995a.

ESRU, *Summary of ESP-r's Data Model*, ESRU Technical Report TR95/2, Energy Systems Research Unit, University of Strathclyde, Glasgow, UK, 1995b.

Fanger, P.O., *Thermal Comfort*, Danish Technical Press, Copenhagen, 1970.

Feustel, H.E., e.a., *Fundamentals of the multizone air flow model COMIS*, Report of the International Energy Agency - Air Infiltration and Ventilation Centre, UK, 1990.

Folk, G.E., *Climatic change and acclimatization*, in K. Cena, J.A. Clark (eds.) 'Bio-engineering, Thermal Physiology and Comfort', pp157-168, Elsevier, Amsterdam, The Netherlands, 1981.

Fountain, M.E., Huizenga, C., *Wincomf: A Windows 3.1 thermal sensation model - Users manual*, Berkeley: Environmental Analytics, 1996.

François, C., Maalej, J., Paillassa, V., *Base de donnees des essais en regime permanent. Resultats d'essais de: plafond, plancher et panneau chauffants, radiateur et convecteur*, Report of the Centre Scientifique et Technique du Batiment (CSTB), Service genie energetique et climatique, GEC/DGE no. 93.016R, February , 1993.

French, S., *Decision theory – an introduction to the mathematics of rationality*, Ellis Horwood, London, 1993.

Froehlich, C., London, J. (eds.), *Revised instruction manual on radiation instruments and measurements*, WCRP publication series n7, WMO Technical Document 149, World Meteorological Organization, Geneva, Switzerland, 1986.

Fürbringer, J.-M., *Sensibilité de modèles et de mesures en aéraulique du bâtiment à l'aide de plans d'expériences*, Ph. D. thesis nr. 1217. École Polytechnique Fédérale de Lausanne, Switzerland, 1994.

Gagge, A.P., Stolwijk, J.A.J., Hardy, J.D., *Comfort and thermal sensations and associated physiological responses at various ambient temperatures*, Environmental Research v1 pp1-20, 1967.

Gagge, A.P., Stolwijk, J.A.J., Nishi, Y., *An effective temperature scale based on a simple model of human physiological regulatory response*, ASHRAE Trans. v70 n1 pp247-262, 1971.

Gagneau, S., Nataf, J.M., Wurtz, E., *An illustration of automatic generation of zonal models*, Proc of the 5th Int. IBPSA Conference 'Building Simulation '97 v2 pp437-444, Prague, September , 1997.

Geurts, C.P.W., *Wind-induced pressure fluctuations on building façades*, Ph.D. Thesis, Eindhoven University of Technology, 1997.

Gids, W.F. de, *Window airing pattern for simulations IEA Annex 27*, Memo to L.G. Mansson, 13 November 1995.

Gokhale, D., Press, S., *Assessment of a prior distribution for the correlation coefficient in a bivariate normal distribution*, J.R. Stat. Soc. A v145 n2 pp237-249, 1982.

Gonçalves, H., *Climate input data and its processing*, in: Jensen, S.Ø. (ed.), EUR 13034 EN - The PASSYS Project phase I, Subgroup model Validation and Development, Research report of the subgroup model validation and development for the Commission of the European Communities, DG XII, Thermal Insulation Laboratory, Technical University of Denmark, Copenhagen, Denmark, 1990.

Gonzalez, R.R., Berglund, L., Gagge, A.P., *Indices of thermoregulatory strain for moderate exercise in the heat*, J. Applied Physiology: Respiration Environment Exercise Physiology v44 n6 pp889-899,1978.

Grosso, M., *Wind pressure distribution around buildings: a parametrical model*, Energy and Buildings v18 pp101-131, 1992.

Grosso, M., Marino, D., Parisi, E., *A wind pressure distribution calculation program for multizone airflow models*, Proc. of the 3rd Int. Conf. on Building Performance Simulation, pp105-118, Madison, USA, 1995.

Haar, T.R. ter, Retief, J.V. & Dunaiski, P.E., Towards a more rational approach of the serviceability limit states design of industrial steel structures. *Proc. 2nd World Conference on Steel in Construction*, paper 283, San Sebastian, Spain, 1998.

Halcrow, Sir William and partners, *Report on "heat transfer at internal surfaces*, Report for the Energy Technology Support Unit of the Dep. of Energy, Wiltshire, England, 1987.

Hamilton, G.F., *Effects of velocity distribution wind loads on walls and low buildings*, Tech publication series, TP6205 of the Department of Mechanical Engineering, University of Toronto, November, 1962.

Harper, F.T., et al., *Joint US/NRC/CEC Consequence Uncertainty Study: Summary of Objectives, Approach, Application, and Results for the Dispersion and Deposition Uncertainty Assessments* , Main report prepared under contracts NUREG/CR-6244; EUR 15855; SAND94-1453, Sandia National Laboratories and Delft University of Technology, 1994.

Heiselberg, P., Murakami, S., Roulet, C.-A. (eds.), *Ventilation of Large Spaces in Buildings, Analysis and Prediction Techniques*, Report of the International Energy Agency, Energy Conservation in Buildings and Community Systems Programme, Annex 26: Energy Efficient Ventilation of Large Enclosures, Aalborg University, Aalborg, Denmark, 1998.

Hoelscher, N., *WTG-Ringversuche in Grenzschichtwindkanälen*, Bochum, November 1997.

Holtslag, A.A.M., Estimates of diabatic wind speed profiles from near-surface weather observations, Boundary-Layer Meteorology v29 pp225-250, 1984.

Howarth, A.T., *The prediction of air temperature variations in naturally ventilated rooms with a convective heating*, Build. Serv. Eng. Res. Technol. v6 pp169-175, 1985.

Humphreys, M.A., *Outdoor temperatures and comfort indoors*, Building Research and Practice v6 n2, 1978.

Hussain, M., Lee, B.E., *An investigation of wind forces on three-dimensional roughness elements in a simulated atmospheric boundary layer, Pts. 1,2 and 3*, Reports BS55, BS56 and BS57 of the University of Sheffield, Dept. of Building Science, UK, 1980.

Iman, R.L., Conover, W.J., *Small sample sensitivity analysis techniques for computer models, with application to risk assessment*, Communications in Statistics vB11 pp311-334, 1980.

Iman, R.L., Helton, J.H., *A comparison of uncertainty and sensitivity analysis techniques for computer models*, Internal report NUREG ICR-3904, SAND 84-1461, Sandia National Laboratories, Albuquerque, New Mexico, US, 1985.

Inard, C., Bouia, H., Dalicieux, P., *Prediction of air temperature distributions in buildings with a zonal model*, Energy and Buildings v24 pp125-132, 1996.

Iqbal, M., *An introduction to solar radiation*, Academic Press, London, 1983.

ISO, *ISO-International Standard 7730: Moderate Thermal Environments - Determination of the PMV and PPD Indices and Specification of the conditions of Thermal Comfort, 2nd ed.*, ISO, Geneva, 1994.

ISSO, *Heat transfer and solar transmission of window systems (in Dutch)*, Report 12.1, ISSO, Rotterdam, The Netherlands, 1993.

ISSO, *Reference points for temperature simulations (in Dutch)*, Publication 32, ISSO, Rotterdam, The Netherlands, 1994.

Ito, N., Kimura, K., Oka, J., *A field experiment study on the convective heat transfer coefficient on the exterior surface of a building*, ASHRAE Trans. V78 n1 pp184-191, 1972.

Janssen, P.H.M., Heuberger, P.S.C., Sanders, R., *UNCSAM 1.1: a Software Package for Sensitivity and Uncertainty Analysis; Manual*, Report 959101004 of the Rijksinstituut voor volksgezondheid en milieuhygiene (RIVM), Bilthoven, The Netherlands, 1992.

Janssen, P.H.M., Slob, W., Rotmans, J., *Sensitivity analysis and uncertainty analysis: an inventory of ideas, methods and techniques*, Report 958805001 of the Rijksinstituut voor volksgezondheid en milieuhygiene, Bilthoven (RIVM), The Netherlands, 1990.

Jensen, M., Franck, N., *Model scale tests in turbulent wind, Part II. Phenomena dependent on the velocity pressure. Wind loads on buildings.*, Danish Technical Press, Copenhagen, 1965.

Jensen, S.Ø. (ed.), *EUR 13034 EN - The PASSYS Project phase I, Subgroup model Validation and Development*, Research report of the subgroup model validation and development for the Commission of the European Communities, DG XII, Thermal Insulation Laboratory, Technical University of Denmark, Copenhagen, Denmark, 1990.

Jensen, S.Ø. (ed.), *EUR 15115 EN - The PASSYS Project, Validation of building energy simulation programs; a methodologyI*, Research report of the subgroup model validation and development for the Commission of the European Communities, DG XII, Contract JOUE-CT90-0022, Thermal Insulation Laboratory, Technical University of Denmark, Copenhagen, Denmark, 1994.

Kahneman, D., Slovic, P., Tversky, A. (eds.), *Judgment under uncertainty: heuristics and biases*, Cambridge University Press, NY, 1982.

Keeney, R.L., *Measurement scales for quantifying attributes*, Behavioral Science v26 pp29-36, 1981.

Khalifa, A.J.N., *Heat transfer processes in buildings*, Ph. D. thesis University of Wales College of Cardiff, Chapter 8, 1989.

Khalifa, A.J.N., Marshall, R.H., *Validation of heat transfer coefficients on interior building surfaces using a real-sized indoor test-cell*, Int. J. Heat and Mass Transfer, v33 n10 pp2219-2236, 1990.

Kimani, G., *Weather data adjustment for ventilation and thermal modeling of buildings,* MSc Thesis, Brunel University, Uxbridge, UK, 1998.

Kleijnen, J.P.C., *Sensitivity analysis and related analyses: a review of some statistical techniques,* Journal of Statistical Computation and Simulation v57 pp111-142, 1997.

Knoll, B., Phaff, J.C., Gids, W.F. de , *Pressure simulation program,* Proc. of the 16th AIVC Conference on Implementing the Results of Ventilation Research, Palm Springs, California, USA, March, 1995.

Knoll, B., Phaff, J.C., *The C_p-generator, a simple method to assess wind pressures (in Dutch),* Bouwfysica v7 n4 pp13-17, 1996.

Kraan B.C.P., Cooke R.M., *Processing Expert Judgement Assessments into Parameter Uncertainties*, in: P.C. Cacciabue and I.A. Papazoglou (Eds.), Probabilistic Safety Assessment and Management (ESREL '96 - PSAM III, June 24-28, 1996, Crete, Greece), v1 pp625-630, Springer, 1996.

Kraan, B.C.P., *Probabilistic inversion in uncertainty analysis and related topics (in preparation)*, Ph. D. thesis Delft University of Technology, Delft, Netherlands, 2001.

Kraan, B.C.P., Cooke, R.M., *Post-processing techniques for the joint CEC/USNRC uncertainty analysis of accident consequence codes*, J. Stat. Computation and Simulation v57 pp243-260, 1997.

Kraan, B.C.P., Cooke, R.M., *Uncertainty in Compartmental Models for Hazardous Materials - A case study*. Journal of Hazardous Material v 71 pp253-268, 2000.

Kruehne, H., *Experimental and theoretical investigations on displacement ventilation*, Ph. D thesis Technical University Berlin, Berlin, Germany, 1995.

Kullback, S. *Information theory and statistics*, Wiley, NY, 1959.

Lemaire, A., *Room air and contaminant flow, Evaluation of Computational Methods*, Summary report of the International Energy Agency, Energy Conservation in Buildings and Community Systems Programme, Annex 20: Air Flow Patterns within Buildings, Subtask-1, TNO Building and Construction Research, Delft, December 1993.

Li, L., Beckman, W., Mitchell, J., *An experimental study of natural convection in an office room,* Report of the Solar Energy Laboratory, University of Wisconsin, Madison, US, 1987.

Liddament, M. W., *Air infiltration calculation techniques - an applications guide,* Report AIC-AG-1-86 of the International Energy Agency-Air Infiltration and Ventilation Centre, UK, 1986.

Linden, A.C. van der (ed.), *Building physics (in Dutch)*, Spruyt, Van Mantgem en De Does BV, Leiden, Netherlands, 1996.

Linden, P.F., Cooper, P., *Multiple sources of buoyancy in a naturally ventilated enclosure*, J. Fluid Mechanics v311 pp177-192, 1996.

Linden, P.F., Lane-Serff, G.F., Smeed, D.A., *Emptying filling boxes: the fluid mechanics of natural ventilation*, J. Fluid Mechanics v212 pp309-335,1990.

Lomas, K.J., Bowman, N.T., *Developing and testing tools for empirical validation,* In: An investigation into analytical and empirical validation techniques for dynamic thermal models of buildings, Final BRE/SERC report, Vol. VI, Building Research Establishment, Watford, UK, 1988.

Lomas, K.J., Eppel, H., *Sensitivity analysis techniques for building thermal simulation problems*, Energy and Buildings v19 pp21-44, 1992.

Lomas, K.J., *Applicability study 1 – Executive summary*, Report for the Energy Technology Support Unit, contract ETSU S 1213, School of the Built Environment, De Montfort University, Leicester, UK, 1993.

Loomans, M.G.L.C., *The measurement and simulation of indoor air flow*, Ph. D. thesis Eindhoven University of Technology, Eindhoven, Netherlands, 1998.

Lugtenburg, A., Den Ouden, H., De Gids, W., *Air flow around buildings - pressure measurements on flue outlets (in Dutch)*, Report C302 of IG-TNO, Netherlands, 1972.

Lund, H., *Test Reference Years TRY-Weather data sets for computer simulations of solar energy systems and energy consumption in buildings*, Report EUR9765 of the Commission of the European Communities, DG XII, 1985.

Lusch, G., Truckenbrodt, E., *Wind tunnel experiments on buildings with rectangular floorplans and flat or gable roofs (in German).*, Berichte aus der Bauforschung v41 pp25-69, 1964.

Maalej, J., *Heaters in buildings: thermal behavior and performance study (in French)*, Ph. D. thesis University of Valenciennes and Hainaut-Cambresis, Valenciennes, France, 1994.

MacDonald, I.A., Clarke, J.A., Strachan, P.A., *Assessing uncertainty in building simulation*, Proc. Building Simulation '99, Paper B-21, Kyoto, 1999.

Martin, C., *Quantifying errors in the predictions of SERI-RES*, Report of the Energy Technology Support Unit, contract ETSU S 1368, Energy Monitoring Company Ltd, UK, 1993.

McKay, M.D., Beckmann, R.J., Conover, W.J., *A comparison of three methods for selecting values of input variables in the analysis of output from a computer code*, Technometrics v21 pp239-245, 1979.

McKay, M.D., *Evaluating prediction uncertainty*, Report for the Division of Systems Technology, Office of Nuclear Regulatory Research, USNRC, contract NUREG/CR-6311, Los Alamos National Laboratory, Los Alamos, US, 1995.

Meeuwissen, A., Cooke, R.M., *Tree dependent random variables*, Report 94-28 of Dept. Mathematics, Delft University of Technology, 1994.

Min, T., Schutrum, L., Parmelee, G., Vouris, J., *Natural convection and radiation in a panel-heated room*, ASHRAE Trans. v62 pp337-358, 1956.

Morris, M.D., *Factorial sampling plans for preliminary computational experiments*, Technometrics v33 n2 pp161-174, 1991.

Mundt, E., *The performance of displacement ventilation systems*, Ph. D thesis Royal Institute of Technology, Stockholm, Sweden, 1996

Negrao, C.O.R., *Conflation of computational fluid dynamics and building thermal simulation*, Ph. D. thesis University of Strathclyde, Glasgow, UK, 1995.

NEN 5067, *Cooling load calculation for buildings (in Dutch)*, Nederlands Normalisatie Instituut, The Netherlands, 1985.

NEN-ISO 7726, *Thermal environments - Instruments and methods for measuring physical quantities*, Nederlands Normalisatie Instituut, The Netherlands, 1989.

Nicol, F., *Thermal Comfort - A Handbook for Field Studies Toward an Adaptive Model*, University of East London, UK, 1993.

Niu, J., *Modeling of cooled-ceiling air conditioning systems*, Ph. D. thesis Delft University of Technology, Delft, Netherlands, 1994.

NLR, *LST; Low Speed Wind Tunnel*, Report National Aerospace Laboratory (NLR), Emmeloord, Netherlands, July 1993.

NOVEM, *Guidelines for the design of naturally ventilated office buildings (in Dutch)*, Rapport E 234-1 van de Nederlandse Maatschappij voor energie en Milieu B.V. (NOVEM), Sittard, Netherlands, 1992.

Paciuk, M., *The role of personal control of the environment in thermal comfort and satisfaction at the workplace*, in: R.I. Selby, K.H. Anthony, J. Choi, B. Orland, 'Coming of age', Publication 21 of the Environmental Design Research Association, Oklahoma City, Oklahoma, US, 1990.

Peng, X., *Modeling of indoor thermal conditions for comfort control in buildings*, Ph. D. thesis Delft University of Technology, Delft, Netherlands, 1996.

Pernot, C.E.E., *Internal convection*, in: Jensen, S.Ø. (ed.), EUR 13034 EN - The PASSYS Project phase I, Subgroup model Validation and Development, Research report of the subgroup model validation and development for the Commission of the European Communities, DG XII, Thermal Insulation Laboratory, Technical University of Denmark, Copenhagen, Denmark, 1990.

Phaff, J.C., *Continuation of model tests of the wind pressure distribution on some common building shapes*, Report C429 of TNO, Delft, June, 1979.

Phaff, J.C., *Model tests of the wind pressure distribution on some common building shapes (in Dutch)*, Report C403 of TNO, Delft, November, 1977.

Pinney, A.A., Parand, F., Lomas, K., Bland, B.H., Eppel, H., *The choice of uncertainty limits on program input parameters within the applicability study 1 project*, Applicability Study 1, Research report 18 for the Energy Technology Support Unit of the Department of Energy, UK, Contract no E/5A/CON/1213/1784, Environmental Design Unit, School of the Built Environment, Leicester Polytechnic, UK, 1991.

Plate, E.J., *Urban climates and urban climate modeling: an introduction*, In: Cermak, J.E. (ed.) Wind climate in cities, Kluwer, The Netherlands, 1995.

Polytechnical Almanac (in Dutch), Koninklijke PBNA, Arnhem, The Netherlands, 1995.

Prosser, C.L. (ed.), *Physiological Adaptation*, Am. Physiol. Soc., Washington D.C., 1958.

Rahni, N., Ramdani, N., Candau, Y., Dalicieux, P., *Application of group screening to dynamic building energy simulation models*, J. Statist. Comput. Simul. v57 pp285-304, 1997.

Ramsay, F., *Truth and probability*, in Braithwaite (ed.), The Foundations of Mathematics, Kegan Paul, London, pp156-198, 1931.

RGD, *Indoor climatic conditions in office spaces of new buildings (in Dutch)*, Report of the Rijksgebouwendienst, Hoofdafdeling Bouw, Afdeling Warmte- en Luchttechniek, The Hague, The Netherlands, 1979.

Rodriguez, E.A., Alvarez, S., Caceres, I., *Prediction of indoor temperature and air flow patterns by means of simplified zonal models*, Proc. ISES Solar World Congress v6 pp473-479, Budapest, 1993.

Saltelli, A., Andres, T.H., Homma, T., *Sensitivity analysis of model output, An investigation of new techniques*, Computational statistics & Data Analysis v15 pp211-238, 1993.

Sandberg, M., *Air-exchange efficiency, ventilation efficiency and thermal efficiency in a cellular office*, Report of the National Swedish Institute for Building Research M85:24, January, 1986.

Santamouris, M., Argiriou, A. (eds.), Final report of the PASCOOL CE Project JOU2-CT92-0013, DG XII of the Commission of European Communities, Brussels, 1995.

Savage, L.J., *The foundations of statistics*, 1st edition, Wiley, New York, 1954.

SBR, *Design of energy efficient office buildings*, Publikatie 300, Stichting Bouwresearch, Rotterdam, Netherlands, 1994.

Schalkoort, T.A.J., *Standards for an acceptable indoor climate (in Dutch)*, TVVL magazine v23 n5 pp21-27, 1994.

Sensharma, N.P., Woods, J.E., Goodwin, A.K., *Relationships between indoor environment and productivity: a literature review*, ASHRAE Transactions v104 part 1A pp686-700, 1998.

Sharples, S., *Full-scale measurements of convective energy losses from exterior building surfaces*, Building and Environment v19 n1 pp31-39, 1984.

Sherman, M.H., Grimsrud, D.T., *Wind and infiltration interaction for small buildings.*, Annual meeting of the American Society of Civil Engineers, New Orleans, 1982.

Siegel, R., Howell, J.R., *Thermal Radiation Heat Transfer*, McGraw Hill, NY, 1981.

Simiu, E., Scanlan, R.H., *Wind effects on structures, 3rd edition*, Wiley International, New York, 1996.

Soerensen, L.C., *Wind tunnel tests of a low building in a city environment*, Report Boundary Layer Windtunnel Facility, University of Western Ontario, October, 1998.

Spitler, J.D., *Annotated guide to load calculation models and algorithms*, ISBN 1-883413-33-8, ASHRAE, Atlanta, USA, 1996.

Stanzel, B., *External longwave radiation*, in: Jensen, S.∅. (ed.), EUR 13034 EN - The PASSYS Project phase I, Subgroup model Validation and Development, Research report of the subgroup model validation and development for the Commission of the

European Communities, DG XII, Thermal Insulation Laboratory, Technical University of Denmark, Copenhagen, Denmark, 1990.

Strachan, P, Martin, C., *External convection,* in: Jensen, S.Ø. (ed.), EUR 13034 EN - The PASSYS Project phase I, Subgroup model Validation and Development, Research report of the subgroup model validation and development for the Commission of the European Communities, DG XII, Thermal Insulation Laboratory, Technical University of Denmark, Copenhagen, Denmark, 1990.

Straw, M.P., Robertson, A.P., Baker, C.J., *Experimental measurements and computations on the wind induced ventilation of a cubic structure,* Proc. 10th International Conference on Wind Engineering, Copenhagen v3 pp1951-1958, Denmark, 1999.

Swami, M.V., Chandra, P.E., *Correlations for pressure distributions on buildings and calculation of natural ventilation air flow,* ASHRAE Transactions v94 n1 pp243-266, 1988.

Tieleman, H.W., Gold, R.R., *Wind tunnel investigation of Care Inc. single family dwelling,* Report VPI-E-76-8 of the Virginia Polytechnic Institute and State University,Virginia, USA, 1976.

Unsworth, M.J., Monterth, *Longwave radiation at the ground,* Quart. J. Royal Meteorological Society v101 pp1-13, 1971.

Velds, C.A., *Solar radiation in The Netherlands (in Dutch),* Thieme-Baarn / KNMI-De Bilt, The Netherlands, 1992.

Vickery, B.J., Baddour, R.E., Karakatsanis, C.A., *A study of the external wind pressure distributions and induced internal ventilation flow in low-rise industrial and domestic structures,* Report no BLWT-SS2-1983 of the Boundary Layer Wind Tunnel Labaratory, University of Western Ontario, January, 1983.

Von Neumann, J., Morgenstern, O., *Theory of games and economic behavior,* 2nd edition, Princeton University Press, 1947.

Voskamp, P., *Handbook health and safety in offices: recommendations, guidelines, standards and codes (in Dutch),* SDU Uitgeverij, Den Haag, Netherlands, 1995.

Vrouwenvelder, A.C.W.M., Oosterhout, G.P.C., *Vibrations in tall buildings due to wind loading,* Proceedings of the IABSE conference, Copenhagen, June 1996.

Walker, I.S., Wilson, D.J., Forest, T.W., *Wind shadow model for air infiltration sheltering by upwind obstacles,* HVAC&R Research v2 n4 pp265-283, 1996.

Walker, I.S., Wilson, D.J., *Practical methods for improving estimates of natural ventilation rates,* Proc. of the 15th AIVC Conference on The Role of Ventilation, Buxton, UK, September, 1994.

Wapenaar, P., *Design guidelines for naturally ventilated office buildings (in Dutch),* Report E 234-1 for the NOVEM (Dutch Society for Energy and Environment), Peutz & Associes BV, Zoetermeer, The Netherlands, 1992.

Wells, Hoxey, *Measurements of wind loads on full-scale glasshouses,* J. Wind Eng. Ind. Aer. v6 pp139-167, 1980.

Wieringa, J., *Representative roughness parameters for homogeneous terrain,* Boundary-Layer Meteorology v63 n4 pp323-364, 1993.

Wieringa, J., Rijkoort, P.J., *Wind climate of The Netherlands (in Dutch),* Staatsuitgeverij, Den Haag, The Netherlands, 1983.

Willemsen, E., *Pressure measurements on a 1:250 model for ventilation study TU-Delft (in Dutch),* Report DNW-TR-98.07 of German-Dutch Wind tunnel (DNW), The Netherlands, 1998.

Wiren, B.G., *Effects of surrounding buildings on wind pressure distributions and ventilation losses for single-family houses,* Bulletin M85:19 of the National Swedish institute for Building Research, Gavle, Sweden, 1985.

Wijsman, A.J.Th.M., *Building Thermal Performance Programs: Influence of the Use of a PAM,* BEP '94 Conference, York, UK, April 5-8 1994.

Wit, M.S. de, *Training for experts participating in a structured elicitation of expert judgment - wind engineering experts,* Report of B&B group, Faculty of Civil Engineering, Delft University of Technology, 1997a.

Wit, M.S. de, *Influence of modeling uncertainties on the simulation of building thermal comfort performance,* Proc. Building Simulation '97, 5th International IBPSA Conference, September 8-10, Prague, Czech Republic, 1997b.

Wit, M.S. de, *Identification of the important parameters in thermal building simulation models,* J. Statistical Computation and Simulation v57 n1-4 pp305-320, 1997c.

Wit, M.S. de, *Training for experts participating in a structured elicitation of expert judgment –air temperature distribution,* Report of B&B group, Faculty of Civil Engineering, Delft University of Technology, 1998.

Wit, M.S. de, *Final report of the expert judgment study on wind pressure coefficients, part 2, Unprocessed data,* Report of B&B group, Subfaculty of Civil Engineering, Delft University of Technology, June 1999a.

Wit, M.S. de, Linden, A.C. van der, Raue, A.K., *Evaluation of performance indicators for thermal comfort in buildings (in Dutch),* Report PG-110, ISSO, Rotterdam, Netherlands, 1999b.

Wit, M.S. de, *Uncertainty in wind pressure coefficients for low-rise buildings,* In: Larsen, A., Larose, G.L., Livesey, F.M. (eds.), Wind Engineering into the 21st Century, v3 pp1859-1866, Balkema, Rotterdam, 1999c.

Wit, M.S. de, *Uncertainty in wind pressure coefficients for low-rise buildings,* HERON v44 n1 pp45-59, Netherlands School for Advanced Studies in Construction, Delft, Netherlands, 1999d.

Wit, M.S. de, *Final report of the expert judgment study on air temperature distribution, part 2, Rationales,* Report of B&B group, Faculty of Civil Engineering, Delft University of Technology, 2001.

Yoshizawa, S., Kimura, K., Ikeda, K., Tanabe, S., Iwata, T. (eds.), Proc. Indoor Air '96, Nagoya, Japan, 1996.

Appendix A

A.1. Model data

Figure A.1 shows the plan of the top floor of the building under study. The dashed line encloses the modeled building section.

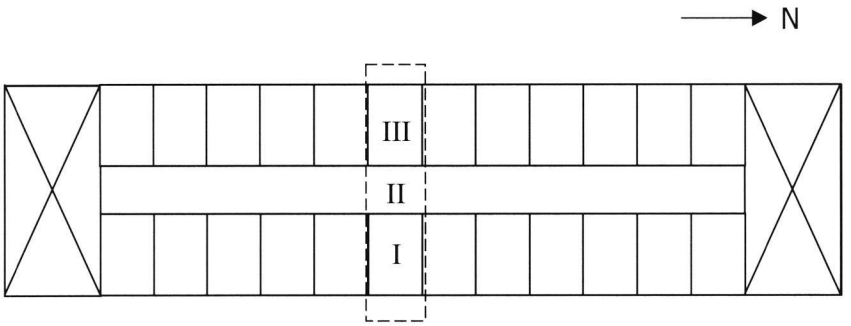

Figure A.1. Plan of the top floor. A corridor separates the two rows of office spaces at the long façades. The crosses at both ends of the building indicate the stairwells, which are separated from the corridors by airtight fire doors. The orientation of the building is indicated. The dashed rectangle encloses the part of the building that is modeled in detail.

Space I (east office space)

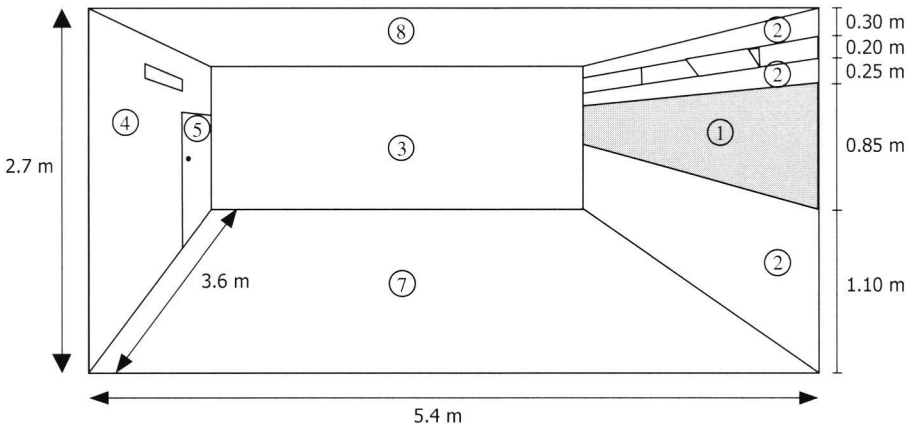

Figure A.2. Office space I with dimensions ($l \times w \times h$) 5.4m × 3.6m × 2.7 m. Cross-ventilation of the space takes place through a cantilever window in the façade and a rectangular vent in the opposite wall. The wall components are numbered. Wall component 6 is the missing separation wall.

Properties wall components

Table A.1. Wall components space I

nr. (see Figure A.2)	description	wall type (see Table A.8)
1	window	1
2	parapet	2
3	separation wall left	3
4	separation wall back	3
5	door	4
6	separation wall right	3
7	floor	5
8	ceiling/roof	6

Table A.2. Wall components space I, continued. The values between brackets apply when the sunblind is down.

nr.	$\alpha_{c,int}$ [W/m²K]	$\alpha_{c,ext}$[33] [W/m²K]	a_s[33] [-]	t_s[33] [-]	ε[33] [-]	viewfactors[33] ground	buildings	sky
1	2.5	25 (8)	0.15[34]	0.7	0.9	0.4 (0)	0.2 (0)	0.4 (0)
2	2.5	25	0.65	0.0	0.9	0.4	0.2	0.4
3	2.5	-	-	-	-	-	-	-
4	2.5	-	-	-	-	-	-	-
5	2.5	-	-	-	-	-	-	-
6	2.5	-	-	-	-	-	-	-
7	3.0	-	-	-	-	-	-	-
8	2.0	25	0.65	0.0	0.9	0.0	0.0	1.0

where

$\alpha_{c,int}$ internal convective heat transfer coefficient
$\alpha_{c,ext}$ external convective heat transfer coefficient
a_s solar absorption factor
t_s solar transmission factor
ε emittance of external surface (=absorptance, gray radiator).

Ventilation

Table A.3. Ventilation openings space I

Location	Type	Cross-sectional area	Discharge coefficient
façade	cantilever window	0.18 m²	0.7
separation wall	vent	0.18 m²	0.7

[33] Values are only specified for wall components, which are part of the building envelope.
[34] Absorption of solar radiation is assumed to be equally divided over the two windowpanes.

Solar radiation

Table A.4. Properties of the external sunblind. For details on the operation see 'Scenario data'.

	$\alpha_{c,int}$	$\alpha_{c,ext}$[33]	a_s[35]	t_s[33]	ε[33]	viewfactors		
	[W/m²K]	[W/m²K]	[-]	[-]	[-]	ground	buildings	sky
sunblind	12	30	0. 5	0.18	0.9	0.4	0.2	0.4

The cavity between the sunblind and the window pane is ventilated with outdoor air at a rate of 0.5 m³/s.

Table A.5. Distribution of solar radiation in the space

Description	Value	Reference
Solar radiation entering the space:		
• division of absorption over furniture/enclosure	10% / 90%	
• distribution of absorption over enclosure	100% at floor	ISSO, 1994

Space II (corridor)

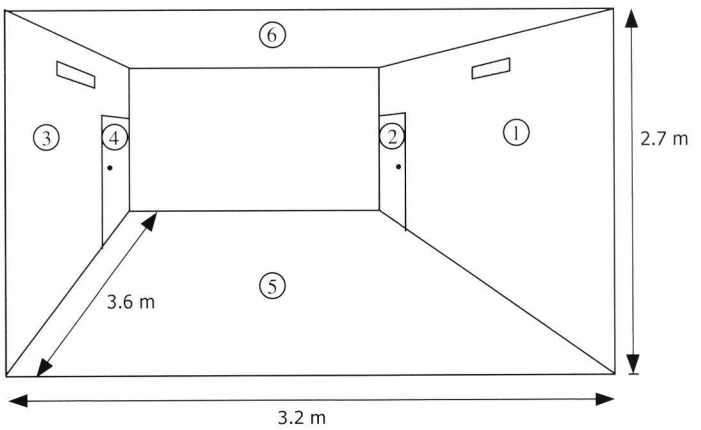

Figure A.3. Space II with dimensions (l × w × h) 3.2 m × 3.6 m × 2.7 m. Cross-ventilation of the space takes place through two rectangular vents in the separation walls with office spaces I and III. The wall components are numbered.

Ventilation

Table A.6. Ventilation openings space II

Location	Type	Cross-sectional area	Discharge coefficient
separation wall east	vent	0.18 m²	0.7
separation wall west	vent	0.18 m²	0.7

[35] Values are only specified for wall components, which are part of the building envelope.

Properties wall components

Table A.7. Wall components space II

nr. (see Figure A.1)	description	wall type number (see Table A.8)	$\alpha_{c,int}$ [W/m^{2}K]
1	separation wall east	3	2.5
2	door east	4	2.5
3	separation wall west	3	2.5
4	door west	4	2.5
5	floor	5	3.0
6	ceiling	6	2.0

Space III (west office space)

Identical to east office space (space I).

Wall types

Table A.8. Properties of wall types, attributed to wall-components in Table A.1 en Table A.7.

Wall type	Layer[36]	description	λ [W/m K]	ρ c [J/m^3 K]	d [m]
1	1	glass pane	0.8	2.1 10^6	0.004
	2	air layer[37]	1.0	0	0.17
	3	glass pane	0.8	2.1 10^6	0.005
2	1	rabat	0.17	1.2 10^6	0.02
	2	insulation	0.04	2.9 10^4	0.12
	3	underlayment	0.23	1.3 10^6	0.01
	4	insulation	0.04	2.9 10^4	0.12
	5	plaster	0.70	8.4 10^5	0.015
3	1	sand-lime	1.0	1.7 10^6	0.10
4	1	internal door	0.17	1.2 10^6	0.04
5	1	concrete	2.0	2.0 10^6	0.22
	2	carpet	0.07	5.9 10^5	0.004
6	1	roofing	0.2	1.8 10^6	0.004
	2	insulation	0.04	2.9 10^4	0.12
	3	concrete	2.0	2.0 10^6	0.22
	4	cavity[38]	1.0	0	0.20
	5	ceiling	0.2	1.0 10^6	0.02

[36] Layers are numbered from the outside of the space towards the inside. Layers in separation walls between an office space and the corridor are numbered from the outside of the office space.
[37] This combination of values represents a thermal resistance R_t = 0.17 m^2 K/W.
[38] This combination of values represents a thermal resistance R_t = 0.20 m^2 K/W.

where

λ	conductivity
ρ	density
c	specific heat
d	thickness

General data

Table A.9. General data

Description	Value	Reference
location building site	The Netherlands	
albedo	0.2	
density of air	1.2 kg/m^3	
specific heat of air	1000 J/kg K	
wind reduction factor	0.7 (urban terrain)	Liddament, 1986
pressure coefficients set	sheltered, flat roof, aspect ratio of floor plan 2:1	Liddament, 1986
model for sky radiant temperature		Unsworth and Monterth, 1971
ground parameters		
conductivity	1.3 W/m K	
heat capacity	1.3 10^6 J/m^3 K	
thickness	1.2 m	

A.2. Scenario data

The scenario contains the external conditions under which the responses of the building (model) are observed.

Climate data

- April through September in the Test Reference Year for De Bilt, The Netherlands (Lund, 1985)
- Isotropic sky radiance distribution
- Ground temperature at 1.2 m depth: as default in ESP-r (ESRU, 1995b)

Operation of the building

- Office hours from 8.00 – 18.00, 7 days per week
- Internal heat load[39] in spaces I and III (see Figure A.1): 20 W/m^2 during office hours
- Internal heat load in space II equal to 0

Control

- Internal office doors closed at all times
- Automatic control of the solar shading (threshold level at 250 W/m^2 at the façade (ISSO, 1994)).
- When (dry bulb) air temperature in either space I or space III tends to drop below 20°C, an (idealized) heating system is activated, which keeps the air temperature at exactly 20°C until it rises again.
- Empirical control law for window opening according to Gids (1995):
  window opening R in percentage of the maximum opening:

  $$R = R_{wind} * R_{temp}$$

  with
  $R_{wind} = 1 - 0.1\ U$
  $R_{temp} = 0.2 + T_a/25$

  where
  U local mean wind speed at roof height (m/s)
  T_a outdoor ambient temperature (°C)

Additional data for static Rgd-comfort model (see section 2.4.2)

- metabolism: 70 W/m^2
- clothing resistance: 0.11 m^2 K/W
- relative humidity: 50%
- air velocity: 0.10 m/s

[39] Specified as load per m^2 floor area in the space. It is assumed that all heat is emitted convectively to the ambient indoor air.

Appendix B

Tables with ranges, quantifying the specification uncertainties. In the uncertainty analysis, 'Low', 'Base' and 'High' have been interpreted as 2.5%, 50% and 97.5% quantile values respectively. The symbols and the numbers in the column 'Reference' are explained below the table.

Variable	Low	Base	High	Unit	Reference
Spaces					
height	2.68	2.70	2.72	m	10
width	3.58	3.60	3.62	m	10
length	5.38	5.40	5.42	m	10
Wall component 1 (window)					
Layer 1 (float glass)					
d	4.8	5.0	5.2	mm	1
λ	0.760	0.955	1.15	W/mK	2
ρ c	1.85	2.10	2.35	J/m^{3}K	Calculated from 2
a_s	0.12	0.13	0.14	-	Base: 4, range: 10
t_s	0.79	0.81	0.83	-	Calculated from 5
ε	0.81	0.83	0.85	-	6
Layer 2 (air)					
R_t	0.16	0.18	0.20	m^{2}K/W	
Layer 3 (float glass)					
d	3.8	4.0	4.2	mm	1
λ	0.760	0.955	1.15	W/mK	2
ρ c	1.85	2.10	2.35	10^6 J/m^{3}K	Calculated from 2
a_s	0.08	0.09	0.10	-	Base:4, ranges: 10
t_s	0.83	0.845	0.86	-	Calculated from 5
Wall component 2 (parapet)					
Layer 1 (rabat)					
d	18	20	22	mm	Relative variation as plywood in 6
λ	0.11	0.13	0.15	W/mK	6, 7
ρ c	0.5	1.0	1.4	10^6 J/m^{3}K	Calculated from 7
a_s	0.60	0.65	0.70	-	6
ε	0.82	0.88	0.94	-	5, 6
Layer 2 (insulation)					
d	10.5	12	13.5	mm	Relative variation as in 5
λ	0.024	0.040	0.056	W/mK	6, 7
ρ c	0.8	2.4	4.0	10^4 J/m^{3}K	Calculated from 6, 7

Layer 3 (underlayment)					
d	9	10	11	mm	Relative variation as plywood in 6
λ	0.21	0.23	0.25	W/mK	10
ρ c	1.0	1.3	1.6	10^6 J/m^{3}K	10
Layer 4 (insulation): See layer 2					
Layer 5 (plasterboard)					
d	14	15	16	mm	Absolute variation as in 5
λ	0.14	0.30	0.46	W/mK	4, 7
ρ c	0.70	1.05	1.40	10^6 J/m^{3}K	Calculated from 4, 7
Wall component 3 (separation wall left)					
Layer 1 (sand-lime brick)					
d	98	100	102	mm	Absolute variation as for brick (inner) in 5
λ	0.92	1.00	1.08	W/mK	Base: 4, relative variation as for brick (inner) in 2
ρ c	1.5	1.7	1.9	10^6 J/m^{3}K	Base: 4, relative variation calculated from 2
Wall component 4 (separation wall left): see wall component 3					
Wall component 5 (internal door)					
d	38	40	42	mm	10
λ	0.11	0.13	0.15	W/mK	Based on plywood data in 6, 7
ρ c	0.5	1.0	1.4	10^6 J/m^{3}K	Calculated from plywood data in 7
Wall component 6 (separation wall right): see wall component 3					
Wall component 7 (floor)					
Layer 1 (concrete slab)					
d	200	220	240	mm	Relative variation as in 5
λ	1.40	1.65	1.90	W/mK	4 (reinforced concrete)
ρ c	1.7	1.9	2.1	10^6 J/m^{3}K	Calculated from 2, 4
Layer 2 (carpet)					
d	3.0	4.5	6.0	mm	5
λ	0.045	0.075	0.100	W/mK	8
ρ c	1.8	3.3	4.8	10^5 J/m^{3}K	Calculated from 5
Wall component 8 (ceiling/roof)					
Layer 1 (roofing)					
d	3.6	4.0	4.4	mm	10
λ	0.18	0.20	0.22	W/mK	10
ρ c	1.6	1.8	2.0	10^6 J/m^{3}K	10
a_s	0.80	0.85	0.90	-	10
ε	0.82	0.88	0.94	-	5, 6

Layer 2 (insulation) : layer 2 in wall component 2					
Layer 3 (concrete slab): see layer 1 in wall component 7					
Layer 4 (air cavity)					
R_t	0.15	0.18	0.21	m^2K/W	8
Layer 5 (plasterboard)					
d	18	20	22	mm	10
λ	0.14	0.30	0.46	W/mK	4, 7
ρ c	0.70	1.05	1.40	$10^6 J/m^3K$	4, 7
Ground					
d	1.20	1.20	1.20	m	Fixed
λ	0.8	1.3	1.8	W/mK	range dry-wet in 4
ρ c	1.3	1.5	1.7	$10^6 J/m^3K$	9
Sunblinds					
a_s	0.45	0.5	0.55	-	Estimated from 3
t_s	0.16	0.18	0.20	-	Estimated from 3
ε	0.81	0.83	0.85	-	10
Windows					
$A_{eff, max}$	0.124	0.138	0.152	m^2	10
Vents					
A	0.17	0.18	0.19	m^2	10

Explanation references:
NEN 3265
Clarke et al. (1990)
ISSO (1975)
ISSO (1994)
Pinney et al. (1991)
Jensen (1994)
Lomas and Bowman (1988)
CIBSE (1986)
Polytechnic Almanac (1995)
Assumed

Explanation symbols:
λ conductivity
ρ density
c specific heat
d thickness
a_s solar absorption factor
t_s solar transmission factor
ε emittance (=absorptance, gray radiator)
R_t heat resistance
A opening area

Appendix C

C.1. Combination of expert assessments

Introduction

In an expert judgment study, quantile values are elicited from the experts for each variable. The aim is to obtain a single (marginal) probability distribution over each variable. This marginal probability distribution is referred to as the 'distribution for the decision-maker', or the 'DM'.

The calculation of the DM from the elicited quantile values takes two steps:

1. Construction of a probability distribution for each expert from his quantile values
2. Combination of the experts' distributions

For both steps Cooke (1991) proposes an approach, which is embedded in a solid mathematical framework. An outline is given in the following sections.

Construction of a distribution from quantile values

Introduction

The construction of a probability distribution from given quantile values involves two issues:

a) intrinsic ranges
b) minimally informative distributions

Intrinsic ranges

In this study experts assess 5%, 50% and 95% quantile values for each variable. Their 5% and 95% quantile assessments bound 90% of the probability mass. About the location or distribution of the probability mass below the 5% or above the 95% quantile point however, no information is provided by the experts.

To cope with this, we assume that all probability mass is distributed over a finite interval, the 'intrinsic range'. A common choice for this intrinsic range is the interval with 10% overshoot below and above the interval that is bounded by the smallest and the greatest of all the experts' quantile assessments for the variable at hand (Cooke, 1991). In this study we adhere to this practice if no other constraints on the intrinsic range are suggested or imposed by the context of the variable.

Minimally informative distributions

Defining an intrinsic range for a variable is equivalent with assigning values to the 0% and 100% quantiles. For all experts the same 0% and 100% quantile values are used. Hence, together with the elicited quantile values, a set of 5 quantile points is obtained for each variable and each expert. This set does not uniquely define a probability distribution: many distributions can be constructed, which satisfy these quantile values.

In this study we select from all these distributions that distribution, which has *minimum information* relative to the uniform distribution on the intrinsic range.
In practice this means that we distribute the probability mass uniformly between each pair of successive quantile points. An illustration is given in Figure C.1.

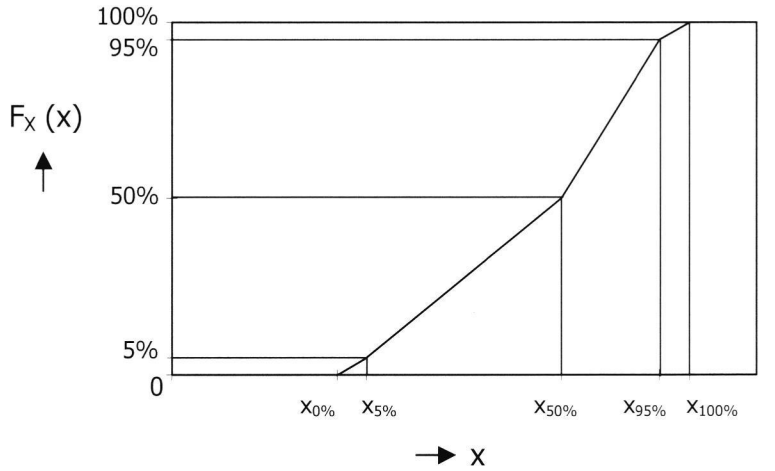

Figure C.1. An expert's cumulative probability distribution over variable X, corresponding to the given quantile values x_r *(r = 0%, 5%, 50%, 95% and 100%) and minimally informative relative to the uniform distribution on the intrinsic range* $[x_{0\%}, x_{100\%}]$.

It can be shown (Kullback, 1959) that this distribution minimizes:

$$I(f,u)=\int f(x)\frac{f(x)}{u(x)}dx \tag{C.1}$$

where f is the probability density function over the variable X, u is the uniform probability density function on the intrinsic range, and I is the relative information of f relative to u. Loosely stated, I expresses what we learn from f if we initially believe u.

Combination of the experts' distributions

Introduction

In this study, a single probability distribution for the decision-maker (DM) is calculated as a weighted average of the experts' distributions. In determining the weights, two methods can be distinguished. In the first strategy, each expert receives the same weight. The resulting *equal weight* DM is the arithmetic average of the experts' distributions.
The second method uses performance-based weights. An expert's performance is obtained from a comparison of his assessments and measured realizations on the *seed* variables. Seed variables are those variables for which a realization is available to the analyst but not to the experts, e.g. from unpublished measurements. This method is applied in this study.

The scoring of the experts to obtain their performances and the performance-based combination of their distributions are carried out according to the classical model, developed by Cooke (1991). An outline is given in the following sections.

Scoring experts

In the classical model, an expert's performance is calculated from a comparison of his assessments with measured realizations of the seed variables. Performance can be scored per variable (item), or globally. An expert's item performance w_i on variable i is the product of two measures, calibration C and information score I_i:

$$w_i = C_e I_i \tag{C.2}$$

Roughly, calibration measures 'agreement with observations', whereas the information score indicates how closely an expert's quantile assessments determine a variable.

Analogously, the global performance w of an expert is calculated from:

$$w = C I \tag{C.3}$$

where his global informativeness I is his average information score over all variables.

Calibration

For each variable, an expert assigns 3 quantile values, i.e. the 5%, 50% and 95% quantile values. These quantile values define 4 probability 'bins' (see Figure C.2).

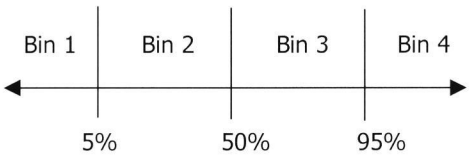

Figure C.2. Illustration of the 4 probability bins defined by the expert's quantile assessments. Note that no 'intrinsic range' is used in scoring the experts.

The probability mass function p over these bins is shown in Figure C.3. As an expert assesses the same quantiles for each variable, all variables are assigned the same distribution p over their associated bins.

When realizations become available, it is tallied in which bin they fall. In this way, a sample mass function s is constructed. An example is shown in Figure C.3. Obviously, the more the sample mass function s resembles the probability mass function p, the better the observed data support expert's assessments. As a measure of discrepancy between the mass functions p and s, the relative information $I(s, p)$ of s relative to p is used, which is defined analogously to (C.1). $I(s, p) = 0$ only if $s = p$ and higher values correspond to a greater discrepancy.

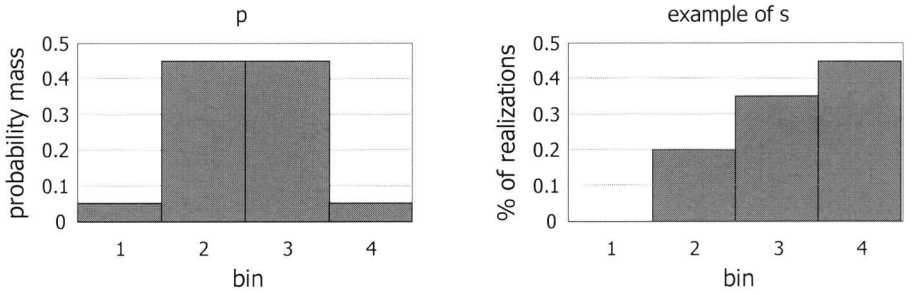

Figure C.3. Illustration of the probability mass function p over the 4 bins (left) and an example of a sample distribution for an expert (right). This expert is significantly overconfident (45% of the realizations fall outside bin 2+3, which constitute his 90%-confidence intervals) and has a tendency to underestimate (80% of the realizations end up above his median values (the boundary between bins 2 and 3).

In scoring calibration, an expert is now regarded as the hypothesis:

H: s results from independent sampling from p.

To test this hypothesis, the conditional probability is calculated that a sample mass function *s'* would be observed which differs more from *p* than the actually observed *s*, the difference between two mass functions being expressed in terms of relative information:

$$P\{I(s', p) \geq I(s, p) | H\} \tag{C.4}$$

This probability is the expert's calibration score. Clearly, the value of the calibration score is between 0 and 1 and higher scores are better.

To calculate this probability, the statistic $2NI(s', p)$ is used in stead of $I(s', p)$ as it can be shown that this quantity, which statisticians may recognize as a log likelihood ratio, becomes χ^2-distributed with 3 degrees of freedom (the number of bins − 1) for a large number of variables N. Hence the calibration score C equals:

$$C = 1 - \chi_3^2(2NI(s, p)) \tag{C.5}$$

where $2NI(s, p)$ can be calculated with a discrete version of (C.1):

$$2NI(s, p) = 2N \sum_{j=1}^{4} s_j \ln \frac{s_j}{p_j} \tag{C.6}$$

In practice, a minimum value of 1.10^{-4} is used for the calibration score. This prevents that a badly calibrated expert (with a score say 1.10^{-5}) would dominate an very badly calibrated expert with a score of e.g. 1.10^{-6}.

A calibration score is related to the *power* of the calibration test, i.e. the effective number of variables from which it is calculated (cf. classical hypothesis testing). If calibration scores from two experiments with a different number of seed variables are to be compared, it is important to reduce the power of the test with the highest number of variables to the same level as the power of the other test. This can be achieved by introducing an extra factor β in expression (C.5):

$$C = 1 - \chi^2_3(2\beta N_1 I(s, p)) \tag{C.7}$$

where the factor $\beta = N_2/N_1$ ($N_2 \leq N_1$), the ratio between the numbers of seed variables in the two experiments.

Information

The information score (or informativeness) is the degree to which an expert's probability distribution defines the value of a variable or item. It is scored per item i as the relative information of the probability mass function p to the uniform distribution on the intrinsic range:

$$I_i = \ln(x_{i,4} - x_{i,0}) + \sum_{j=1}^{4} p_j \ln \frac{p_j}{(x_{ij} - x_{ij-1})} \tag{C.8}$$

In this equation, x_{ij} , $j = 0,\ldots,4$ are the expert's 0%, 5%, 50%, 95% and 100% quantile assessments respectively on variable i. I_i expresses what we learn from the assessments of the expert if we initially believe that variable i is uniformly distributed on the intrinsic range $[x_{e,i,0}, x_{e,i,4}]$.
Information scores are always positive and all other thing being equal, higher scores are preferred.

Combination of the experts' distributions

The experts' distributions are combined to obtain, for each variable, a single (marginal) distribution. This distribution is referred to as the distribution for the decision maker, or simply DM.
Combination of the experts' distributions according to the classical model uses linear pooling, which means that the resulting distributions are weighted averages of the experts' distributions. This reduces the problem of combining expert judgments to the problem of determining the expert weights.

Two types of performance based weights can be used, *global* or *item* weights. When global weights are used, each expert is assigned a single weight, which is applied in the construction of the DM's marginal distributions for all variables. In case of combination on the basis of item weights, an expert receives a separate weight for each variable. Both techniques are briefly discussed here.

Global weights
For each expert e, the non-normalized global weight G_e is equal to his global performance score, modified by an indicator function:

$$G_e = C_e I_e 1_\alpha(C_e) \tag{C.9}$$

In this expression, C_e and I_e are the expert's calibration and information score respectively and the indicator function

$$1_\alpha(C_e) = \begin{cases} 1 & C_e \geq \alpha \\ 0 & \text{otherwise} \end{cases} \tag{C.10}$$

is used to express whether an expert (who is regarded as a statistical hypothesis) is rejected at the significance level α or not. In other words, if an expert's calibration score is below the significance level, to be set by the analyst, he receives a zero weight. The analyst can adjust the value of the significance level to optimize the performance of the DM.

In combining the experts' assessments, their weights must add up to 1, so the normalized weight g_e for each expert is given by:

$$g_e = \frac{G_e}{\sum_{e=1}^{E} G_e} \tag{C.11}$$

where E is the number of experts.

Item weights
Item weights are also calculated analogously to (C.9):

$$G_{i,e} = C_e I_{i,e} 1_\alpha(C_e) \tag{C.12}$$

where the weights are item-specific. For each variable, the weights have to sum to 1, so the normalized weights are calculated analogously to (C.11).

Although the performance score is composed of two elements, calibration and information, it is the calibration score, which predominantly differentiates between experts. Calibration is a fairly *fast* function, i.e. on the basis of say 10 realizations we can distinguish four or more orders of magnitude in calibration. Informativeness, on the other hand, is comparatively slow. A variation in information score of more than a factor 5 is rarely found. Therefore, the information score mainly serves to discriminate between experts, who are more or less equally well calibrated.
It can be shown (Cooke, 1991) that both the global and the item weights or scores are asymptotically strictly proper, which means that experts on the long run receive the highest weights if they state assessments according to their true beliefs.

C.2. Results expert elicitation

This appendix lists the experts' assessments. The full rationales of the experts can be found in Wit (1999).

Expert 1

Quantile assessments

orientation	variable	quantiles		
		5%	50%	95%
0°	ΔC_{p1}	0.24	0.44	0.64
	ΔC_{p2}	0.04	0.24	0.44
30°	ΔC_{p1}	0.13	0.53	0.93
	ΔC_{p2}	0.01	0.41	0.81
60°	ΔC_{p1}	0.04	0.44	0.84
	ΔC_{p2}	-0.07	0.33	0.73
90°	ΔC_{p1}	-0.30	0.10	0.50
	ΔC_{p2}	-0.30	0.10	0.50
120°	ΔC_{p1}	-1.21	-0.81	-0.41
	ΔC_{p2}	-1.32	-0.92	-0.52
150°	ΔC_{p1}	-1.58	-1.18	-0.78
	ΔC_{p2}	-1.74	-1.34	-0.94
180°	ΔC_{p1}	-1.48	-1.28	-1.08
	ΔC_{p2}	-1.66	-1.46	-1.26
210°	ΔC_{p1}	-1.48	-1.18	-0.88
	ΔC_{p2}	-1.64	-1.34	-1.04
240°	ΔC_{p1}	-1.11	-0.81	-0.51
	ΔC_{p2}	-1.22	-0.92	-0.62
270°	ΔC_{p1}	-0.20	0.10	0.40
	ΔC_{p2}	-0.20	0.10	0.40
300°	ΔC_{p1}	0.07	0.37	0.67
	ΔC_{p2}	-0.10	0.20	0.50
330°	ΔC_{p1}	0.0	0.40	0.80
	ΔC_{p2}	-0.18	0.22	0.62

Dependency assessments (conditional probabilities)

Arc	Dependency	Arc	Dependency
1	0.25	7	0.95
2	0.60	8	0.95
3	0.85	9	0.50
4	0.85	10	0.25
5	0.85	11	0.30
6	0.85		

Expert 2

Quantile assessments

orientation	variable	quantiles		
		5%	50%	95%
0°	ΔC_{p1}	0.40	1.00	1.20
	ΔC_{p2}	0.40	1.00	1.30
30°	ΔC_{p1}	0.30	1.00	1.40
	ΔC_{p2}	0.30	1.00	1.30
60°	ΔC_{p1}	0.10	0.70	0.80
	ΔC_{p2}	0.20	0.30	0.50
90°	ΔC_{p1}	-0.60	0.00	0.60
	ΔC_{p2}	-0.30	0.00	0.30
120°	ΔC_{p1}	-0.80	-0.40	-0.20
	ΔC_{p2}	-0.70	-0.40	-0.30
150°	ΔC_{p1}	-1.35	-1.10	-0.30
	ΔC_{p2}	-1.45	-1.20	-0.50
180°	ΔC_{p1}	-1.35	-1.10	-0.75
	ΔC_{p2}	-1.45	-1.20	-0.85
210°	ΔC_{p1}	-1.20	-0.90	-0.55
	ΔC_{p2}	-1.20	-0.90	-0.60
240°	ΔC_{p1}	-1.00	-0.60	-0.20
	ΔC_{p2}	-0.90	-0.60	-0.30
270°	ΔC_{p1}	-0.60	0.00	0.60
	ΔC_{p2}	-0.40	0.00	0.40
300°	ΔC_{p1}	0.10	0.40	1.10
	ΔC_{p2}	0.05	0.30	1.00
330°	ΔC_{p1}	0.20	0.60	1.40
	ΔC_{p2}	0.10	0.60	1.10

Dependency assessments (conditional probabilities)

Arc	Dependency	Arc	Dependency
1	0.10	7	0.95
2	0.80	8	0.95
3	0.75	9	0.55
4	0.65	10	0.20
5	0.75	11	0.20
6	0.75		

Expert 3

Quantile assessments

orientation	variable	quantiles		
		5%	50%	95%
0°	ΔC_{p1}	0.4	1.0	1.4
	ΔC_{p2}	0.0	0.9	1.4
30°	ΔC_{p1}	0.4	1.0	1.4
	ΔC_{p2}	0.0	0.9	1.4
60°	ΔC_{p1}	0.3	0.7	1.1
	ΔC_{p2}	0.0	0.5	1.0
90°	ΔC_{p1}	-0.3	0.0	0.3
	ΔC_{p2}	-0.3	0.0	0.3
120°	ΔC_{p1}	-1.3	-0.9	-0.5
	ΔC_{p2}	-1.3	-0.9	-0.5
150°	ΔC_{p1}	-1.5	-1.2	-0.8
	ΔC_{p2}	-1.3	-1.0	-0.7
180°	ΔC_{p1}	-1.5	-1.2	-0.8
	ΔC_{p2}	-1.3	-1.0	-0.7
210°	ΔC_{p1}	-1.5	-1.2	-0.8
	ΔC_{p2}	-1.3	-1.0	-0.7
240°	ΔC_{p1}	-1.3	-0.9	-0.5
	ΔC_{p2}	-1.3	-0.9	-0.5
270°	ΔC_{p1}	-0.3	0.0	0.3
	ΔC_{p2}	-0.3	0.0	0.3
300°	ΔC_{p1}	0.3	0.7	1.1
	ΔC_{p2}	0.0	0.5	1.0
330°	ΔC_{p1}	0.4	1.0	1.4
	ΔC_{p2}	0.0	0.9	1.4

Dependency assessments (conditional probabilities)

Arc	Dependency	Arc	Dependency
1	0.5	7	0.9
2	0.8	8	0.9
3	0.75	9	0.6
4	0.8	10	0.5
5	0.75	11	0.5
6	0.75		

Expert 4

Quantile assessments

orientation	variable	quantiles		
		5%	50%	95%
0°	ΔC_{p1}	0.3	0.7	1.3
	ΔC_{p2}	0.3	0.6	0.9
30°	ΔC_{p1}	0.3	0.8	1.4
	ΔC_{p2}	0.3	0.8	1.4
60°	ΔC_{p1}	-0.5	0.5	1.2
	ΔC_{p2}	-0.5	0.5	1.2
90°	ΔC_{p1}	-0.6	0.1	0.7
	ΔC_{p2}	-0.6	0.1	0.7
120°	ΔC_{p1}	-1.2	-0.5	0.3
	ΔC_{p2}	-1.2	-0.5	0.3
150°	ΔC_{p1}	-1.5	-1.1	-0.6
	ΔC_{p2}	-1.7	-1.2	-0.6
180°	ΔC_{p1}	-1.5	-1.1	-0.6
	ΔC_{p2}	-1.7	-1.2	-0.6
210°	ΔC_{p1}	-1.5	-1.1	-0.6
	ΔC_{p2}	-1.7	-1.2	-0.6
240°	ΔC_{p1}	-1.2	-0.5	0.3
	ΔC_{p2}	-1.2	-0.5	0.3
270°	ΔC_{p1}	-0.6	0.1	0.7
	ΔC_{p2}	-0.6	0.1	0.7
300°	ΔC_{p1}	-0.5	0.5	1.2
	ΔC_{p2}	-0.5	0.5	1.2
330°	ΔC_{p1}	0.3	0.8	1.4
	ΔC_{p2}	0.3	0.8	1.4

Dependency assessments (conditional probabilities)

Arc	Dependency	Arc	Dependency
1	0.4	7	0.8
2	0.7	8	0.7
3	0.9	9	0.6
4	0.9	10	0.4
5	0.9	11	0.4
6	0.9		

Expert 5

Quantile assessments

orientation	variable	quantiles		
		5%	50%	95%
0°	ΔC_{p1}	0.55	0.80	1.05
	ΔC_{p2}	0.40	0.70	1.00
30°	ΔC_{p1}	0.55	0.75	0.95
	ΔC_{p2}	0.35	0.65	0.85
60°	ΔC_{p1}	0.35	0.60	0.85
	ΔC_{p2}	0.25	0.55	0.85
90°	ΔC_{p1}	-0.15	0.05	0.25
	ΔC_{p2}	-0.15	0.05	0.25
120°	ΔC_{p1}	-1.20	-0.85	-0.50
	ΔC_{p2}	-1.20	-0.85	-0.50
150°	ΔC_{p1}	-1.50	-1.10	-0.70
	ΔC_{p2}	-1.55	-1.15	-0.75
180°	ΔC_{p1}	-1.35	-1.10	-0.85
	ΔC_{p2}	-1.45	-1.20	-0.95
210°	ΔC_{p1}	-1.45	-1.10	-0.75
	ΔC_{p2}	-1.50	-1.15	-0.80
240°	ΔC_{p1}	-1.15	-0.85	-0.55
	ΔC_{p2}	-1.15	-0.85	-0.55
270°	ΔC_{p1}	-0.10	0.05	0.20
	ΔC_{p2}	-0.10	0.05	0.20
300°	ΔC_{p1}	0.35	0.60	0.85
	ΔC_{p2}	0.20	0.50	0.80
330°	ΔC_{p1}	0.45	0.65	0.85
	ΔC_{p2}	0.30	0.55	0.80

Dependency assessments (conditional probabilities)

Arc	Dependency	Arc	Dependency
1	0.20	7	0.60
2	0.80	8	0.70
3	0.80	9	0.55
4	0.80	10	0.30
5	0.90	11	0.40
6	0.95		

Expert 6

Quantile assessments

orientation	variable	quantiles		
		5%	50%	95%
0°	ΔC_{p1}	0.69	1.59	2.49
	ΔC_{p2}	0.69	1.59	2.49
30°	ΔC_{p1}	-0.41	0.49	1.39
	ΔC_{p2}	-0.41	0.49	1.39
60°	ΔC_{p1}	0.02	0.37	0.72
	ΔC_{p2}	0.02	0.37	0.72
90°	ΔC_{p1}	-0.30	0.0	0.30
	ΔC_{p2}	-0.30	0.0	0.30
120°	ΔC_{p1}	-0.67	-0.47	-0.27
	ΔC_{p2}	-0.67	-0.47	-0.27
150°	ΔC_{p1}	-1.09	-0.94	-0.79
	ΔC_{p2}	-1.09	-0.94	-0.79
180°	ΔC_{p1}	-1.30	-1.15	-1.00
	ΔC_{p2}	-1.30	-1.15	-1.00
210°	ΔC_{p1}	-1.09	-0.94	-0.79
	ΔC_{p2}	-1.09	-0.94	-0.79
240°	ΔC_{p1}	-0.67	-0.47	-0.27
	ΔC_{p2}	-0.67	-0.47	-0.27
270°	ΔC_{p1}	-0.31	-0.01	0.29
	ΔC_{p2}	-0.31	-0.01	0.29
300°	ΔC_{p1}	0.12	0.42	0.72
	ΔC_{p2}	0.12	0.42	0.72
330°	ΔC_{p1}	0.11	0.46	0.81
	ΔC_{p2}	0.11	0.46	0.81

Dependency assessments (conditional probabilities)

Arc	Dependency	Arc	Dependency
1	0.40	7	1.00
2	0.50	8	0.60
3	0.90	9	0.60
4	0.90	10	0.25
5	1.00	11	0.40
6	1.00		

Global weight DM

Quantile assessments

orientation	variable	quantiles		
		5%	50%	95%
0°	ΔC_{p1}	0.40	1.00	1.20
	ΔC_{p2}	0.40	1.00	1.30
30°	ΔC_{p1}	0.30	1.00	1.40
	ΔC_{p2}	0.30	1.00	1.30
60°	ΔC_{p1}	0.10	0.70	0.80
	ΔC_{p2}	0.20	0.30	0.50
90°	ΔC_{p1}	-0.60	0.00	0.60
	ΔC_{p2}	-0.30	0.00	0.30
120°	ΔC_{p1}	-0.80	-0.40	-0.20
	ΔC_{p2}	-0.70	-0.40	-0.30
150°	ΔC_{p1}	-1.35	-1.10	-0.30
	ΔC_{p2}	-1.45	-1.20	-0.50
180°	ΔC_{p1}	-1.35	-1.10	-0.75
	ΔC_{p2}	-1.45	-1.20	-0.85
210°	ΔC_{p1}	-1.20	-0.90	-0.55
	ΔC_{p2}	-1.20	-0.90	-0.60
240°	ΔC_{p1}	-1.00	-0.60	-0.20
	ΔC_{p2}	-0.90	-0.60	-0.30
270°	ΔC_{p1}	-0.60	0.00	0.60
	ΔC_{p2}	-0.40	0.00	0.40
300°	ΔC_{p1}	0.10	0.40	1.10
	ΔC_{p2}	0.05	0.30	1.00
330°	ΔC_{p1}	0.20	0.60	1.40
	ΔC_{p2}	0.10	0.60	1.10

Dependency assessments (conditional probabilities)

Arc	Dependency	Arc	Dependency
1	0.10	7	0.95
2	0.80	8	0.95
3	0.75	9	0.55
4	0.65	10	0.20
5	0.75	11	0.20
6	0.75		

C.3. Wind tunnel results

This section presents the results of the wind tunnel tests in more detail than in Chapter 4. For more information on the set-up of the experiments see Wit (1999) or Willemsen (1998) for the test in the DNW-LST or Soerensen (1998) for the experiment in UWO-BLWT1.

Low speed German-Dutch wind tunnel (DNW-LST)

Figure C.4 shows the pressure coefficients, measured at the taps 1a, 1b, 2a and 2b and the corresponding pressure difference coefficients as a function of the wind angle.

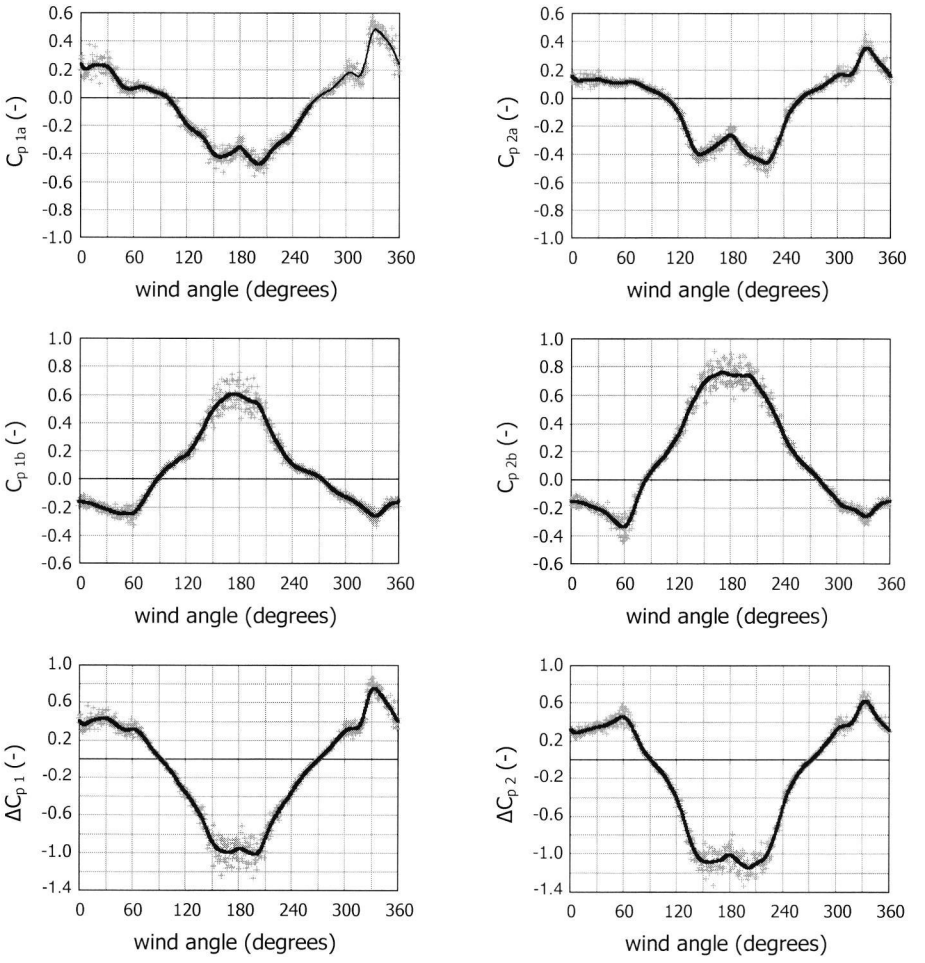

Figure C.4. Results of the pressure measurements in the DNW-LST. The drawn lines show moving averages, obtained by convolution of the measured signals with a gaussian profile with a standard deviation of 4° (corresponding to 4 seconds at the angular velocity of the turntable of 1°/s). The realizations, used to score the experts, were taken from these moving average curves.

For pressure data from the other taps see Willemsen (1998).

Boundary layer wind tunnel UWO-BLWT1

Figure C.5 shows the pressure coefficients, measured at the taps 1a, 1b, 2a and 2b and the corresponding pressure difference coefficients as a function of the wind angle. For comparison, the moving average curves of the DNW-results are also shown.

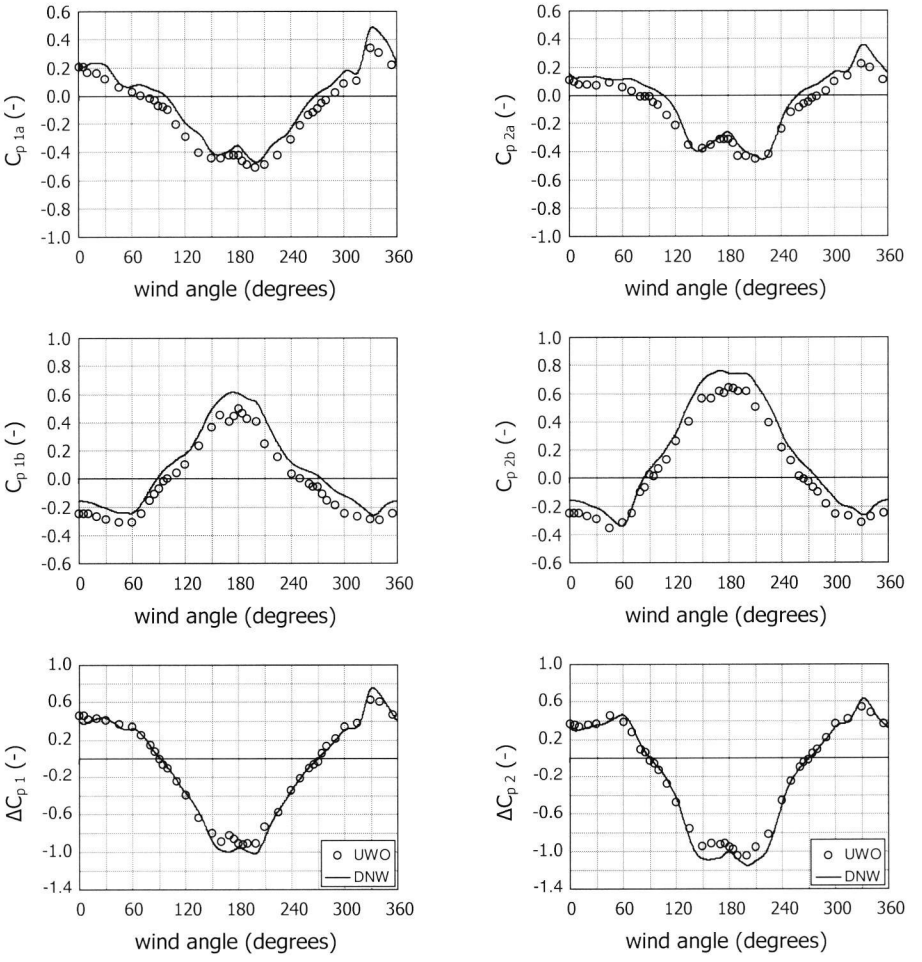

Figure C.5. Wind tunnel results from both DNW-LST and UWO-BLWT1 tunnels. The symbols are the 30s averages, measured in the UWO tunnel. The drawn lines show moving averages of the DNW-result (see Figure C.4).

For pressure data from the other taps see Soerensen (1998).

Discussion and conclusion

The pressure coefficients measured at UWO seem negatively biased compared to the DNW-values for all 4 taps under study, whereas the pressure difference coefficients agree fairly well. This suggests that there may be a bias in the static pressure measurements between both experiments. This is supported by the observation that in the DNW experiment the pitot-static tube was used to measure the background pressure, whereas the UWO-experiment obtained this pressure from a floor tap.

The main deviations in the wind pressure difference coefficients between the tests occur for the 'isolated' wind angles. At these angles the pressure differences are most sensitive to the characteristics of the simulated boundary layer.

The following realizations were extracted from the data as reference material for the expert judgment study.

Realizations used in the expert judgment experiment.

Wind angle	DNW-LST		UWO-BLWT1	
(degrees)	ΔC_{p1}	ΔC_{p2}	ΔC_{p1}	ΔC_{p2}
0	0.39	0.31	0.46	0.36
30	0.44	0.35	0.41	0.36
60	0.32	0.47	0.34	0.38
90	0.03	0.01	0.00	-0.03
120	-0.36	-0.40	-0.39	-0.47
150	-0.88	-1.07	-0.80	-0.94
180	-0.95	-0.99	-0.91	-0.95
210	-0.87	-1.10	-0.73	-0.95
240	-0.35	-0.49	-0.34	-0.45
270	-0.01	-0.02	-0.03	-0.02
300	0.30	0.31	0.34	0.36
330	0.77	0.64	0.63	0.54

Appendix D

D.1. Air temperature profile in natural convection regime

In the literature, data on the effect of convective heat sources on the temperature profile are mainly available from studies on two types of configurations:

- Spaces with displacement ventilation
- Radiator heated spaces

Displacement ventilation

Linden, Lane-Serff, Smeed (1990), quoted in Cooper and Linden (1996), performed a theoretical study on a displacement ventilation system, driven by one single point source of heat. They show that the vertical temperature difference ΔT between the upper and lower regions of the space depends on the convective internal heat gain, i.e. the convective heat flow from the heat source Q as:

$$\Delta T \sim Q^{2/3} \tag{D.1}$$

Cooper, Linden (1996) and Linden, Cooper (1996) generalize this result for multiple point sources (non-interfering plumes). In that case Q in (D.1) represents the sum of the convective heat flows from the sources.

In another study (Chen, 1992), the temperature field, the velocity field and the contaminant concentration distribution are studied numerically as a function of various parameters. One element in the study concerns the vertical temperature profile as a function of the total convective heat gain, while all other parameters are kept at a fixed value.

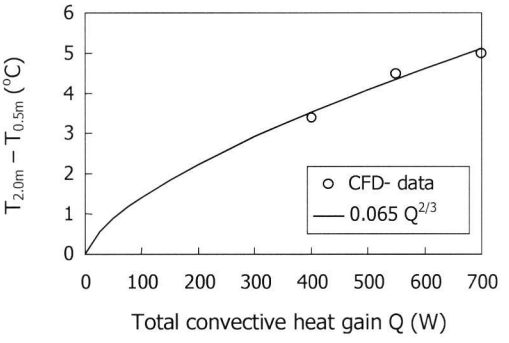

Figure D.1. The air temperature difference between 2.0 m and 0.5 m above the floor as a function of the total heat gain from both internal heat sources and (solar) heat gain from the window as reported in the Chen (1992). The circles show the Computational Fluid Dynamics results. The drawn line is the best fit of (D.1) to the data.

Figure D.1 shows the temperature difference between 2.0 m and 0.5 m above the floor as a function of the total convective heat gain in the space. With (D.1) a close fit through the data points can be obtained as shown by the drawn line. This suggests that (D.1) might also be applied in situations with heat sources of finite dimensions.

Radiator heated spaces

Maalej (1994) presents a comprehensive experimental study of vertical air temperature differences in spaces heated with radiators. He varies the location of the radiator in reference to the (cold) window, the type of radiator and most importantly for this study, the convective heat flow from the radiator. He concludes that for a given configuration (type and location of the radiator) a the vertical temperature difference ΔT between 2.4m and 0.1m above the floor can be well modeled by a power law function of the convective heat load Q from the radiator[40]:

$$\Delta T = a\,Q^{c} \tag{D.2}$$

where a and b are empirical constants, which depend on the configuration.

The results of these studies suggest that the effect of convective heat sources on the air temperature difference between two vertically separated locations in a space can be modeled by a power law in Q, where Q denotes the total convective heat gain. In each of the studies the form of the vertical temperature profile does not significantly depend on Q, which implies that:

- the vertical temperature difference between any two points with arbitrary but fixed height within the space will closely follow a power law in Q
- z_{mean}, the level above the floor at which the temperature is equal to the mean air temperature, will be fairly independent of Q

Hence, in the one-dimensional approach of the temperature profile, the power law model can be applied to $\Delta T_{out} = T(z_{out}) - T(z_{mean})$ and $\Delta T_{out} \approx T(\bar{z}_{occ}) - T(z_{mean})$, where $\bar{z}_{occ}$ = 0.7 m, half the height of a sitting person.

D.2. Case structure

The values and ranges of the case-structure variables are discussed per variable.

Air flow rate Φ_V

The ventilation flow through the spaces are mainly driven by wind-induced pressure differences between windward and leeward facades. Under suitable assumptions for wind reduction factor and wind pressure coefficients, the 90% quantile value for the pressure difference between two opposite facades was estimated at 8 Pa in the reference year 1964. This pressure difference induces a volume flow rate of approximately 2.1 10^{-1} m^3/s, if the flow crosses two identical spaces with specification as in given in Appendix A, one at the windward façade and one at the leeward façade with an

[40] A similar result was found for the difference between air temperatures at 1.8m and 0.1m.

corridor in-between. This value was adopted as the maximum value considered for Φ_V in this study.
Two other values were used for Φ_V, i.e. 2.8 10^{-2} and 7.0 10^{-2} m^3/s, corresponding to air change rates of 2 and 5 hr^{-1} respectively. These are commonly used values in building simulations (ISSO, 1994).

Internal heat gain Q_{srce}

NOVEM (1992) reports on a study, which investigates the influence of various design parameters on summer comfort conditions in office buildings in The Netherlands. One of these parameters is the internal heat gain. The report indicates that it is quite a challenge to maintain comfortable conditions in a naturally ventilated space with an internal heat gain of 30 W/m^2. This corresponds to a gain of approximately 600 W in the case at hand, which is chosen as the maximum value considered for the internal heat gain in this study. It is assumed that all heat is emitted convectively.
The minimum value of the internal heat gain is set to 0, representing the situation that the space is unoccupied.

Solar heat gain Q_{sol} and convective fraction $Q_{sol,c}$

With a maximum total solar gain of 900 W/m^2 on the façade (Van der Linden, 1996), the solar gain entering the space through an external solar shading is 500 W or less. This value is adopted as the maximum value of the solar gain Q_{sol}. The minimum value is set to 0 for obvious reasons.
The fraction $Q_{sol,c}$, which is absorbed by the furniture and convectively emitted to the air, is set to the 10% of Q_{sol} in all cases. This is a commonly used value in building simulations (ISSO, 1994).

The temperature of the incoming air, T_{in}

This variable is a balancing item in the case structure design. In the model, T_{in} only occurs in the temperature differences T_{in}-T_{air} or T_{in}-T_{out}. From a range of simulations of the temperature in the space for different scenarios, it appears that in about 90% of the cases, T_{in}-T_{air} falls in the range [-7 °C, +4°C]. These simulations were performed with the default assumptions of uniform air temperature, a convective heat transfer coefficient of 3 W/m^2 °C and for a range of possible internal heat gains.
Hence it was decided to assign values to T_{in}, which yield values of T_{in}-T_{air} in this interval under the same default assumptions in each of the cases.
Due to the structure of the models for ΔT_{out} and ΔT_{occ}, equally many cases were selected with T_{in}-$T_{air} \geq 0$ as with T_{in}-$T_{air} < 0$.

Mean surface temperature of the enclosure T_{wall}

The physical processes determining the airflow are highly insensitive to the absolute temperature level in the space. Therefore T_{wall} was set at a fixed value of 23°C in all cases.

D.3. Results expert elicitation

Expert 1

Quantile assessments on seed variables

	$T_{2.4\,m}$-$T_{0.1\,m}$(°C)			$T_{1.5\,m}$ (°C)		
Case	5%	50%	95%	5%	50%	95%
A	-1.0	0.4	2.0	17.0	19.6	23.0
B	-1.0	0.8	3.0	18.0	19.6	22.0
C	-2.0	0.8	4.0	17.0	19.7	23.0
D	-2.0	0.4	4.0	17.0	19.9	23.0
E	2.0	5.1	9.0	18.0	20.8	24.0

Quantile assessments on elicitation variables

	T_{out}-T_{air} (°C)			T_{air} (°C)			T_{occ}-T_{air} (°C)		
Case	5%	50%	95%	5%	50%	95%	5%	50%	95%
1	-1.0	0.0	1.0	21.0	23.0	25.0	-1.0	0.0	1.0
2	0.0	1.6	4.0	23.0	24.6	26.0	-2.0	0.0	2.0
3	-1.0	0.2	1.0	21.0	23.1	25.0	-1.0	0.0	1.0
4	-1.0	1.5	4.0	18.0	20.0	22.0	-3.0	0.0	2.0
5	0.0	2.5	5.0	23.0	25.3	28.0	-2.0	0.0	2.0
6	0.0	1.7	3.0	22.0	23.4	25.0	-2.0	0.0	2.0
7	-0.3	0.2	0.7	20.0	21.5	23.0	-1.0	0.0	1.0
8	-1.0	0.2	1.0	25.0	26.4	28.0	-1.0	0.0	1.0
9	-1.0	0.4	3.0	15.0	19.3	21.0	-2.0	0.0	2.0

Dependency assessments on elicitation variables

	Variable 1	Variable 2	Variable 1	Variable 2
Case	T_{air}	T_{out}-T_{air}	T_{occ}-T_{air}	T_{out}-T_{air}
1	0.5		0.75	
2	0.3		0.75	
3	0.3		0.75	
4	0.4		0.65	
5	0.35		0.6	
6	0.35		0.55	
7	0.45		0.55	
8	0.45		0.60	
9	0.45		0.55	

Expert 2

Quantile assessments on seed variables

	$T_{2.4\,m}$-$T_{0.1\,m}$(°C)			$T_{1.5\,m}$ (°C)		
Case	5%	50%	95%	5%	50%	95%
A	0.7	1.3	2.0	19.5	20.5	21.5
B	1.3	2.6	4.0	20.6	21.0	23.5
C	1.0	2.0	3.0	20.4	21.4	23.2
D	0.0	0.5	1.5	18.9	19.9	20.9
E	2.0	3.6	5.0	19.0	20.0	21.0

Quantile assessments on elicitation variables

	T_{out}-T_{air} (°C)			T_{air} (°C)			T_{occ}-T_{air} (°C)		
Case	5%	50%	95%	5%	50%	95%	5%	50%	95%
1	0.0	0.5	1.0	22.0	23.0	24.0	-0.5	-0.3	0.0
2	0.9	1.6	2.9	24.1	25.5	27.5	-1.5	-0.8	-0.4
3	0.2	0.4	1.2	22.2	23.2	24.2	-0.6	-0.2	-0.1
4	0.2	0.7	2.1	19.1	21.2	22.4	-1.0	-0.4	-0.1
5	1.2	2.1	3.6	24.3	26.2	28.1	-1.8	-1.0	-0.6
6	0.2	0.6	2.0	23.1	24.1	25.1	-1.0	-0.3	-0.1
7	0.1	0.4	1.1	20.0	21.6	22.6	-0.6	-0.2	-0.1
8	0.5	0.9	1.7	23.9	25.7	27.0	-0.9	-0.4	-0.3
9	0.1	0.3	0.9	16.8	19.6	22.0	-0.5	-0.2	-0.1

Dependency assessments on elicitation variables

Case	Variable 1 T_{air}	Variable 2 T_{out}-T_{air}	Variable 1 T_{occ}-T_{air}	Variable 2 T_{out}-T_{air}
1	0.6		0.25	
2	0.6		0.25	
3	0.6		0.25	
4	0.6		0.25	
5	0.6		0.25	
6	0.6		0.25	
7	0.6		0.25	
8	0.6		0.25	
9	0.6		0.25	

Expert 3

Quantile assessments on seed variables

	$T_{2.4\ m}$-$T_{0.1\ m}$(°C)			$T_{1.5\ m}$ (°C)		
Case	5%	50%	95%	5%	50%	95%
A	0.20	1.10	2.00	20.60	21.00	21.50
B	0.60	2.30	4.00	21.40	22.50	23.70
C	0.50	1.50	2.60	21.20	22.40	23.50
D	0.10	0.70	1.25	20.00	20.50	21.00
E	5.60	9.80	14.00	23.40	23.90	24.40

Quantile assessments on elicitation variables

	T_{out}-T_{air} (°C)			T_{air} (°C)			T_{occ}-T_{air} (°C)		
Case	5%	50%	95%	5%	50%	95%	5%	50%	95%
1	0.10	0.60	1.25	22.00	23.00	24.00	-0.60	-0.30	-0.05
2	0.05	0.53	1.00	24.00	25.25	26.50	-1.50	-0.90	-0.30
3	0.10	0.60	1.25	22.50	23.50	24.50	-0.60	-0.30	-0.05
4	0.10	0.60	1.25	21.00	22.00	23.00	-1.90	-1.20	-0.50
5	0.10	1.00	1.90	24.50	26.30	28.10	-1.50	-0.80	-0.10
6	0.10	0.60	1.25	23.10	24.10	25.10	-1.00	-0.75	-0.50
7	0.10	0.60	1.25	20.75	21.75	22.75	-1.40	-0.80	-0.30
8	0.10	0.60	1.25	24.90	26.30	27.60	-0.60	-0.30	-0.05
9	0.10	0.60	1.25	18.00	19.35	20.70	-0.60	-0.30	-0.05

Dependency assessments on elicitation variables

	Variable 1	Variable 2	Variable 1	Variable 2
Case	T_{air}	T_{out}-T_{air}	T_{occ}-T_{air}	T_{out}-T_{air}
1	0.5		0.5	
2	0.25		0.25	
3	0.25		0.25	
4	0.4		0.4	
5	0.3		0.3	
6	0.4		0.4	
7	0.4		0.4	
8	0.25		0.25	
9	0.25		0.25	

Expert 4

Quantile assessments on seed variables

	$T_{2.4\ m}$-$T_{0.1\ m}$(°C)			$T_{1.5\ m}$ (°C)		
Case	5%	50%	95%	5%	50%	95%
A	1.50	2.00	2.50	20.30	20.80	21.60
B	3.00	4.00	5.00	20.20	21.00	22.40
C	1.80	3.00	4.20	18.90	20.00	21.00
D	1.50	2.00	2.50	14.70	17.30	19.20
E	4.00	5.50	7.00	17.50	19.80	21.40

Quantile assessments on elicitation variables

	T_{out}-T_{air} (°C)			T_{air} (°C)			T_{occ}-T_{air} (°C)		
Case	5%	50%	95%	5%	50%	95%	5%	50%	95%
1	-0.70	0.00	0.47	22.20	23.00	23.60	-0.22	0.00	0.30
2	-2.11	-0.27	0.95	24.20	25.90	28.10	-0.56	0.05	1.01
3	-1.22	-0.07	0.48	22.10	23.30	24.10	-0.30	0.01	0.54
4	0.00	1.96	5.91	18.20	20.40	22.10	-2.71	-0.20	1.51
5	-4.91	-1.33	0.07	25.10	27.20	29.70	-1.27	0.14	2.16
6	-0.19	1.28	3.66	22.60	24.10	26.10	-1.93	-0.18	1.03
7	0.00	1.17	3.34	19.10	20.50	21.90	-1.63	-0.12	0.97
8	-1.76	-0.38	0.10	25.50	27.00	28.30	-0.54	0.04	0.88
9	0.00	1.29	4.16	16.20	18.10	20.20	-1.98	-0.13	1.18

Dependency assessments on elicitation variables

	Variable 1	Variable 2	Variable 1	Variable 2
Case	T_{air}	T_{out}-T_{air}	T_{occ}-T_{air}	T_{out}-T_{air}
1	0.8		0.3	
2	0.8		0.3	
3	0.8		0.3	
4	0.4		0.3	
5	0.5		0.3	
6	0.4		0.3	
7	0.2		0.3	
8	0.6		0.3	
9	0.4		0.3	

Item weight DM

Quantile assessments on seed variables

	$T_{2.4\,m}$-$T_{0.1\,m}$(°C)			$T_{1.5\,m}$ (°C)		
Case	5%	50%	95%	5%	50%	95%
A	-0.39	1.26	2.00	18.92	20.49	21.70
B	-0.71	2.21	3.97	18.40	20.93	23.45
C	-0.27	1.98	3.27	18.57	21.36	23.20
D	-0.44	0.50	1.96	17.47	19.90	22.21
E	2.00	3.80	8.55	18.61	20.02	22.52

Quantile assessments on elicitation variables

	T_{out}-T_{air} (°C)			T_{air} (°C)			T_{occ}-T_{air} (°C)		
Case	5%	50%	95%	5%	50%	95%	5%	50%	95%
1	-0.58	0.47	1.00	21.83	23.00	24.17	-0.54	-0.30	0.14
2	0.11	1.60	3.65	23.09	25.00	27.35	-1.53	-0.80	-0.01
3	-0.60	0.39	1.19	21.97	23.20	24.33	-0.63	-0.20	0.04
4	-0.48	0.78	3.54	18.26	20.81	22.38	-1.30	-0.40	0.35
5	0.10	2.18	4.70	23.27	25.97	28.10	-1.82	-0.99	0.21
6	0.10	0.77	2.76	22.22	23.96	25.10	-1.07	-0.30	0.15
7	-0.27	0.33	1.09	20.00	21.56	22.89	-0.83	-0.20	0.56
8	-0.83	0.78	1.68	24.02	26.02	27.90	-0.90	-0.40	-0.10
9	-0.53	0.31	2.21	15.33	19.43	21.88	-0.60	-0.20	0.08

Realizations on seed variables

Realizations on the seed variables were obtained from measurements by François et al. (1993). The values are listed below.

Case	$T_{2.4\,m}$ –$T_{0.1\,m}$ (°C)	$T_{1.5\,m}$ (°C)
A	0.9	20.5
B	3.0	20.9
C	4.5	20.9
D	0.8	19.8
E	5.7	20.5

D.4. Marginal distributions target variables

quantile	a_0	a_1	a_2	a_3	a_4	α_c	b_0	b_1	b_2	b_3	b_4
	$x10^0$ °C	$x\ 10^{-3}$ °C/W	$x\ 10^{-3}$ °C/W	$x10^2$ s^2/m^6	$x\ 10^{-3}$ °C/W	$x10^0$ W/m^2K	$x10^0$ °C	$x\ 10^{-3}$ °C/W	$x\ 10^{-3}$ °C/W	$x10^2$ s^2/m^6	$x\ 10^{-3}$ °C/W
0.0025	-3.75	-13.8	-94.8	1.01	-26.4	0.31	-1.13	-5.13	-20.05	1.01	-9.00
0.01	-2.59	-9.81	-50.2	1.03	-21.8	0.49	-1.03	-4.44	-14.51	1.03	-8.50
0.02	-1.80	-9.62	-37.5	1.03	-18.3	0.49	-0.80	-3.96	-12.78	1.06	-4.39
0.03	-1.39	-6.99	-23.4	1.04	-17.9	0.66	-0.76	-3.59	-11.61	1.08	-4.03
0.04	-0.77	-6.35	-5.93	1.05	-17.3	0.79	-0.68	-3.16	-10.60	1.11	-3.62
0.05	-0.53	-5.64	-4.65	1.06	-16.4	1.12	-0.66	-2.95	-10.54	1.13	-3.21
0.06	-0.52	-5.57	-4.65	1.09	-14.9	1.31	-0.63	-2.62	-10.18	1.15	-2.98
0.07	-0.47	-4.96	-3.56	1.11	-13.8	1.47	-0.61	-2.36	-10.18	1.17	-2.67
0.08	-0.46	-4.27	-3.18	1.13	-13.4	1.51	-0.61	-2.30	-9.75	1.19	-2.38
0.09	-0.44	-3.51	-3.18	1.14	-13.0	1.67	-0.59	-2.19	-9.29	1.21	-2.14
0.10	-0.41	-3.06	-3.18	1.16	-12.3	1.84	-0.57	-2.11	-9.01	1.22	-1.94
0.11	-0.41	-2.74	-3.04	1.18	-11.6	1.97	-0.57	-1.94	-8.93	1.23	-1.74
0.12	-0.41	-2.74	-2.68	1.19	-11.0	2.07	-0.57	-1.83	-8.79	1.25	-1.41
0.13	-0.37	-2.52	-2.39	1.20	-10.6	2.16	-0.56	-1.76	-8.37	1.26	-1.18
0.14	-0.32	-1.89	-1.59	1.24	-10.4	2.27	-0.54	-1.63	-8.20	1.29	-1.06
0.15	-0.30	-1.43	-1.23	1.24	-10.1	2.36	-0.53	-1.56	-8.20	1.31	-0.87
0.16	-0.27	-1.08	-1.07	1.25	-9.77	2.42	-0.52	-1.47	-8.20	1.33	-0.71
0.17	-0.23	-0.75	-1.07	1.27	-9.54	2.49	-0.51	-1.39	-8.14	1.36	-0.60
0.18	-0.22	-0.61	-0.73	1.29	-9.27	2.52	-0.51	-1.33	-7.76	1.38	-0.54
0.19	-0.22	-0.47	0.30	1.30	-8.70	2.58	-0.50	-1.24	-7.55	1.39	-0.46
0.20	-0.18	-0.40	0.83	1.31	-8.36	2.62	-0.49	-1.20	-7.25	1.40	-0.46
0.21	-0.16	-0.40	1.21	1.34	-8.14	2.68	-0.48	-1.12	-7.17	1.42	-0.39
0.22	-0.15	-0.33	1.49	1.36	-7.66	2.74	-0.47	-1.06	-7.04	1.44	-0.32
0.23	-0.01	-0.27	1.81	1.40	-7.42	2.81	-0.46	-1.00	-6.94	1.45	-0.24
0.24	-0.01	-0.24	2.01	1.42	-7.32	2.88	-0.44	-0.99	-6.61	1.45	-0.07
0.25	-0.01	-0.21	2.18	1.44	-6.99	2.94	-0.43	-0.95	-6.36	1.47	-0.04
0.26	0.00	-0.18	2.35	1.48	-6.77	3.01	-0.42	-0.91	-6.13	1.50	0.01
0.27	0.00	-0.14	2.47	1.50	-6.55	3.08	-0.40	-0.90	-5.97	1.53	0.02
0.28	0.00	-0.04	2.75	1.53	-6.42	3.10	-0.39	-0.87	-5.81	1.54	0.04
0.29	0.00	0.09	2.95	1.54	-6.24	3.13	-0.39	-0.85	-5.57	1.57	0.05
0.30	0.03	0.15	3.01	1.58	-5.98	3.17	-0.38	-0.83	-5.51	1.61	0.07
0.31	0.04	0.20	3.27	1.60	-5.63	3.22	-0.37	-0.81	-5.42	1.64	0.10
0.32	0.05	0.24	3.40	1.61	-5.27	3.25	-0.36	-0.78	-5.26	1.65	0.16
0.33	0.06	0.28	3.40	1.62	-5.04	3.30	-0.36	-0.76	-5.20	1.66	0.19
0.34	0.06	0.31	3.88	1.65	-4.78	3.30	-0.35	-0.74	-5.04	1.68	0.21
0.35	0.07	0.34	4.20	1.67	-4.65	3.33	-0.32	-0.74	-4.95	1.70	0.23
0.36	0.08	0.39	4.49	1.68	-4.48	3.36	-0.28	-0.71	-4.80	1.72	0.27
0.37	0.08	0.42	4.74	1.72	-4.22	3.41	-0.26	-0.69	-4.62	1.75	0.31
0.38	0.09	0.44	4.89	1.74	-4.18	3.46	-0.23	-0.69	-4.54	1.77	0.34
0.39	0.10	0.45	5.17	1.75	-3.85	3.51	-0.20	-0.67	-4.50	1.79	0.36
0.40	0.10	0.48	5.37	1.78	-3.58	3.55	-0.19	-0.63	-4.38	1.81	0.39
0.41	0.11	0.53	5.69	1.78	-3.33	3.63	-0.18	-0.61	-4.30	1.83	0.40
0.42	0.13	0.58	5.95	1.78	-2.95	3.70	-0.17	-0.59	-4.28	1.87	0.50
0.43	0.13	0.63	6.22	1.78	-2.71	3.75	-0.16	-0.56	-4.18	1.90	0.65
0.44	0.14	0.68	6.57	1.80	-2.63	3.84	-0.15	-0.53	-3.96	1.92	0.69
0.45	0.15	0.74	6.81	1.82	-2.44	3.89	-0.14	-0.53	-3.82	1.94	0.87
0.46	0.16	0.74	7.15	1.83	-2.36	3.92	-0.13	-0.51	-3.68	1.95	1.00
0.47	0.19	0.76	7.69	1.86	-2.23	4.00	-0.13	-0.49	-3.53	1.98	1.25
0.48	0.20	0.78	7.87	1.88	-2.12	4.04	-0.12	-0.47	-3.46	1.98	1.38

quantile (continued)	a_0 $x10^0$ °C	a_1 $x\ 10^{-3}$ °C/W	a_2 $x\ 10^{-3}$ °C/W	a_3 $x10^2$ s^2/m^6	a_4 $x\ 10^{-3}$ °C/W	α_c $x10^0$ W/m^2K	b_0 $x10^0$ °C	b_1 $x\ 10^{-3}$ °C/W	b_2 $x\ 10^{-3}$ °C/W	b_3 $x10^2$ s^2/m^6	b_4 $x\ 10^{-3}$ °C/W
0.49	0.22	0.83	8.38	1.90	-2.05	4.08	-0.11	-0.45	-3.36	2.00	1.42
0.50	0.24	0.88	8.63	1.94	-1.97	4.12	-0.11	-0.43	-3.31	2.01	1.46
0.51	0.25	0.90	9.10	1.98	-1.88	4.18	-0.10	-0.41	-3.13	2.03	1.48
0.52	0.28	0.91	9.35	2.01	-1.80	4.23	-0.09	-0.38	-2.81	2.05	1.50
0.53	0.32	0.94	9.57	2.02	-1.71	4.27	-0.09	-0.35	-2.61	2.06	1.55
0.54	0.34	0.98	9.79	2.04	-1.61	4.31	-0.08	-0.33	-2.54	2.08	1.61
0.55	0.35	1.03	10.06	2.07	-1.55	4.37	-0.07	-0.26	-2.35	2.11	1.69
0.56	0.36	1.08	10.32	2.09	-1.49	4.41	-0.06	-0.22	-2.17	2.14	1.80
0.57	0.40	1.11	10.36	2.12	-1.49	4.46	-0.05	-0.12	-2.03	2.15	1.87
0.58	0.43	1.15	10.48	2.15	-1.42	4.53	-0.04	-0.09	-1.84	2.18	1.91
0.59	0.46	1.19	10.73	2.19	-1.30	4.53	-0.03	-0.03	-1.69	2.20	1.93
0.60	0.51	1.25	10.99	2.21	-1.24	4.53	-0.02	0.00	-1.55	2.22	1.99
0.61	0.52	1.26	11.27	2.25	-1.13	4.53	-0.01	0.01	-1.48	2.24	2.08
0.62	0.54	1.28	11.52	2.26	-1.04	4.56	-0.01	0.01	-1.40	2.24	2.10
0.63	0.54	1.30	11.81	2.28	-0.96	4.59	-0.01	0.02	-1.29	2.25	2.10
0.64	0.55	1.31	11.83	2.31	-0.82	4.59	0.00	0.02	-1.14	2.29	2.19
0.65	0.57	1.35	12.20	2.32	-0.68	4.62	0.00	0.02	-1.06	2.33	2.19
0.66	0.58	1.38	12.56	2.33	-0.68	4.65	0.00	0.03	-0.95	2.37	2.19
0.67	0.60	1.38	12.80	2.34	-0.68	4.72	0.00	0.04	-0.82	2.40	2.19
0.68	0.60	1.38	13.12	2.35	-0.66	4.77	0.00	0.06	-0.72	2.43	2.24
0.69	0.62	1.38	13.35	2.35	-0.65	4.77	0.00	0.11	-0.65	2.45	2.28
0.70	0.63	1.42	13.75	2.38	-0.58	4.82	0.00	0.16	-0.60	2.48	2.33
0.71	0.65	1.46	14.08	2.39	-0.52	4.85	0.00	0.21	-0.52	2.51	2.41
0.72	0.67	1.51	14.51	2.42	-0.39	4.89	0.00	0.25	-0.42	2.53	2.44
0.73	0.67	1.52	14.71	2.44	-0.30	4.96	0.00	0.28	-0.29	2.55	2.51
0.74	0.68	1.59	15.03	2.45	-0.22	5.01	0.00	0.30	-0.22	2.57	2.62
0.75	0.69	1.60	15.39	2.47	-0.02	5.12	0.00	0.34	-0.16	2.57	2.76
0.76	0.70	1.64	15.65	2.48	0.00	5.20	0.00	0.39	-0.12	2.58	2.77
0.77	0.71	1.67	15.79	2.52	0.10	5.26	0.00	0.42	-0.06	2.58	2.90
0.78	0.73	1.70	15.84	2.54	0.31	5.35	0.00	0.45	0.17	2.60	2.98
0.79	0.74	1.77	16.10	2.54	0.43	5.42	0.00	0.47	0.29	2.63	3.13
0.80	0.76	1.85	16.66	2.56	0.57	5.46	0.00	0.52	0.41	2.63	3.20
0.81	0.78	1.92	16.76	2.60	0.68	5.47	0.00	0.62	0.51	2.63	3.21
0.82	0.80	1.95	17.35	2.61	0.76	5.51	0.00	0.68	0.61	2.67	3.36
0.83	0.83	1.98	17.84	2.63	0.82	5.55	0.01	0.76	0.73	2.69	3.57
0.84	0.85	2.03	18.62	2.65	0.90	5.59	0.01	0.86	0.79	2.70	3.69
0.85	0.89	2.08	19.17	2.67	0.96	5.65	0.01	1.00	0.86	2.73	3.83
0.86	0.93	2.09	19.82	2.69	1.00	5.80	0.01	1.00	1.02	2.74	4.03
0.87	0.95	2.13	21.33	2.70	1.05	6.04	0.01	1.00	1.15	2.74	4.24
0.88	0.96	2.23	22.22	2.73	1.12	6.23	0.02	1.12	1.22	2.74	4.44
0.89	1.00	2.28	23.90	2.75	1.21	6.31	0.03	1.12	1.34	2.76	4.69
0.90	1.02	2.32	25.72	2.77	1.34	6.51	0.04	1.39	1.44	2.78	4.89
0.91	1.03	2.48	27.85	2.79	1.40	6.74	0.05	1.39	1.68	2.82	5.13
0.92	1.03	2.64	29.39	2.81	1.46	6.85	0.06	1.39	2.66	2.85	5.33
0.93	1.09	2.97	30.89	2.85	1.48	7.06	0.07	1.39	4.35	2.87	5.64
0.94	1.15	3.30	31.76	2.86	1.55	7.42	0.07	1.51	5.95	2.90	5.90
0.95	1.22	3.95	32.24	2.88	1.66	7.60	0.09	2.00	9.41	2.93	6.35
0.96	1.24	5.56	35.87	2.89	2.56	8.03	0.11	2.03	11.65	2.94	7.53
0.97	1.49	7.33	39.22	2.91	3.69	8.49	0.15	2.19	15.71	2.95	9.58
0.98	1.83	9.79	41.09	2.94	5.22	8.75	0.22	2.19	19.67	2.95	15.79
0.99	2.83	19.4	44.15	2.97	7.36	8.84	0.30	2.47	22.28	2.97	15.79
0.9975	3.27	23.7	51.99	2.99	18.64	9.19	0.54	3.95	41.29	2.99	20.32

Symbols and abbreviations

Lower case

a	absorption factor
c_p	specific heat of air
d	displacement height
d	elementary effect
d	thickness
$\underline{d}$	vector with model parameters
g	non-normalized expert weight
k	number of parameters
m	sample mean
n	general exponent
p	pressure
p	probability mass function
p	number of grid levels
q	heat flux
r	number of replicates
s	sample distribution
t	time
t	transmission factor
w	expert performance score
z	height
z_o	roughness length

Upper case

A	area
C	expert calibration score
C	general constant
C	heat capacity
C_d	discharge coefficient
C_p	pressure coefficient
DM	probability distribution for the decision maker
E	expected value
G	normalized expert weight
GTO	Dutch performance indicator for thermal comfort
H	ceiling height
H	obstacle height
I	expert information score
M	model
P	probability
Q	heat gain
R	heat resistance
R	window opening

S	standard deviation
T	temperature
TO	Dutch performance indicator for thermal comfort, (static model)
TO*	Dutch performance indicator for thermal comfort (adaptive model)
U	mean wind velocity
U	utility

Greek

α	heat transfer coefficient
α	significance level
γ	wind reduction factor
ε	emittance
λ	conductivity
ρ	density
ξ	stratification parameter
χ^2	chi-square distribution
Φ	air mass flow rate
Φ_V	air volume flow rate

Subscripts

. m	at . m height above floor
a	ambient (outdoor)
c	convective
e	expert
env	environment
ext	external
in	incoming (supply) air
int	internal
occ	occupant
out	outgoing (exhaust) air
pot	potential
r	radiant
sol	solar
srce	heat source
w	wall

Abbreviations

TRY	test reference year
PMV	predicted mean vote
PPD	predicted percentage dissatisfied
HVAC	heating, ventilation and air conditioning
ET	effective temperature
DM	decision maker
ACH	air changes per hour
NLP	non-linear programming
CFD	computational fluid dynamics

Samenvatting

In keuzes tussen ontwerpvarianten van een gebouw spelen gebouwprestaties een belangrijke rol. Deze grootheden vormen een kwantitatieve schaal waarop de beslisser kan afmeten in hoeverre een gebouwvariant voldoet aan de eisen en doelstellingen. Bij de bepaling van de gebouwprestaties in de ontwerpfase moet rekening worden gehouden met onzekerheden. Kwantificering van deze onzekerheden kan bijdragen tot rationelere ontwerpbeslissingen en kan sturing geven aan de ontwikkeling en keuze van methoden om de gebouwprestatie te berekenen.
In de huidige ontwerppraktijk worden bij het berekenen van gebouwprestaties in de meeste gevallen die onzekerheden niet gekwantificeerd. Dit geldt ook voor prestaties die zijn gerelateerd aan de warmtehuishouding van een gebouw. In de literatuur over simulatie van deze prestaties wordt wel enige aandacht besteed aan onzekerheden, maar verschillende vragen blijven liggen.
Op de eerste plaats wordt in een aantal studies onderkend, dat veel van de onzekerheden niet zonder meer kunnen worden bepaald op basis van een statistische analyse van beschikbare gegevens. Dit roept de vraag op welke methode dan wel geschikt zou zijn om deze onzekerheden te kwantificeren en of een dergelijke methode ook in de ontwerppraktijk zou kunnen worden toegepast.
Daarnaast zijn op diverse plaatsen in de literatuur intuïtieve argumenten te vinden, die onderstrepen dat kwantitatieve informatie over onzekerheden van belang is voor ontwerpbeslissingen. Nergens wordt echter uitgewerkt hoe een beslisser deze informatie zou kunnen gebruiken om zijn beslissing te verbeteren.
In dit proefschrift is een onzekerheidsanalyse uitgewerkt voor een specifieke gebouwprestatie, en voor een specifiek gebouw. Expertmeningen zijn gebruikt om onzekerheden te bepalen die niet via statistische weg kunnen worden afgeleid. Hoe kwantitatieve onzekerheden geïntegreerd kunnen worden in (de analyse van) ontwerpbeslissingen is geïllustreerd in de context van de Bayesiaanse beslissingstheorie.

Het prestatieaspect dat voor de studie is gekozen betreft thermische behaaglijkheid in de zomer. Het gebouw waarvan de prestatie is bestudeerd, is een kantoorgebouw van vier verdiepingen zonder koelinginstallatie of mechanisch ventilatiesysteem. Om de gebouwprestatie te bepalen zijn twee indicatoren gehanteerd, namelijk TO en TO*. Beide indicatoren voorspellen het aantal uren per jaar, waarin in het gebouw een klimaat heerst dat door meer dan 10% van de mensen zou worden beoordeeld als 'oncomfortabel warm'. De indicatoren verschillen echter in de onderliggende comfortmodellen. De TO-indicator is gebaseerd op het statische comfortmodel volgens Fanger (1970), terwijl het adaptieve comfortmodel van De Dear en Brager (1998) ten grondslag ligt aan de TO*-indicator. De indicatoren zijn berekend op basis van numeriek gesimuleerde temperaturen in het gebouw. Voor de ontwikkeling van het gebouwsimulatiemodel is een standaardaanpak gevolgd met een aanvulling voor de modellering van de luchtstromingen.

Onzekerheid wordt in dit proefschrift gerepresenteerd in termen van subjectieve kansen. Er wordt onderscheid gemaakt tussen onzekerheden uit vier bronnen. Deze worden aangeduid als specificatie-onzekerheid, scenario-onzekerheid, modellerings-onzekerheid en numerieke onzekerheid. Specificatie-onzekerheid ontstaat doordat de ontwerpspecificaties het op te leveren gebouw niet volledig vastleggen. Scenario-onzekerheid vloeit voort uit het feit dat de externe factoren waaraan het gebouw wordt blootgesteld, gedurende de prestatiebepaling niet volledig vastliggen. Modellerings-onzekerheid komt voort uit aannamen en vereenvoudigingen die worden geïntroduceerd in de ontwikkeling van het fysische gebouwmodel. Numerieke onzekerheid, tenslotte, kan ontstaan bij de vertaling van het fysische gebouwmodel in een numeriek computermodel en bij de simulaties met dit computermodel. Scenario-onzekerheid en numerieke onzekerheid zijn in dit proefschrift niet verder onderzocht.

Het onderzoek dat in het eerste deel van het proefschrift wordt beschreven, concentreert zich op een ruwe onzekerheidsanalyse. De onzekerheden zijn door de auteur bepaald op basis van gegevens uit de literatuur en gepropageerd door het gebouwsimulatiemodel. De resulterende onzekerheden in de prestatieindicatoren waren significant blijkens een variatiecoëfficiënt (standaarddeviatie gedeeld door gemiddelde) van 0.5. De waarden voor zowel gemiddelden als standaarddeviaties van de beide indicatoren TO en TO* lagen dicht bij elkaar.
De onzekerheidsanalyse legde verschillende modelparameters bloot, waarvoor de onzekerheid op ad-hoc basis moest worden bepaald. Van deze parameters kon hetzij onvoldoende informatie worden gevonden, of waren de beschikbare gegevens tegenstrijdig, dan wel onbetrouwbaar. De onzekerheid in twee sets van deze parameters is verder geanalyseerd. Deze parameters waren geïdentificeerd als belangrijk bijdragend aan de onzekerheid in de gebouwprestatie.

De eerste set parameters betrof de winddrukverschilcoëfficiënten, die de lokale windsnelheid relateren aan de drukverschillen over het gebouw. Deze drukverschillen vormen de drijvende factor achter de ventilatiestromen door het gebouw. De onzekerheid in deze coëfficiënten is gekwantificeerd in een expertmeningonderzoek met een methode volgens Cooke en Goossens (2000). In dit onderzoek hebben zes experts de onzekerheid in 24 winddrukverschilcoëfficiënten bepaald op basis van generieke kennis en gegevens. Voor elke coëfficiënt is een gewogen gemiddelde van hun schattingen berekend voor toepassing in de onzekerheidsanalyse. De gewichten van de experts zijn bepaald uit een statistische vergelijking van hun schattingen met gemeten waarden die waren verkregen in twee onafhankelijke windtunnelonderzoeken.
De expertmeningstudie bleek succesvol. De statistische vergelijkingen toonden aan, dat de gecombineerde schattingen van de experts goed gekalibreerd zijn. Dit betekent dat deze schattingen geloofwaardig zijn als weerspiegelingen van de onzekerheden in de winddrukverschilcoëfficiënten. Wel bleek het expertmeningonderzoek veel duurder te zijn dan een windtunnelstudie, terwijl de resulterende onzekerheden groter waren. Een voor de hand liggende maatregel om de kosten te drukken door het aantal deelnemende experts te verkleinen is niet aantrekkelijk. Slechts twee van de zes experts in de huidige studie bleken namelijk goed gekalibreerd bij vergelijking van hun schattingen met de gemeten data.

Expertmeningen zijn ook gebruikt om de onzekerheden te bepalen in de luchttemperatuurverdeling in de kantoorvertrekken (hoofdstuk 5). Een belangrijk verschil met de expertmeningstudie aan de winddrukken was het ontbreken van een geschikt model voor de luchttemperatuurverdeling. Dit bood de mogelijkheid om de modelontwikkeling parallel te laten lopen met de onzekerheidsanalyse. Anticiperend op een significante onzekerheid in de luchttemperatuurverdeling, gegeven de beperkte informatie over de randvoorwaarden in de context van een gebouwsimulatie, is een grof, heuristisch model geponeerd met een beperkt aantal empirische parameters. De onzekerheden in de relevante aspecten van de temperatuurverdeling zijn via expertmeningonderzoek bepaald voor negen verschillende sets van randvoorwaarden. Hiervoor werd dezelfde methode gehanteerd als voor de winddrukken, maar deze keer met 5 experts. Daarna is probabilistische inversie toegepast volgens de PREJUDICE-methode van Kraan (2000). Bij probabilistische inversie wordt geprobeerd om een zodanige kansverdeling over de modelparameters te vinden, dat de onzekerheden in de modeloutput in overeenstemming zijn met de gecombineerde schattingen van de experts.

De conclusies uit deze expertmeningstudie zijn sterk vergelijkbaar met die uit de vorige. De gecombineerde schattingen bleken weer goed gekalibreerd en de schattingen en kalibratiescores wisselden sterk van expert tot expert. De probabilistische inversie was succesvol: over de 11 modelparameters kon een verdeling worden gevonden, waarmee de expertmeningen met voldoende nauwkeurigheid konden worden gereproduceerd. Dit geeft aan, dat het voorgestelde model voor de luchttemperatuurverdeling niet te grof is gekozen.
Probabilistische inversie is een krachtig hulpmiddel gebleken om te toetsen of de mate van modelverfijning in overeenstemming is met de onzekerheid in het proces dat door het model beschreven moet worden. De methode is echter kostbaar in termen van rekentijd en vereist in zijn huidige vorm veel specifieke kennis van de gebruiker. De techniek is dan ook niet geschikt voor frequent gebruik in de ontwerppraktijk.

In het eerste deel van hoofdstuk 6 zijn alle onzekerheden in modelparameters door het gebouwmodel gepropageerd om de onzekerheid in de thermische behaaglijkheids-prestatie te bepalen. Voor zowel de TO- als de TO*-indicator is een variatiecoëfficiënt gevonden van 0.6. Dit is een gematigde toename in vergelijking met de waarde van 0.5, die in de initiële onzekerheidsanalyse in hoofdstuk 3 was gevonden.
Het tweede deel van het hoofdstuk illustreert hoe Bayesiaanse beslissingstheorie kan worden gebruikt om kwantitatieve informatie over de onzekerheden constructief in te zetten bij een ontwerpbeslissing. Een voorbeeld wordt beschreven, waarin twee (fictieve) beslissers onder dezelfde omstandigheden de keuze moeten maken om wel of geen koelinginstallatie in het gebouwontwerp op te nemen. Het voorbeeld laat zien hoe de twee beslissers, die in afwezigheid van onzekerheid dezelfde keuze zouden maken, tot verschillende beslissingen komen als gevolg van hun verschillende risico-attitude. Dit onderstreept het belang van expliciete onzekerheidsinformatie voor rationele ontwerpkeuzes.

M.S. de Wit, Uncertainty in predictions of thermal comfort in buildings, Proefschrift TUDelft, 2001.

Dankwoord

Dit boekje gaat over onzekerheden. Dat is niets nieuws zult u zeggen: dat staat met grote letters op de voorkant. Maar het zijn zeker niet alleen de onzekerheden uit de titel die de afgelopen periode hebben beheerst. Veel andere Onzekerheden, met name omtrent de aanpak, de richting, en zelfs de zin van het onderzoek staken regelmatig de kop op. Aan het onder de knie krijgen van zowel de onzekerheden als de Onzekerheden heeft een groot aantal mensen bijgedragen. Ik kan hen niet allemaal noemen, maar een aantal mag ik niet vergeten.

Op de eerste plaats noem ik Fried Augenbroe. Hij heeft me met raad en daad bijgestaan vanaf de eerste schetsen van het onderzoeksplan tot de laatste letter van het proefschrift. Ik denk met veel plezier terug aan de discussies die we hebben gehad, de vele deadlines die we hebben gemist en ik ben hem erg dankbaar voor de onnavolgbare manier waarop hij erin geslaagd is mij steeds weer te motiveren.
Ook Ton Vrouwenvelder was vanaf het begin betrokken bij het onderzoek. Zijn efficiëntie en grote inzicht zijn steeds een voorbeeld voor mij.

De tijd in de sectie GBT van de Faculteit Civiele Techniek was een bijzondere. Ik begon aan het promotie-onderzoek als onderdeel van een driemensschap, samen met Alex Hogeweg en Marrit Pel. Het onderzoek had een moeizame start, waarin ik van Alex en Marrit veel steun heb ervaren. Ook in latere fasen hebben ze mij steeds aangemoedigd om door te zetten. Aan de tijd dat ik met Geert-Jan van Oosterhout op de kamer zat heb ik een bijzonder prettige herinnering, niet in de laatste plaats vanwege onze 'synergie'.
De dynamica-groep van TNO Bouw ben ik erkentelijk voor de ruimte die ze me de afgelopen twee jaar hebben gegeven om het proefschrift af te ronden.

Ook buiten de directe werkkring heb ik veel steun gehad van verschillende mensen. Peter Janssen van het RIVM dank ik voor de correspondentie over uiteenlopende aspecten van onzekerheids- en gevoeligheidsanalyse en het ter beschikking stellen van de software die als basis heeft gediend voor de onzekerheidsanalyses in dit werk. Bij Wil de Gids kon ik altijd terecht met vragen over ventilatie van gebouwen en aanverwante zaken. Met Bernd Kraan heb ik veel gediscussieerd over onzekerheidsanalyse en expertmeningonderzoek. Maar bovenal heeft hij me bijgestaan met zijn kennis en kunde om de probabilistische inversie in hoofdstuk 5 tot een goed einde te brengen.

I want to extend my gratitude to the experts, who participated in the expert judgment studies for a small fee. A special word of thanks goes to Dave Surry, who carried out a wind tunnel experiment free of charge for the benefit of my research.

Mijn familie en vrienden wil ik in het bijzonder bedanken. Zij hebben veel geduld met me gehad steeds wanneer ik het liet afweten omdat er aan 'het boekje' moest worden gewerkt.
Martijn Baljon dank ik hartelijk voor het ontwerpen van de fraaie omslag.
Pa en ma, ik heb jullie niet aflatende belangstelling en steun bijzonder op prijs gesteld en ben jullie daar erg dankbaar voor.
Ik weet dat jullie je vader te weinig gezien hebben, Bas en Roos, maar jullie hebben als geen ander problemen in het onderzoek weten te relativeren door mij steeds weer te laten ervaren dat er veel belangrijker dingen in het leven zijn.
Angélique, je zou in feite mede-auteur van dit boekje moeten zijn. Je hebt mij zonder helder inzicht in planning en precieze vorderingen van het proefschrift steeds weer de ruimte gegeven. Bij mijn verhandelingen over onzekerheden ben je steevast in slaap gevallen, daarmee blijkgevend van een volledig vertrouwen. Maar als ik het had over de Onzekerheden was je altijd één en al oor en heb je me er steeds weer doorheen gesleept.

Curriculum vitae

Sten de Wit werd geboren op 31 mei 1964 te Valkenswaard. In 1976 begon hij op het Hertog-Jan College in Valkenswaard, waar hij in 1982 het Gymnasium-β diploma behaalde. Aansluitend studeerde hij technische natuurkunde aan de Technische Universiteit Eindhoven (TUE). Het ingenieursdiploma werd in 1989 behaald. Na een korte aanstelling als toegevoegd onderzoeker aan de TUE werd de vervangende dienstplicht vervuld bij het FOM-instituut voor plasmafysica 'Rijnhuizen'. In 1991 begon hij als docent natuurkunde aan het Stedelijk Gymnasium te Haarlem en volgde parallel daaraan de lerarenopleiding aan de Rijksuniversiteit Utrecht. Het leraarschap werd in 1993 verruild voor een promotieplaats aan de Technische Universiteit Delft bij de faculteit Civiele Techniek. Van 1994 tot 1999 deed hij daar het promotieonderzoek waarvan de resultaten in dit proefschrift zijn beschreven. Sinds februari 1999 is hij in dienst van TNO Bouw waar hij zich in hoofdzaak bezighoudt met betrouwbaarheid en veiligheid van civiele constructies.